ISSN: 2408-2384 (Online)
ISSN: 1686-5456 (Print)

Environment and Natural Resources Journal

Volume 18, Number 1, January - March 2020

Scopus® Clarivate Analytics EBSCO HOST DOAJ DIRECTORY OF OPEN ACCES JOURNALS ASEAN CITATION INDEX TCI

Environment and Natural Resources Journal (EnNRJ)

Volume 18, Number 1, January-March 2020 ISSN: 1686-5456 (Print)
ISSN: 2408-2384 (Online)

AIMS AND SCOPE

The Environment and Natural Resources Journal is a peer-reviewed journal, which provides insight scientific knowledge into the diverse dimensions of integrated environmental and natural resource management. The journal aims to provide a platform for exchange and distribution of the knowledge and cutting-edge research in the fields of environmental science and natural resource management to academicians, scientists and researchers. The journal accepts a varied array of manuscripts on all aspects of environmental science and natural resource management. The journal scope covers the integration of multidisciplinary sciences for prevention, control, treatment, environmental clean-up and restoration. The study of the existing or emerging problems of environment and natural resources in the region of Southeast Asia and the creation of novel knowledge and/or recommendations of mitigation measures for sustainable development policies are emphasized.

The subject areas are diverse, but specific topics of interest include:

- Biodiversity
- Climate change
- Detection and monitoring of polluted sources e.g., industry, mining
- Disaster e.g., forest fire, flooding, earthquake, tsunami, or tidal wave
- Ecological/Environmental modelling
- Emerging contaminants/hazardous wastes investigation and remediation
- Environmental dynamics e.g., coastal erosion, sea level rise
- Environmental assessment tools, policy and management e.g., GIS, remote sensing, Environmental Management System (EMS)
- Environmental pollution and other novel solutions to pollution
- Remediation technology of contaminated environments
- Transboundary pollution
- Waste and wastewater treatments and disposal technology

Schedule

Environment and Natural Resources Journal (EnNRJ) is a quarterly published journal in January-March, April-June, July-September and October-December.

Publication Fees

There is no cost of the article-processing and publication.

Ethics in publishing

EnNRJ follows closely a set of guidelines and recommendations published by Committee on Publication Ethics (COPE) (http://publicationethics.org/).

Editorial Office Address
Research and Academic Services Section,
Faculty of Environment and Resource Studies, Mahidol University
999, Phutthamonthon Sai 4 Road, Salaya, Phutthamonthon, Nakhon Pathom, Thailand, 73170
Phone +662 441 5000 ext. 2108 Fax. +662 441 9509-10
Website: https://www.tci-thaijo.org/index.php/ennrj/index
E-mail: ennrjournal@gmail.com

Environment and Natural Resources Journal (EnNRJ)

Volume 18, Number 1, January-March 2020 ISSN: 1686-5456 (Print)
ISSN: 2408-2384 (Online)

EXECUTIVE CONSULTANT TO EDITOR

Associate Professor Dr. Kampanad Bhaktikul
(Mahidol University, Thailand)
Associate Professor Dr. Sura Pattanakiat
(Mahidol University, Thailand)

EDITOR

Associate Professor Dr. Benjaphorn Prapagdee
(Mahidol University, Thailand)

EDITORIAL BOARD

Professor Dr. Anthony SF Chiu
(De La Salle University, Philippines)
Professor Dr. Chongrak Polprasert
(Thammasat University, Thailand)
Professor Dr. Gerhard Wiegleb
(Brandenburgische Technische Universitat Cottbus, Germany)
Professor Dr. Hermann Knoflacher
(University of Technology Vienna, Austria)
Professor Dr. Jurgen P. Kropp
(University of Potsdam, Germany)
Professor Dr. Mark G. Robson
(Rutgers University, USA)
Professor Dr. Nipon Tangtham
(Kasetsart University, Thailand)
Professor Dr. Pranom Chantaranothai
(Khon Kaen University, Thailand)
Professor Dr. Shuzo Tanaka
(Meisei University, Japan)
Professor Dr. Warren Y. Brockelman
(Mahidol University, Thailand)
Professor Dr. Yeong Hee Ahn
(Dong-A University, South Korea)
Associate Professor Dr. Kathleen R Johnson
(Department of Earth System Science, USA)
Associate Professor Dr. Sate Sampattagul
(Chiang Mai University, Thailand)
Associate Professor Dr. Sompon Wanwimolruk
(Mahidol University, Thailand)

Associate Professor Dr. Takehiko Kenzaka
(Osaka Ohtani University, Japan)
Associate Professor Dr. Tamao Kasahara
(Kyushu University, Japan)
Associate Professor Dr. Uwe Strotmann
(University of Applied Sciences, Germany)
Assistant Professor Dr. Devi N. Choesin
(Institut Teknologi Bandung, Indonesia)
Assistant Professor Dr. Said Munir
(Umm Al-Qura University, Saudi Arabia)
Dr. Manish Mehta
(Wadia Institute of Himalayan Geology, India)
Dr. Marzuki Ismail
(University Malaysia Terengganu, Malaysia)
Dr. Mohamed Fassy Yassin
(University of Kuwait, Kuwait)
Dr. Norberto Asensio
(University of Basque Country, Spain)
Dr. Thomas Neal Stewart
(Mahidol University, Thailand)

ASSISTANT TO EDITOR

Associate Professor Dr. Kanchana Nakhapakorn
Dr. Chitsanuphong Pratum
Dr. Kamalaporn Kanongdate
Dr. Paramita Punwong
Dr. Witchaya Rongsayamanont

JOURNAL MANAGER

Isaree Apinya

JOURNAL EDITORIAL OFFICER

Supalak Wattanachalarmyot
Parynya Chowwiwattanaporn

Environment and Natural Resources Journal (EnNRJ)

Volume 18, Number 1, January-March 2020 ISSN: 1686-5456 (Print)
ISSN: 2408-2384 (Online)

CONTENT

Green Approach for Decolorization and Detoxification of Textile Dye- CI Direct Blue 201 Using Native Bacterial Strains 1
*Ekanayake EMMS and Pathmalal M. Manage**

Formulation of Natural Fortifiers from Readily Available Materials for Nutrient Enrichment of Organic Fertilizers 9
Taiwo B. Hammed, Godson R.E.E. Ana, and Elizabeth O. Oloruntoba*

Adsorption of Reactive Dyes from Wastewater Using Cationic Surfactant-modified Coffee Husk Biochar 21
*Chatsuda Kosaiyakanon and Suratsawadee Kungsanant**

The Chemical Characteristic and Microbial Diversity of the Hot Spring at Phusang National Park 33
Sureewan Bumrungthai, Sureewan Duangjit, Buntom Somsuwan, and Somchai Inpeng*

Effects of Volcanic Zeolite Tuff on Olive (*Olea Europaea* L.) Growth and Soil Chemistry under a Constant Water Level: Five Years' Monitoring Experience 44
Jalal. A. Al-Tabbal, Naji. K. Al-Mefleh, Kamel. K. Al-Zboon, and Maher. J. Tadros*

Pine Needle Energy Potential in Conifer Forest of Western Himalayan 55
Vishal Sharma and Rajeev Kamal Sharma*

Effect of Plant Spacing and Organic Fertilizer Doses on Methane Emission in Organic Rice Fields 66
Andin Muhammad Abduh, Eko Hanudin, Benito Heru Purwanto and Sri Nuryani Hidayah Utami*

Effects of *Agrobacterium* sp. I26, Manure and Inorganic Fertilizers to Pb Content of Rice Grains Planted in Pb Polluted Soil 75
Retno Rosariastuti, Muhamad Sulthoni Fauzi1, Purwanto, and Suntoro*

Structural Durability Assessment of Stilt Houses to Flash Flooding: Case Study of Flash Flood-Affected Sites in Thailand 85
Olarn Charoenchai and Kampanad Bhaktikul*

Association of Community-level Traits with Soil Properties in a Tropical Coastal Sand Dune 101
*Dokrak Marod, Sarawood Sungkaew, Hiromi Mizunaga, and Jakkaphong Thongsawi**

Green Approach for Decolorization and Detoxification of Textile Dye- CI Direct Blue 201 Using Native Bacterial Strains

Ekanayake EMMS and Pathmalal M. Manage*

Centre for Water Quality and Algae Research, Department of Zoology, University of Sri Jayewardenepura, Nugegoda 10250, Sri Lanka

ARTICLE INFO

Received: 19 Feb 2019
Received in revised: 6 Jun 2019
Accepted: 14 Jun 2019
Published online: 14 August 2019
DOI: 10.32526/ennrj.18.1.2020.01

Keywords:
Bioremediation/ Decolorization/ *Alcaligenes faecalis*/ *Micrococcus luteus*/ *Staphylococcus warneri*

*** Corresponding author:**
E-mail: pathmalal@sjp.ac.lk

ABSTRACT

One hundred and fifty six native bacterial strains with different morphological characters were isolated from water and soil samples collected from textile wastewater effluent sites, Sri Lanka. Three isolated bacterial strains were more effective on decolorization of CI Direct Blue 201 textile dye and 16s rRNA analysis reveals that the bacterial strains were *Alcaligenes faecalis* (MK166784), *Micrococcus luteus* (MK166783) and *Staphylococcus warneri* (MK256311). *A. faecalis, M. luteus* and *S. warneri* showed complete decolorization of CI Direct Blue 201 textile dye within 60, 64, and 72 h of incubation time respectively under the static conditions at 28 ºC. Decolorization was effective at a temperature range from 24 ºC to 40 ºC and pH range from 7 to 9. The presence of tryptone, peptone or yeast in the Mineral Salt Medium enhanced the decolorization of the dye. Phytotoxicity assay based on the seed germination percentages of *Oryza sativa* and *Vigna radiate* showed that the detoxification of CI Direct Blue 201 textile dye after the bacterial treatment was effective signifying the potential applicability of the *A. faecalis, M. luteus* and *S. warneri* to develop a green application to treat textile wastewater.

1. INTRODUCTION

The natural coloring materials which derived from plant, animal or mineral sources have played an important role in every civilization, until the first synthetic dye: "mauveine" was discovered in the late nineteenth century (Hunger, 2003). However, synthetic dyes have invaded the textile dyeing industry rapidly due to the excellent color fastness ability, lower production cost, broad range of color spectra, etc. (Bechtold and Mussak, 2009). At present, more than 7×10^5 kg of synthetic dyes are consumed annually in the forms of 100,000 structurally different colors to fulfill the requirement of rapidly changing fashion trends (Gupta et al., 2012).

Textile dyeing industry consumes a huge quantity of water in their manufacturing processes including dyeing, washing, and seizing etc. Around 10-20 L of water is required for dyeing and finishing 1 kg of fabric (Naresh et al., 2013). Annually, more than one thousand tons of dyes together with different types of flame retardants, aromatic amines, bisphenols, heavy metals, etc. are discharged directly either into waterways or to the environment (Rovira and Domingo, 2018). Therefore, textile wastewater effluent interrupts the wellbeing of aquatic ecosystems by deteriorating the quality of surface and groundwater (Ileperuma, 2000; Mahagamage and Manage, 2014; Mahagamage et al., 2015). Finally, the discharges trigger the formation of carcinogenic, microtoxic, mutagenic diseases in terrestrial animals as well as in human beings (Gupta et al., 2009).

Although there are various important control measures for textile wastewater effluents, treatment of textile wastewater is difficult due to the huge daily load of wastewater, high recalcitrance for natural degradation processes, presence of sulfur like additives, high COD levels, etc. (Saratale et al., 2009). Most of the color removal methods work either by concentrating color molecules into sludge or complete degradation of color molecules by breaking the complex structures into colorless daughter products by chemical treatment (Pearce et al., 2003). Most physical and chemical based treatment methods such as electrokinetic coagulation, membrane filtration, activated carbon or peat concentrate the colored effluent by forming a huge amount of sludge

Citation: Ekanayake EMMS, Manage PM. Green approach for decolorization and detoxification of textile dye- CI direct blue 201 using native bacterial strains. Environ. Nat. Resour. J. 2020;18(1):1-8. DOI: 10.32526/ennrj.18.1.2020.01

(Konsowa, 2003; Robinson et al., 2001). Therefore, such application methods create secondary pollution and require millions of dollars for the treatment process to remove the sludge which is highly toxic and recalcitrant for natural degradation processes and has become one of the major problems in terms of point source environmental pollution. Thus, such methods are not applicable all over the world. Countries like Sri Lanka, India, and Bangladesh which are the leading suppliers of apparel to the world, are facing environmental pollution problems with huge use of textile dyes in the textile industries and are compelled to explore alternative novel treatment methods to achieve the required wastewater consent limits and for further expansion of their productions.

Biological treatment of textile wastewater is one of the emerging techniques as an eco-friendly alternative for existing physiochemical treatments. Decolorization by biological agents involved in the biotransformation of toxic textile dyes to non-toxic secondary metabolites with a very little amount of sludge (Kalyani et al., 2008; Saratale et al., 2009). Biological agents including bacteria (Ekanayake and Manage, 2017; Kalyani et al., 2008), fungi (Ekanayake et al., 2018), aquatic plants (Ekanayake and Manage, 2016) and algae (Anandhana et al., 2018) have been reported by a number of investigators with reference to decolorization of various textile dyes to date.

In Sri Lanka, Somasiri et al. (2005) and Wijetunga et al. (2007) have recorded the decolorization of a few acid dyes by anaerobic mixed cultures. According to the author's knowledge, only a limited number of studies are available in Sri Lanka regarding decolorization of di-azo direct dyes (Ekanayake and Manage, 2017), which is a class of dye having the highest rate of toxicity among all the synthetic dye classes (Shore, 1996). Therefore, the present study was designed to isolate, identify and optimize the CI Direct Blue 201 (DB), a di-azo direct textile dye, decolorizing native bacteria as per the request of local textile dyeing industries to achieve the greener certificate of textile wastewater treatment focusing Sri Lankan textile industry into "Product without Guilt Concept".

2. METHODOLOGY

2.1 Synthetic dye and chemicals

A questionnaire survey was conducted to select major dyes used in Sri Lankan textile dyeing industry and based on the results, CI Direct Blue 201 (DB), synthetic azo dye, was selected as the model dye for the study. The chemical structure of the DB textile dye consists of two azo bonds, three sulphate groups on seven aromatic rings having a molecular weight of 834 g/mol (Chemical Book, 2017). The selected dye is generally bound into cotton and other cellulosic materials by electrostatic forces when the aqueous dye bath consists of salts and electrolyte (Hunger, 2003). The DB synthetic azo dye was provided by local textile industry, Poogoda, Sri Lanka. All the culture media, organic and inorganic compounds are in microbiology and analytical grade with the highest purity, obtained from Sigma Aldrich.

2.2 Medium

Luria Bertani (LB) medium consisted of (g/L) Yeast extract (4.6), tryptone water (15) was selected as the general growth medium and modified Mineral Salt Medium (MSM) with (g/L) 3.39 Na_2HPO_4, 15.0 KH_2PO_4, 5.0 NH_4Cl, 2.5 NaCl, 3.5 $MgCl_2$ (Asad et al., 2007) was selected for the decolorization experiment. 1.5% bacteriological agar was added when solid medium was required. The pH of the medium was adjusted to 7.0.

2.3 Isolation and screening of textile dye decolorizing bacteria

The wastewater and soil samples collected from textile wastewater effluent sites in Awissawella (6º58'58.02" N, 80º07'23.86" E) and Biyagama (6º57'28.85" N, 79º59'41.21" E) were subjected to enrichment studies for 14 days at 28±1 ºC under static conditions, spiking of 50 mg/L of DB dye as the sole carbon source. Exactly 1 mL of enriched samples were subjected to serial dilution and plated on LB agar to isolate bacterial colonies with different morphological features and the isolated bacterial strains were maintained in LB slants at 4 ºC (Liyanage and Manage, 2016).

2.4 Textile dye decolorization experiments

2.4.1 Dye assay and dye decolorization by isolated bacterial strains

Decolorization of textile dye could be seen visually compare to the control setup, and determination was done numerically by measuring the absorption using UV-Vis spectrophotometer at relevant wavelength. The pH of DB dye was found to be 8.1, thus, the pH of the culture medium was adjusted to 7.0. Accordingly, the maximum absorption spectra were recorded for pH 6, 7, 8, and 9 in order to ensure the effect of pH changes on color spectrum

of DB dye and all the spectra were found as the same at λ max of 570 nm. The decolorization percentage of the dye was calculated using the equation given below (Gupta et al., 2012), where C1 is the initial concentration and C2 is the final concentration.

Decolorization percentage (%) = [(C1-C2)/C1] 100

Overnight exponentially grown bacterial cultures were washed with 0.9% saline solution following centrifugation and starved overnight (Idroos and Manage, 2018) to remove all the remaining carbon sources in the medium and then the turbidity of the each bacterial suspension was equalized to 0.350 at the wave length of 590 nm using a UV-Vis spectrophotometer (Manage et al., 2000; Manage et al., 2009). The equalized bacterial suspension (5% v/v) was introduced into modified MSM spiked with filter sterilized dye (final concentration of 50 mg/L) as the sole carbon source and further incubated at 28±1 ºC for a period of 14 days under static condition. Triplicate sample setup was maintained for each bacterial strain while controls were maintained under the same conditions without the addition of bacteria. The primary screening was carried out for all the bacterial strains isolated in the present study. The changes in absorbance were measured at 14 days of incubation, and the decolorization percentages were calculated accordingly. Any bacterial strain which showed over 80% of decolorization was selected for further studies.

In secondary screening, decolorization was further analyzed by subsampling of 3 mL of aliquots at twenty-four hours' intervals. The most promising bacterial strains showing decolorization of DB were screened and identification was done by 16S rRNA analysis via the service obtained from GENETECH (PVT), Sri Lanka. The 16S rRNA sequences of selected bacterial strains were aligned to the most similar sequences in the National Center for Biotechnology Information (NCBI) using the align sequence program (NCBI, 2018). The pre-aligned 16S rRNA sequences were deposited in GenBank (NCBI, 2018) and accession numbers were obtained.

2.4.2 Optimization of bacterial decolorization of DB textile dye

Decolorization of DB textile dye by the selected isolated bacterial strains were optimized by altering the temperature (24, 28, 32, 36, 40 ºC), pH (6, 7, 8, 9), carbon sources (starch, glucose, yeast), nitrogen sources (tryptone, peptone, urea) and static or shaking conditions (100 rpm). Decolorization experiments were carried out by changing one parameter at once, in the modified MSM at 50 mg/L of final dye concentration following the procedure described in 2.4.1. Moreover, the decolorization potential of selected bacteria strains for different dye concentrations (25, 50, 75, and 100 mg/L) was studied. Repeated usability of selected bacterial strains in decolorization process was studied by addition of 50 mg/L DB textile dye at the end of each decolorization cycle without supplement of nutrients further. All the experiments were carried out in triplicates and controls were maintained for each experiment set up under the same experimental conditions without addition of bacteria.

2.5 Phytotoxicity study

Phytotoxicity assay was employed for the evaluation of toxicity of the original dye and the end product of the bacterial decolorized dye solutions from each bacterial strain employed by the method described by Kalyani et al. (2008) with minor modifications. Thirty seeds of *Oryza sativa* (monocot) and *Vigna radiate* (dicot) were placed on moisture chambers having several layers of tissues on petri dishes and seeds were watered (5 mL) from DB textile dye (50 mg/L) and decolorized dye solutions for each bacterial decolorized dye solutions separately. Modified MSM without addition of dye was used for the control set. Seed germination percentage was calculated at five days of incubation.

3. RESULTS AND DISCUSSION

3.1 Isolation and identification of DB textile dye decolorizing bacteria

A questionnaire survey was conducted among Sri Lankan textile dyeing industries to select a model dye for the study. Based on the results of the survey, DB dye was selected for the present study. The selected DB dye is widely used in small scale textile dyeing industries (5-50 kg/day) where the proper treatment methods are not practiced due to the high cost.

Ekanayake and Manage (2016) recorded that DB, is highly recalcitrant to natural photolysis and removal was suggested via biodegradation processes. However, it has been recorded that dyes having azo and sulfo groups on the aromatic components are highly inhibiting the breakdown through bacterial degradation processes (Saratale et al., 2009).

In the present study, 156 bacterial strains having different morphological characteristics were isolated from water and soil samples collected from textile wastewater effluent sites in Sri Lanka and their decolorization capability of DB textile dye was evaluated. The selected bacterial strains were identified using the 16S rRNA analysis (Table 1) and the nucleotide sequences were deposited on the GenBank and accessions were obtained as *Alcaligenes faecalis* (MK166784), *Micrococcus luteus* (MK166783), and *Staphylococcus warneri* (MK256311) respectively.

Table 1. Identification of isolated bacterial strains

Isolate	Number base pair of sequence	Number base pair of homology	Similarity percentage (%)	GenBank accession number
Alcaligenes faecalis	1031	940	99	MK166784
Micrococcus luteus	1018	945	99	MK166783
Staphylococcus warneri	1003	945	99	MK256311

3.2 Optimization of the decolorization under selected parameters

A. faecalis, M. luteus, and *S. warneri* showed complete decolorization of the DB dye within 60, 64 and 72 h of incubation under static conditions, respectively (Table 2). Hassan et al. (2013) have recorded that 70% decolorization of Novacron Orange by the bacterium *M. luteus* within 72 h of incubation suggesting that the dye decolorization potential of bacteria vary with the type of the textile dye. Further, *S. warneri* (Chen et al., 2005) and *A. faecalis* (Shah et al., 2012) have also been recorded as potential textile dye decolorizing bacteria. A recent study of Ekanayake and Manage (2017) recorded 50% decolorization of DB textile dye by *Micrococcus* sp. within 14 days of incubation. However the present study showed complete decolorization of DB dye by the bacterium *M. luteus* indicating that decolorization of textile dyes are species specific. Nevertheless, decolorization of DB was not attributed for the bacteria; *A. faecalis* and *S. warneri* which is studied in the present study.

Table 2. Decolorization of DB dye by selected bacterial strains

Isolate	Decolorization percentage	Time (h)
A. faecalis	CD	60
M. luteus	CD	64
S. warneri	CD	72

*CD: Complete decolorization

Real textile wastewater effluents are a mixture of different colors with a high concentration of COD, BOD, turbidity, and Electric conductivity with high temperature. Bacteria which live in such conditions should be able to tolerate the harsh conditions and must be able to decolorize the dyes effectively without exhaustion. Thus, the decolorization of DB textile dye by the selected bacterial strains was further evaluated under different selected conditions. According to the Sri Lankan wastewater guidelines, the temperature in the effluent water should be less than 40 °C (BOI, 2011). Kalyani et al. (2008) showed that decolorization of Scarlet R textile dye by *M. glutamicus* is dependent on the variation of temperature applied. Therefore, the effect of temperature on decolorization of DB dye at static condition was evaluated. It was found that over 90% of decolorization of DB dye when temperature changed from 24 to 40 °C for all three bacterial strains (Figure 1), suggesting the applicability of the selected bacterial strains for practical applications.

The tolerant limit of the pH in textile wastewater effluent should be within the range of 6.0-8.5 at ambient temperature (BOI, 2011). Therefore, decolorization of DB textile dye by selected bacterial strains were evaluated the pH range of 6.0 to 9.0 at 28 °C under static conditions. Saratale et al. (2009) recorded that the decolorization of most textile dyes by bacterial strains is more effective at pH 7. In the present study, the range of pH 7 to 9 was appeared to be more favorable for all bacterial strains and rapid decolorization of DB textile dye was detected (Table 3). It was found that *A. faecalis* s howed the highest decolorization potential even at slightly alkaline (pH 9) conditions rather than the other two bacteria species. Saratale et al. (2009) recorded the decolorization of an azo dye (Scarlet R) was not possible for both pure and mixed bacterial consortium developed with *Micrococcus* sp. at alkaline pH range of 9 to 12, where above 90% of decolorization was recorded in the present study by the bacterium *M. luteus* contrasting to the previous studies.

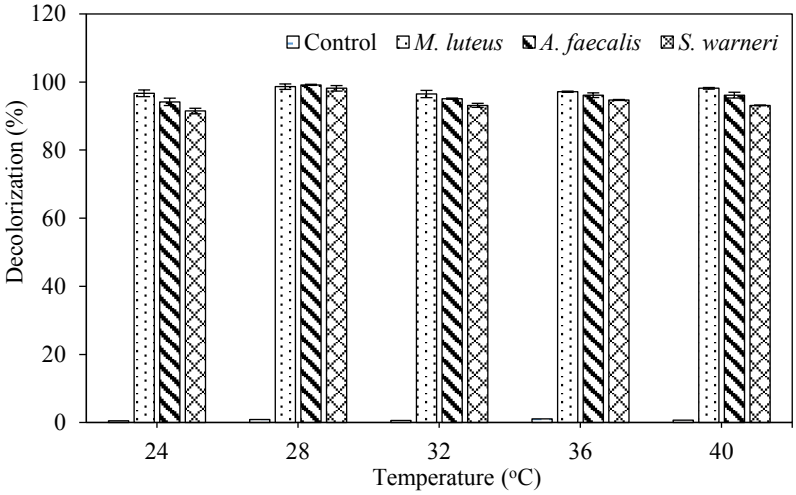

Figure 1. Effect of temperature on decolorization of DB dye by the bacteria: *A. faecalis, M. luteus,* and *S. warneri.* When error bars are not shown, the standard deviation was less than the width of the symbol. (Dotted: *M. luteus*, Diagonal: *A. faecalis,* Diamond: *S. warneri,* Dashed line: Control).

In terms of the effect of dye concentration, complete decolorization of DB textile dye was recorded up to 50 mg/L by all three bacterial strains and descending decolorization trend was found with the increase of the dye concentrations (Table 3). More or less similar result were recorded by other studies suggesting that declining potential of decolorization may be due to the toxic effect of the dye coupled with inadequate production of bacterial biomass (Jadhav et al., 2008; Saratale et al., 2009).

Most textile dyes are deficient in easily available carbon or nitrogen sources in their structures (Padmavathy et al., 2003; Senan and Abraham, 2004). Therefore, decolorization performances by *A. faecalis, M. luteus* and *S. warneri* were evaluated with the supplement of additional carbon or nitrogen sources into the synthetic MSM. In the present study, complete decolorization of DB was obtained using the bacteria: *A. faecalis* and *M. luteus* with the presence of tryptone and peptone in the medium within 48 h of incubation (Table 4). However, supplement of starch, glucose and urea did not play noteworthy role in decolorization of DB dye by the bacteria: *A. faecalis, M. luteus* or *S. warneri*. Saratale et al. (2010) recorded that decolorization of Green HE4BD dye with mixed bacterial consortium consists of *Proteus vulgaris* and *M. glutamicus* were efficient when the synthetic medium was supplemented with tryptone or urea and decolorization was not evident without supplement of any carbon or nitrogen source. Thus, it has been suggested that the efficiency of decolorization depends on carbon or nitrogen sources employed. This may be due to the stimulatory or inhibitory effects on the enzyme of the bacteria that are involved in the degradation of the structure of the textile dyes (Jadhav et al., 2010).

The static condition was more favorable for effective decolorization of DB textile dye as the three strains of bacteria employed in the present study yield complete decolorization of the dye within 72 h while shaking conditions taking more than 14 days for the same conditions (Figure 2). More or similar comparable decolorization patterns were recorded by other studies for decolorization of different textile dyes using bacteria (Moosvi et al., 2007; Shah et al., 2012). Moosvi et al. (2007) recorded that the most of textile dye decolorizing bacterial enzymes such as azo reductase are normally inhibited with the presence of oxygen due to the completion in oxidation of reduced electron carriers with either oxygen or azo groups, supporting the significant relationship between dissolve oxygen and decolorization of DB by *A. faecalis*, *M. luteus*, and *S. warneri* in the present study.

The effect of consecutive addition of DB dye showed that decolorization of DB textile dye was successive up to three consecutive cycles for *A. faecalis*, *M. luteus*, and *S. warneri* and then a descending pattern of decolorization of the dye was observed (Table 5). The declining pattern of decolorization might be due to the reduction of bacterial cells with exhaustion of nutrients. However, results of the present study emphasize the effectiveness of isolated bacterial strains: *A. faecalis, M. luteus,* and *S. warneri* for its practical approaches of bioremediation of textile dyes.

Table 3. Effect of different pH and initial dye concentrations on decolorization of DB textile dye by the bacteria; *A. faecalis, M. luteus,* and *S. warneri.*

Bacterial strain	Decolorization (%) (at 72 h of incubation)							
	pH				DB dye concentration (mg/ L)			
	6	7	8	9	25	50	75	100
Control	0	0	0	0	1	0	0	0
A. faecalis	78	CD	98	93	CD	CD	75	66
M. luteus	60	CD	97	90	CD	CD	81	73
S. warneri	60	CD	96	90	CD	CD	71	58

*CD: Complete decolorization

Table 4. Decolorization of DB textile dye by *A. faecalis, M. luteus,* and *S. warneri* with the presence of different carbon and nitrogen sources.

Bacterial strain	Decolorization (%) (at 48 h of incubation)						
	Without C or N source	Starch	Glucose	Yeast	Tryptone	Peptone	Urea
Control	0	0	0	0	1	1	0
A. faecalis	56	27	57	85	CD	CD	58
M. luteus	64	22	73	91	CD	CD	43
S. warneri	38	21	33	83	95	94	54

*CD: Complete decolorization

Table 5. Repeated addition of textile dye along with different bacteria strains; *A. faecalis, M. luteus,* and *S. warneri*

Bacterial strain	Decolorization percentages at the end of each cycle			
	1st cycle	2nd cycle	3rd cycle	4th cycle
A. faecalis	CD (60 h)	CD (48 h)	98% (48 h)	86% (52 h)
M. luteus	CD (64 h)	CD (48 h)	96% (48 h)	72% (52 h)
S. warneri	CD (72 h)	CD (54 h)	92% (52 h)	68% (58 h)

*CD: Complete decolorization

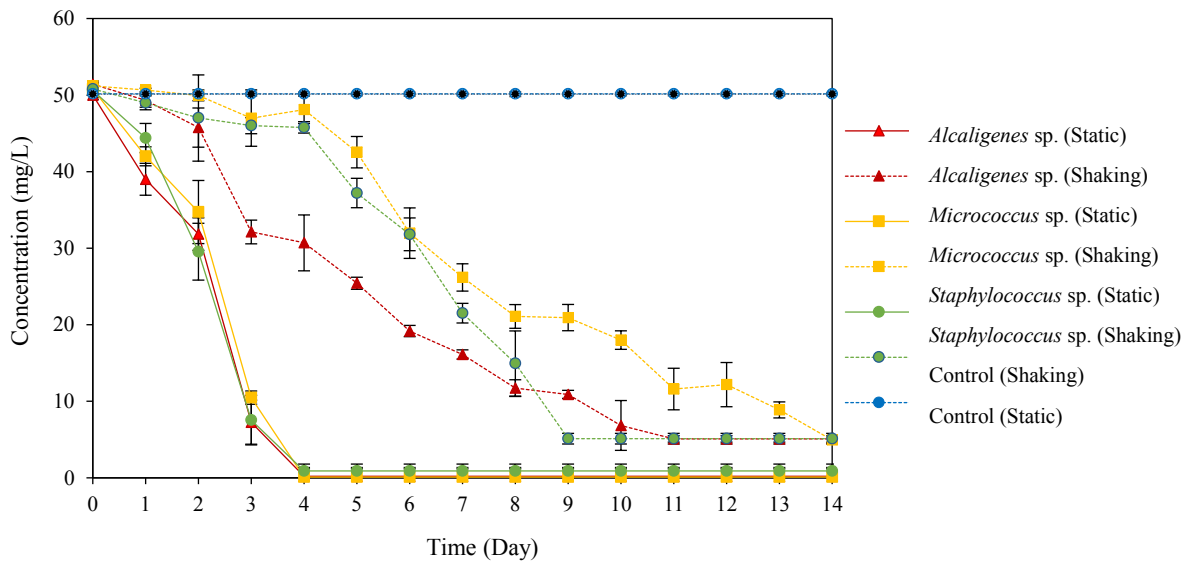

Figure 2. Decolorization of DB textile dye by *A. faecalis, M. luteus,* and *S. warneri* (Closed triangle: *A. faecalis,* Closed squre: *M. luteus,* Closed diamand: *S. warneri,* Closed circle: Control, Solid lines: decolorization at static conditions, Dotted lines: Decolorization at shaking conditions at 100 rpm).

3.3 Phytotoxicity study

Though the untreated textile dye effluent water cannot be used for further uses due to the toxic nature, the treated textile wastewater effluents can be used for agrarian purposes if treatment is possible to remove the toxic nature. In some instances, the secondary byproducts are more toxic in some synthetic chemicals than their original forms (Guruge et al., 2007). Therefore, a seed germination assay was employed to assess the toxicity of the by-products which were generated after the bacterial treatment. In the present study, *O. sativa* and *V. radiate* seeds which were treated with DB dye, showed 8% and 12% germination respectively (Table 6). The resulted low germination percentages of these seeds emphasis the toxic effect which lead to environmental problems when the dyes are released to the environment without any treatment. Interestingly, the seeds treated with the decolorized dye solutions by *A. faecalis, M. luteus,* and *S. warneri*, showed around 100% germination for both *O. sativa* and *V. radiate* indicating the detoxification of DB textile dye by the bacterial treatments.

Table 6. Phytotoxicity of DB textile dye and the bacteria treated water

Bacterial strain	Germination percentage (%)	
	Oryza sativa	*Vigna radiate*
Control (MSM only)	100	100
DB (50 mg/L)	08	12
Decolorized dye by *A. faecalis*	100	100
Decolorized dye by *M. luteus*	100	100
Decolorized dye by *S. warneri*	99	100

4. CONCLUSION

Three potential bacterial strains for decolorization of CI Direct Blue 201 textile dye were isolated from textile wastewater effluent sites in Sri Lanka and identified as *A. faecalis* (MK166784), *M. luteus* (MK166783), and *S. warneri* (MK256311) through their molecular characteristics. *A. faecalis, M. luteus,* and *S. warneri* showed complete decolorization of the DB dye within 60, 64, and 72 h of incubation under static conditions, respectively. The effective temperature range was 24 to 40 ºC where pH ranged from 7 to 9 with the presence of tryptone, peptone or yeast in the medium. Further, phytotoxicity assay confirmed detoxification of the DB textile dye by the bacterial treatment giving 100% seed germination after application of the bacterial treated textile dye effluent water. Therefore, the isolated bacterial strains in the present study can be used as the potential biological treatment agents for future applications in textile dye treatment processes.

ACKNOWLEDGEMENTS

The authors would like to acknowledge the Research Council of the University of Sri Jayewardenepura for funding the research project under the research grant no. ASP/01/RE/SCI/2016/10 and the Centre for Water Quality and Algae Research, University of Sri Jayewardenepura for providing bench space and all the equipment facilities.

REFERENCES

Anandhana M, Prabhahar RSS, Thanikachalamc J, Arunrajd T. Evaluation of phycoremediation potentials of microalgae with reference to textile dyeing industrial effluent. International Journal of Applied Engineering Research 2018;13(8):6440-5.

Asad S, Amoozegar MA, Pourbabaee A, Sarbolouki MN, Dastgheib SMM. Decolorization of textile azo dyes by newly isolated halophilic and halotolerant bacteria. Bioresource Technology 2007;98(11):2082-8.

Bechtold T, Mussak R. Colours in civilizations of the world and natural colorants history under tension. In: Bechtold T, Mussak R. editors. Handbook of Natural Colorants. 1st ed. Hoboken: John Wiley and Sons; 2009. p. 21-7.

Board of Investment of Sri Lanka (BOI). Environmental Norms: Textile Wastewater Effluent Guide Lines. Sri Lanka: Board of Investment of Sri Lanka; 2011.

Chemical Book. CI direct blue 201 basic information [Internet]. 2017 [cited 2019 March 6]. Available from: https://www.chemicalbook.com/ProductChemicalPropertiesCB01453522_EN.htm.

Chen H, Hopper SL, Cerniglia CE. Biochemical and molecular characterization of an azoreductase from *Staphylococcus aureus*, a tetrameric NADPH-dependent flavorprotein. Microbiology 2005;151(5): 1433-41.

Ekanayake EMMS, Manage PM. Decolorization of textile dye (Cl Direct Blue 201) by selected aquatic plants. Proceeding of the 2nd Environmental and Natural Resources International Conference; 2016 Nov 13-14; Bangkok: Thailand; 2016.

Ekanayake EMMS, Pathmalal MM. Decolorization of CI Direct Blue 201 textile dye by native bacteria. International Journal of Multidisciplinary Studies 2017;4(1):49-58.

Ekanayake EMMS, Udayanga D, Jayawardana DT, Manage PM. Effectiveness of *Aspergillus aculeatus* on decolorisation of mixture of two different textile dye classes. Proceedings of International Forestry and Environment Symposium; 2018 Nov 23-24; Citrus Hotel, Colombo: Sri Lanka; 2018.

Gupta VK, Carrott PJM, Ribeiro Carrott, MML. Low-cost adsorbents: Growing approach to wastewater treatment: a review. Critical Reviews in Environmental Science and Technology 2009;39(10):783-842.

Gupta VK, Jain R, Mittal A, Saleh TA, Nayak A, Agarwal S, Sikarwar S. Photo-catalytic degradation of toxic dye amaranth on TiO_2/UV in aqueous suspensions. Materials Science and Engineering 2012;32(1):12-7.

Guruge KS, Taniyasu S, Yamashita N, Manage PM. Occurrence of perfluorinated acids and fluorotelomers in waters from Sri Lanka. Marine Pollution Bulletin 2007;54(10):1667-72.

Hassan MM, Alam MZ, Anwar MN. Biodegradation of textile azo dyes by bacteria isolated from dyeing industry effluent. International Research Journal of Biological Science 2013;2(8):27-31.

Hunger K. Dye classes for principal applications. In: Hunger K. editor. Industrial Dyes: Chemistry, Properties, Applications. 1st ed. Frankfurt, Germany: Wiley-VCH; 2003. p. 158-78.

Idroos FS, Manage PM. Biodegradation of microcystins by *Bacillus cereus* and *Rahnella aquatilis* isolated from freshwater bodies. Asian Journal of Microbiology Biotechnology and Environmental Sciences 2018; 20(3):24-32.

Ileperuma OA. Environmental pollution in Sri Lanka: A review. Journal of the National Science Foundation of Sri Lanka 2000;28(4):301-25.

Jadhav JP, Kalyani DC, Telke AA, Phugare SS, Govindwar SP. Evaluation of the efficacy of a bacterial consortium for the removal of color, reduction of heavy metals, and toxicity from textile dye effluent. Bioresource Technology 2010;101(1): 165-73.

Jadhav UU, Dawkar VV, Ghodake GS, Govindwar SP. Biodegradation of direct red 5B, a textile dye by newly isolated *Comamonas* sp. UVS. Journal of Hazardous Matererials 2008;158:507-16.

Kalyani DC, Patil PS, Jadhav JP, Govindwar SP. Biodegradation of reactive textile dye Red BLI by an isolated bacterium *Pseudomonas* sp. SUK1. Bioresource Technology 2008; 99(11):4635-41.

Konsowa AH. Decolorization of wastewater containing direct dye by ozonation in a batch bubble column reactor. Desalination 2003;158(1-3):233-40.

Liyanage GY, Manage PM. Evaluation of Amoxicillin and Sulfonamide removal by *Bacillus cereus*, *Enterobacter ludwigii* and *Enterobacter* sp. Journal of Environment and Natural Resources 2016;14(1):39-43.

Mahagamage MGYL, Chinthaka SDM, Manage PM. Multivariate analysis of physico-chemical and microbial parameters of surface water in Kelani river basin. International Journal of Multidisciplinary Studies 2015;1(1):55-61

Mahagamage MGYL, Manage PM. Water quality index (CCME-WQI) based assessment study of water quality in Kelani river basin, Sri Lanka. Proceeding of the 1st Environment and Natural Resources International Conference; 2014 Nov 6-7; the Sukosol hotel, Bangkok: Thailand; 2014.

Manage PM, Edwards C, Singh BK, Lawton LA. Isolation and identification of novel microcystin-degrading bacteria. Applied and Environmental Microbiology 2009;75(21):6924-8.

Manage PM, Kawabata ZI, Nakano SI. Algicidal effect of the bacterium *Alcaligenes denitrificans* on *Microcystis* spp. Aquatic Microbial Ecology 2000;22(2):111-7.

Moosvi S, Kher X, Madamwar D. Isolation, characterization and decolorization of textile dyes by a mixed bacterial consortium JW-2. Dyes and Pigments 2007;74(3):723-9.

Naresh B, Preethi C, Sneha S, Bhagyashree R, Parizad P. Microbial decolorization of disperse textile dye brown 21 by *Enterobacter gergoviae* isolated from textile effluent. International Research Journal of Environmental Science 2013;2:31-36.

National Center for Biotechnology Information (NCBI). U.S. National Library of Medicine, 8600 Rockville pike Bethesda MD, 20894 USA [Internet]. 2018 [cited 2018 Nov 21]. Available from: https://www.ncbi.nlm.nih.gov.

Padmavathy V, Vasudevan P, Dhingra SC. Biosorption of nickel (II) ions on baker's yeast. Process Biochemistry 2003; 38(10):1389-95.

Pearce CI, Lloyd JR, Guthrie JT. The removal of colour from textile wastewater using whole bacterial cells: A review. Dyes and Pigments 2003;58(3):179-96.

Robinson T, McMullan G, Marchant R, Nigam P. Remediation of dyes in textile effluent: A critical review on current treatment technologies with a proposed alternative. Bioresource Biotechnology 2001;77(3):247-55.

Rovira J, Domingo JL. Human health risks due to exposure to inorganic and organic chemicals from textiles: A review. Environmental Research 2018;168:62-9.

Saratale RG, Saratale GD, Chang JS, Govindwar SP. Decolorization and biodegradation of textile dye navy blue HER by *Trichosporon beigelii* NCIM-3326. Journal of Hazardous Materials 2009;166(2):1421-8.

Saratale RG, Saratale GD, Chang JS, Govindwar SP. Decolorization and biodegradation of reactive dyes and dye wastewater by a developed bacterial consortium. Biodegradation 2010;21(6):999-1015.

Senan RC, Abraham TE. Bioremediation of textile azo dyes by aerobic bacterial consortium aerobic degradation of selected azo dyes by bacterial consortium. Biodegradation 2004;15(4): 275-80.

Shah PD, Dave SR, Rao MS. Enzymatic degradation of textile dye Reactive Orange 13 by newly isolated bacterial strain *Alcaligenes faecalis* PMS-1. International Journal of Biodeterioration and Biodegradation 2012;69:41-50.

Shore BW. The Theory of Coherent Atomic Excitation, 2 Volume Set. 1st ed. Wiley-VCH: 1996.

Somasiri W, Ruan W, Li X, Jian C. Biological decolourization of simulated textile wastewater in UASB reactor system by anaerobic granular sludge. Tropical Agricultural Research and Extension 2005;8:53-64.

Wijetunga S, Xiufen L, Wenquan R, Chen J. Removal mechanisms of acid dyes of different chemical groups under anaerobic mixed culture. Ruhuna Journal of Science 2007;2(1):96-110.

Formulation of Natural Fortifiers from Readily Available Materials for Nutrient Enrichment of Organic Fertilizers

Taiwo B. Hammed*, Godson R.E.E. Ana, and Elizabeth O. Oloruntoba

Department of Environmental Health Sciences, Faculty of Public Health, College of Medicine, University of Ibadan, Ibadan, Nigeria

ARTICLE INFO

Received: 2 Jan 2019
Received in revised: 22 May 2019
Accepted: 6 Jun 2019
Published online: 13 Aug 2019
DOI: 10.32526/ennrj.18.1.2020.02

Keywords:
Agronomic parameters/ Biodegradable matter/ Fortified fertilizers/ Market waste/ Natural materials

*** Corresponding author:**
E-mail:
hammetab2003@yahoo.co.uk

ABSTRACT

Studies have shown that organic fertilizer, a product of biodegradable organic matter, is not popular among Nigerian farmers because of its low quality. To alleviate this problem, this study was designed to explore the effect of nutrient-rich materials on quality of fertilizer made from market organic wastes. It adopted an experimental study design, comprising organic fertilizer preparation, fortification with natural fortifiers, farm plot experiments and laboratory analyses. The experiment was laid out in a randomized complete block design with factorial arrangement and three replications. The main plots comprised three crops - maize (cereal), soybean (legume) and yam (tuber) while five different fortified organic fertilizers at three rates of applications -2.0, 2.5, and 3.0 ton/ha and control (organic fertilizers without fortification) - formed subplots. Nutrient-rich materials sourced from animal, plant and rock changed the chemical composition of organic fertilizer made from market wastes and yielded better agronomic performances than the synthetic fertilizer. Hence, fortification of organic fertilizer with natural materials which are readily available and environmentally friendly should be promoted among the farmers.

1. INTRODUCTION

In Nigeria and many other developing countries, synthetic fertilizers account for the largest source of nutrients such as nitrogen, phosphorus and potassium that are needed for plant growth (Lenis and Liverpool-Tasie, 2017). However, the use of compost or other organic-based fertilizers has been employed only to a limited extent. Despite this, synthetic fertilizer application, estimated at 13 kg/ha in 2009 by the Federal Ministry of Agriculture and Rural Development, is far lower than the 200 kg/ha recommended by the United Nations Food and Agriculture Organization (FAO) (Otu et al., 2014) for soil in Nigeria. The low fertilizer application is acknowledged to be among the many reasons for low agricultural productivity in Nigeria (Lenis and Liverpool-Tasie, 2017). According to Takeshima et al. (2015) during 2000/01-2002/03, the average fertilizer use in Sub-Saharan Africa (excluding South Africa), estimated at 9 kg/ha, was much lower than it is obtainable elsewhere in the world (for example, 86 kg/ha in Latin America, 104 kg/ha in South Asia, and 142 kg/ha in Southeast Asia). In the late 1970s, inorganic fertilizers such as urea, Single Super-phosphate (TSP) and different formulations of NPK (nitrogen, phosphorus and potassium) were heavily subsidized up to 95% (Takeshima et al., 2015). But after subsidy was removed in the 1990s, the price of fertilizer skyrocketed and corrupt practices prevented timely and efficient distribution of it to farmers (Obi-egbedi and Bankole, 2017).

Chemical fertilizers are made in factories by turning nitrogen gas into ammonia and by treating rock phosphate with acid while organic fertilizers are derived naturally from plants and animals and also include minerals that occur naturally (Vinneras, 2002). One major advantage of chemical fertilizers is that they quickly break down to provide specific nutritional needs to plants. However, they normally cause rapid release of nutrients and possible unbalanced growth (Rowlings et al., 2013; Fernando et al., 2015) and salty environment which wreak havoc on plants and soil through over-fertilization and water pollution (Vance et al., 2003; Carey et al., 2012). Organic fertilizers contain relatively low concentrations of actual nutrients and depend on soil

Citation: Hammed TB, Ana GREE, Oloruntoba EO. Green approach for decolorization and detoxification of textile dye- CI direct blue 201 using native bacterial strains. Environ. Nat. Resour. J. 2020;18(1):9-20. DOI: 10.32526/ennrj.18.1.2020.02

organisms to break them down to release these nutrients. Since nutrient released by microbial activities, in general, occurs gradually over time, one potential drawback is that the organic fertilizers may not release enough of their principal nutrients when the plant needs them for growth.

According to Marion (2000), organic fertilizers perform important functions which the chemical formulations do not. Organic fertilizers tend to bring the balance back to the soil and provide long-term fertility. They also impact significant physical and biological properties by increasing water-holding capacity of the soil; enhancing soil stability, structure and texture (Ludwig et al., 2011); improving soil microbial activities; controlling weed and common pest growth; minimizing the dependence on expensive inorganic fertilizers; preventing soil erosion; binding toxic chemicals in soils and making them unavailable to plants; and reducing soil and water pollution. Various studies have shown the importance of organic nutrient sources in improving maize yields (Heluf, 2002; Mucheru-Muna et al., 2007). The decline in yam yields associated with loss of soil fertility has led to the conclusion that yam requires high level of nutrient for growth (O'Sullivan and Ernest, 2008). Nitrogen (N) and potassium (K) are largely stored in the tubers (Diby, 2005; O'Sullivan and Ernest, 2008) while the calcium (Ca) is mainly accumulated in the leaves and returns to the soil with dead leaves (Diby, 2005). Soybean has been described in various ways. Some call it the "miracle bean" or the "golden bean" because it is a cheap, protein-rich grain. It contains 40% high quality protein, 20% edible vegetable oil, and a good balance of amino acids (Pawar et al., 2011).

Increasing the nutrient levels in the organic fertilizers and optimizing its quality is a great challenge. There have been, and there will continue to be, efforts towards developing and refining methods of improving and up-grading the quality of stable and mature compost, also known as organic fertilizer, with cheap, locally and readily available organic materials up to the level that could be compared to the synthetic fertilizer counterparts. Sridhar et al. (2001) and Adeoye et al. (2008) noted that supplementing with natural sources of fortifiers is more environmentally friendly than opting for chemical sources. Up till now, no one universally accepted and applied method for upgrading organic fertilizer quality into chemical fertilizer status exists. Hence, any research in this direction may likely provide solution to the problems inherent in the organic fertilizers and promote their usage among the farmers. Therefore, the objectives were to characterize various natural and synthetic fortifiers for their nutrients and selected heavy metals; produce organic fertilizer, fortified the fertilizer for crop specific use; and determine the effects of fortified organic fertilizers on agronomic parameters of test crops.

2. METHODOLOGY

2.1 Description of the study area

The experiment was conducted in Ibadan, Nigeria. Ibadan (Yoruba: Ìbàdàn or fully Ìlú Ẹ̀bá-Ọ̀dàn, the town at the point of the savannah and the forest) is the capital city of Oyo State and the third largest metropolitan area in Nigeria in terms of population after Lagos and Kano, as the 2006 Nigerian Census revealed. It is located in south-western Nigeria, 128 km inland Northeast of Lagos and 530 km Southwest of Abuja, the Federal Capital Territory. It is also a prominent transit point between the coastal region and the areas to the North. In addition, about 36.25 km^2 (34.9% of the land area) is allotted for land use (such as residential area, public buildings and facilities, markets, industrial and commercial areas as well as educational institutions, amenities and open spaces. The remaining 63.75 km^2 is allotted for non-urban uses such as fallow land, forest reserves, farmland and water environment (Areola, 1992). The field was located behind Alesinloye Waste Recycling facility, Alesinloye Market, Ibadan. At the facility, all organic wastes generated in the market were converted to organic fertilizer while plastic and nylon wastes were recycled into useful materials such as plastic pellets and chips for plastic manufacturing industries. The recycling complex is situated next to the market abattoir where an average of 30 cows is slaughtered daily. Animal waste from the abattoir including blood and bone was also used in the production of organic fertilizer in the facility.

2.2 Materials

The test materials used for fortifying organic fertilizer comprised both natural and synthetic materials. Natural materials were Plant-based (PB), Animal/Human-based (AB) and Rock- based (RB). Synthetic materials were urea and Single Super-phosphate (SSP). The urea contained 45% N per 50 kg bag and had 18% P_2O_5. Plant-based included

Cotton Seed Meal (CSM), Palm Kernel Shell (PKS), Neem Seed (NS) and Palm Kernel Residue (PKR) all which were sourced from Ibadan neighborhoods. Animal-based comprised of Chicken Feathers (CF), Hoof Meal (HM), Horn Meal (HM), Human Hair, and Bone Meal (BM). Human hair was collected from the market at barber's shops; chicken feather was collected from fowl sellers' shops behind the recycling premises; and, the rest were sourced from Alesinloye Market abattoir beside the complex. Rock-based comprised Rock Phosphate (RP) was sourced from Agronomy Department, University of Ibadan. In addition, test crops were maize (*Zea mays* L), Soybean (*Glycine max*; TX 114) and Yam (*Dioscorea rotundata* Poir), representing cereals, legume and tuber respectively. The maize had commercial name of 'Oba Super 2', yield capacity of 5 to 7 ton/ha and germination rate of 90%. Both maize and soybean were sourced from the Generic Laboratory of International Institute for Tropical Agriculture (IITA), Ibadan; while the yam was sourced from a local market in Ibadan. Also, soil samples were taken from the farm plots before crop planting at depth of 0-10 cm for baseline data.

2.3 Study design

The study design was experimental and comprised compost preparation and fortification, farm plot experiments and laboratory analyses. Plot experiments design was simple Randomized Complete Block Design (RCBD) with three replications. Main plots were for three crops selected for the study - maize (cereal), soybean (Legume) and yam (tuber) - while five different Fortified Organic Fertilizers (FOFs) at three levels of applications -2.0, 2.5, and 3.0 ton/ha, and control plot, applied with ordinary compost without fortification, formed subplots. This translated to 0.20, 0.25 and 0.50 kg/plant, respectively (i.e., one 50 g bag was used for 250, 200, and 100 plant stands, respectively). In the maize and soybean subplots, each of the treatments and control plot was designed in 3×3 factorial with three replications. For yam, 2×3 factorial was used. All the plots were labelled according to the type of fertilizer formulation applied to them viz: Control which is ordinary organic fertilizer (compost) without fortifiers (C), PB, AB, RB, Organic-based fertilizer (OM, mixture of PB, AB, and RB), and mixture of urea and SSP (SC, synthetic chemical).

2.4 Methods of data collection

The data were collected using different methods; laboratory measurements were used to appraise the quality of raw organic wastes, organic fertilizers, natural fortifiers (nutrient-rich materials), chemical fortifiers, soil samples and quality of FOFs produced, using standard analytical methods as described by Motsara and Roy (2008). The following chemical parameters were determined: total organic-carbon (OC), total nitrogen (TN), C:N ratio, total phosphorus (P), calcium (Ca), magnesium (Mg) and sodium (Na) as well as some selected heavy metals such as lead (Pb), chromium (Cr), nickel (Ni), zinc (Zn), manganese (Mn), Iron (Fe) and Cadmium (Cd). Samples taken from the materials were air-dried, milled and digested for the purpose of phosphorus and heavy metal determination, using spectrophotometry. About 0.2 g of each sample was digested with nitric, perchloric and sulphuric acid mixture in the ratio of 5:1:1 in a 100 mL conical flask (Motsara and Roy, 2008). Determination of total phosphorus in the samples was carried out spectrophotometrically, using the Mo (molybdo-vanadate) blue colour method of Murphy and Riley (1962). Total carbon content of the samples was determined according to Walkey Black wet oxidation method (Walkley and Black, 1934) and total nitrogen was determined, using regular Macro-Kjeldahl method (Kjeldahl, 1883). Potassium content of raw samples was determined according to Mehlich 3 procedure (Mehlich, 1984).

Prior to laboratory analyses, pH of samples was measured with the aid of a pH digital meter. Also, moisture content and dry matter content were determined using AOAC Official Method (2005) by measuring 2 g of the sample into a previously weighed crucible. The crucible plus sample was transferred into the oven set at 100 ºC to dry to a constant weight for 24 h. At the end of the 24 h, the crucible plus sample was removed from the oven and transferred to the desiccator, cooled for ten minutes and weighed. The values obtained were subjected to Equations 1-2:

$$\%\ \text{Dry Matter (DM)} = \frac{W_3 - W_0 \times 100}{W_1 - W_0} \quad (1)$$

$$\%\ \text{Moisture} = \frac{W_1 - W_3 \times 100}{W_1 - W_0} \quad (2)$$

Where: W_0=weight of empty crucible, W_1=weight of crucible plus sample, W_3=weight of crucible plus oven-dried sample, and %Moisture=100 - %DM.

Organic fertilizer was produced by mixing sorted organic waste with cow intestinal waste in ratio 3:1, following the method used in the facility (Hammed et al., 2011). Farm practices and performances of different FOFs on agronomic parameters (growth and yield data) of the three test crops on the field were also monitored. Agronomic data measured included number of leaves, by counting; plant height, leave area, and stem girth (in centimeters) by metric rule; and crop yield by weighing scale. Maize leaf area was calculated thus: L × B × 0.745 (Agboola and Unamma, 1991). Plant height was measured as the distance from the base of the plant to the height of the first tassel branch and ear height as the distance to the node bearing the upper ear (Badu-Apraku et al., 2010).

2.4.1 Procedures for fortification of organic fertilizer with natural fortifiers

Results obtained from baseline chemical analyses of all the materials were used to determine the amount of fortifiers needed to enrich the organic fertilizer. The fortification was carried out in view of two major macro-nutrients in fertilizer (N and P). Initial levels of these nutrients in the organic fertilizer were increased to P=2.5% and N=3.5%, in accordance with the national quality standard of organic fertilizer (Otu et al., 2014). The dilution formula (Equation 3) was used to fortify the compost and achieved all the formulations tested on the field.

$$C_1W_1 = C_2W_2 \quad (3)$$

Where, C_1 is an initial level of N or P in the organic fertilizer, C_2 is the final level of N of P in the formulation, W_1 is the quantity of the fortifier that is required to produce the quantity that is needed (W_2). For instance, nitrogen and phosphorus fortification using RB fortifier was carried out viz.

Nitrogen: where C_1=9.4% N, W_2=1.5 kg, C_2=2.5% N, W_1=?

$9.4 \times W_1 = 2.5 \times 1.5$

$W_1 = \frac{2.5 \times 1.5}{9.4} = 0.399$ kg (i.e., 399 g) of hair

Phosphorus: where C_1=17% P, W_2=1.5 kg, C_2=1.5% P, W_1=?

$17 \times W_1 = 1.5 \times 1.5$

$W_1 = \frac{1.5 \times 1.5}{17} = 0.132$ kg (i.e., 132 g) of phosphate rock

RB formulation = 399 g Hair + 132 g Phosphate Rock + 969 g Organic fertilizer

2.4.2 Procedures for plot experiment

Size of beds constructed for each type of crop - maize, soybean or yam - was 1 m × 1 m = 1 m^2. For the maize and soybean, 9 seeds were planted per bed. In the case of yam, only four yam tubers could be planted due to the size of a tuber. Distance of 45 cm was maintained between one crop stand and another. Quantity of fertilizer was estimated on assumption that 1 ha of land is equivalent to 10,000 m^2. As such, 2.0 ton/ha was translated to 0.2 kg of fertilizer per 1 m^2 (size of a bed). For maize and soybean with 9 seeds per bed, each plant was applied with 22 g (i.e., 0.2 kg ÷ 9 = 0.022 kg or 22 g). In the case of a yam bed with 4 seeds, each plant was applied with 50 g of fertilizer (i.e., 0.2 kg ÷ 4 = 0.05 kg or 50 g). Similar calculation was used for other two rates of applications, 2.5 ton/ha and 3.0 ton/ha, carried out in this study. A total of 72 yam tubers (each yam weighed 0.55 g) were planted on the yam ridges. Thrash removed from the ground during the clearing was used as mulch and FOFs were applied to the yam using ring method, a month after planting and at the first appearance of shoot. Fertilizer application to maize and soybean was also carried out, using ring method - 3 cm deep and 5 cm away from stem two weeks after germination. Effects of FOFs on agronomic parameters (number of leaves (NL), plant height (PH), stem girth (SG), leaf area (LA) and crop yield) were assessed in these experiments.

3. RESULTS

3.1 Chemical composition of samples

The baseline characteristics of soil, nutrient and heavy metal compositions of fortifiers and organic fertilizer before fortification are indicated in Table 1, Figures 1 and 2. The soil had more sand content (79.2±0.0%) than both silt (13.4±0.0%) and clay (7.4±0.0%). Levels of macro nutrients were: N (0.2±0.0%); P (2.6±0.0%) and C (0.9±0.0%) (Table 1). Urea, organic mixture and bone were very rich in phosphorus and, in addition to this, urea had the highest quantity of nitrogen followed by cotton, animal blood and neem (Figure 2). Among all the materials, blood, followed by the bone, was found with the least quantity of heavy metals with the exception of iron. Organic fertilizer contained the highest level of Zn while neem and horn had the highest quantity of Cu (Figure 2).

Table 1. Characteristics of soil used for plot experiment

S/N	Parameter	Value (Mean±SD, n=4)
1	IM KCL	6.9±0.0
2	pH (H_2O)	7.6±0.0
3	E.C_{25} (mmho/cm)	18.0±0.0
4	Org. C (%)	0.9±0.0
5	Total N (%)	0.2±0.0
6	Av. P (mg/kg)	2.6±0.0
7	Sand (%)	79.2±0.0
8	Silt (%)	13.4±0.0
9	Clay (%)	7.4±0.0
Exchangeable bases (Cmol/kg)		
10	Ca	0.5±0.0
11	Mg	1.0±0.0
12	Na	2.0±0.0
13	K	0.7±0.0
14	Ex. Acidity	0.2±0.0
15	CEC	4.50±0.0
Extractable micronutrient (mg/kg)		
16	B. Sat	95.6±0.0
17	Mn	268.1±0.1
18	Fe	186.0±0.1
19	Cu	2.8±0.0
20	Zn	7.5±0.0

Organic carbon was found highest in C while nitrogen and carbon were higher in all the FOFs compared to P and K. Effects of fortification were more predominant in TN and OC than in other nutrients as shown in Figure 3. There were no significant differences in the nutrient values of all formulations. Chemical analysis of FOFs revealed organic-carbon (%): 33.2±0.0, 38.4±0.2, 27.7±0.1, 34.8±0.0, 28.4±0.2, 32.8±0.21; TN (%): 5.69±0.0, 5.74±0.0, 5.85±0.0, 6.05±0.0, 6.15±0.0, 3.21±0.0, phosphorus (%): 0.3±0.0, 0.5±0.0, 0.2±0.0, 0.8±0.0, 0.2±0.0, 0.7±0.1 and potassium (%): 0.5±0.0, 0.7±0.0, 0.4±0.0, 1.0±0.0, 0.4±0.0, 0.9±0.0 for PB, AB, RB, OM, SC and C respectively. The C had significantly higher phosphorus and potassium but lower value of TN than any of the formulations; it is also rich in carbon content among the formulations. Considering the levels of heavy metal in the FOFs, Iron (Fe) dominated the contents of all the formulations; it was significantly higher in AB compared to any other fertilizers and rock-based fertilizer contained the lowest quantity of Fe (Figure 4). Zinc was also found higher in compost and organic mixture than any other formulations. Generally, all the FOFs had low quantity of other heavy metals apart from Fe and Zn. There was no significant difference in the nutrient composition of the compost fortified with different nutrient-rich organic materials when compared to chemical fertilizer.

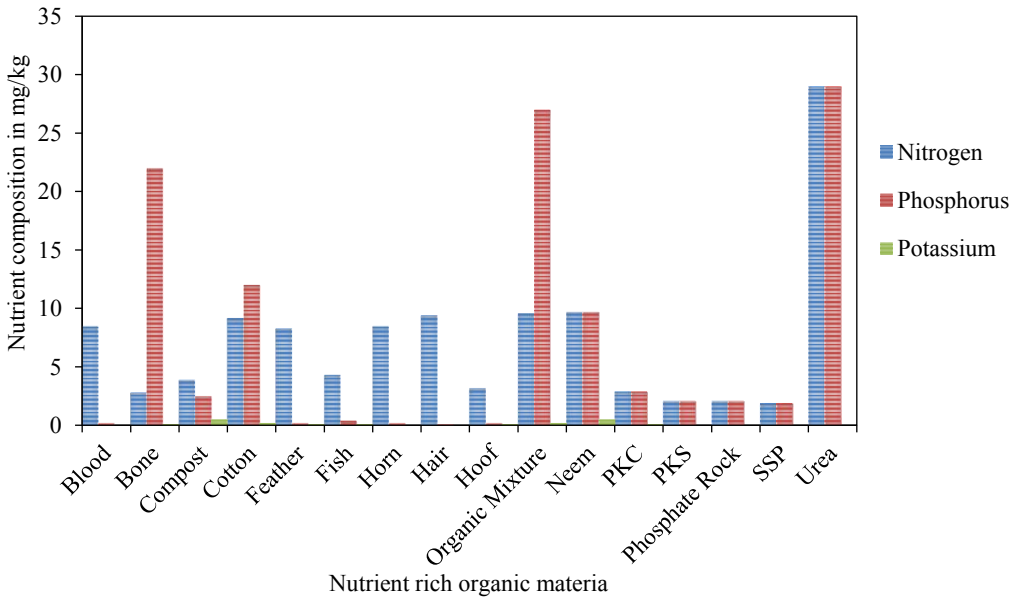

Figure 1. Nutrient composition of organic-rich materials

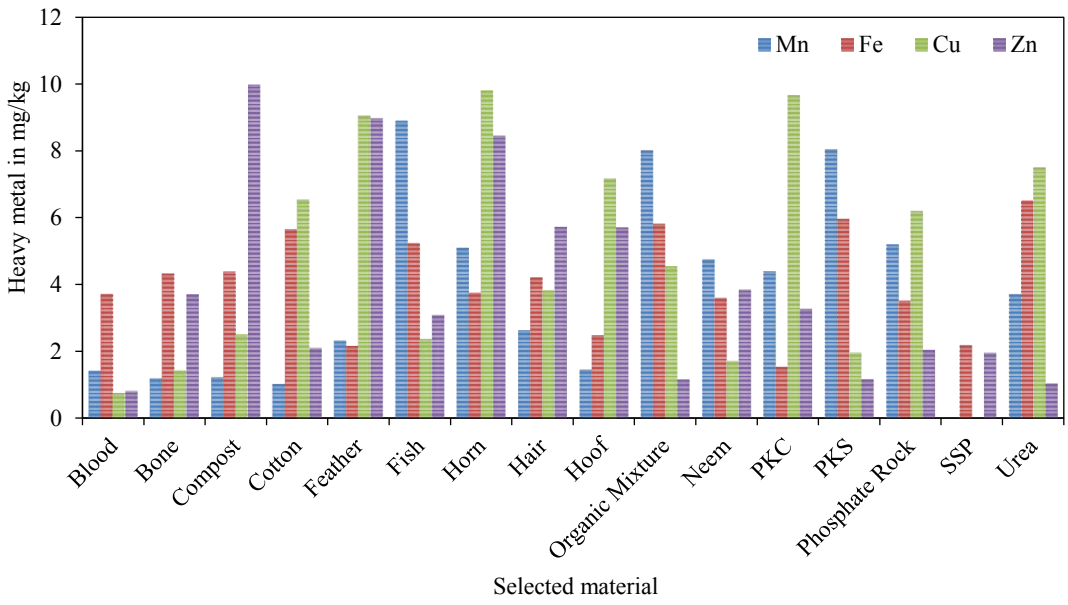

Figure 2. Heavy metal composition of organic-rich materials

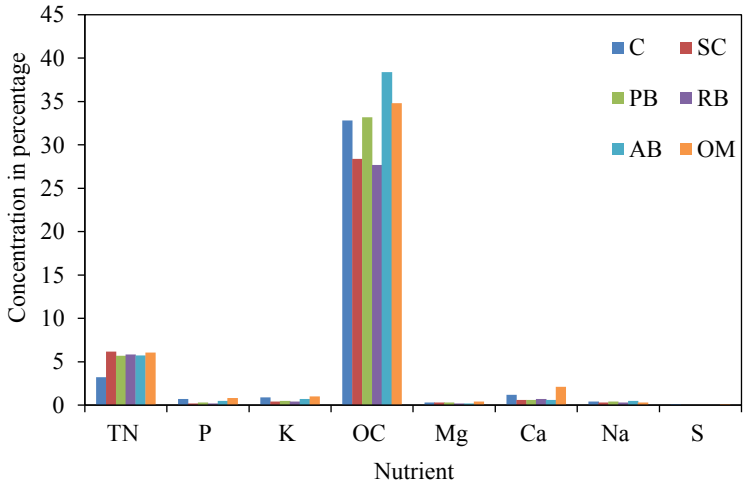

Figure 3. Nutrients composition of fertilizer (formulation) (Legend: C-Control; PB-Plant-based fertilizer; AB-Animal/Human-based fertilizer; RB-Rock-based fertilizer; OM-Organic-based fertilizer (Mixture of PB, AB, and RB); and, SC-Synthetic chemical fertilizer).

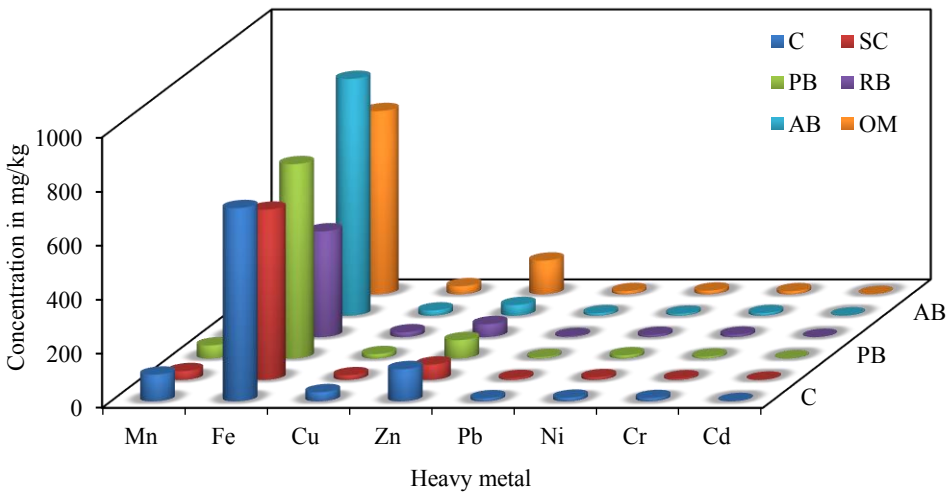

Figure 4. Heavy metal composition of fertilizer (Legend: C-Control; PB-Plant-based fertilizer; AB-Animal/Human-based fertilizer; RB-Rock-based fertilizer; OM-Organic-based fertilizer (Mixture of PB, AB, and RB); and, SC-Synthetic chemical fertilizer).

3.2 Effect of fertilizer on the agronomic parameters of crops

The effect of fertilizer formulations on the agronomic parameters of maize, soybean and yam are indicated in Tables 2, 3 and 4. The test crops were formulation specific as different crops were selective in their positive responses to different FOFs. There were significant differences at two weeks of application for all the crops (p=0.05) and much more significant effects were noted at maturity. That is, all the fertilizers showed direct relationship pattern to the agronomic parameters from germination to the maturity. However, there was no indication that any of the fertilizers had effect on the stem girth of yam. The SC showed highest effect only in soybean plant height as at first week after the fertilizer application (13.9±5.4 cm). Specifically, OM and RB for maize [NL (10.0±1.1; 9.2±1.0), PH (23.9±5.4 cm; 22.7±3.6 cm), SG (2.2±0.4 cm; 2.2±0.4 cm), LA (2.7±0.1 cm^2; 3.4±0.7 cm^2)]; AB and RB for soybean [NL (20.3±10.1; 15.3±4.5), PH (12.0±3.5 cm; 10.8±5.8 cm), SG (0.4±0.1 cm; 0.4±0.1 cm), LA (21.0±15.7 cm^2; 18.7±7.2 cm^2)] and RB for yam [PH (44.0±24.0 cm); SG (0.8±0.1 cm)] respectively gave the best crops' performances in agronomic parameters among all the formulations and the control. Apart from crops being selective to FOFs, agronomic parameters were similarly found to be formulation specific. This means that an agronomic parameter showed better performance while applied with a specific formulation. The following formulation and agronomic parameters specificities were found among the crops: Maize: (PH-OM; NL-OM; SG-RB; LA-RB), Soybean: (PH-SC; NL-AB; SG-AB; LA-RB), and Yam (SG-RB; LA-RB).

Table 2. Effect of fertilizer on the agronomic parameters of maize (Mean±SD, n=9)

Agronomic parameter	Treatment						F value	P value
	C	SC	PB	RB	AB	OM		
After 2 weeks of application								
Plant height	16.4±4.9^{a}	16.7±6.6^{a}	11.8±4.1^{a}	22.7±3.6^{b}	22.8±4.1^{b}	23.9±5.4^{b}	8.8	*0.0
Leaf area	2.0±1.0^{ab}	1.4±0.6^{a}	2.14±0.1^{abc}	3.4±0.7^{d}	2.9±0.1^{cd}	2.7±0.1^{bcd}	4.9	*0.0
Stem girth	1.2±0.5^{ab}	1.5±0.3^{a}	1.7±0.6^{b}	2.2±0.4^{c}	2.2±0.4^{c}	2.2±0.4^{c}	9.8	*0.0
No. of leaves	6.3±1.5^{a}	6.3±1.6^{a}	8.3±1.9^{b}	9.2±1.0^{bc}	8.8±1.2^{bc}	10.0±1.1^{c}	10.7	*0.0
At maturity (12 weeks)								
Plant height	218.2± 28.5^{a}	274.2± 30.6^{b}	284.9± 18.7^{bc}	313.6± 17.0^{bc}	301.8± 5.2^{bc}	326.9± 18.1^{c}	6.8	*0.0
Leaf area	4.4±0.2^{a}	5.7±0.2^{bc}	5.3±0.0^{b}	6.5±0.4^{c}	5.8±0.2^{bc}	6.2±0.1^{c}	6.9	*0.0
Stem girth	2.1±0.5^{a}	2.4±0.2^{ab}	2.4±0.4^{ab}	2.8±0.4^{b}	2.6±0.4^{b}	2.6±0.4^{b}	6.0	*0.0
No. of leaves	12.4±1.2^{a}	12.8±1.6^{ab}	14.2±2.4^{bc}	14.9±1.5^{cd}	14.2±1.2^{bc}	15.9±1.2^{d}	3.5	*0.0

Different letters (a, b, c and d) indicate significant differences along the rows
*Significant at p=0.05; KEY: Plant height (cm); Leaf area (cm^2); Stem girth (cm)

Table 3. Effect of fertilizer on the agronomic parameters of soybean (Mean±SD, n=9)

Agronomic parameter	Treatment						F value	P value
	C	SC	PB	RB	AB	OM		
After 2 weeks of application								
Plant height	9.6±3.0^{ab}	13.9±5.4^{b}	12.0±4.8^{ab}	10.8±5.8^{ab}	12.0±3.5^{ab}	8.9±4.7^{a}	1.4	*0.0
Leaf area	10.6±4.8^{a}	17.0±8.4^{a}	17.0±12.1^{a}	18.7±7.2^{a}	21.0±15.7^{a}	12.4±7.4^{a}	1.4	0.3
Stem girth	0.3±0.1^{a}	0.4±0.1^{a}	0.4±0.1^{a}	0.4±0.1^{a}	0.4±0.1^{a}	0.3±0.1^{a}	1.4	0.3
No. of leaves	11.2±5.6^{a}	17.3±8.6^{ab}	14.1±8.7^{ab}	15.3±4.5^{ab}	20.3±10.1^{b}	10.2±4.9^{a}	2.3	*0.0
At maturity (12 weeks)								
Plant height	51.8±6.6^{a}	53.7±7.0^{a}	51.7±5.6^{a}	55.6±6.0^{a}	53.4±11.7^{a}	53.5±6.7^{a}	0.3	0.9
Leaf area	40.0±8.8^{a}	44.1±10.8^{a}	47.3±9.5^{ab}	57.5±15.1^{b}	46.8±7.4^{ab}	46.7±11.7^{ab}	2.6	*0.0
Stem girth	0.7±0.1^{ab}	0.8±0.1^{b}	0.7±0.1^{ab}	0.7±0.1^{ab}	0.7±0.1^{ab}	0.6±0.1^{a}	2.5	*0.0
No. of leaves	70.1± 24.7^{a}	98.0± 27.6^{ab}	86.7± 35.5^{ab}	110.1± 33.2^{b}	98.8± 37.7^{ab}	71.8± 20.0^{a}	2.5	*0.0

Different letters (a, b, c and d) indicate significant differences along the rows
*Significant at p=0.05; KEY: Plant height (cm); Leaf area (cm^2); Stem girth (cm)

Table 4. Effect of fertilizer on the agronomic parameters of yam (Mean±SD, n=9)

Agronomic parameter	Treatment						F value	P value
	C	SC	PB	RB	AB	OM		
After 2 weeks of application								
Plant height	21.7±24.3^{ab}	13.0±10.1^{a}	13.9±11.2^{a}	44.0±24.0^{b}	19.0±15.5^{a}	15.3±23.6^{a}	2.2	*0.0
Stem girth	0.8±0.0^{cd}	0.7±0.1^{bcd}	0.4±0.3^{ab}	0.8±0.1^{d}	0.4±0.3^{abc}	0.2±0.4^{a}	5.1	*0.0
At maturity (12 weeks)								
Plant height	67.5±9.7^{a}	58.3±13.0^{a}	70.4±9.5^{a}	65.8±3.1^{a}	69.5±7.1^{a}	83.2±13.6^{b}	4.0	*0.0
Stem girth	0.8±0.2^{a}	1.0±0.2^{a}	0.9±0.1^{a}	1.0±0.1^{a}	1.0±0.1^{a}	1.0±0.1^{a}	0.9	0.5

Different letters (a, b, c and d) indicate significant differences along the rows
*Significant at p=0.05; KEY: Plant height (cm); Leaf area (cm^2); Stem girth (cm)

3.3 Effect of different rates of application on the test crops

The effects of different rates of AB application on agronomic parameters of maize and soybean are indicated in Figure 5. Also, the effects of different rates of RB application on maize, soybean and yam are shown in Figure 6. The AB formulation greatly increased the plant height of maize at 2.0 ton/ha while RB formulation enhanced the maize plant height mostly at 2.5 ton/ha. The RB formulation gave best performance on the soybean number of leaves and the leaf area when applied at 2.5 ton/ha. Apart from type of FOFs, another major factor that affected the plant growth was rate of application of FOFs, indicating that plant growth performance also depended on rate of fertilizer application.

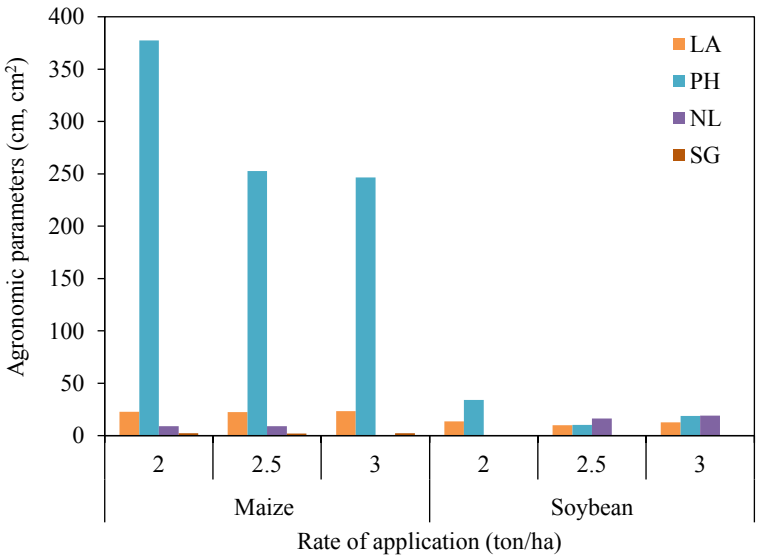

Figure 5. Effect of different rate of application of RB on agronomic parameters of the test crops (Legend: Plant Height, Leaf Area, Stem Girth, No. of Leaves).

4. DISCUSSION

4.1 Chemical composition of samples

The soil taken from the farm plot had low nitrogen content due to a high level of sand and low level of silt contents that are usually rich in humus and natural source nitrogen in the soil. This is an indication of no interference of nutrients (NPK) from their background levels in the soil that could have resulted from humus and loamy soil. The capacity to produce plant biomass remains an essential function of the soil productivity. Among all the fortifiers, blood and bone had the least quantity of heavy metals: Lead, Manganese, Nickel, Zinc, and Cadmium; and highest concentration of Iron. This could be due to the fact that animals (including humans) have threshold levels of these chemicals beyond which they may not survive (Veeken and Haneters, 2002). In addition, Fe is a major component of food taken by animals. Li et al. (2007) stated that application of organic matter increases concentration of Fe in the soil. In this study, all the fortifiers increased nutrients of the organic fertilizer after the fortification, with reference to macro nutrients: carbon, nitrogen, phosphorus, and potassium.

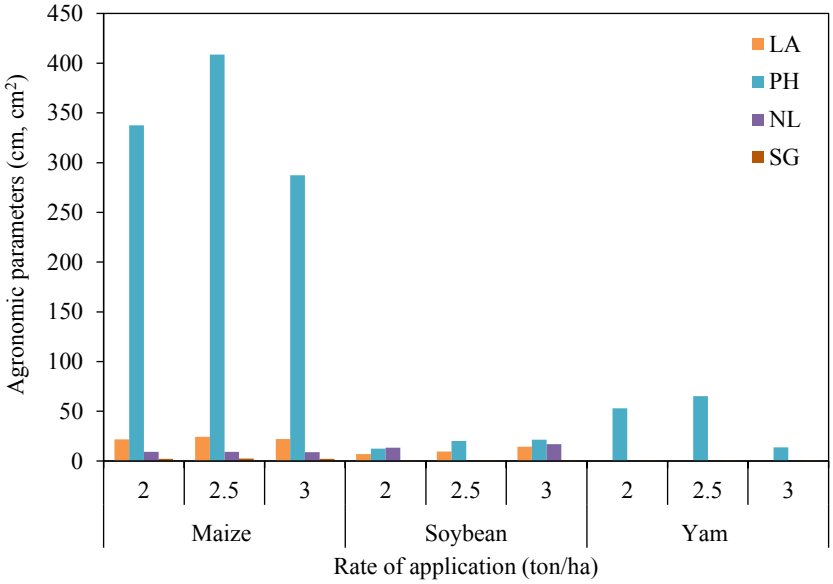

Figure 6. Effect of different rates of application of RB on agronomic parameters of the test crops (Legend: Plant Height (PH), Leaf Area (LA), Stem Girth (SG), No. of Leaves (NL)).

The primary nutrients required by microorganisms for growth are C, N, P, and K (Tchobanoglouse et al., 1993). The C and N play the most important role in the composting process: C is used by microorganisms for energy and growth while N is needed for protein and production (Metcalf and Edd, 2003). Neem and horn, among the fortifiers, had the highest quantity of Cu while the presence of high Cu content in the compost confirmed its high molecular weight humic acid, generally found in soil with well-decomposed organic matter (Prechthai et al., 2008) and which reduces the bioavailability of the heavy metals and their toxicity in plant (Inaba and Takenaka, 2005). The similarity in the nutrient composition of the organic fertilizer fortified with different nutrient- rich organic materials (FOFs) and chemical fertilizer is a clear indication of such effectiveness of fortification which raised the nutrient composition of the organic fertilizer to the status of synthetic chemical fertilizer. This observation corroborates with Mayer et al. (2008), Bouis et al. (2011), and Thavarajah and Thavarajah (2012). Also Fang et al. (2008) reported that the goal of compost fortification is not only to increase yield of crops and their qualities, but also to meet the demand for minerals required by humans. In composting process, Zn and Pb are significant contaminants and could have been responsible for the highest level of Zn noticed in the organic fertilizer. Likewise, Mariachiara et al. (2005) reported that at the end of composting process the concentration is 2.6 times the initial value for Zn and 1.6 times the initial value for Pb. Application of compost increased Mn, Cu and Zn contents of the soil but lowered Fe content (Courtney and Mullen, 2008). Several high revenue food crops such as beans, citrus, corn and rice are highly susceptible to Zn deficiency and bio-fortification is considered as a promising method to accumulate high content of Zn especially in grains (Christos et al., 2018), making the types of fertilizers used in this study more advantageous to plant growth.

4.2 Effect of fortified organic fertilizers on the agronomic parameters of crops

The FOFs generally improved agronomic parameters of the test crops, though selectively. In an experiment conducted by Ayoola and Makinde (2008) to assess the growth and yield of maize applied with nitrogen-enriched with cow dung, the plants were comparable in height and leaf area with those grown with inorganic fertilizer. Application of organic fertilizer improved growth and yield of bean plants compared with those amended with mineral fertilizer (Fernandez-Luqueno et al., 2010). The results of FOFs' performances obtained in this study are in agreement with findings of Francesco and Lionello (1992) who tested effects of compost fortified with organic and inorganic materials on agronomic parameters of maize. They concluded that growth responses to inorganic fertilizers do not provide better performance. The reasons for the FOFs being selective on the type of crop and agronomic parameters could be associated with different chemical forms of nutrients in the fortifiers and

genetic factors of test crops. In selecting any type of the FOFs, one should consider which part of a plant is better prioritized: leaf area, plant height and so on. In contrary, Sajal et al. (2018) observed that the agronomic parameters of grain and straw did not differ significantly among the organic amendments. Maize stem girth generally reduced at maturity and the maize number of leaf was constant at the appearance of husk because growth of the plant had stopped. All FOFs performed better than synthetic fertilizer in number of leaves. This finding is not in agreement with that of Olubunmi et al. (2011) who reveals that increase in relation to number of leaves of *Corchorus olitorus* are in order of NPK>poultry manure>cow dung>urea.

4.3 Effect of different rates of fortified organic fertilizers application on the crops

Type of FOFs and rate of application were major factors that affected the plant growth. Kolade et al. (2005) indicated that the composts could be applied to maize at 4 ton/ha to obtain yields comparable to those of organo-mineral fertilizer and chemical fertilizer which are popular among Nigerian farmers. Bolanle et al. (2010) found application of NPK fertilizer gave a lower yield of maize (5.40 ton/ha) to that of organo-mineral fertilizer (6.06 ton/ha) when applied at a rate of 6 ton/ha. The lower rate (2.0 and 2.5 ton/ha) of application with enhanced agronomic performances observed in this study indicated that the FOFs were better than fortified composts used by the previous researchers (Kolade et al., 2005; Bolanle et al., 2010; Rady et al., 2016). The rates were also far below poultry manure (10 ton/ha) and cow dung (ton/ha) utilized by Olubunmi et al. (2011) when compared the effect of poultry manure, cow dung, NPK 20:10:10 and urea fertilizers on growth, nutrients content and yield of *Corchorus olitorus* and *Celosia argentina.* Also, Yang et al. (2011) found that the best growth performance was recorded by application of 40 ton/ha organic fertilizer which does not match up with effectives rate of FOFs utilized in this study.

Very similarly, Sutharsan et al. (2016) showed that different rates of nitrogen and phosphorous had significant increases in plant height, leaf area, plant dry biomass as well as root nodulation of soybean when applied with 50N:125P:75K kg/ha. Also, performances of FOFs are in consonance with findings of Roba (2018) who assessed the effect of mixing organic with inorganic fertilizer on soil fertility and productivity. The study revealed that appropriate application of organic with inorganic fertilizers increases the productivity without negative effect on yield quality and improves soil fertility than the values obtained by organic or inorganic fertilizers separately.

5. CONCLUSION

The composted market organic waste, fortified with nutrient-rich naturally available materials, performed better than the organo-mineral fertilizer on agronomic parameters of the three crops (maize, soybean and yam). The implication of this is that ordinary organic fertilizer can be fortified with nutrient-rich natural materials and applied at low rate of 2 ton/ha. This process facilitates desired growth performances of the three crops comparable to those of organo-mineral fertilizer and chemical fertilizer (NPK) which are popular among Nigerian farmers. Different fortified organic fertilizers influence the crops differently, and in selecting any of the fertilizers for a certain crop, the part of a plant (leaf area, plant height and others) to be considered is very important. Thus, OM and RB are recommended for maize; AB and RB for soybean; and RB for yam. The study recommends another study focusing on the effect of seasonal variation on effectiveness of organically fortified fertilizers, using the three test crops.

REFERENCES

Adeoye GO, Sridhar MKC, AdeOluwa OO, Oyekunle M, Makinde EA, Olowoake AA. Comparative evaluation of organo-mineral fertilizer (OMF) and mineral fertilizer (NPK) on yield and quality of maize (*Zea mays* L Moench). Nigeria Journal of Soil Science 2008;18:141-7.

Agboola AA, Unamma RPA. Maintenance of soil fertility under traditional farming system and organic fertilizer in the Nigerian Agriculture: present and future. Proceedings of a National Organic Fertilizer Conference; 1991 March 26-27; Durbar Hotel, Kaduna: Nigeria; 1991.

Association of Official Analytical Chemist (AOAC). Official Method of Analysis. 18th ed. AOAC International, Gaithersburg, MD, USA: Official Method; 2005. p. 64-87.

Areola O. The spatial growth of Ibadan city and its implication on rural hinterland in Ibadan region. Ibadan, Nigeria: RexCharles and Cann Publication; 1992. p. 98-106.

Ayoola OT, Makinde EA. Performance of green maize and soil nutrient changes with fortified cow dung. African Journal of Plant Science 2008;23:19-22.

Badu-Apraku B, Menkir A, Ajala SO, Akinwale RO, Oyekunle M, Obeng-Antwi K. Performance of tropical early-maturing maize cultivars in multiple stress environments. Canadian Journal of Plant Science 2010;90:1-22.

Bolanle W, Sridhar MKC, Ayorinde AA. Improving food security through environmental management in Ibadan: the

case of the Ayeye community. Urban Agriculture Magazine 2010;23:20-5.

Bouis HE, Hotz C, McClafferty B, Meenakshi JV, Pfeiffer WH. Biofortification: A new tool to reduce micronutrient malnutrition. Food Nutrition Bulletin 2011;32(1):31-40.

Carey RO, Hochmuth GJ, Martinez CJ, Boyer TH, Nair VD, Dukes MD. A review of turf grass fertilizer management practices: Implications for urban waste quality. Horticulture Technology 2012;22:280-91.

Christos N, Miltiadis T, Theodore K. Zinc in soils, water and food crops. Journal of Trace Elements in Medicine and Biology 2018;49:252-60.

Courtney R, Mullen G. Application of high copper and zinc compost and its effects on soil properties and growth of barley. Communication in Soil Science and Plant Anal 2008;39(1):82-95.

Diby NL. Etude de l'elaboration du rendement chez deux espèces d'igname (*Dioscorea* spp.) [dissertation]. Abidjan: Universite de Cocody; 2005. p. 180.

Fang MS, Zhao FJ, Fairweather-Tait SJ, Poulton PR, Dunham SJ, McGrath SP. Evidence of decreasing mineral density in wheat grain over the last 160 years. Journal of Trace Elements in Medicine and Biology 2008;22:315-24.

Fernandez-Luqueno FV, Reyes-Verela C, Martinez-Suarez G, Salomon-Hernandez, Yanez-Meneses CJ. Effects of different nitrogen sources on plant characteristics and yield of common bean (*Phaseolus vulgaris* L.). Bioresources Technology 2010;1:396-403.

Fernando L, Fabian F, Maria FV. Mineral fertilizers, bio-fertilizers and PGPRS: Advantages and disadvantages of its implementation. In: Sinha S, Pant KK, Bajpai S, editors. Advances in Fertilizer Technology. Vol. 2. USA: Studium Press LLC; 2015. p. 276-90.

Francesco D, Lionello B. Economic evaluation of compost use: Short-term results on a maize crop. Acta Horticulturae 1992;302:315-24.

Hammed TB, Soyingbe AA, Adewole DO. An abattoir waste water management through composting: a case study of Alesinloye waste recycling complex. International Journal of Interdisciplinary Social Sciences 2011;6(2):67-78.

Heluf G. Soil and Water Management Research Program Summary Report of 2000/2001 Research Activities, Alemaya Research Center, Alemaya University; 2002. p. 95.

Inaba S, Takenaka C. Effects of dissolved organic matter on toxicity and bioavailability of copper for lettuce sprouts. Environment International 2005;31:603-8.

Kjeldahl J. Neue méthode zur bestimmung des stickstFOFs in organischen körpern Z. Analytical Chemistry 1883;22:366-82.

Kolade OO, Coker AO, Sridhar MKC, Adeoye GO. Palm kernel waste management through composting and crop production. Journal of Environmental Health Research 2005;5(2):81-5.

Lenis Saweda O, Liverpool-Tasie. Is fertilizer use inconsistent with expected profit maximization in sub-Saharan Africa? Evidence from Nigeria. Journal of Agricultural Economics 2017;68(1):22-44.

Li BY, Zhou DM, Cang L, Zhang HL, Fan XH, Qin SW. Soil micronutrient availability to crops as affected by long-term inorganic and organic fertilizer applications. Soil and Tillage Research 2007;96(1-2):166-73.

Ludwig B, Geisseler D, Michel K, Joergenen RG, Schulz E, Mecbach I. Effects of fertilization and soil management on crop yields and carbon stabilization in soils: A review. Agronomy for Sustainable Development 2011;31:361-72.

Mariachiara Z, Fabrizio C, Daniele F, Franco F, Bruno P. Heavy metal contamination in compost: A possible solution. Annali di Chimica 2005;95(3):247-56.

Marion J. Composting 12,000 tons of food residuals a year. BioCycle 2000;41:30-5.

Mayer GE, Pfeiffer WH, Beyer P. Bio fortified crops to alleviate micronutrient malnutrition. Current Opinion in Plant Biology 2008;11(2):166-70.

Mehlich A. Mehlich-3 soil test extractant: A modification of Mehlich-2 extractant. Journal of Communications in Soil Science and Plant Analysis 1984;15:1409-16.

Metcalf and Eddy Inc. Wastewater Engineering: Treatment and Reuse. 4th ed. New York, USA: McGraw-Hill; 2003. p. 1546-54.

Motsara MR, Roy RN. Guide to Laboratory Establishment for Plant Nutrient Analysis. Rome, Italy: Fertilizer and Plant Nutrition Bulletin, FAO; 2008. p. 103-23.

Mucheru-Muna M, Mugendi D, Kungu J, Mugwe J, Bationo A. Effects of organic and mineral fertilizer inputs on maize yield and soil chemical properties in a maize cropping system in Meru South District, Kenya. Agroforest System 2007;69:189-97.

Murphy J, Riley JP. Method of phosphorus determination 36 in soil samples. Analytica Chimica Acta 1962;2:27-31.

Obi-egbedi O, Bankole OA. Determinants of participation in fertilizer subsidy programme among rice farmers in Ogun State, Nigeria. Journal of Development and Agricultural Economics 2017;9(6):162-7.

Olubunmi S, Makinde M, Imisu UE, Adeyinka M, Samuel AL. Comparative effect of mineral fertilizers and organic manures on growth, nutrient content and yield of *Chorcorus olitorus* and *Celosia argentina*. Research Journal of Botany 2011;6(4):150-6.

O'Sullivan JN, Ernest J. Yam Nutrition and Soil Fertility Management in the Pacific. Brisbane, Australia: Australian Centre for International Agricultural Research; 2008. p. 143.

Otu WI, Idiong CI, Nsikan EB, Ekaette SU. Food security and productivity of urban food crop farming households in southern Nigeria. Agricultural Science 2014;2(3):1-12.

Pawar RS, Wagh VM, Panaskar DB, Adaskar VA, Pawar PR. A Case study of soybean crop production, installed capacity and utilized capacity of oil plants in Nanded District, Maharashtra, India. Advances in Applied Science Research 2011;2:342-50.

Prechthai T, Padmasri M, Visvanathan C. Quality assessment of mined MSW from an open dumpsite for recycling potential. Resources Conservation and Recycling 2008;53:70-8.

Rady MM, Semida WM, Hemida KA, Abdelhamid TM. The effect of compost on growth and yield of *Phaseolus vulgaris* plants grown under saline soil. International Journal of Recycling of Organic Waste in Agriculture 2016;5:311-21.

Roba TB. Review on the effect of mixing organic and inorganic fertilizer on productivity and soil fertility. Open Access Library Journal 2018;5:e4618.

Rowlings DW, Grace PR, Scheer C, Kiese R. Influence of nitrogen fertilizer application and timing on greenhouse gas emissions from a lychee (*Litchi chinensis*) orchard in humid subtropical Australia. Agriculture, Ecosystem and Environment 2013; 179:168-78.

Sajal RMD, Abul Kashem K, Towhid O. The Uptake of Phosphorous and Potassium of Rice as Affected by Different Water and Organic Manure Management. Journal of Plant Sciences 2018;6(2):31-40.

Sridhar MKC, Adeoye GO, Adeoluwa OO. Alternate nitrogen amendments for organic fertilizers, in optimizing nitrogen management in food and energy production and environmental protection. Proceedings of the 2nd International Nitrogen Conference on Science and Policy; 2001 June 2-5; Lagos, Nigeria: The Scientific World; 2001. p. 16.

Sutharsan S, Yatawatte V, Srikrisnah S. Effect of different rates of nitrogen and phosphorous on growth and nodulation of glycine max in the eastern region of Sri Lanka. World Journal of Engineering and Technology 2016;4:14-7.

Takeshima H, Liverpool-Tasie, Lenis SO. Fertilizer subsidies, political influence and local food prices in sub-Saharan Africa: Evidence from Nigeria. Food Policy 2015;54(C):11-24.

Tchobanoglouse G, Theisen H, Vigil S. Integrated Solid Waste Management. New York: McGraw-Hill, Inc; 1993. p. 135-46.

Thavarajah D, Thavarajah P. Evaluation of chickpea micronutrient composition: bio-fortification opportunities to combat global micronutrient malnutrition. Food Resources International 2012; 49(1):99-104.

Vance CP, Uhde-Stone C, Allan DL. Phosphorous acquisition and use: critical adaptations by plants for securing a non-renewable resource. New Phythologist 2003;157:423-47.

Veeken A, Hamelers B. Sources of Cd, Cu, Pb and Zn in biowaste. Science of the Total Environment 2002;300(1-3):87-98.

Vinnerås B. Possibilities for Sustainable Nutrient Recycling by Faecal Separation Combined with Urine [dissertation]. Uppsala, Sweden: Swedish University of Agricultural Sciences; 2002.

Walkley A, Black IA. Method of total organic carbon determination in soil samples. Soil Science 1934; 37:29-38.

Yang XY, Li PR, Zhang SL, Sun BH, Chen XP. Longterm-fertilization effects on soil organic carbon, physical properties, and wheat yield of a loess soil. Journal of Plant Nutrition and Soil Science 2011;174:775-84.

Adsorption of Reactive Dyes from Wastewater Using Cationic Surfactant-modified Coffee Husk Biochar

Chatsuda Kosaiyakanon and Suratsawadee Kungsanant*

Department of Chemical Engineering, Faculty of Engineering, Prince of Songkla University, Hat-Yai, Songkhla 90110, Thailand

ARTICLE INFO

Received: 28 Feb 2019
Received in revised: 4 Jun 2019
Accepted: 14 Jun 2019
Published online: 30 Jul 2019
DOI: 10.32526/ennrj.18.1.2020.03

Keywords:
Reactive dye/ Coffee husk/ Biochar/ Cationic surfactant/ Dye adsorption

*** Corresponding author:**
E-mail: suratsawadee.k@psu.ac.th

ABSTRACT

A solid agricultural waste, coffee husk, was applied as an adsorbent for reactive dye-polluted wastewater treatment. Coffee husk biochar was pyrolyzed at 450 °C and then chemically activated using 50% $ZnCl_2$ solution. The surface of activated coffee husk biochar was modified using a cationic surfactant, Cetyltrimethylammonium bromide (CTAB), to create CTAB-modified coffee husk biochar (MCH), to improve reactive adsorption of anionic dyes from synthetic wastewater. The selected reactive dyes were reactive yellow 145 (RDY145), reactive red 195 (RDR195), and reactive blue 222 (RDB222). The adsorption kinetics fit well using a pseudo-second order model for all three dyes. The adsorption isotherms matched well with the Langmuir model . The removal efficiency of RDY145 (83.7%) was the highest, followed by RDR195 (71.1%) and RDB222 (59.6%). The amount of RDY145 adsorbed by MCH was about 9-fold that adsorbed by conventional activated carbon. Additionally, the solution pH had no effect on reactive dye removal efficiency using MCH.

1. INTRODUCTION

The growth of textile industry plays an important economic role in Thailand but its large water consumption creates a considerable amount of wastewater effluents. Dyes released to the environment are estimated at around 200,000 tons annually (Ogugbue and Sawidis, 2011). Normally, the dyes in textile industry are categorized as anionic (acid, direct, and reactive dyes), cationic (basic dyes), and nonionic dyes (dispersed dyes) (Ghazi Mokri et al., 2015). Generally, around 20 to 30% of the dyes used are of a reactive type, so representatives of these were selected for this study. Reactive dyes are also known as azo dyes because they contain one or more azo groups (-N=N-). In addition, reactive dyes containing aromatic amines can decompose and the amine groups formed are suspected to be carcinogenic (Mook et al., 2016; Moazzam et al., 2017). Thus, improper wastewater treatment can have negative environmental impacts affecting aquatic life and ecosystems.

Reactive dye contaminants should be removed from wastewaters. There are several methods to remove dyes from industrial effluents, including adsorption by activated carbon, electrochemical or membrane separations, and coagulation (Sun et al., 2013; Mook et al., 2016; Puasa et al., 2018). Among these, adsorption by activated carbon (AC) is a well-known technique for dye removal. The advantages of this technique include comparatively small need of land area, environmental friendliness, and ease of operation. However, the cost of AC remains the key to economic feasibility.

Nowadays, agricultural residues with high carbon content, such as palm shell, coconut coir, and rice husk have been studied as potential alternative adsorbents for AC (Sun et al., 2013; Ahmad et al., 2014; Mook et al., 2016; Mi et al., 2016). Typically, they can be applied to produce biochar by thermal degradation in oxygen-limited conditions, and consequently utilized as a low-cost adsorbent for pollutant separation from air, or heavy metals as well as textile dye removal from wastewater (Mi et al., 2016; Moazzam et al., 2017; Rehman and Razzaq, 2017). Biochar adsorption has been intensively studied because it has excellent adsorption capability and satisfies the need for cost effective adsorbents.

In southern Thailand, Robusta coffee has been planted on a large scale and it accounts for 98% of the coffee production in Thailand (Maleangpoothong

Citation: Kosaiyakanon C, Kungsanant S. Adsorption of reactive dyes from wastewater using cationic surfactant-modified coffee husk biochar. Environ. Nat. Resour. J. 2020;18(1):21-32. DOI: 10.32526/ennrj.18.1.2020.03

et al., 2013). Consequently, abundant amounts of coffee husk are generated and these could be converted to AC, as the husks are highly porous with high carbon content. Additionally, making biochar from coffee husk is not only promising for agricultural waste minimization, but it provides value-added adsorbents.

Furthermore, many studies have reported that adsorption with biochar is effective in the removal of reactive dyes from aqueous solution, such as reactive black 5 removal using palm shell biochar (Mook et al., 2016), reactive red 2 removal using coir pith biochar (Thitame and Shukla, 2016), and reactive blue 171 removal using *Enteromorpha prolifera* biochar (Sun et al., 2013). Besides, surface modification of the biochar with surfactants could enhance the adsorption capacity and ensure environmental friendliness (Puasa et al., 2018). Mi et al. (2016) reported that biochar prepared from cornstalk and modified by Cetyltrimethylammonium bromide (CTAB) had up to 53% improved adsorption of negatively charged anionic dye from water. In addition, all the studies have agreed that using biochar as a precursor for AC for reactive dye removal provided a great adsorption performance, cheap treatment costs, no unexpected by-products, and minimal waste. Thus, biochar was suggested to be promising for AC development.

Therefore, this work aimed to apply the CTAB-modified coffee husk biochar (MCH) for reactive dye removal from synthetic wastewater. The reactive dyes were reactive yellow 145 (RDY145), reactive red 195 (RDR195), and reactive blue 222 (RDB222). The dye removal and adsorption capacities of MCH and AC are compared and discussed in terms of kinetic models and adsorption isotherms. The effects of pH on reactive dye removal using MCH are also discussed.

2. METHODOLOGY

2.1 Materials

Husk of Robusta coffee was obtained from Thamsing Coffee Group Community Enterprise, located in Tham Sing sub-district, Mueang Chumphon district, Chumphon province, Thailand. The geographic location of coffee plantation is at latitude from 10°22'45.19"N to 10°26'28.82"N and longitude from 99°02'13.11"E to 99°07'19.75"E. The plantation covers an area of 2,891 ha, as shown in Figure 1 (GEO-Informatics Research Center for Natural Resource and Environment, Southern Regional Center of Geo-Informatics and Space Technology, 2019). The coffee husk was dried under sunlight for 4 days. It was then pyrolyzed at 450 °C for 1.5 h in a furnace tube under nitrogen atmosphere to remove the volatile matter (Ahmad et al., 2014). The obtained coffee husk biochar (CH) was then crushed and controlled for size in the range 0.6-1.41 mm. Food grade AC made from coconut shell was purchased from C. Gigantic Carbon Co., Ltd., Thailand. The cationic surfactant (CTAB) and zinc chloride ($ZnCl_2$) were purchased from Ajax Finechem Pty Ltd. (100% purity). All commercial reactive dyes (RDY145, RDR195, and RDB222) were received from KPT Corporation (Thailand) Co., Ltd. , Thailand. The properties of chemicals are summarized in Table 1. All the chemicals were used as received.

2.2 CH activation

A quantity of 50 g of CH was impregnated with 150 g of 50%wt. $ZnCl_2$ solution and left at room temperature for 24 h. Then, it was dried in an oven at 105 °C for 24 h, followed by heating at 500 °C for 2 h in a furnace tube under nitrogen blanket at a flow rate of 0.25 L/min (Mozammel et al., 2002; Kula et al., 2008). The obtained activated coffee husk biochar (ACH) sample was washed with distilled water until the pH of water was neutral. Then, it was dried again in the oven at 105 °C for 24 h.

2.3 ACH pretreatment using cationic surfactant

A quantity of 10 g of ACH was mixed with 1,000 mL of 7.5 mM CTAB solution. The samples were shaken for 7.5 h in the incubator shaker at 30 °C and 170 rpm shaking speed. After that, the obtained MCH samples were washed and dried at 60 °C for 15 h, and finally stored in desiccators for further use (Lin et al., 2013).

2.4 Adsorption study

A 1 g quantity of MCH was mixed with 100 mL of synthetic wastewater containing a reactive dye (RDY145, RDR195, or RDB222). The concentrations of reactive dyes were varied in the range 50-700 mg/L. The sample bottles were kept in an incubator shaker at 30 °C with 170 rpm shaking speed. Liquid samples were collected from each bottle every 10 min and were immediately analyzed for residual dye concentration using a UV-Visible Spectrophotometer (HP 8453) at 417, 541, and 614 nm for RDY145, RDR195, or RDB222, respectively.

The pH of the solutions was adjusted by adding HCl or NaOH solution (1 mol/L) (Oei et al., 2009; Ghazi Mokri et al., 2015). The cases were run randomly in triplicate and the standard deviation was less than 4%. The standard deviation is shown as y-error bars in graphs of Figures 3, 4, 5, and 7.

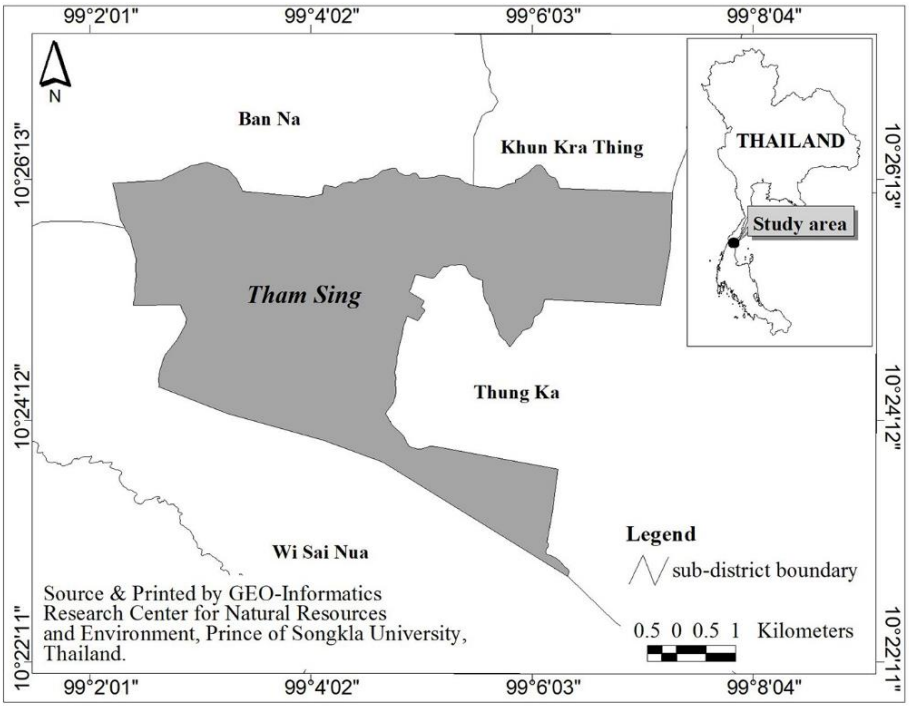

Figure 1. Map of coffee plantation, Tham Sing sub-district in Mueang Chumphon District, Chumphon Province, Thailand (GEO-Informatics Research Center for Natural Resource and Environment, Southern Regional Center of Geo-Informatics and Space Technology, 2019).

Table 1. The chemicals used in this study

Chemical	Scientific name	Molecular formula	Molecular weight (MW, g/mol)
CTAB[a]	Cetyltrimethylammonium bromide	$C_{19}H_{42}BrN$	364.5
RDY145[b]	Tetrasodium;7-[[2-(carbamoylamino)-4-[[4-chloro-6-[3-(2-sulfonatooxyethyl sulfonyl)anilino]-1,3,5-triazin-2-yl] amino]phenyl]diazenyl]naphthalene-1,3,6-trisulfonate	$C_{28}H_{20}ClN_9Na_4O_{16}S_5$	1026.2
RDR195[c]	Pentasodium;(3E)-5-[[4-chloro-6-[3-(2-sulfonatooxyethylsulfonyl)anilino]-1,3,5-triazin-2-yl]amino]-3-[(1,5-disulfonatonaphthalen-2-yl)hydrazinylidene]-4-oxonaphthalene-2,7-disulfonate	$C_{31}H_{19}ClN_7Na_5O_{19}S_6$	1136.3
RDB222[d]	Hexasodium;5-amino-3-[(1,5-disulfonatonaphthalen-2-yl)diazenyl]-4-oxido-6-[[3-sulfonato-5-[[4-[4-(2-sulfooxyethyl sulfonyl)anilino]-1,3,5-triazin-2-yl] amino]phenyl]diazenyl]naphthalene-2,7-disulfonate	$C_{37}H_{24}N_{10}Na_6O_{22}S_7$	1323.0

Remark: Letters a, b, c, and d express data cited from NCBI (2004), NCBI (2005), Guidechem (2017), and NCBI (2015), respectively.

2.5 Data analysis

For the kinetics study, the quantity of adsorbed dyes per unit weight of adsorbent was calculated as in Equation (1), and the dye removal efficiency (% Sorption) was determined with Equation (2) (Amin, 2008; de Franco et al., 2017):

$$q_t = \frac{C_0 - C_t}{m} V \quad (1)$$

$$\% \text{ Sorption} = \frac{C_0 - C_t}{C_0} \times 100 \quad (2)$$

Here, C_0 is the initial dye concentration (mg/L), C_t is the residual dye concentration in the solution after adsorption, V is the solution volume (L), and m is the mass of adsorbent (g) (Mi et al., 2016).

Then, the adsorption kinetics was assessed against both pseudo-first order and pseudo-second order models. The pseudo first order model is based on assumed physical multilayer absorption that is reversible.In contrast, the pseudo-second order model assumes chemical monolayer adsorption that is irreversible (Ibrahim et al., 2010; Ghazi Mokri et al., 2015; Mook et al., 2016). The pseudo-first order and pseudo-second order equations are presented as Equation (3) and Equation (4), respectively:

$$\ln\left(\frac{q_e}{q_e - q_t}\right) = k_1 t \quad (3)$$

$$q_t = \frac{q_e^2 k_2 t}{1 + q_e k_2 t} \quad (4)$$

Here, q_t is the amount of adsorbed dye on adsorbent (mg/g), q_e is amount of adsorbed dye on adsorbent at equilibrium (mg/g), k_1 is the rate constant of pseudo-first order model (min^{-1}), k_2 is the rate constant of pseudo-second order model (g/mg-min), and t is the time (min) (Ibrahim et al., 2010; Ghazi Mokri et al., 2015; Mook et al., 2016; de Franco et al., 2017).

Equilibrium dye adsorption isotherms were plotted as suggested by Langmuir and Freundlich models. The Langmuir model describes monolayer adsorption on a homogenous surface. The Freundlich model describes multilayer adsorption on a heterogeneous surface (Ibrahim et al., 2010; Ghazi Mokri et al., 2015; Mi et al., 2016). The Langmuir and Freundlich models are expressed in Equation (5) and Equation (6), respectively:

$$\frac{q_e}{q_{max}} = \frac{k_L C_e}{1 + k_L C_e} \quad (5)$$

$$q_e = k_f \, C_e^{1/n} \quad (6)$$

Here, q_e is the amount of adsorbed dye on the adsorbent at equilibrium (mg/g), q_{max} is the maximum adsorption of dye on the adsorbent (mg/g), C_e is residual dye concentration at equilibrium (mg/L), k_L is Langmuir constant related to the energy of adsorption (L/mg), k_F is Freundlich constant indicating adsorption capacity (mg/g $(L/mg)^{1/n}$), and n is Freundlich exponent accounting for adsorption intensity or the energetic heterogeneity of the adsorbing surface (de Franco et al., 2017; Markandeya et al., 2017). Additionally, the dimensionless separation factor (R_L) from the Langmuir model could indicate the affinity of adsorbent to adsorbate and is determined using Equation (7):

$$R_L = \frac{1}{1 + k_L C_0} \quad (7)$$

Here, a value of R_L equal to zero indicates that the adsorption is irreversible, while R_L in the range from zero to one indicates favorable adsorption. Besides, if R_L is equal to one, then adsorption is linear. A value of R_L greater than one represents unfavorable adsorption (Meng et al., 2018; Wang et al., 2018).

3. RESULTS AND DISCUSSION

3.1 Characterization of adsorbents

The surfaces of studied adsorbents, designated as CH, ACH, MCH, and AC, were imaged using SEM, as shown in Figure 2.

It can be seen that the pores of the ACH and MCH were similar and larger than those observed in CH and AC. The use of $ZnCl_2$ solution in activation could create more pores onto the CH surfaces resulting in increasing the porosity of CH. SEM images also indicate that the adsorption of CTAB on adsorbent MCH surfaces (Figure 2(c)) provides surface structure similar to ACH (Figure 2(b)). The pores of ACH and MCH are large and randomly distributed on the surfaces, whereas, the pores of AC are quite small and uniform. In addition, the porosities and surface areas of all adsorbents were assessed using the BET technique, with results listed in Table 2.

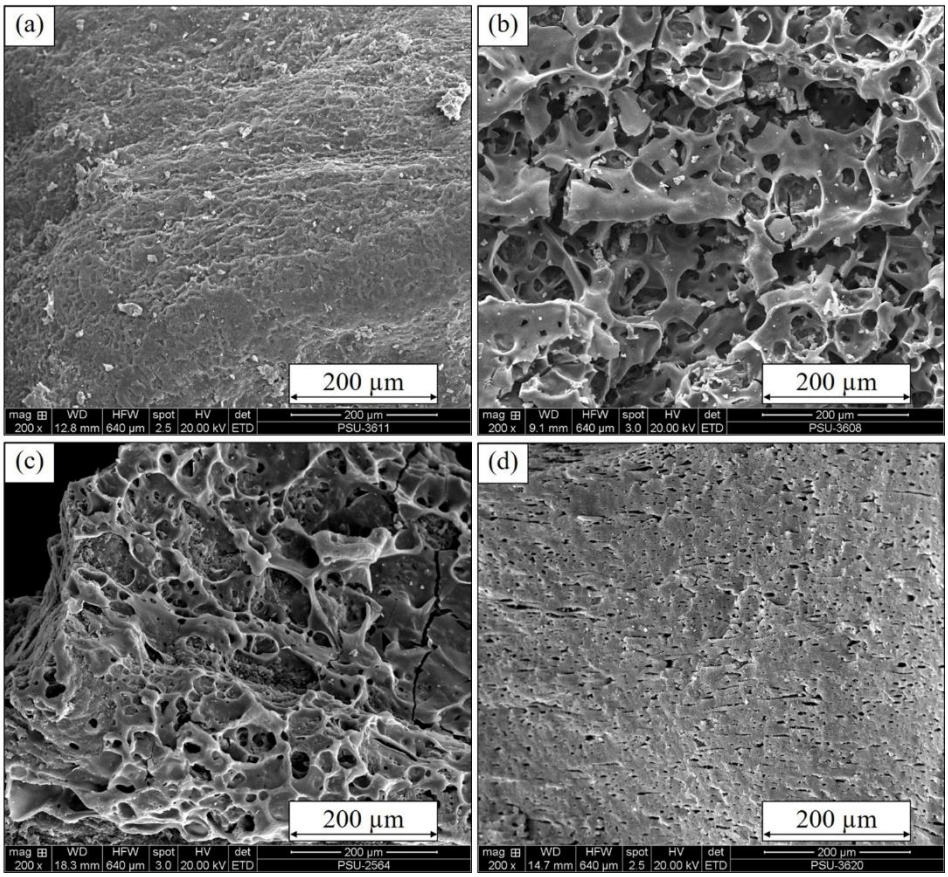

Figure 2. SEM images of CH (a), ACH (b), MCH (c), and AC (d) at × 200

Table 2. BET surface area analysis for the adsorbents

Parameter	CH	ACH	MCH	AC
BET surface area (m^2/g)	0.5	750.1	557.4	1099.8
Adsorption average pore diameter (Å)	43.4	18.9	22.9	17.0
Pore volume (cm^3/g)	0.0006	0.3541	0.3192	0.4684

The results from BET analysis agree well with the SEM images. It could be noted that the surface area and pore volume of ACH were significantly higher than those of CH, due to activation, while its average pore diameter was decreased. The increase in porosity was caused by removal of ash, tar, and nonvolatile residues from CH surfaces in the $ZnCl_2$ solution. However, as the ACH was modified using CTAB to obtain the MCH, the pores of MCH are wider and its surface area is slightly lower than those of ACH. This might be caused by further removal of organic residues in CTAB from ACH surfaces increasing the pore diameter and reducing the surface area of MCH.

According to the pore size diameter, MCH could be classified as mesoporous material with pore diameters in the range 20-500 Å, whereas the AC having pore diameters less than 20 Å is considered microporous (Ip et al., 2009). Though surface area and pore volume of MCH are lower and pore diameter is slightly larger than for the AC, many studies have reported that the specific surface area of synthesized biochar for reactive dye removal from wastewater should be in the range 600-900 m^2/g (Vijayaraghavan et al., 2009; Sun et al., 2013; Mook et al., 2016; Thitame and Shukla, 2016). In this study, the specific surface area of MCH was slightly lower than those in prior reports. Therefore, the use of MCH as an AC alternative for reactive dye removal is challenging and should be intensively examined.

3.2 Comparative adsorption of the reactive dyes by ACH, MCH, and AC

The sorbent dosage was fixed at 1 g. The adsorbents, namely ACH, MCH, and AC, were used for RDY145 removal from synthetic wastewater. The

initial RDY145 concentration was 700 mg/L. The experiment was conducted at pH 7, 30 °C, and 170 rpm shaking speed for 3 h. The RDY145 removal efficiencies by ACH, MCH, and AC are shown in Figure 3.

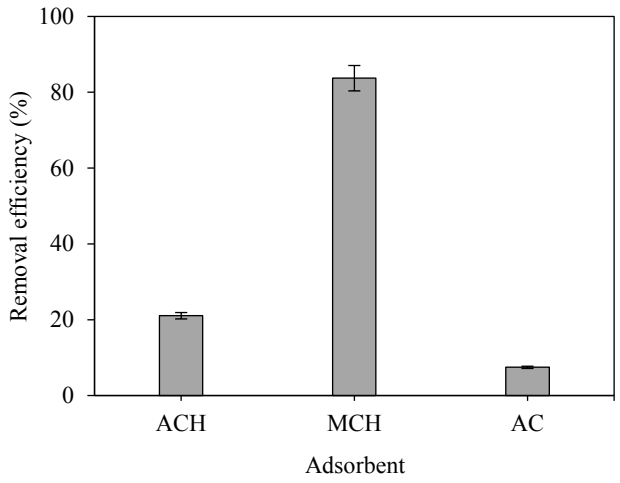

Figure 3. RDY145 removal efficiencies by ACH, MCH, and AC. Operating conditions: 700 mg/L of C_0, 30 °C, pH 7, and 170 rpm shaking speed for 3 h.

The results show 20, 83, and 7% removal of RDY145 by ACH, MCH, and AC, respectively. Interestingly, the higher adsorption efficiency of ACH than that of AC indicates that wider pores could facilitate reactive dye molecule accessibility to interior pore surfaces resulting in better reactive dye adsorption. This result combined with the data in Table 2 demonstrates that pore size of an adsorbent plays a crucial role in reactive dye removal. In addition, the MCH could increase RDY145 removal efficiency by up to 4-fold of ACH and 11-fold of AC, respectively. The increase in adsorption affinity for anionic dye might be due to CTAB modifying the surface charges on ACH. Our preliminary study shows that the ACH had a large capacity to adsorb CTAB (around 78.6% of the initial CTAB dosage) because of the large specific surface and hydrophobic attraction. CTAB could be adsorbed as individual molecules on the ACH surface, forming a monolayer, following the Langmuir adsorption isotherm (data not shown). The cationic surfactant CTAB has both a polar hydrophilic head (positive charge) and a non-polar hydrophobic tail. The tails of CTAB adsorb on hydrophobic sites of the ACH surface through Van der Waals attraction forces (Krivova et al., 2013; Ahmad et al., 2014; Puasa et al., 2018). Additionally, the positively charged heads can effectively adsorb negatively charged RDY145 molecules from wastewater by electrostatic interactions (Mi et al., 2016; Puasa et al., 2018). Thus, the MCH modified with this cationic surfactant has potential for anionic dye removal from wastewater.

3.3 Effect of pH on RDY145 removal using MCH

The removal of RDY145 from wastewater using MCH was tested at 700 mg/L C_0, 1 g of MCH, 30 °C, and 170 rpm shaking speed. The pH of wastewater from textile industry in Thailand is reported to be in the range 7-9 (Department of Industrial Works, Ministry of Industry, 2013). Typically, dye adsorption is a pH dependent process. The variation of pH in bulk solution could impact the surface properties of adsorbent and disturb the adsorbent-adsorbate interaction. Thus, in this work, the pH of solution was set at 3, 6, or 9 using HCl or NaOH. The relationship between adsorption and pH of solution is shown in Figure 4.

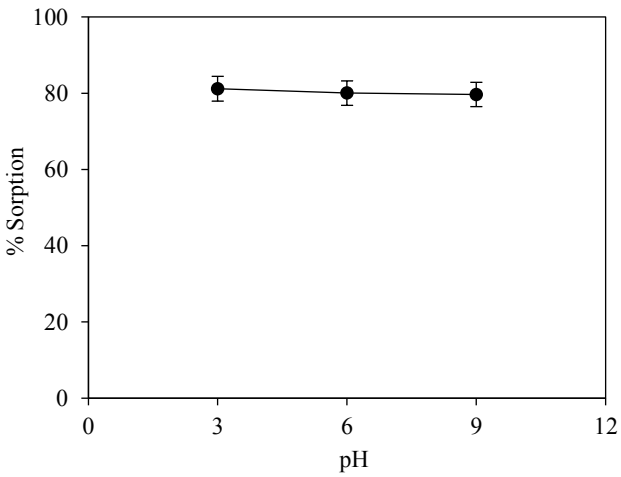

Figure 4. The adsorption percentages of RDY145 at different pH. Operating conditions: 700 mg/L of C_0, 1 g of MCH, 30 °C, and 170 rpm shaking speed.

It is seen that the pH of the solution had no effect on RDY145 removal efficiency. When NaOH was added to increase the pH, the small extra amount of hydroxyl groups (OH^-) present in the solution did not significantly interfere with adsorption of RDY145 on binding sites of MCH. Similarly, HCl decreased solution pH and provided free hydrogen ions (H^+), but these did not alter the positively charged CTAB-modified surface of MCH. Therefore, the removal efficiency of RDY145 was unaffected. These results were also consistent with the studies of pH variation in the range of 3-9 on reactive dyes removal using AC. They reported that the variation of solution pH had no effect on reactive dyes' removal

efficiency (Nabil et al., 2014; Mook et al., 2016). Thus, the observed results also support the use of MCH as an alternative for AC application in a variety of environmental pH.

3.4 Adsorption of reactive dyes

A 1 g quantity of MCH was applied for reactive dyes (RDY145, RDR195, or RDB222) removal from synthetic wastewater, indicated by MCH-RDY145, MCH-RDR195, or MCH-RDB222 as shown in Figure 5. Besides, the dye removal efficiencies of MCH and AC were compared using RDY145, with these cases labeled as MCH-RDY145 and AC-RDY145 in Figure 5, respectively. The quantity of AC was also controlled at 1 g. The particle sizes of the adsorbents were similar and controlled within 0.6-1.41 mm. The initial dye concentration was 700 mg/L. The experiment was conducted at pH 7, 30 °C, and 170 rpm shaking speed. The relationship between the adsorbed reactive dye quantity and contact time is shown in Figure 5.

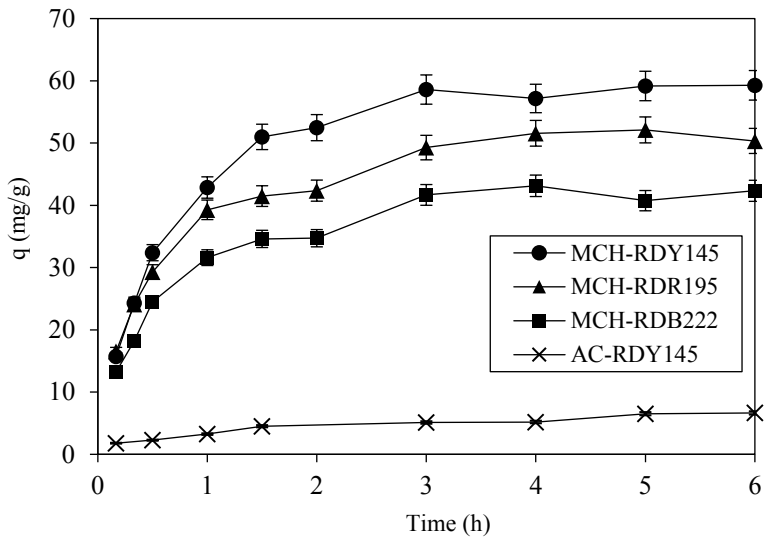

Figure 5. Reactive dye adsorption at various contact times for MCH-RDY145, MCH-RDR195, MCH-RDB222, and AC-RDY145, respectively. Operating conditions: 700 mg/L of C_0, 30 °C, pH 7, and 170 rpm shaking speed.

The results show that dye adsorption rapidly increased with contact time at initial uptake, after which it slowly increased and eventually saturated. The adsorption process reached equilibrium within 3 h for all reactive dyes and adsorbents. The large number of available active sites on adsorbents in the initial stage enables fast dye adsorption, and then the dye adsorption rate on the remaining surface slows down due to the repulsive forces and blocking by the adsorbed dye ions, as the competitive dye adsorption nears equilibrium (Brito et al., 2018). The adsorption of RDY145, RDR195, and RDB222 on MCH was 586.0, 498.0, and 416.7 mg/L, respectively. The dye removal percentage of RDY145 (83.7%) was the highest, followed by RDR195 (71.1%) and RDB222 (59.6%). While CTAB introduced positive charge on ACH surfaces and increased adsorption affinity of MCH for negative dyes, the observed differences in dye removal might be due to dye molecule sizes. Among the three dyes, RDY145 shows the highest adsorption capacity because it is the smallest molecule. The molecular weights of the dyes are shown in Table 1. It should be noted that small-sized molecules could not only adsorb on the adsorbent surface but also possibly penetrated into pores by diffusion and this should increase the adsorption capacity (Vijayaraghavan et al., 2009; Ahmad et al, 2014). In contrast, RDB222 is the largest molecule and its size might complicate the diffusion into the adsorbent pores. The adsorption might occur mainly on the external surfaces of MCH leading to the lowest adsorption efficiency (Ip et al., 2010; Krivova et al., 2013; Ahmad et al., 2014; de Franco et al., 2017).

Additionally, it should be noted that though MCH has a lower surface area than that of AC (data shown in Table 2), the higher RDY145 adsorption capacity using MCH was attributed to the wider average pore diameter of MCH compared to AC. These results are also consistent with the data illustrated in Figure 3 and supported by a study reporting that pore size of adsorbent plays an

important role on adsorbate molecular size and influences its adsorption behavior. Typically, adsorbate molecules could be adsorbed in pores with diameters 1.3-1.8 times their molecular diameter (Ip et al., 2010; Krivova et al., 2013; Ahmad et al., 2014; de Franco et al., 2017). Thus, as shown in Figure 6 (the molecular structure of RDY145 was illustrated by ACD/ChemSketch), a suitable pore size for uptake of RDY145 should be in the range 16.25-22.50 Å. It is seen that the average pore size of AC was below that of MCH, which might slow down the dye adsorption rate.

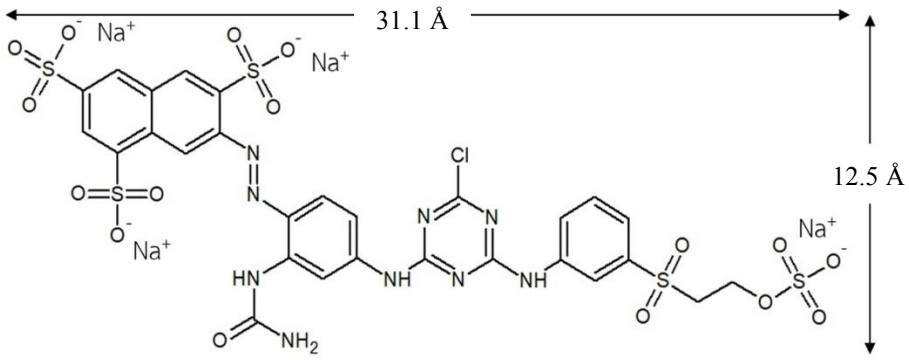

Figure 6. Molecular structure of RDY145

Moreover, AC surface is more hydrophobic than the positively charged MCH surface (Puasa et al., 2018). This non-polar attraction force is weaker than the electrostatic interaction that dominated RDY145 adsorption by MCH, and apparently is not sufficient to enhance the capacity of AC to adsorb the anionic RDY145 (Mi et al., 2016). Therefore, the large pore size of MCH facilitated the diffusion of RDY145 in MCH pores and its adsorption on MCH surfaces, and its positively charged CTAB modified surface provided strong attraction of anionic RDY145 dye molecules, leading to high dye removal efficiency.

Subsequently, the data were fitted with the aforementioned adsorption kinetics models. The kinetic parameters are given in Table 3.

Table 3. Parameters of fitted pseudo-first order and pseudo-second order models for adsorption of reactive dyes by MCH or by AC

Sample	Pseudo-first order			Pseudo-second order		
	k_1 (1/min)	q_e (mg/g)	R^2	k_2 (g/mg-min)	q_e (mg/g)	R^2
MCH-RDY145	0.0184	48.0	0.980	0.00040	68.5	0.997
MCH-RDR195	0.0135	36.5	0.959	0.00071	54.6	0.994
MCH-RDB222	0.0159	34.4	0.939	0.00073	46.5	0.990
AC-RDY145	0.4880	4.8	0.939	0.23700	6.2	0.965

The coefficient of determination (R^2) indicates that the pseudo-second order equation was suitable for fitting the adsorption of all the reactive dyes on MCH and AC. The equilibrium adsorption capacity (q_e) had the rank order RDY145 > RDR195 > RDB222 for reactive dye removal using MCH, and the q_e of MCH-RDY145 was significantly higher than that of AC-RDY145. The results were consistent with the data shown in Figure 5. This suggests that all the dyes were chemically adsorbed irreversibly on the MCH or AC surface and the adsorption rate is controlled by this step (Ibrahim et al., 2010; Ghazi Mokri et al., 2015; Mook et al., 2016). This agrees well with many prior studies (Sun et al., 2013; Ghazi Mokri et al., 2015; Thitame and Shukla, 2016). In addition, the value of k_2 also reflected the dye removal efficiency. A lower value of k_2 indicates higher dye removal. It should be noted that the sort order of k_2 agrees well with the order of q_e, and supports the concept that a small-sized dye could be highly adsorbed with good removal efficiency.

3.5 Equilibrium adsorption of reactive dyes

MCH was used to remove the reactive dyes (RDY145, RDR195, or RDB222) from synthetic wastewater, in experiments labeled as MCH-

RDY145, MCH-RDR195, or MCH-RDB222 shown in Figure 7. The dye adsorption performance of MCH and AC is compared using RDY145 (cases MCH-RDY145 and AC-RDY145) in Figure 7. The adsorbent quantity was controlled at 1 g. The initial dye concentration was varied from 50 to 700 mg/L. The experiment was conducted at pH 7 and 30 °C. The samples were shaken at 170 rpm for 3 h in order to achieve equilibrium. The equilibrium adsorbed reactive dye quantity (q_e) and residual dye concentration are shown in Figure 7. Then, the isotherm data were fitted with the Langmuir and Freundlich isotherms models, and the model parameters are shown in Table 4.

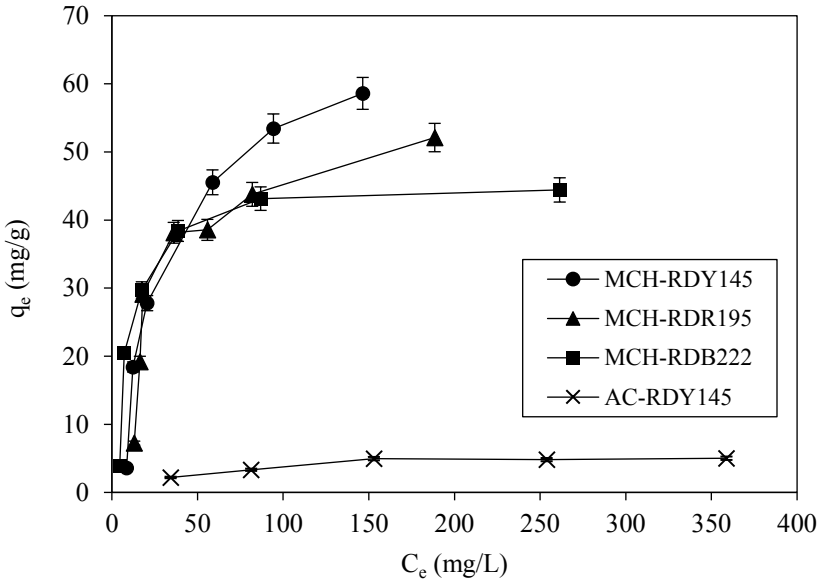

Figure 7. The equilibrium reactive dye adsorption by MCH-RDY145, MCH-RDR195, MCH-RDB222, and AC-RDY145. Operating conditions: 50-700 mg/L of C_0, 30 °C, pH 7, and 170 rpm shaking speed for 3 h.

Table 4. Identified parameters in Langmuir and Freundlich isotherm models for reactive dyes adsorbed by MCH and for RDY145 adsorbed by AC

Dye	Langmuir				Freundlich		
	q_{max} (mg/g)	k_L (L/mg)	R_L	R^2	k_F (mg/g (L/mg)$^{1/n}$)	n	R^2
MCH-RDY145	73.0	0.029	0.0476	1.000	6.30	2.15	0.968
MCH-RDR195	58.8	0.039	0.0354	0.992	9.58	2.94	0.813
MCH-RDB222	46.1	0.104	0.0136	0.999	15.32	4.69	0.855
AC-RDY145	6.4	0.014	0.0930	0.967	0.83	3.22	0.882

The R^2 values of model fits indicate that the Langmuir isotherm was suitable for all the reactive dyes on MCH or RDY145 on AC. According to the Langmuir theory, all reactive dyes were adsorbed on adsorbent surfaces as monolayer. The adsorbent surface was possibly homogenous (Ibrahim et al., 2010; Ghazi Mokri et al., 2015; Mi et al., 2016). The Langmuir parameter q_{max} has the rank order MCH-RDY145 > MCH-RDR195 > MCH-RDB222 > AC-RDY145. These results show similar trends as the experimental data and adsorption kinetics (Figure 5 and Table 3, respectively). Additionally, k_L reveals the interaction forces between adsorbed dye molecules and the surface sites. A higher k_L indicates greater strength of the adsorption forces (Markandeya et al., 2017). The order of k_L values is reversed from the order of q_{max}. For homologous adsorbent, the results confirm that RDB222 has the largest molecules and the least adsorption capacity on MCH (lowest q_{max}), while it had the strongest Van der Waals attraction forces (highest k_L) on MCH. Moreover, the q_{max} of AC-RDY145 was significantly lower than that of MCH-RDY145. Their difference in k_L values indicates that the attraction forces between RDY145 and MCH are much stronger than those with AC, which is consistent with the

aforementioned results (Markandeya et al., 2017). Besides, the values of R_L for all dyes were in the range from zero to one, indicating that adsorption under the experimental conditions were favorable.

Furthermore, many studies have tested various adsorbents obtained from agricultural waste biomass for removing anionic dyes from wastewater, reporting the Langmuir maximum adsorptions q_{max} listed in Table 5. It should be noted that the maximum adsorption capacity was 146.20 mg/g of light green dye on using cationic surfactant (Hexadecylpyridinium bromide, CPB) modified peanut husk (Zhao et al., 2017), while the adsorption capacity was 23.61 mg/g of reactive black 5 using activated carbon from palm shell (Mook et al., 2016). MCH had adsorption capacities in the range 46.10-73.00 mg/g for all three reactive dyes tested. This comparison shows MCH to be an effective adsorbent for reactive dye removal from water.

Table 5. Langmuir isotherm fit based capacities reported by prior studies on adsorption of anionic dye by an adsorbent based on agricultural solid waste

Adsorbent	Dye	q_{max} (mg/g)	Reference
Activated carbon (Palm shell)	Reactive black 5	23.61	Mook et al. (2016)
Activated carbon (*Enteromorpha prolifera*)	Reactive red 23	59.88	Sun et al. (2013)
Activated carbon (*Enteromorpha prolifera*)	Reactive blue171	71.94	Sun et al. (2013)
Activated carbon (*Enteromorpha prolifera*)	Reactive blue 4	131.93	Sun et al. (2013)
CTAB modified Biochar (Cornstalk)	Orange II	26.90	Mi et al. (2016)
CTAB modified wheat straw	Congo red	71.20	Zhang et al. (2014)
CPB modified wheat straw	Light green	70.01	Su et al. (2013)
CPB modified peanut husk	Light green	146.20	Zhao et al. (2017)
MCH	RDY145	73.00	This work
MCH	RDR195	58.80	This work
MCH	RDB222	46.10	This work

4. CONCLUSION

The study demonstrated that the MCH derived from coffee husk was effectively used as an adsorbent to remove reactive dyes (RDY145, RDR195, and RDB222) from synthetic wastewater. The results suggest that wider pores and smaller dye molecules could contribute to adsorption capacity. The mesoporous surface of MCH could enhance the reactive dye-MCH accessibility. Surface modification with CTAB could increase reactive dye removal efficiency by MCH by up to 80%. The dye adsorption kinetics was found to follow the pseudo second-order model. Additionally, the Langmuir isotherm described the dye adsorption equilibrium well. The pH did not significantly affect dye removal performance by MCH. Moreover, MCH provided better dye removal performance than AC. Thus, this work suggests that MCH is a promising adsorbent for reactive dye removal from water, and is comparable to AC and other adsorbents derived from agricultural waste.

ACKNOWLEDGEMENTS

We would like to acknowledge the Thamsing Coffee Group Community Enterprise for supplying coffee husk material, and all the commercial reactive dyes (RDY145, RDR195, and RDB222) were provided by KPT Corporation (Thailand) Co., Ltd. We are grateful for the financial support from the Faculty of Engineering's Graduate Study Scholarship, the Graduate School of Prince of Songkla University (PSU), and for facilities support from the Department of Chemical Engineering, Faculty of Engineering, PSU. Additionally, we would like to thank the PSU research and development office and Assoc. Prof. Seppo Karrila for reviewing the English of this article.

REFERENCES

Ahmad M, Rajapaksha AU, Lim JE, Zhang M, Bolan N, Mohan D, Vithanage M, Lee SS, Ok YS. Biochar as a sorbent for contaminant management in soil and water: a review. Chemosphere 2014;99:19-33.

Amin NK. Removal of reactive dye from aqueous solutions by adsorption onto activated carbons prepared from sugarcane bagasse pith. Desalination 2008;223(1-3):152-61.

Brito MJP, Veloso CM, Santos LS, Bonomo RCF, Fontan R da CI. Adsorption of the textile dye Dianix® royal blue CC onto carbons obtained from yellow mombin fruit stones and activated with KOH and H_3PO_4: kinetics, adsorption equilibrium and thermodynamic studies. Powder Technology 2018;339:334-43.

Department of Industrial Works, Ministry of Industry. Wastewater Management Guidance Manual from Textile Factories. Bangkok, Thailand: Department of Industrial Works, Ministry of Industry; 2013.

de Franco MAE, de Carvalho CB, Bonetto MM, Soares RD, Féris LA. Removal of amoxicillin from water by adsorption onto activated carbon in batch process and fixed bed column: kinetics, isotherms, experimental design and breakthrough curves modelling. Journal of Cleaner Production 2017;161:947-56.

GEO-Informatics Research Center for Natural Resource and Environment, Southern Regional Center of Geo-Informatics and Space Technology. Area of Tham Sing sub-district in Mueang Chumphon District, Chumphon Province, Thailand. Songkhla, Thailand: Prince of Songkla University; 2019.

Ghazi Mokri HS, Modirshahla N, Behnajady MA, Vahid B. Adsorption of C.I. acid red 97 dye from aqueous solution onto walnut shell: kinetics, thermodynamics parameters, isotherms. International Journal of Environmental Science and Technology 2015;12(4): 1401-8.

Guidechem. Reactive Red 195 [Internet]. 2017 [cited 2019 Feb 26]. Available from: https://www.guidechem.com/reference/dic-276579.html#Properties.

Ibrahim S, Fatimah I, Ang HM, Wang S. Adsorption of anionic dyes in aqueous solution using chemically modified barley straw. Water Science and Technology 2010;62(5):1177-82.

Ip AWM, Barford JP, McKay G. A comparative study on the kinetics and mechanisms of removal of reactive black 5 by adsorption onto activated carbons and bone char. Chemical Engineering Journal 2010;157(2-3):434-42.

Ip AWM, Barford JP, McKay G. Reactive black dye adsorption/desorption onto different adsorbents: effect of salt, surface chemistry, pore size and surface area. Journal of Colloid and Interface Science 2009; 337(1):32-8.

Krivova MG, Grinshpan DD, Hedin N. Adsorption of C_nTABr surfactants on activated carbons. Colloids and Surfaces A: Physicochemical and Engineering Aspects 2013;436:62-70.

Kula I, Uğurlu M, Karaoğlu H, Çelik A. Adsorption of Cd(II) ions from aqueous solutions using activated carbon prepared from olive stone by $ZnCl_2$ activation. Bioresource Technology 2008;99(3):492-501.

Lin S-Y, Chen W-f, Cheng M-T, Li Q. Investigation of factors that affect cationic surfactant loading on activated carbon and perchlorate adsorption. Colloids and Surfaces A: Physicochemical and Engineering Aspects 2013;434:236-42.

Maleangpoothong J, Photha P, Siriwongyotha C, Paksa W, Rommanee W, Taweesuk D, Srichoo C. Thailand experiences from the grassroots: value chain finance best practices, initiatives, strategies and trends in agriculture. Bangkok, Thailand: Asia-Pacific Rural and Agricultural Credit Association; 2013.

Markandeya, Shukl SP, Dhiman N. Characterization and adsorption of disperse dyes from wastewater onto cenospheres activated carbon composites. Environmental Earth Sciences 2017;76(20):1-12.

Meng L, Xu X, Bai B, Ma M, Li S, Hu N, Wang H, Suo Y. Surface carboxyl-activated polyester (PET) fibers decorated with glucose carbon microspheres and their enhanced selective adsorption for dyes. Journal of Physics and Chemistry of Solids 2018;123:378-88.

Mi X, Li G, Zhu W, Liu L. Enhanced adsorption of orange II using cationic surfactant modified biochar pyrolyzed from cornstalk. Journal of Chemistry 2016;2016:1-7.

Moazzam A, Jamil N, Nadeem F, Qadir A, Ahsan N, Zameer M. Reactive dye removal by a novel biochar/MgO nanocomposite. Journal of the Chemical Society of Pakistan 2017;39(1):26-34.

Mook WT, Aroua MK, Szlachta M. Palm shell-based activated carbon for removing reactive black 5 dye: equilibrium and kinetics studies. BioResources 2016;11(1):1432-47.

Mozammel HM, Masahiro O, Bhattacharya SC. Activated charcoal from coconut shell using $ZnCl_2$ activation. Biomass and Bioenergy 2002;22(5):397-400.

Nabil GM, El-mallah NM, Mahmoud ME. Enhanced decolorization of reactive black 5 dye by active carbon sorbent-immobilized-cationic surfactant (AC-CS). Journal of Industrial and Engineering Chemistry 2014;20(3):994-1002.

National Center for Biotechnology Information (NCBI). PubChem Compound Database; CID=5974 [Internet]. 2004 [cited 2018 Jul 30]. Available from: https://pubchem.ncbi.nlm.nih.gov/compound/5974.

National Center for Biotechnology Information (NCBI). PubChem Compound Database; CID=157317 [Internet]. 2005 [cited 2018 Jul 20]. Available from: https://pubchem.ncbi.nlm.nih.gov/compound/157317.

National Center for Biotechnology Information (NCBI). PubChem Compound Database; CID=102407104 [Internet]. 2015 [cited 2018 Jul 20]. Available from: https://pubchem.ncbi.nlm.nih.gov/compound/102407104.

Oei BC, Ibrahim S, Wang S, Ang HM. Surfactant modified barley straw for removal of acid and reactive dyes from aqueous solution. Bioresource Technology 2009;100(18):4292-5.

Ogugbue CJ, Sawidis T. Bioremediation and detoxification of synthetic wastewater containing triarylmethane dyes by aeromonas hydrophila isolated from industrial effluent. Biotechnology Research International 2011;2011:1-11.

Puasa SW, Ismail KN, Khairi NAIA. Direct surfactant-impregnated activated carbon for adsorption of reactive blue 4. International Journal of Engineering and Technology 2018;7(4):5-8.

Rehman HA, Razzaq R. Benefits of biochar on the agriculture and environment: a review. Journal of Environmental Analytical Chemistry 2017;4(3):1-3.

Su Y, Zhao B, Xiao W, Han R. Adsorption behavior of light green anionic dye using cationic surfactant-modified wheat straw in batch and column mode. Environmental Science and Pollution Research 2013;20(8):5558-68.

Sun D, Zhang Z, Wang M, Wu Y. Adsorption of reactive dyes on activated carbon developed from *Enteromorpha prolifera*. American Journal of Analytical Chemistry 2013;4(7A):17-26.

Thitame PV, Shukla SR. Adsorptive removal of reactive dyes from aqueous solution using activated carbon synthesized from waste biomass materials. International Journal of Environmental Science and Technology 2016;13(2):561-70.

Vijayaraghavan K, Won SW, Yun Y-S. Treatment of complex Remazol dye effluent using sawdust- and coal-based activated carbons. Journal of Hazardous Materials 2009; 167(1-3):790-6.

Wang X, Jiang C, Hou B, Wang Y, Hao C, Wu J. Carbon composite lignin-based adsorbents for the adsorption of dyes. Chemosphere 2018;206:587-96.

Zhang R, Zhang J, Zhang X, Dou C, Han R. Adsorption of Congo red from aqueous solutions using cationic surfactant modified wheat straw in batch mode: kinetic and equilibrium study. Journal of the Taiwan Institute of Chemical Engineers 2014;45(5):2578-83.

Zhao B, Xiao W, Shang Y, Zhu H, Han R. Adsorption of light green anionic dye using cationic surfactant-modified peanut husk in batch mode. Arabian Journal of Chemistry 2017;10(Supplement 2):S3595-602.

The Chemical Characteristic and Microbial Diversity of the Hot Spring at Phusang National Park

Sureewan Bumrungthai[1*], Sureewan Duangjit[2], Buntom Somsuwan[3], and Somchai Inpeng[3]

[1]*Division of Microbiology and Parasitology, School of Medical Sciences, University of Phayao, Phayao 56000, Thailand*
[2]*Division of Pharmaceutical Chemistry and Technology, Faculty of Pharmaceutical Sciences, Ubon Ratchathani University, Ubon Ratchathani 34190, Thailand*
[3]*Phusang National Park, Department of National Parks, Wildlife and Plant Conservation, Phayao 56000, Thailand*

ARTICLE INFO

Received: 7 Feb 2019
Received in revised: 29 May 2019
Accepted: 12 Jun 2019
Published online: 26 Aug 2019
DOI: 10.32526/ennrj.18.1.2020.04

Keywords:
Bacterial hot spring/ Sequencing/ Metagenomic/ Phusang warm pool/ Bacterial diversity

*** Corresponding author:**
E-mail:
sureewan.b@windowslive.com

ABSTRACT

The Phusang waterfall is located in Phusang National Park in Phayao Province, Thailand. The robustness of Phusang's warm waterfall is regionally recognized as the only one with a temperature range of 35-36 °C which makes it an outstanding place to visit in Thailand. Surprisingly, Phusang waterfall originates from the Phusang warm pool (hot spring). However, data about the bacterial community and characteristics of this water are still obscure. Therefore, this study investigated the bacterial community and characteristics of water in the Phusang hot spring. Tests to determine its physical characteristics such as pH, color and turbidity were performed. Trace elements such as sodium, bicarbonates, iron, and fluoride were detected as chemical characteristics. The biological properties were verified by 16S ribosomal RNA sequencing. Illumina metagenomic analysis was directly demonstrated from the water after DNA extraction via a membrane filtration pore of 0.45 µm. The range of pH, color and turbidity of water from the Phusang hot spring was 7.33-7.53, 0.05-0.18 Pt.Co and 9.55-10.91 NTU, respectively. The biological study of microorganisms found less than 300 CFU/mL. Coliform bacteria such as *Staphylococcus aureus* and other examples such as *Aeromonas veronii*, *Acinetobacter* sp. *Neisseriaceae bacterium* were abundant. Shotgun metagenomic sequencing defined the phylum as Proteobacteria (84%), Bacteroidetes (13%), Cyanobacteria (1%), and unclassified (2%). Moreover, the amount of sodium and strontium detected was 6.00-7.52 and 1.40-1.58 mg/L respectively. These studies show that a high abundance of Proteobacteria were present in samples from this hot spring. Phusang hot spring has been classified as having low mineral content water.

1. INTRODUCTION

Terrestrial geothermal springs are distributed all over the world. They are associated with bacterial communities under temperature and chemical stress. These bacterial communities were associated with early earth environments (Purcell et al., 2007) including the hot springs in Thailand.

Phusang waterfall or Phusang warm waterfall is located in Phusang National Park, Phayao Province, Thailand (19°39'50.2"N 100°22'35.6"E). Phusang waterfall is regionally recognized as the only one with a water temperature range of 35-36 °C which makes it an outstanding place to visit in Thailand. The Phusang waterfall originates from Phusang warm pool (Phusang hot spring). The warm pool is five meters deep with a temperature range of 35-38 °C. Possibly, the water of the warm pool is derived from both a hot spring and surface water.

Hot springs are found around the world and their waters exhibit specific physical and chemical characteristics, including different pH and more levels of several trace elements than fresh or groundwater. The community of microorganisms in each hot spring depends on pH, temperature, and

Citation: Bumrungthai S, Duangjit S, Somsuwan B, Inpeng S. The chemical characteristic and microbial diversity of the hot spring at Phusang National Park. Environ. Nat. Resour. J. 2020;18(1):33-43. DOI: 10.32526/ennrj.18.1.2020.04

other physicochemical parameters of the geothermal regions (Valeriani et al., 2018; Heni and Julinar, 2015). Thus, the chemical composition, such as a high level of sulfur or hydrogen carbonate, can be associated with the natural selection and involved with the bionetwork (Valeriani et al., 2018). Several factors, including biotic and abiotic pathways in hot springs impact bacteria diversity (Valeriani et al., 2018). One study found that temperature and sulfide have a more detectable effect than any other abiotic variables (Purcell et al., 2007). In the eastern lowlands, the Elegedi hot spring in the Alid volcanic area of Eritrea has a high temperature and increased concentrations of iron and sulfates. Phylum Proteobacteria (6.2-82.3%), Firmicutes (1.6-63.5%), Deinococcus-*Thermus* (0.0-19.2%) and Bacteroidetes (2.7-8.4%) were abundant. These generacorrelate with the temperature, carbonate, iron, sodium and sulfate levels in the water (Ghilamicael et al., 2017). In India, the Bakreshwar hot spring (54 °C) in West Bengal predominantly included the bacterial phylum Firmicutes (65.85%) and Synergistetes (27.24%) and water from the hot spring (65 °C) exhibited the diversity of the phylum Firmicutes (96.10%) and Proteobacteria (3.36%) based on sequencingV3 hypervariable 16S rRNA fragments (Chaudhuri et al., 2017). The bacterial diversity in this hot spring, situated at a high altitude, is dominated by phylum Proteobacteria which has been confirmed in several studies based on 16S rRNA analysis.

Phylum Proteobacteria have been found in other hot springs (Rozanov et al., 2017) including in Thailand (Valeriani et al., 2018) along with other bacteria such as phylum Firmicutes-*Bacillus*, phylum Deinococcus-*Thermus,* etc. (Purcell et al., 2007; Kanasawud et al, 1992). In nine districts with hot spring in northern Thailand, phylum Cyanobacteria-*Synechococcus lividus* and *Synechococcus* sp. (40-80 °C) and *Phormidium boryanu*m (30-60 °C) dominated (Udomluk et al., 2005). The Bor Khlueng hot spring (Ratchaburi province, Thailand) (50-57 °C) was characterized as having phylum Acidobacteria (23%), Bacteriodetes (19%), Nitrospirae (13%), Proteobacteria (12%), Deinococcus-*Thermus* (11%) by PCR using 16S rRNA amplified and restriction fragment length polymorphism (RFLP) analysis (Kanokratana et al., 2004). From a hot spring in northern Thailand, the phylum Thermotogae-*Thermotoga* sp. strain PD524 was isolated (70-85 °C, pH 6.0-8.5, NaCl 0-10 g/L) (Kanoksilapatham et al., 2015). In a hot spring pond in the Krabi province (Thailand), the genus *Planosporangium*, a novel filamentous bacterial strain, HSS8-18 (T), was isolated from the soil (Thawai et al., 2013). Infections in humans may be caused by waterborne opportunistic pathogens hidden in a hot spring (Jardine et al., 2017). Because hot springs are common tourist attractions, authorities should be attentive to probable risks and provide measures and guidelines to ensure safety without causing undue alarm to tourists (Sukthana et al., 2005). *Escherichia coli* or *Enterococcus* are the main thermotolerant bacteria which are an indicator of the water quality. Nevertheless, the majority of environmental bacteria are unculturable. Consequently, culture methods may not be able to detect all pathogens. Illumina sequencing can be more comprehensive. A precise evaluation of ecological bacterial pathogens can be applied to improve risk valuation methods and promote public health awareness (Ghilamicael et al., 2018).

Thermophilic Actinobacteria can produce several enzymes including amylases, DNA polymerases, pullulanases, proteases, lipases and xylanases (Valeriani et al., 2018). Other bacteria such as *Bacillus licheniformis*, potential producers of thermostable enzymes such as amylase, protease, and cellulase, might be beneficial in industrial applications (Mohammad et al., 2017; Ibrahim et al., 2013). One of the key metabolites (violacein, purple pigment) of *Chromobacterium* may affect gastroente-rological diseases e.g. colorectal cancer, inflammatory gastric lesions (Giselle and Nelson, 2017), and also inhibit *Bacillus* sp. growth, Plasmodium growth (Stefanie et al., 2009) with anti-MRSA and anti-fungal properties (Mahajan and Balachandran, 2017). *Thermus*, a genus found in Thailand produced an extracellular protease (Kanasawud et al., 1992). In the Tao Dam hot spring, the TD1 bacterial strain may be a good candidate as a pectate lyase producer (Yasawong et al., 2011). A neopullulanase-like enzyme from Bor Khleung hot spring (Tang et al., 2008) and lipolytic enzymes potential can be used in industrial applications (Tirawongsaroj et al., 2008). However, the microbial communities of hot springs in Thailand have been poorly studied. In particular, the data from the hot spring of Phusang warm pool has not been studied until now.

Therefore, this study investigated the bacterial community and the characteristics of the water from Phusang hot spring. Tests to determine its physical characteristics, such as pH, color and turbidity, were

performed. Trace elements such as potassium, sodium, chlorides, bicarbonates, calcium, sulfates, strontium, iron, fluoride and etc. were detected as chemical characteristics. Biological properties were identified using a bacterial culture in nutrient agar and sequencing by 16S ribosomal RNA (16S rRNA). Illumina metagenomic sequencing analysis was performed with directly extracted DNA from warm water trapped onto membranes with a filtration pore size of 0.45 µm.

2. METHODOLOGY

2.1 Sampling methods

Water samples were collected at three different periods (Season) in a year (June 2017 to May 2018) from Phusang hot spring (35-38 ºC) located in Phusang National Park, Phayao Province, Thailand (19°39'50.2"N 100°22'35.6"E). The characteristics such as pH, color (Pt. Co), turbidity, and trace elements (such as bicarbonate, iron (Fe), fluoride (F), sulfate (SO_4), sodium (Na), potassium (K), zinc (Zn), calcium (Ca), chloride (Cl), strontium (Sr)), total hardness (as $CaCO_3$), and total dissolved solids (TDS) of water samples were analyzed twice using inductively coupled plasma (ICP, Perkin Elmer, USA) and standard methods for examination of water following the recommend-dations of the American Public Health Association (APHA) and the American Water Works Association (AWWA). For sample analysis of chemical characteristics, eight liters (L) of water were obtained under the surface of the pool near the water inlet and stored on ice. After that, the samples were placed in sterile glass containers and stored on ice for future microorganisms analysis.

2.2 DPPH assay

Three water samples of 50 mL were collected and then filtered using a 0.45 µm filter membrane. A stock solution including 1, 1-Diphenyl-2-picryl-hydrazyl (DPPH) (Sigma-Aldrich USA) was prepared in methanol and methanol/buffer with an acetic acid buffer (0.1 M, pH 5.5). The methanol/buffer was prepared by mixing 40 mL of 0.1 M acetate buffer (pH 5.5) with 60 mL methanol. The reaction tubes were kept at 30 °C for 30 min in the dark wrapped in aluminum foil (at least 5 layers). In the dim light, spectrophotometric measurements were done at 517 nm using a Spectronic Genesys 5 spectrophotometer. The data are mean ±SD. Ascorbic acid and butylated hydroxytoluene (BHT) (E. Merck, India), and propylgallate (Sisco Research Laboratories, Mumbai, India) were used.

2.3 Bacterial isolation

To isolate the bacteria, 100 µL of water was spread onto nutrient agar (NA) plates in triplicates (NA, Hi-Media Laboratories Pvt, Ltd., Mumbai, India). NA plates were incubated at 37 °C for 24 h and the total colonies were counted as CFU/mL. The growth colonies were re-streaked on NA plates and a single colony was transferred into Luria-Bertani (LB, HiMedia Laboratories Pvt, Ltd., Mumbai, India) broth for DNA extraction.

2.4 DNA extraction

Bacterial pellets or a 0.45 µm filter membrane were used for total DNA extraction. The cell lysis solution (Tris-HCl 10 mM, pH 7.8; EDTA 5 mM; SDS 0.5%; lysozyme) and proteinase K 50 µL (stock 20 mg/mL) were added and incubated at 65 °C for 1 h. 5 M potassium acetate (400 µL) was used for protein precipitation and then centrifuged at 12,000xg for 10 min at 4 °C. The supernatant was collected and an equal volume of phenol: chloroform: isoamyl (25: 24:1) was added, then centrifugation at 12,000xg for 10 min at 4 °C was done. Isopropanol was used for DNA precipitation from an aqueous phase by centrifugation at 12,000xg for 10 min at 4 °C and washed with 70% ethanol. DNA was rehydrated in TE buffer (10 mM Tris [pH 7.8] and 1 mM EDTA) and stored at -20 °C until analysis by agarose gel electrophoresis was performed. The DNA quality was checked via staining with Redsafe™ (iNtRON Biotechnology, Inc., Burlington, MA, USA) and examined using a gel documentation system (Bio-Rad, Hercules, California, USA).

2.5 Polymerase chain reaction (PCR) amplify-cation and sequencing

DNA extracted from the bacterial cells was subjected to PCR. Then 27F/1492R universal primers were used for PCR amplification (16S rRNA genes). OnePCR™ plus a master mix (GeneDireX, Las Vegas, Nevada, USA), 0.4 pmol primer pair 27F/ 1492R, 100-200 ng DNA template and Dnase/Rnase free water to 25 µL. The PCRs conditions were pre-denaturation at 96 °C for 5 min and 35 cycles of denaturation at 96 °C for 45 s, annealing at 58 °C for 45 s, extension at 72 °C for 2 min and a final extension at 72 °C for 7 min. The PCR product size was close to 1500 bps on 1.5%

agarose gel electrophoresis. DNA sequencing was used for species identification. PCR was done before sequencing by 27F/1492R primers. The result of 16S rRNA sequence was done using NCBI's (BLASTN).

2.6 Metagenomics

Shotgun metagenomic sequencing was used to analyze the bacterial biodiversity of the hot spring water. We filtered 20 L of water using a 0.45 µm filter membrane. The bacterial pellet was eluted by a PBS buffer. Phenol-chloroform was used to extract DNA followed the 2.4 DNA extraction process. The extracted DNA might represent all bacterial cells from the water sample. A high-quality and sufficient amount of DNA must be acquired for ensuing library production and sequencing. Fraction steps were checked by Agilent 2100 and Q-PCR to certify that enough targeted DNA existed. This was a range of end repairing. For tailing construction, sequencing adapters were ligated, and enrichment steps of PCR were used to produce a library. Agarose electrophoresis was used for DNA purity and integrity. The sequencing was performed using the Illumina platform after library clustering with paired-end reads. Phylum abundance data by shotgun metagenomics sequencing were based on a 16S rRNA gene sequence and included phylum data of other functional genes.

3. RESULTS AND DISCUSSION

The present study provides the physical, chemical and biological characteristics of water sampling from Phusang hot spring. An environmental valuation of this hot spring was significantly influenced by risk assessment methods and the promotion of public health awareness for both the government and tourists. These intrinsic characteristics of water from Phusang hot spring may be the variables that influence the number of tourists and visitors in this location. An examination of the pH, color, and turbidity was performed to identify the physical characteristics of the water from Phusang hot spring. The temperature of the Phusang hot spring varied due to the activity of the springs, ranging from 35-38 °C (mean 36±1.5 °C). The pH of spring water was in a range of 7.2-7.5 (mean 7.3±0.1). The color and turbidity were 0.05-0.18 Pt.Co and 9.55-10.91 NTU, respectively (Table 1).

Moreover, our results suggested that the water from the Phusang hot spring has no effect on an antioxidant when compared to vitamin E (Figure 1).

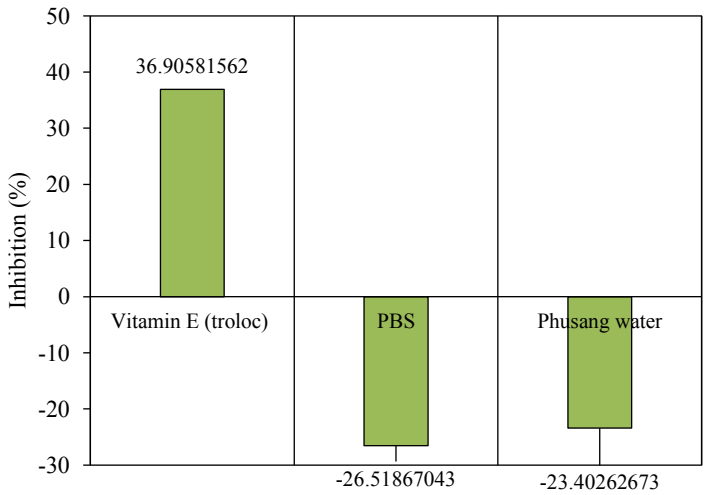

Figure 1. Antioxidant activity by DPPH assay of Phusang springs water

The total amount of solids found were <500 mg/L. Calcium, sodium, and strontium were found at 147.40, 6.00-7.52, and 1.40-1.58 mg/L, respectively. The other trace elements identified included potassium, bicarbonates, sulfates, iron, fluoride, etc. as shown in Table 1. These results indicated that Phusang hot spring should be classified as low mineral content water (Quattrini et al., 2017). The sodium is <20 mg/L and this is indicated as a low sodium definition (Quattrini et al., 2017).

The total bacterial counts of the water samples from Phusang warm water were observed on the NA medium by spread plate technique. After 20 replicates in the three periods of one year were counted, a majority of the samples showed a mean of $2.5\pm1.7\times10^2$ CFU/mL (Table 2). *Staphylococcus*

aureus and other bacteria such as *Acinetobacter* sp., *Aeromonas veronii*, *Bacillus licheniformis*, *Chromobacterium* sp., *Enterobacter* sp., *Staphylococcus* spp, *Pseudogulbenkiania* sp. were found but *Salmonella* spp. and *Clostridium perfringens* were not found by PCR and sequencing (Table 3).

Shotgun metagenomic sequencing showed these phylum abundance results: bacteria 93% of the amplicon library, unknown 7%, virus 0.02%, Archea 0.02% and Eukaryota 0.02%.

Based on these total sequences read numbers, this study found phylum Proteobacteria (84%), Bacteriodetes (13%), Cyanobacteria (1%), and unclassified (2%). The phylum Proteobacteria included, 71% from class Gammaproteobacteria, 22% from class Betaproteobacteria, 4% from class Alphaproteobacteria, 0.3% from class Deltaproteobacteria. As for the top 10 phyla found via the analysis, the most common was phylum Proteobacteria, followed by Bacteriodetes, Cyanobacterium, Firmicutes, Actinobacteria, Chloroflexi, Verrucomicrobia, Planctomycetes, Acidobacteria and Euryarchaeota. Moreover, the top ten families, genus and species are shown in Figures 2-4.

Table 1. The water turbidity, color, pH and trace elements analysis

Category	Composition (mg/L or ppm)	Unit	Phusang
Physical	Color	Pt.Co	0.05-0.18
	Turbidity	NTU	9.55-10.91
	pH	-	7.33-7.53
Chemical	Total Solids	mg/L	392.5-400
	Total Hardness (as $CaCO_3$)	mg/L	320-330
	Chloride	mg/L	6.59-7.95
	Iron	mg/L	0.75-0.94
	Strontium	mg/L	1.40-1.58
	Sulfate	mg/L	<0.0-<5.0
	Zinc	mg/L	Not-detected-<0.01
	Fluoride	mg/L	0.95-1.16
	Bicarbonate	mg/L	336.60-341.70
	Calcium	mg/L	147.40
	Potassium	mg/L	1.41-4.11
	Sodium	mg/L	7.52-8.90
Microbiological	*E. coli*	MPN/100 mL	Not-detected-<1.1
	S. aureus		Not-detected-Detected
	Salmonella spp.		Not-detected
	Cl. perfringens		Not-detected

Table 2. Total bacterial counts using a spread plate technique

Months	No. of CFU $\times 10^2$/mL								CFU/mL)mean±SD)
	1	2	3	4	5	6	7	8	
April	4.5	2.1	1.2	1.2	0.6	0.8	2.7	3.1	$2.0\times10^2\pm1.3\times10^2$
August	4.2	1.4	4.0	2.5	1.3	1.8	-	-	$1.9\times10^2\pm1.3\times10^2$
December	6.6	2.8	5.8	2.2	3.2	2.0	-	-	$3.8\times10^2\pm1.9\times10^2$
Mean									$2.5\times10^2\pm1.7\times10^2$

*CFU/mL =colony forming unit/mL

Table 3. 16S rRNA gene sequences analysis of bacteria isolated from the Phusang hot spring.

April	August	December
Bacillus mojavensis	*Acinetobacter* sp.	*Acinetobacter* sp.
Bacillus halotolerans	*Aeromonas jandaei*	*Aeromonas veronii*

Table 3. 16S rRNA gene sequences analysis of bacteria isolated from the Phusang hot spring (cont.).

April	August	December
Bacillus licheniformis	*Aeromonas* sp.	*Chromobacterium* sp.
Bacillus mojavensis	*Aeromonas veronii*	*Neisseriaceae bacterium*
Bacillus paramycoides	*Aquaphilus dolomiae*	*Pseudogulbenkiania* sp.
Bacillus safensis	*Bacillus amyloliquefaciens*	
Bacillus tropicus	*Brevibacillus agri*	
Staphylococcus cohnii	*Brevibacillus* sp.	
Staphylococcus epidermidis	*Cellulomonas hominis*	
Staphylococcus warneri	*Chromobacterium rhizoryzae*	
Staphylococcus aureus	*Enterobacter cloacae*	
Micrococcus luteus	*Enterobacter* sp.	
	Escherichia coli	
	Flavobacterium sp.	
	Microbacterium sp.	
	Pseudogulbenkiania sp.	
	Rheinheimera sp.	
	Sphingomonas zeae	
	Staphylococcus arlettae	
	Staphylococcus epidermidis	
	Staphylococcus pasteuri	
	Staphylococcus sp.	
	Terrimonas sp.	
	Uncultured *Asticcacaulis* sp.	
	Uncultured *bacterium*	
	Uncultured *Xylella*	

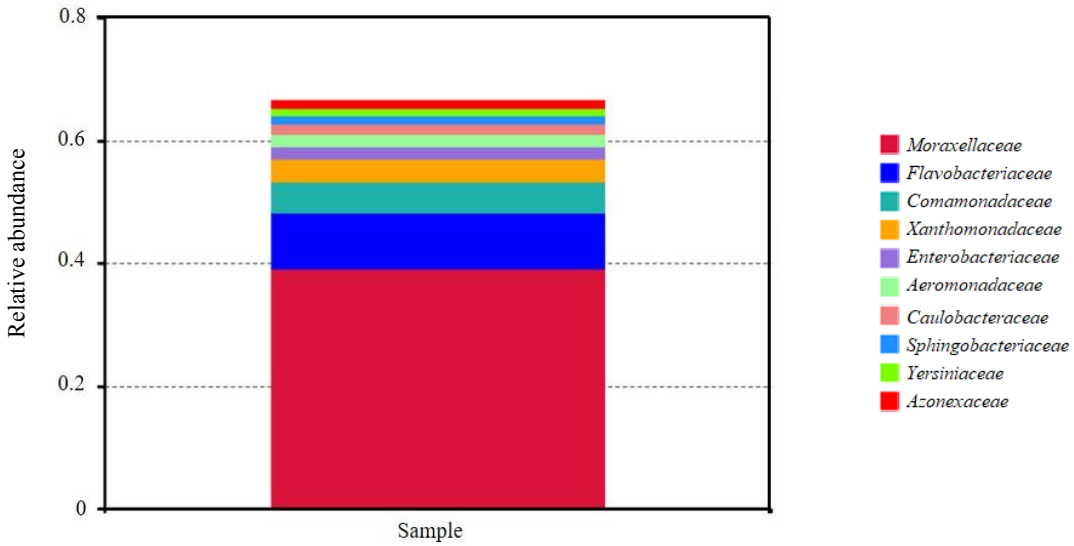

Figure 2. Top ten families found by shotgun sequencing

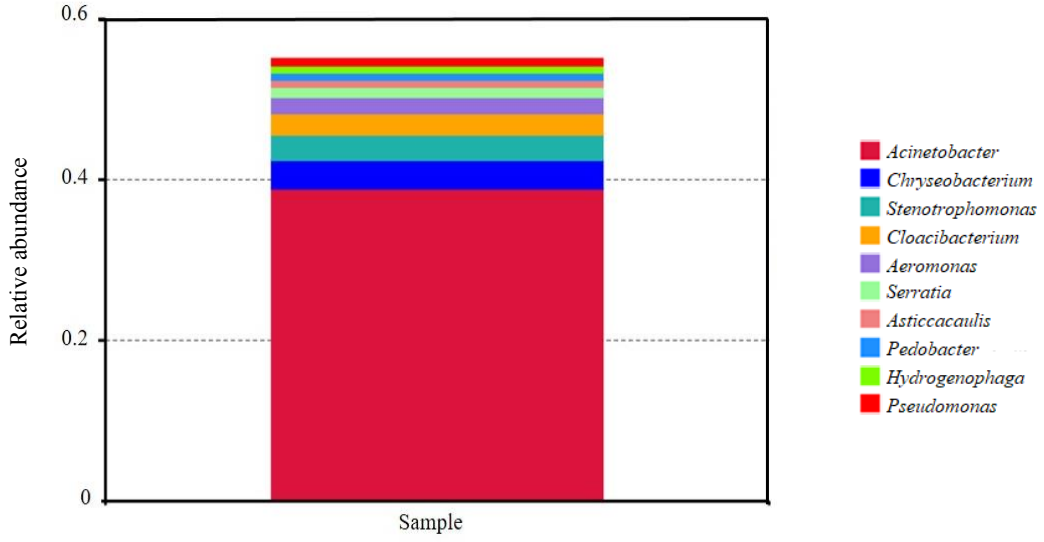

Figure 3. Top ten genus found by shotgun sequencing

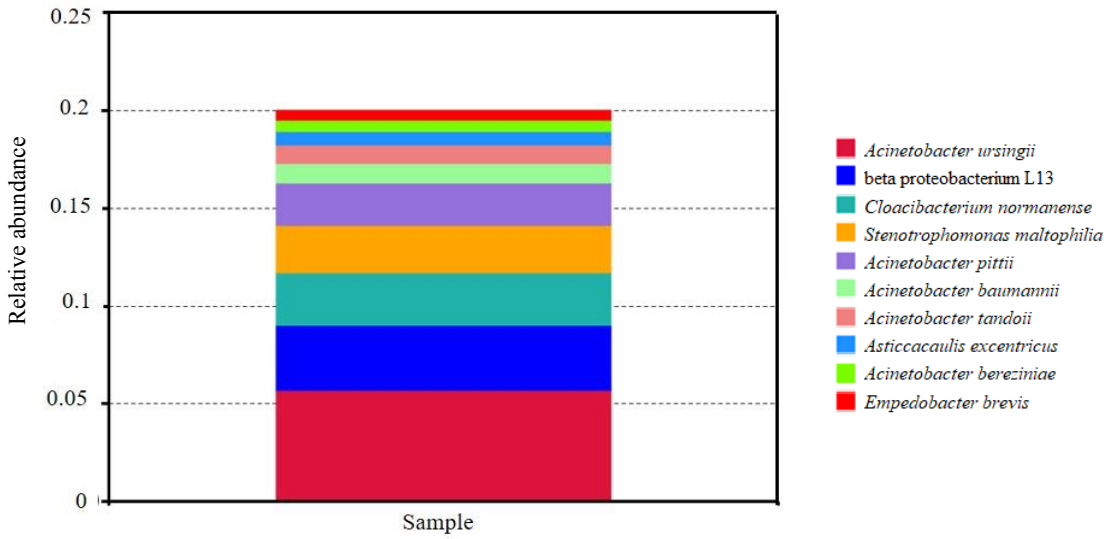

Figure 4. Top ten species found by shotgun sequencing

In Figure 5, an antibiotic mixture of two or more antibiotics is labeled in the form of an acronym. The relative abundance in unit ppm is the result of magnifying 10^6 times of the original abundance data. For antibiotic analysis, the most common was bacitracin, followed by CA, tetracycline, and sulfonamide as shown in Figure 5.

The water from Phusang hot spring ranged from neutral pH to alkaline pH. The water samples showed no evidence of antioxidants when compared to vitamin E. The Phusang water could be applied for use as a commercial cosmetic product such as a moisturizer or mineral aqua for skin care with no antioxidant claim.

The low amount of sodium found in the water (<20 mg/L) might be useful for drinking in cases of hypertension (Quattrini et al., 2017; Ha, 2014). Reducing dietary salt consumption to decrease deaths ratio from hypertension, cardiovascular disease and stroke has been recommended by the World Health Organization (WHO) (Ha, 2014). Tap water exhibited a large range of strontium concentration (0-1.9 mg/L) in the United States (US) (Lesley et al., 2012). Strontium was detected in 650 different European natural water samples (<0.0002-22.8 mg/L) (Voerkelius et al., 2010).

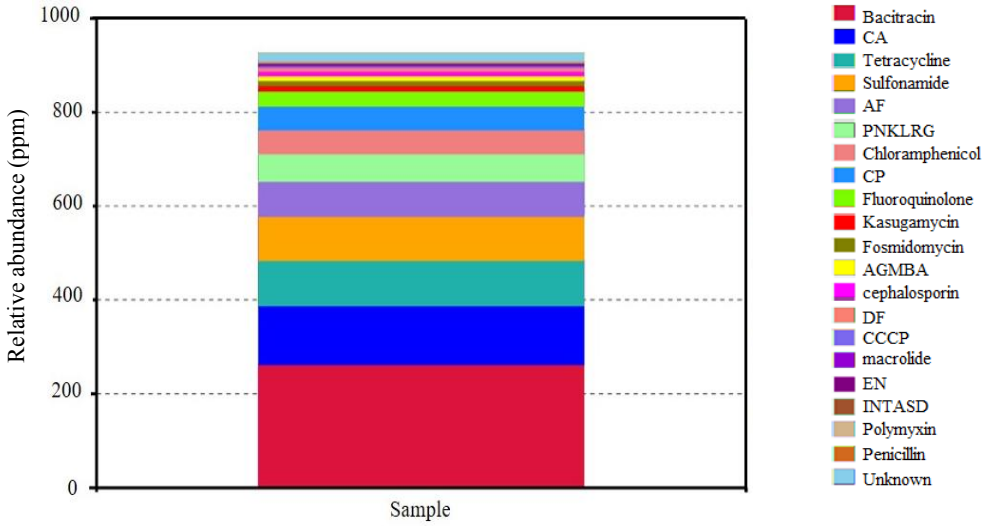

Figure 5. The abundance of the antibiotics in each sample

In this study, the amount of strontium may be beneficial to the elderly but not to children. Risk of osteoporotic vertebral and nonvertebral fractures might be reduced by strontium, seemingly through a decrease of resorption and an increase of bone formation (Voerkelius et al., 2010; Meunier et al., 2004; Reginster et al., 2005; Seeman et al., 2006; Meunier et al., 2009; Roux, 2008). A smell of sulfur is not present in Phusang hot spring according to the result of this study (<5.0 mg/L).

Phylum Proteobacteria and Chloroflexi were most commonly found in samples from Tato Field, Tatta Pani, and Murtazaabad according to this study (Ghilamicael et al., 2017; Chaudhuri et al., 2017; Amin et al., 2017). In the Murtazaabad hot springs (90-95 °C), phylum Thermotogae was favored with the higher temperature, whereas the phylum Proteobacteria has favored growth in the Tatta Pani thermal spring (60 °C) (Amin et al., 2017). The Bakreshwar hot springs (65 °C) showed an abundance of the phylum Firmicutes (96.10%) and Proteobacteria (3.36%) (Chaudhuri et al., 2017). The Bor Khlueng hot spring (Ratchaburi Province, Thailand), contains sulfide-rich mineral water (50-57 °C) and Proteobacteria was found at levels of 12% (Kanokratana et al., 2004). Phylum Chloroflexi were dominant at locations with low silica and high temperature (Amin et al., 2017). Therefore, the community structures are dependent upon temperature (Purcell et al., 2007; Amin et al., 2017) and sulfide rather than by any other abiotic (Valeriani et al., 2018; Purcell et al., 2007). This study supports the idea that temperature has an effect on predominately Proteobacteria in low-temperature hot springs such as the Phusang hot spring. The presence of domain Archaea (Chaudhuri et al., 2017) in the hot springs was confirmed at 0.02% including *Halorubrum kocurii*, *Haloferax natronorubrum*, *Halorubrum aethiopicum*. Similarly, a study of the Bor Khlueng hot spring (Ratchaburi Province, Thailand) found Crenarahaeota (Kanokratana et al., 2004). A significant correlation with abundant salinity occurring was found between Halobacteria, Actinobacteria and Cyanobacteria in Garbanabra and Gelti (Ghilamicael et al., 2017). The occurrence of some Cyanobacteria was highly dependent on temperature (Strunecky et al., 2018). Therefore, this study could be a biological basis to confirm that the Phusang warm pool was derived from hot spring water.

This study found 1% of the bacteria could not be unassigned an identity using shotgun sequencing, suggesting many undiscovered and unexplored microbiota were present. The novel insights of nature ecology interactions and bacterial communities that were found in this study might help in determining future study courses in these locations (Amin et al., 2017). In Bor Khlueng (Thailand), the majority of the detected prokaryotic sequences were unknown (approximately 80%) (Kanokratana et al., 2004). For example, Kanoksilapatham et al. (2015) studied a hot spring in northern Thailand where a strain of hyperthermophilic *Thermotoga* sp. (strain PD524) was isolated. Some studies at a hot spring pond in the Krabi Province (Thailand) found a novel filamentous bacterial strain HSS8-18 (T) genus *Planosporangium* that was isolated from the soil (Thawai et al., 2013) and a strain CC-KL-3^{T} showed the highest sequence

of *Hydrogenophaga bisanensis*. This is similar to the result of the current study that found *Hydrogenophaga* sp. T4, *Hydrogenophaga flava*, *Hydrogenophaga taeniospiralis*, etc. and unassigned *Hydrogenophaga* that need to be evaluated in a further study (Lin et al., 2017).

The family Moraxellaceae (genus *Acinetobacter*) constitutes 42% of the total bacteria. Family Enterobacteriaceae (genus *Enterobacter* 0.5%, *Klebsiella* 0.5%, *Shigella* 0.09%, *Salmonella* 0.09%, *Escherichia* 0.08%, *Cronobacter* 0.08%) constitutes 2% of total bacteria. Family Yersiniaceae (genus *Serratia*) constitutes 1% of the total bacteria. In hot springs, human pathogens can survive and grow. The main thermotolerant bacteria frequently used to estimate a load of pathogenic bacteria in water are *Escherichia coli* or *Enterococcus*. (Thorolfsdottir and Marteinsson, 2013; Signorelli et al., 2006; McClung et al., 2017; Rebellon et al., 2018). *Legionella* was a pathogen found in samples from 57.8% (48/83 samples) (Viroj, 2005) of the studied places at natural hot springs in northern, southern eastern and central Thailand. This study found *Listeria monocytogenes* (0.002%). Because there can be possible risks of exposure to hazardous pollutants in public waters, and since spas and natural springs are popular tourist attractions, authorities should be aware of possible hazards and provide tactful measures and guidelines to ensure safety without causing undue alarm to tourists (Sukthna et al., 2005; Rebellon et al., 2018; Hayasaka et al., 2018). This location should be managed in a way that is similar to the practice near the Khao-Than hot spring, Surat Thani Province, southern Thailand, that found high natural radium radiation (Bhongsuwan and Auisui, 2015). Therefore, this study suggests that the water from Phusang must be treated before use.

Emerging waterborne opportunistic pathogens that can cause infections in humans may harbor in hot spring water. This study investigated the diversity and antimicrobial resistance of emerging and opportunistic bacterial pathogens. Isolates were found to have resistance to ten antibiotics (bacitracin, CA, tetracycline, sulfonamide, AF, PNKLRG, chloramphenicol, CP, fluoroquinolone, kasugamycin etc.). This study suggests that a potential reservoir for emerging opportunistic pathogens are hot springs. Multiple antibiotic-resistant strains highlight the occurrence of unknown populations of emerging and possible waterborne opportunistic pathogens in the environment (Jardine et al., 2017).

Moreover, the results suggest that Actinobacteria might be producing antimicrobial molecules and biopharmaceuticals more than other bacteria. Thermophilic Actinobacteria was a producer of several enzymes such as DNA polymerases, amylases, xylanases, lipases and proteases (Valeriani et al., 2018; Ghilamicael et al., 2017) or lipolytic enzymes from Jae Sawn hot spring (Thailand), which lead to the isolation of a novel esterase (Est1) and patatin-like phospholipase (PLP) with potential use in industrial applications (Tirawongsaroj et al., 2008). This study found *Bacillus licheniformis* is a potential producer of a thermostable enzyme such as amylase, cellulose, gelatins, lecithin, and protease. This supports future studies to explore further environmental and industrial applications (Mohammad et al., 2017; Ibrahim et al., 2013). Their quick reaction time, thermostability, and decreased risk of contamination are an adeptness of thermophilic microorganisms and their enzymes. Thus, a good source for isolating efficient biomass degrading thermophiles and thermozymes was a hot spring (Lee et al., 2018).

Moreover, *Chromobacterium* was found in this study and further study of it might evaluate the function of this metabolite to inhibit cancer and other bacterial growth (Giselle and Nelson, 2017; Stefanie et al., 2009; Mahajan and Balachandran, 2017).

4. CONCLUSION

These studies conclude that a high abundance of Proteobacteria and Chloroflexi exist in samples from the hot springs in the Phusang zone was present. The most common was Family Moraxellaceae, followed by Enterobacteriaceae and Yersiniaceae. Phusang hot spring was classified as having low mineral content water. Strontium and low sodium might be beneficial to the elderly and hypertension patients, respectively.

ACKNOWLEDGMENT

We thank the Thalassemia Unit, University of Phayao for use of the PCR machine and gel documentation system. Department of National Parks, Wildlife and Plant Conservation. Phusang National Park. Assist. Prof. Dr. Bhundit Innawong, Department of Food Technology, Faculty of Engineering and Industrial Technology, Silpakorn University for idea thinking. Chamnan Sangkeo (Director) and the Adventure team, University of Phayao. Student from Special problem class (2016-

2018), University of Phayao for preparing materials, spread plate and DNA extraction. This work was supported by funding grant no. RDG59A0013-02-03 from Area-Based Collaborative Research (ABC)/ University of Phayao; grant no. 601007 (2017) from the School of Medical Science, University of Phayao; and grant no. RD62057 from University of Phayao.

CONFLICT OF INTEREST

The authors declare no conflict of interest associated with this manuscript.

REFERENCE

Amin A, Ahmed I, Salam N, Kim BY, Singh D. Diversity and distribution of thermophilic bacteria in hot springs of Pakistan. Microbial Ecology 2017;74(1):116-27.

Bhongsuwan T, Auisui SA. A high natural radiation area in Khao-Than hot spring, Southern Thailand. Radiation Protection Dosimetry 2015;167(1-3):284-8.

Chaudhuri B, Chowdhury T, Chattopadhyay B. Comparative analysis of microbial diversity in two hot springs of Bakreshwar, West Bengal, India. Genomic Data 2017;12:122-9.

Ghilamicael AM, Boga HI, Anami SE, Mehari T, Budambula NLM. Potential human pathogenic bacteria in five hot springs in Eritrea revealed by next generation sequencing. PLoS ONE 2018;13(3): e0194554.

Ghilamicael AM, Budambula NLM, Anami SE, Mehari T, Baga HI. Evaluation of prokaryotic diversity of five hot springs in Eritrea. BMC Microbiology 2017;17(1):203.

Giselle ZJ, Nelson D. Action and function of *Chromobacterium violaceum* in health and disease: Violacein as a promising metabolite to counteract gastroenterological diseases. Best Practice and Research Clinical Gastroenterology 2017;31(6): 649-56.

Ha SK. Dietary salt intake and hypertension. Electrolyte Blood Press 2014;12(1):7-18.

Hayasaka S, Uchida M, Hattori M, Watanabe H, Ojima T. Association between having a hot spring water supply in the home and prevention of long-term care. Complementary Therapies in Clinical Practice 2018; 33:142-8.

Heni Y, Julinar M. Isolation and phylogenetic analysis of thermophile community within Tanjung Sakti hot spring, South Sumatera, Indonesia. HAYATI Journal of Biosciences 2015;22(3):143-8

Ibrahim D, Zhu HL, Yusof N, Isnaeni, Hong LS. *Bacillus licheniformis* BT5.9 isolated from Changar hot spring, Malang, Indonesia, as a potential producer of thermostable α-amylase. Tropical Life Sciences Research 2013;24(1):71-84.

Jardine JL, Abia ALK, Mavumengwana V, Ubomba JE. Phylogenetic analysis and antimicrobial profiles of cultured emerging opportunistic pathogens (Phyla Actinobacteria and Proteobacteria) identified in Hot Springs. International Journal of Environmental Research and Public Health 2017;14(9):1070.

Kanasawud P, Teeyapan S, Lumyong S, Holst O, Mattiason B. *Thermus* 2S from Thai hot springs: Isolation and immobilization. World Journal of Microbiology and Biotechnology 1992;8(2):137-40.

Kanokratana P, Chanapan S, Pootanakit K, Eurwilaichitr L. Diversity and abundance of bacteria and archaea in the Bor Khlueng hot spring in Thailand. Journal of Basic Microbiology 2004;44(6):430-44.

Kanoksilapatham W, Keawram P, Gonzalez JM, Robb FT. Isolation, characterization, and survival strategies of *Thermotoga* sp. strain PD524, a hyperthermophile from a hot spring in Northern Thailand. Extremophiles 2015;19(4):853-61.

Lee LS, Goh KM, Chan CS, Annie TGY, Yin WF. Microbial diversity of thermophiles with biomass deconstruction potential in a foliage-rich hot spring. Microbiology Open 2018:e00615.

Lesley AC, Brett JT, Glen NM, Scott AH, James RE. Strontium isotopes in tap water from the coterminous USA. Ecosphere 2012;3(7):67.

Lin SY, Hameed A, Wen CZ, Hsu YH, Liu UC. *Hydrogenophaga aquatica* sp. nov., isolated from a hot spring. International Journal of Systematic and Evolutionary Microbiology 2017;67(10):3716-21.

Mahajan GB, Balachandran. Sources of antibiotics: Hot springs. Biochemical Pharmacology 2017;134:35-41.

McClung R, Roth D, Vigar M, Roberts V, Kahler A. Waterborne disease outbreaks associated with environmental and undetermined exposures to water-United States, 2013-2014. Morbidity and Mortality Weekly Report 2017;66:1222-5.

Meunier PJ, Roux C, Ortolani S, Diaz CM, Compston J. Effects of long-term strontium ranelate treatment on vertebral fracture risk in postmenopausal women with osteoporosis. Osteoporosis International 2009;20: 1663-73

Meunier PJ, Roux C, Seeman E, Ortolani S, Badurski JE. The effects of strontium ranelate on the risk of vertebral fracture in women with postmenopausal osteoporosis. New England Journal of Medicine 2004:350:459-68

Mohammad BT, Daghistani HI, Jaouani A, Abdel-Latif S, Kennes C. Isolation and characterization of thermophilic bacteria from Jordanian hot springs: *Bacillus licheniformis* and *Thermomonas hydrothermalis* isolates as potential producers of thermostable enzymes. International Journal of Microbiology 2017:ID 6943952.

Purcell D, Sompong U, Yim LC, Barraclough TG, Peerapornpisal Y. The effects of temperature, pH and sulphide on the community structure of hyperthermophilic streamers in hot springs of northern Thailand. FEMS Microbiology Ecology 2007;60(3):456-66.

Quattrini S, Pampaloni B, Brandi ML. Natural mineral waters: Chemical characteristics and health effects. Clinical Cases in Mineral and Bone Metabolism 2017;13(3):173-80.

Rebellon SDE, Avendano SA, Mendez FYR. Hot springs as sources of infection: An environment overlooked by public health practitioners. Journal of Infection and Public Health 2018;18:30314-9.

Reginster JY, Seeman E, De Vernejoul MC, Adami S, Compston J. Strontium ranelate reduces the risk of nonvertebral fractures in postmenopausal women with osteoporosis: Treatment of Peripheral Osteoporosis (TROPOS) study. Journal of Clinical Endocrinology and Metabolism 2005;90:2816-22

Roux C. Strontium ranelate: Short- and long-term benefits for post-menopausal women with osteoporosis. Rheumatology 2008;47:20-2

Rozanov AS, Bryanskaya AV, Ivanisenko TV, Malup TK, Peltek SE. Biodiversity of the microbial mat of the Garga hot spring. BMC Evolutionary Biology 2017;17 (Suppl 2):254.

Seeman E, Vellas B, Benharnou C, Aquino JP, Semler J. Strontium ranelate reduces the risk of vertebral and nonvertebral fractures in women eighty years of age and older. Journal of Bone and Mineral Research 2006;21:1113-20

Signorelli C, Pasquarella C, Saccani E, Sansebastiano G. Treatment of thermal pool waters. Igiene e Sanita Pubblica 2006;62:539-52

Stefanie CP, Yara CB, Giselle ZJ, Paulo AN, Francisco LS. Violacein extracted from *Chromobacterium violaceum* inhibits *Plasmodium* growth in vitro and in vivo. Antimicrobial Agents and Chemotherapy 2009; 53(5):2149-52.

Strunecký O, Kopejtka K, Goecke F, Tomasch J, Lukavsky J. High diversity of thermophilic cyanobacteria in Rupite hot spring identified by microscopy, cultivation, single-cell PCR and amplicon sequencing. Extremophiles 2018;23(1):35-48.

Sukthana Y, Lekkla A, Sutthikornchai C, Wanapongse P, Vejjajiva A. Spa, springs and safety. Southeast Asian Journal of Tropical Medicine and Public Health 2005;36(Suppl4):10-6.

Tang K, Kobayashi RS, Champreda V, Eurwilaichitr L, Tanapongpipat S. Isolation and characterization of a novel thermostable neopullulanase-like enzyme from a hot spring in Thailand. Bioscience, Biotechnology, and Biochemistry 2008;72(6):1448-56.

Thawai C, Thamsathit W, Kudo T. *Planosporangium thailandense* sp. nov., isolated from soil from a Thai hot spring. International Journal of Systematic and Evolutionary Microbiology 2013;63(3):1051-5.

Thorolfsdottir BOT, Marteinsson VT. Microbiological analysis in three diverse natural geothermal bathing pools in Iceland. International Journal of Environmental Research and Public Health 2013; 10:1085-99.

Tirawongsaroj P, Sriprang R, Harnpicharnchai P, Thongaram T, Champreda V. Novel thermophilic and thermostable lipolytic enzymes from a Thailand hot spring metagenomic library. Journal of Biotechnology 2008;133(1):42-9.

Udomluk S, Hawkins PR, Besley C, Peerapornpisal Y. The distribution of cyanobacteria across physical and chemical gradients in hot springs in northern Thailand. FEMS Microbiology Ecology 2005;52(3):365-76.

Valeriani F, Crognale S, Protano C, Gianfranceschi G, Orsini M. Metagenomic analysis of bacterial community in a travertine depositing hot spring. New Microbiologica 2018;41(2):126-35.

Viroj W. Legionella and free living amoeba contamination in natural hot spring pools in Thailand: Overview. Bentham Science 2005;4:29-32.

Voerkelius S, Lorenz GD, Rummel S, Qutel CR. Strontium isotopic signatures of natural mineral waters, the reference to a simple geological map and its potential for authentication of food. Food Chemistry 2010;118:933-40.

Yasawong M, Areekit S, Pakpitchareon A, Santiwatanakul S, Chansiri K. Characterization of thermophilic halotolerant *Aeribacillus pallidus* TD1 from Tao Dam hot spring, Thailand. International Journal of Molecular Sciences 2011;12(8):5294-303.

Effects of Volcanic Zeolite Tuff on Olive (*Olea Europaea* L.) Growth and Soil Chemistry under a Constant Water Level: Five Years' Monitoring Experience

Jalal. A. Al-Tabbal[1*], Naji. K. Al-Mefleh[2], Kamel. K. Al-Zboon[3], and Maher. J. Tadros[2]

[1]*Al-Huson University College, Al-Balqa Applied University, Department of Nutrition and food processing, Irbid, Jordan*
[2]*Departments of Natural Resources and Environment, Faculty of Agriculture, Jordan University of Science and Technology, Jordan*
[3]*Al-Huson University College, Al-Balqa Applied University, Department of Environmental Engineering, Irbid, Jordan*

ARTICLE INFO

Received: 11 Apr 2019
Received in revised: 18 Jul 2019
Accepted: 26 Jul 2019
Published online: 9 Sep 2019
DOI: 10.32526/ennrj.18.1.2020.05

Keywords:
Nutrients/ Plant water status/ Soil amendment/ Volcanic zeolite tuff/ Olive tree

*** Corresponding author:**
E-mail: jaltabbal@bau.edu.jo

ABSTRACT

This study investigated the effects of using fine and coarse volcanic zeolite tuff on the growth of olive (*Olea europaea* L.) trees and the silty clay soil in which they were grown. Olive trees were grown in four different soil treatments: silty clay soil (S1, control), silty clay soil covered with coarse volcanic zeolite tuff (S2), silty clay soil mixed with fine volcanic zeolite tuff (S3), and silty clay soil mixed with fine volcanic zeolite tuff covered with coarse volcanic zeolite tuff (S4). The morphological and physiological characteristics of the olive plants were then monitored over a 5-year period from 2012 to 2016, and the leaf and soil chemistry were analyzed at the end of the monitoring period. It was found that the addition of volcanic zeolite tuff (treatments S2, S3, and S4) had a positive effect on shoot length (relative increases of 10%, 21%, and 29%, respectively), plant height (0.53%, 1.29%, and 3.5%), plant weight (13%, 22%, and 32.26%), number of branches (14%, 27%, and 41.5%), number of leaves (9%, 22%, and 43%), trunk diameter (9%, 22%, and 29%), and shoot diameter (12%, 22%, and 36%), as well as the relative water content (15%, 22%, and 36%) and leaf water potential (16%, 26%, and 32%) compared with the control treatment (S1). Furthermore, the contents of N and P in the plant leaves, and most of the soil chemical parameters measured significantly increased following the addition of volcanic zeolite tuff. These results highlight the benefits of using volcanic zeolite tuff as a natural, readily available, and low-cost material for soil amendment due to its large effects on plant growth and soil fertility.

1. INTRODUCTION

Jordan is ranked as the second and eighth largest exporter of table olives and olive oil, respectively. Olive oil production is an important source of income to over 180,000 Jordanian families and contributes over 150 million US dollars to the national economy (ILO, 2014).

In recent decades, olive tree (*Olea europea* L.) plantations have transitioned from traditional rain-fed to irrigated production systems. Most olive plantations occur in the Middle East and North Africa (MENA) region, in which most countries are suffering from a scarcity of water. Consequently, water management and soil amendment are key solutions to minimizing soil moisture evaporation and enhancing plant nutrient uptake, which may increase plant yield and ensure the sustainability of this tree in arid and semi-arid regions. Water conservation leads to better management of the environmental resources, support the ecological systems especially in the arid areas, and reduce the drought stress on human communities and the agriculture.

Several different approaches can be taken to conserve soil moisture and reduce the effects of water stress, such as the addition of crop residues, mulch plants, waste, straw, stubble, and synthetic materials like hydro-plus zeolites to the soil (Silberbush et al., 1993). Recently, there has been a noticeable trend toward using natural materials to augment soil

Citation: Al-Tabbal JA, Al-Mefleh NK, Al-Zboon KK, Tadros MJ. Effects of volcanic zeolite tuff on olive (*Olea Europaea* L.) growth and soil chemistry under a constant water level: five years' monitoring experience. Environ. Nat. Resour. J. 2020;18(1):44-54. DOI: 10.32526/ennrj.18.1.2020.05

fertility, such as waste materials, gypsum, earthworms, and natural volcanic zeolite tuff.

Zeolitic tuff which is a normally volcanogenic sedimentary mineral made basically out of aluminosilicates is widely distributed in Jordan (Almjadleh et al., 2014). The mineral has a three dimensional precious stone cross section, with approximately bound cations, equipped for hydrating and getting dried out without changing the gem structure (Ramesh and Reddy, 2011). The unique three dimensional porous structure gives natural zeolites various application possibilities. Zeolite may help in total procedure in the soil that assumes an extensive job in improving the soil physical qualities, for example, pressure driven conductivity, penetration and ventilation (Mirzaei et al., 2015) just as in improving the carbon sequestration in soil (Lal, 2015).

Natural zeolite was shown to improve soils and reduce the harmful effects of water stress in arid and semi-arid area (Ghanbari and Ariafar, 2013) due to their ability to improve water storage, making it available for plant growth and production (Manivannan et al., 2007; Zhang et al., 2007). Because of the excess of negative charge on the surface of zeolite, which results from isomorphic replacement of silicon by aluminum in the primary structural units, natural zeolites belong to the group of cationic exchangers and thus it tends to be utilized to improve the soil (Najafi-Ghiri, 2014). Natural zeolite-enriched soils increased water holding capacity by (18-19%) and cation exchange capacity by 30-40% (Jakkula and Wani, 2018). The utilization of zeolite in dry season periods significantly affects fundamental oil yield of Medicinal Peppermint (Ghanbari and Ariafar, 2013). The expansion of zeolite had a constructive outcome on physicomorpological qualities of Moldsvian Balm (Gholizadeh et al., 2010).

Several studies have reported the positive impact of volcanic zeolite tuff additions on plant growth (Bybordi and Ebrahimian, 2013; Ozbahce et al., 2015), plant yield (Ozbahce et al., 2015), soil moisture content (Al-Busaidi et al., 2008), soil nutrient levels (Perez-Caballero et al., 2008), improve soil physio-chemical properties, and the soil biota (Da Silva et al., 1993; Giuffrida and Consoli, 2015). The addition of zeolites to soil helps to control soil pH and improve ammonium retention (Jakkula and Wani, 2018). Due to its superior adsorbent properties, Jordanian volcanic zeolite tuff has been used successfully in many engineering applications, such as water decontamination (Al-Zouby et al., 2017), heavy metal removal (Al-zboon et al., 2016), gas adsorption (Al-Harahsheh et al., 2014), and soil amendment (Al-Tabbal et al., 2016). Zeolite can hold supplements in the root zone of plants until required. This prompts increasingly effective utilization of N and K manures, utilizing less compost for a similar yield or use of same measure of compost for longer enduring and creating higher yields (Gamze, 2007; Khodaei-Joghan and Asilan, 2012).

A few studies have evaluated the benefits of using Jordanian natural volcanic zeolite tuff on plant growth and soil properties in the agricultural field, and those that have only measured short-term plant growth in crops such as salvia (*Salvia officinalis*) (Owais et al., 2013), tomato (*Solanum lycopersicum*) (Al-Qarallah et al., 2013), and cucumber (*Cucumis sativus*) (Manolov et al., 2005).

Therefore, this paper investigated the effects of natural volcanic zeolite tuff as a low-cost natural material on the morphological and physiological characteristics of olive trees, as well as the soil and leaf chemistry over a 5-year monitoring period. The comprehensive monitoring procedure, long monitoring period (5 years), analysis of plant growth (olive tree), and suite of parameters that were considered are key strengths of this research.

2. METHODOLOGY

2.1 Soil treatments

A pot experiment was conducted in an open field at Al-Huson University College of Al Al-Balqa' Applied University in the northern part of Jordan (32°27′N, 35°27′E). This site is at an altitude of 650 m and receives an average annual rainfall of 450 mm. The research was conducted using the olive cultivar “Nabali baladi”, which is widely planted in orchards and nurseries. One-year-old transplants of this cultivar were obtained from a government nursery (Faisal Nursery) and planted in 20-l pots filled with different media. Growth was then measured over five successive seasons from 2012 to 2016. The soil taxonomy system can be classified as vertisol (Chromoxeret).

Four different soil media were used as treatments: The control soil was silty clay texture (S1), silty clay soil covered with coarse volcanic zeolite tuff (S2), silty clay soil mixed with fine volcanic zeolite tuff (S3), and silty clay soil mixed with fine volcanic zeolite tuff covered with coarse

volcanic zeolite tuff (S4). The coarse volcanic zeolite tuff cover with size of 6-20 mm was added on the soil surface to a depth of 5 cm, whereas the fine volcanic zeolite tuff with size of <0.06 mm was mixed with the soil at a 1:3 ratio. In the fine volcanic zeolite tuff+ coarse volcanic zeolite tuff treatment, a total of 4 kg of volcanic zeolite tuff was added on the soil surface. X-ray fluorescence (XRF) analyses have previously shown that the volcanic zeolite tuff material consists of 44.56% SiO_2, 11.74% Al_2O_3, 10.78% Fe_2O_3, 10.46% CaO, 8.81% MgO, 1.5% K_2O, 0.52% P_2O, 2.63% TiO_2, 1.87% Na_2O, and 0.11% MnO (Al-zboon et al., 2016). The volcanic zeolite tuff had an average bulk density of 1872 kg/m^3 and a water absorption ratio of 12.7% (Al-zboon and Al-Zouby, 2015; Al-zboon and Al-Zouby, 2017). Silty clay is generally brownish gray, with soft and creamy texture, flow shape and with clay content more than 40% with field capacity equal 35 % (10% sand, 49.4 silt, and 40.6 clay).

The treatments were arranged in a randomized complete block design (RCBD) with four replications. Gravimetric determinations of the water contents of the soil were made by weighing soil samples before and after oven drying to a constant weight at 80 °C. These values were then used to calibrate all measurements of moisture content of the substrates in the pots. Field capacity (FC) was determined 48 h after irrigation, and was calculated according to the equation of Paquin and Mehuys (1980). The level of water was then maintained at between 50% and 70% of FC by manual irrigation and was checked by weighing individual pots each day to maintain the required level of moisture.

At the beginning of the experiment, all trees had a uniform height of 1 m. To enhance root development, the trees were irrigated to the pot capacity for 1 month prior to starting the experiment.

2.2 Plant water status

The two most important indicators of water deficit in plants are the relative water content (RWC) and leaf water potential.

2.2.1 Relative water content

Relative water content was measured in five leaves per plant that were detached from a similar position along the shoots, using three replicate trees per treatment. Following cutting, the petiole of each leaf was immediately immersed in distilled water inside a glass tube. The tube was then sealed, placed in a cold container, and transported to the laboratory, where the increased weight of the tube was used to determine the leaf fresh weight (FW). After 48 h in dim light, the leaf was again weighed to obtain the turgid weight (TW). The dry weight (DW) was then measured after oven drying at 80 °C for 48 h and RWC was calculated as (Ozbahce et al., 2015):

$$\mathrm{RWC} = \left(\frac{\mathrm{FW} - \mathrm{DW}}{\mathrm{TW} - \mathrm{DW}}\right) \times 100$$

2.2.2 Leaf water potential

Leaf water potential (Ψ_w) was measured in the third and fourth fully expanded leaves per plant, with three replicates per treatment. Measurements were made immediately after removing the leaves at midday (12.00) using a Sholander pressure chamber (Model 600; PMS Instruments Co. Corvallis, OR, USA).

2.3 Soil and plant chemistry

At the end of the 5-year experimental period, soil samples were taken at two depths (0-30 cm) from each treatment, air-dried at room temperature, and ground to pass through a 2-mm sieve. These samples were then analyzed for pH, electrical conductivity (EC), Na, Ca, Mg, N, P, K, exchangeable sodium percentage (ESP), sodium adsorption ratio (SAR), total cations, $CaCO_3$, and organic matter. These analyses were carried out according to the standard methods of soil analysis (Van, 2002). Leaves were also collected from the middle of new shoots (fully matured) and analyzed for the nutrients N, P, K, Ca, Mg, and Na according to the Official Methods of Analysis of HORWIZ (2000).

2.4 Morphological indicators

The trunk diameter (approximately 10 cm above the soil surface), number of branches per plant, main shoot diameters, and main shoot lengths (labeled shoot) were monitored annually from the year of planting (2012) to the end of 2016, while measurements of plant height were made from the second year onward. Plant weight (trunk, shoot, and leaves), the number of leaves per plant, and the fresh weight of roots were measured at the end of the 5-year period.

2.5 Statistical analysis

The data for each season were statistically analyzed using analysis of variance (ANOVA) followed by Fisher's Least Significant Difference

(LSD) test using SAS statistical software (SAS, 2004).

3. RESULTS

3.1 The growth of olive tree

The effect of adding volcanic zeolite tuff materials as a mixture and as cover on the soil surface on olive plant characteristics was determined over the 5-year monitoring period. The study clearly demonstrated that the addition of volcanic zeolite tuff material (treatments S2, S3, and S4) improved the vegetative growth characteristics of olive trees compared with the control (S1), with significant effects on shoot length (Figure 1), shoot diameter (Figure 2), trunk diameter (Figure 3), plant height (Figure 4), number of branches (Figure 5), number of leaves (Figure 6) and plant weight (Figure 7). The treatment in which the soil was mixed with fine volcanic zeolite tuff and covered with coarse volcanic zeolite tuff (S4) had a greater effect on all growth characteristics than the treatments in which the soil was covered with coarse volcanic zeolite tuff (S2) or mixed with fine tuff (S3).

The maximum shoot length at the end of experimental period was 64.6 cm for plants in the S4 treatment, with the S2, S3, and S4 treatments increasing the shoot length by 10%, 21%, and 29%, respectively, compared with the control (S1). Similar trends were observed for the other vegetative parameters measured, with the S4 treatment having the greatest effect, and treatments S2, S3, and S4 increasing plant height by 0.53%, 1.29%, and 3.5%; plant weight by 13%, 22%, and 32.26%; the number of branches by 14%, 27%, and 41.5%; the number of leaves by 9%, 22%, and 43%; trunk diameter by 12%, 20%, and 29%; and shoot diameter by12%, 22%, and 36%, respectively, at the end of the experiment. Thus, the impact of the treatments on the vegetative growth of olive trees can be ranked as S4>S3>S2>S1. These differences in growth parameters were observed over all of the experimental periods.

3.2 Relative water content and leaf water potential

The addition of tuff (treatments S2, S3, and S4) significantly increased the RWC and leaf water potential of the leaves compared with the control (S1), resulting in 15%, 22%, and 36% increases in RWC, respectively (Figure 8) and 16%, 26%, and 32% increases in leaf water potential, respectively, compared with S1 (Figure 9).

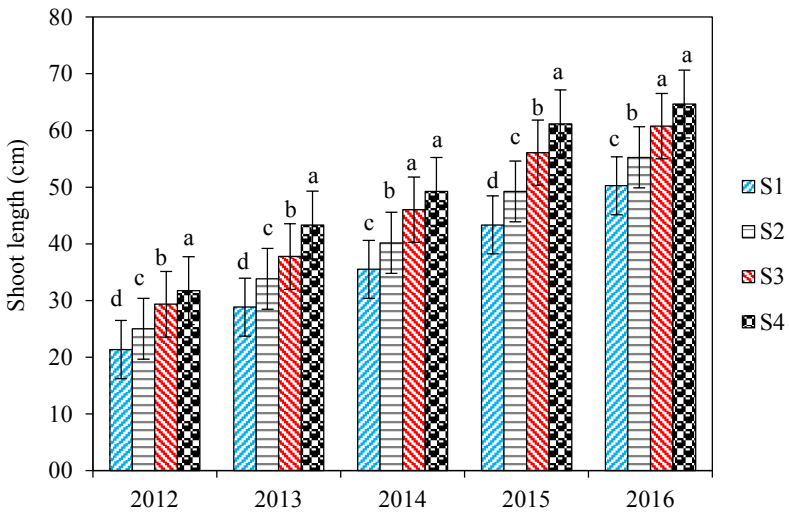

Figure 1. Shoot length of olive trees grown in in four different soil treatments, bars (indicate for standard error) with the same letters are not significantly different at p <0.05.

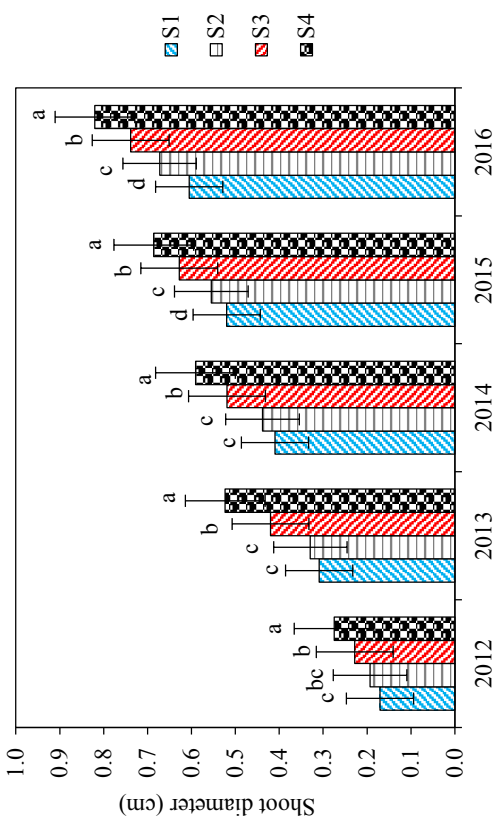

Figure 2. Shoot diameter of olive trees grown in in four different soil treatments, bars (indicate for standard error) with the same letters are not significantly different at $p<0.05$.

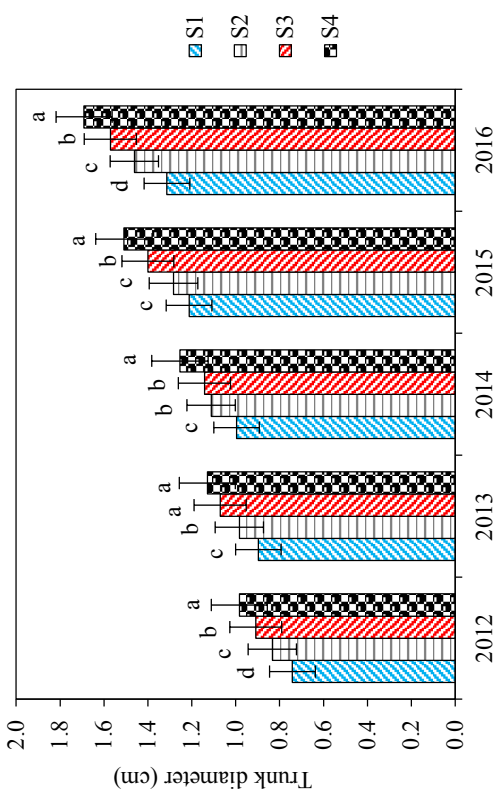

Figure 3. Trunk diameter of olive trees grown in in four different soil treatments, bars (indicate for standard error) with the same letters are not significantly different at $p<0.05$.

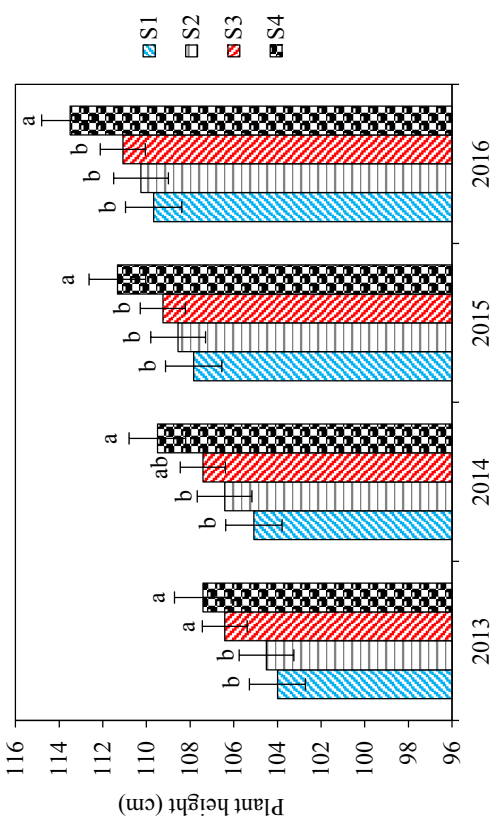

Figure 4. Plant height of olive trees grown in in four different soil treatments, bars (indicate for standard error) with the same letters are not significantly different at $p<0.05$.

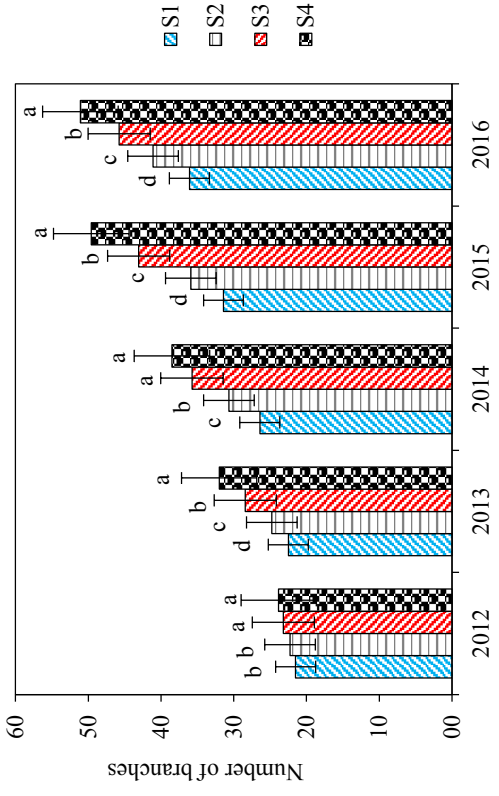

Figure 5. Number of branches of olive trees grown in in four different soil treatments, bars (indicate for standard error) with the same letters are not significantly different at $p<0.05$.

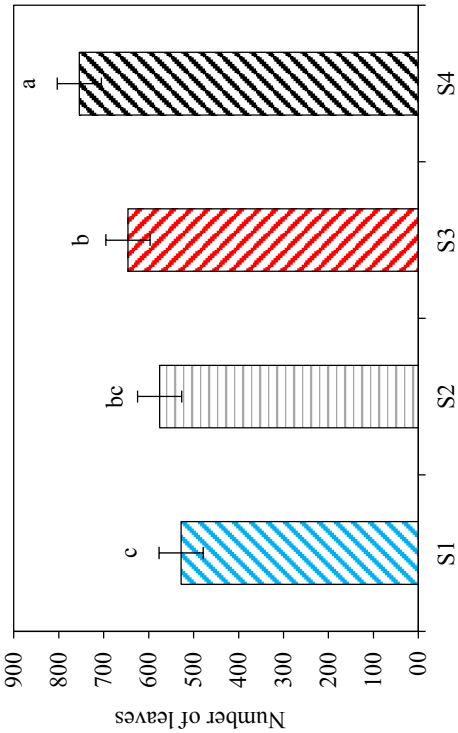

Figure 6. Number of leaves of olive trees grown in in four different soil treatments, bars (indicate for standard error) with the same letters are not significantly different at p<0.05.

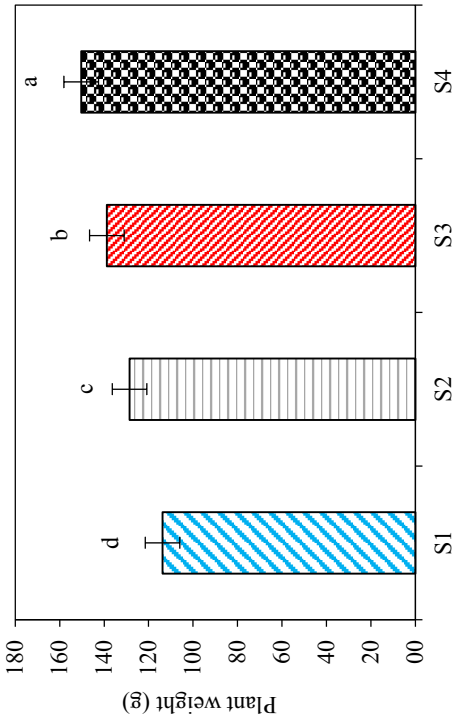

Figure 7. Plant weight of olive trees grown in in four different soil treatments, bars (indicate for standard error) with the same letters are not significantly different at p<0.05.

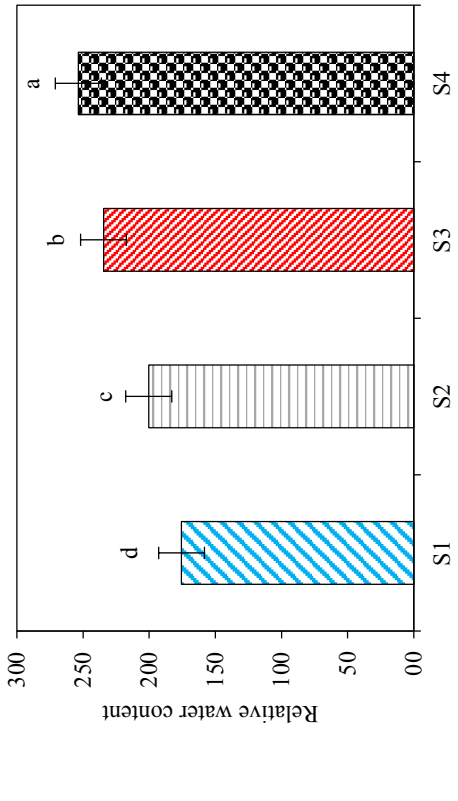

Figure 8. Relative water content of olive leaves grown in in four different soil treatments, bars (indicate for standard error) with the same letters are not significantly different at p<0.05.

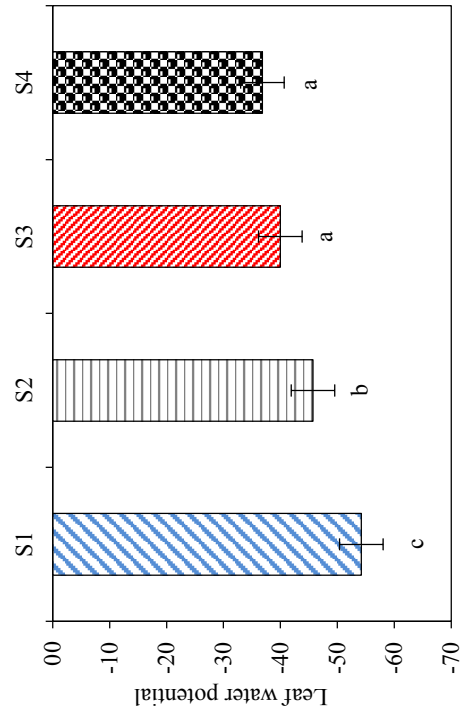

Figure 9. Leaf water potential of olive leaves grown in in four different soil treatments, bars (indicate for standard error) with the same letters are not significantly different at p<0.05.

3.3 Plant leaf chemistry

There were significant increases in the N, P, and Na contents of leaves in plants grown in volcanic zeolite tuff-treated soil, with the S4 treatment leading to 16.8%, 28.6%, and 116% increases, respectively, compared with S1 (Table 1). However, there were no significant differences in the contents of K, Ca, and Mg between treatments.

Table 1. The chemical characteristics of the plant under different soil treatments at the end of the experiment.

Treatment	N	P	K	Na	Ca	Mg
	%	%	%	%	%	%
S4	1.095[a]	0.018[a]	0.348[a]	0.080[a]	2.115[c]	0.402
S3	1.086[a]	0.014[b]	0.339[a]	0.063[b]	2.305[b]	0.407[a]
S2	1.052[a]	0.013[b]	0.342[a]	0.040[c]	2.474[a]	0.398[a]
S1	0.937[b]	0.014[b]	0.363[a]	0.037[d]	2.429[ab]	0.381[a]
F value	**	**	ns	**	ns	ns
C.V. (%)	4.09	8.2	9.52	9.98	9.19	9.02

*,**, ns indicate significant difference at $p \leq 0.05$, $p \leq 0.01$ and non-significant difference, respectively.

3.4 Soil chemistry

Treatment of the soil with volcanic zeolite tuff resulted in an increase in ECe, $CaCO_3$, K, P, SAR, Na, Mg, and Ca, with treatment S4 resulting in the greatest differences from the control (S1), followed by S3 and S2 (Table 2). By contrast, there were no significant differences in the pH and organic matter content between treatments. The soil pH values ranged from 7.73 to 7.78, which are within the most preferable range (6.5-8.5) for agricultural soils, while the organic matter contents ranged from (0.49-0.58%). Based on the pH and ECe values, the soil can be characterized as moderately alkaline (pH=7.5) and unsaline (ECe<0.4 S/m).

4. DISCUSSION

All of the soil amendments used in this study had a significant effect on the morphological traits of olive plants. Plant weight, shoot length, shoot diameter, trunk diameter, the number of branches, plant height, and the number of leaves were significantly higher in plants that were grown in amended soils compared with the control (S1), with the combined fine and coarse tuff treatment (S4) having a larger effect than the fine tuff treatment (S3) and the coarse tuff treatment (S2) alone. The change in plant weight was caused by an increase in the vegetative components such as the number of leaves, number of branches, trunk diameter, and plant height. The observed increase in vegetative growth and plant height in plants grown in the amended soils (S2-S4) indicates that they were not subjected to water stress unlike the control plants (S1). It is known that plants that are not affected by drought stress have an increased plant height as a result of an increase in cell division and assimilate transport, which leads to an increased number of nodes and internode lengths (Wright et al., 1995).

The addition of volcanic zeolite tuff improved the water and nutrient contents of the soil, which explains the improvement in all of the growth parameters measured. The high porosity of volcanic zeolite tuff increases its water holding capacity and allows water to be released when required by plants (Mumpton, 1999). Zeolites are able to lose and gain water reversibly, without any change in their crystal structure, allowing them to be used as fertilizers, stabilizers, and chelators (Perez-Caballero et al., 2008). A layer of coarse tuff covering the soil acts as a mulching material that maintains the humidity at the soil surface and prevents airflow, keeping the moisture in the soil and helping plants to produce more leaves, which results in an improvement in other morphological traits. The RWC of the leaves was considerably higher in olive plants that were grown in amended soils (S2-S4) compared with the control (S1). Leaf RWC is closely related to cell volume and is considered an important criterion of plant water status that indicates the level of water stress in the leaves (Merah, 2001), and the balance between water supply to the leaf and transpiration rate (Farquhar et al., 1989). Thus, leaf RWC reflects

Table 2. The chemical characteristics of the soil treatments at the end of the experiment

Treatment	ECe	pH	OM	$CaCO_3$	N	K	P	ESP	SAR	Na	Mg	Ca
	S/m		%	%	%	mg/kg	mg/kg	%		mg/kg	mg/kg	mg/kg
S4	0.178^{a}	7.78^{a}	0.49^{a}	14.25^{a}	0.11^{a}	265.48^{a}	0.3096^{a}	3.80^{a}	3.60^{a}	31.35^{a}	58.368^{b}	93.386^{a}
S3	0.174^{ab}	7.78^{a}	0.52^{a}	13.35^{b}	0.09^{b}	249.45^{b}	0.2683^{b}	3.57^{a}	3.44^{a}	30.13^{a}	58.854^{a}	94.588^{a}
S2	0.166^{b}	7.73^{a}	0.58^{a}	13.37^{b}	0.08^{b}	247.50^{b}	0.2683^{b}	3.25^{ab}	3.20^{b}	27.73^{b}	55.692^{d}	94.588^{a}
S1	0.152^{c}	7.78^{a}	0.54^{a}	12.98^{b}	0.09^{b}	240.85^{c}	0.2476^{b}	2.82^{b}	2.90^{c}	24.64^{c}	56.665^{c}	87.775^{b}
F value	**	ns	ns	*	**	**	*	ns	**	**	**	**
C.V. (%)	2.62	2.47	9.18	2.65	7.06	0.95	5.93	11.04	2.66	2.77	0.16	1.41

*, **, ns indicate significant difference at $p \leq 0.05$, $p \leq 0.01$ and non-significant difference, respectively.

the metabolic activity in tissues (Flower and Ludlow, 1986), which declines significantly under water stress. When there is a low water content in the soil and roots, plants are unable to compensate for water losses through transpiration, resulting in a reduction in leaf RWC (Shalhevet, 1993; Singh and Singh, 1995; Gadallah, 2000). Therefore, the high RWC that was observed in plants grown in soils treated with volcanic zeolite tuff and volcanic zeolite tuff cover indicates that there was sufficient water in the soils and roots, which contrasts with the lower RWC found in the control treatment. This demonstrates the high impact that volcanic zeolite tuff treatment and volcanic zeolite tuff cover have on water content and subsequently RWC, supporting previous findings (Eskandari Zanjani et al., 2012). Similarly, leaf water potential also tended to be higher in plants that were grown in amended soils, which, combined with the higher RWC, resulted in a higher stomatal conductance and photosynthetic rate. The findings of the present study support those of previous studies, which have suggested that mulching with various materials sequesters water and prevents evaporative water loss from the soil (Hartman et al., 2000; Yamanaka et al., 2004; Sinkevičienė et al., 2009), which, in turn, enhances the photosynthetic rate in the leaves of plants grown under these conditions (Ni et al., 2016). Qin et al. (2015) found that soil mulching reduced evaporation, increased the water potential, and subsequently modified soil temperature, increasing the yields and water use efficiencies of maize (*Zea mays*) and wheat (*Triticum aestivum*) by up to 60%. The positive effect of volcanic zeolite tuff on plant growth and yield can be attributed to its high affinity for nutrients, and high capability of improving N absorption (Bybordi and Ebrahimian, 2013) and the P content of the soil (Pirzad and Mohammadzade, 2014) by preventing nutrient leaching (Gholam-hoseini et al., 2012). It has also previously been shown that zeolite amendment improves the nutrient use efficiency of plants by improving the use of N compounds, increasing P availability, reducing leaching losses of exchangeable cations, especially K^{+}, and acting as a slow-release source of nutrients that are made available when the plant needs them (Barbarick et al., 1990; Bernardi et al., 2008).

Many studies have demonstrated a positive effect of using zeolite on plant leaves, and a favorable effect on the main nutrients (N, P, K, and Ca)

in leaves and fruits (Jakab and Jakab, 2010). For example, Ozbahce et al. (2015) found that zeolite significantly affected the N, K, Zn, Mn, and Cu contents in leaf samples, which increased with increasing rates of zeolite application, and Perez-Caballero et al. (2008) similarly found that the levels of K and N in olive tree leaves increased following the addition of zeolite to the soil due to the absorption of NH_4^+ by the zeolites and the reduced losses of NO_3^- through leaching.

Chemical analysis of the volcanic zeolite tuff indicated that it is rich in Mg, Na, K, and Ca, which explains the increase in the concentrations of these elements in the treated soils. The high ECe values in the treated soils could be attributed to the increase in the concentrations of Na and Mg due to the ability of zeolite to enhance the water and salt holding capacity of soil (Al-Busaidi et al., 2008). A similar result was obtained by Ghazavi (2015), who reported 21.6% and 33% increases in soil ECe following the addition of 10% and 20% zeolite, respectively, to the control soil. The concentrations of the main cations (Ca, Na, and K) were also significantly higher in volcanic zeolite tuff-treated soils than the control soil, whereas the addition of volcanic zeolite tuff had no significant effect on the soil pH. Jakab and Jakab (2010) showed that zeolite volcanic tuff improves N maintenance and increases the mobile K content of soil two to three fold, which explains the increase in nutrients that occurred in the treated soil. Similarly, Perez-Caballero et al. (2008) found that soil K and N contents increased significantly as the application rate of zeolite increased from 0 to 4 kg/m^2, particularly at >3 kg/m^3. Ghorbani and Agha babaei (2008) found that the addition of zeolite to the soil at low rates (<1:20) decreased the soil salinity at an initial water NaCl salinity of 15 dS/m, while a higher rate of zeolite application significantly increased the EC.

5. CONCLUSION

Five years monitoring period of olive trees indicated that amendment of the soil with volcanic zeolite tuff especially fine volcanic zeolite tuff increased both relative water content and leaf water potential. Amended soils also had higher levels of EC, $CaCO_3$, N, K, P, SAR, Na, Mg, and Ca compared with the control soil, while plants that were grown on these soils had higher contents of N, P, and Na in their leaves. Based on the observed changes in physiological parameters and chemistry, it is considered that the amendment of soil with fine and coarse volcanic zeolite tuff ameliorates reduced olive growth under moisture stress by conserving water, increasing nutrient levels in the soil, and preventing nutrient leaching. The outcomes of this research may help in better utilization of water resources in the agricultural sector, optimize the utilization of ZT as a natural material, improve soil fertility, enhance food productivity, subsequently increase the farmers' income, and improve their life.

ACKNOWLEDGEMENTS

We acknowledge the Scientific Research Fund for funding this project, the National Agricultural Research Center (NARC), for their help in chemical analysis and Al-Balqa Applied University for providing the required land for olive cultivation. The authors would like to thank the Jordan University of Science and Technology for supporting this research.

REFERENCES

Al-Busaidi A, Yamamoto T, Inoue MA, Eneji AE, Mori Y, Irshad M. Effects of zeolite on soil nutrients and growth of barley following irrigation with saline water. Journal of Plant Nutrition 2008;31:1159-73.

Al-Harahsheh M, Shawabkeh R, Batiha M, Al-Harahsheh A, Al-Zboon K. Sulfur dioxide removal using natural zeolitic tuff. Fuel Processing Technology 2014;126: 249-58.

Almjadleh M, Alasheh S, Raheb I. Use of natural and modified Jordanian zeolitic tuff for removal of cadmium (II) from aqueous solutions. Jordan Journal of Civil Engineering 2014;8(3):332-43.

Al-Qarallah B, Hamdi MR, El Shair M, Al-Hadidi NA, Hamaideh A, Shiyab S, Thalji T. Plant growth-promoting zeolitic tuff: A potential tool for arid land rehabilitation. American-Eurasian Journal of Agricultural and Environmental Sciences 2013;13(8): 1141-9.

Al-Tabbal J, Al-Zboon K, Al-Zouby J, Al-Smadi B, Ammary BY. Effect of zeolux use on sage (*Salvia officinalis*) plant irrigated by fresh and RO reject waters. Global Nest Journal 2016;18(2):416-25.

Al-Zboon KK, Al-Al-Zouby J. Natural volcanic tuff for sustainable concrete industry. Jordan Journal of Civil Engineering 2017;11(3):408-23.

Al-Zboon KK, Bashar M, Al-Smadi B, Al-Khawaldh S. Natural volcanic tuff-based geopolymer for Zn removal: Adsorption isotherm, kinetic, and thermodynamic study. Water, Air, and Soil Pollution 2016;227(7):227-48.

Al-Zboon KK, Al-Al-Zouby J. Effect of volcanic tuff on the characteristics of cement mortar. European Journal of Environmental and Civil Engineering 2015;20:520-31.

Al-Zouby J, Al-Zboon KK, Al-Tabbal J. Low-cost treatment of grey water and reuse for irrigation of home garden plants. Environmental Engineering and Management Journal 2017;16(2):351-9.

Barbarick KA, MLai TM, Eberl DD. Exchange fertilizer (phosphate rock plus ammonium-zeolite) effects on sorghum-Sudan grass. Soil Science Society of America Journal 1990;54:911-6.

Bernardi ACC, Werneck CG, Haim PG, Rezende NGAM, Monte MBM. Growth and mineral nutrition of rampur lime rootstock cultivated in substrate with zeolite enriched with NPK. Brazilian Magazine of Fruit Culture 2008;30(3):794-800.

Bybordi A, Ebrahimian E. Growth, yield, and quality components of canola fertilized with urea and zeolite. Communications in Soil Science and Plant Analysis 2013;44(19):2896-915.

Da Silva F, Wallach R, Chen Y. Hydraulic properties of sphagnum peat moss and tuff (scoria) and their potential effects on water availability. Plant and Soil 1993;154:119-26.

Eskandari Zanjani K, Shirani Rad AH, Naeemi M, Moradi Aghdam A, Taherkhani T. Effects of zeolite and selenium application on some physiological traits and oil yield of medicinal pumpkin (*Cucurbita pepo* L.) under drought stress. Current Research Journal of Biological Sciences 2012;4(4):462-70.

Farquhar GD, Wong SC, Evans JR, Hubic KT. Photosynthesis and gas exchange. In: Jones HG, Flowers TJ, Jones MB, editors. Plants under Stress. Cambridge, USA: Univ Press; 1989. p 47-69.

Flower DJ, Ludlow MM. Contribution of osmotic adjustment to the dehydration tolerance of water stressed pigeon pea (*Cajanas cajan* (L) Milsp) leaves. Plant, Cell and Environment 1986;9:33-40.

Gadallah MAA. Effects of indole-3-acetic acid and zinc on the growth, osmotic potential and soluble carbon and nitrogen components of soybean plants growing under water deficit. Journal of Arid Environments 2000;44(4):451-67.

Gamze TN. The effects of natural zeolite on salinity level of poultry litter compost. Bioresource Technology 2007;99: 2097-101.

Ghanbari M, Ariafar S. The effect of water deficit and zeolite application on growth traits and oil yield of Medicinal Peppermint (*Mentha piperita* L.). International Journal of Medicinal and Aromatic Plants 2013;3(1):33-9.

Ghazavi R. The application effects of natural zeolite on soil runoff, soil drainage and some chemical soil properties in arid land área. International Journal of Innovation and Applied Studies 2015;13(1):172-7.

Gholamhoseini M, Aghaalikhani M, Khodaei-Joghan A, Zakikhani H, Dolatabadian A. How zeolite controls nitrate leaching and modifies canola grain yield and quality. Agricultural Research and Reviews 2012;1:113-26.

Gholizadeh A, Amin MSM, Anuar AR, Saberioon MM. Water stress and natural zeolite impacts on phisiomorphological characteristics of Moldavian balm (*Dracocephalum moldavica* L.). Australian Journal of Basic and Applied Sciences 2010; 4(10):5184-90.

Ghorbani H, Agha babaei A. The effects of natural zeolite on ions adsorption and reducing solution electrical con ductivity I) Na and K Solutions. International Meeting on Soil Fertility Land Management and Agroclimatology Turkey 2008;Special Issue:947-55.

Giuffrida F, Consoli S. Reusing perlite substrates in soilless cultivation: Analysis of particle size, hydraulic properties, and solarization effects. Journal of Irrigation and Drainage Engineering 2016;142(2): 04015047.

Hartman JR, Pirone TP, Sall MA. Pirone's Tree Maintenance. 7th ed. New York, USA: Oxford University Press; 2000.

Horwiz W. Official Methods of Analysis of the Association of Official Analytical Chemists AOAC (Association of Official Analytical Chemists). 17th ed. Washington, DC: Association of Official Analytical Chemists; 2000.

International Labor Organization (ILO). Draft Report: Market Study and Marketing Strategy of Olive Sector in Irbid. International Labor Organization; 2014.

Jakab S, Jakab A. Effects of the zeolitic tuff on the physical characteristics of haplic luvisol and the quality of fruits on apple orchards. Agriculture and Environment 2010;2:31-7.

Jakkula VS, Wani SP. Zeolites: Potential soil amendments for improving nutrient and water use efficiency and agriculture productivity. Scientific Reviews and Chemical Communications 2018;8:1-15.

Khodaei-Joghan A, Asilan KS. Zeolite influences on nitrate leaching, nitrogen-use efficiency, yield and yield components of canola in sandy soil. Archives of Agronomy and Soil Science 2012;58:1149-69.

Lal R. Restoring soil quality to mitigate soil degradation. Sustainability 2015;7:5875-95.

Manivannan P, Jaleel CA, Kishorekumar A, Sankar BO, Somasundaram R. Propiconazole induced changes in antioxidant metabolism and drought stress amelioration in *Vigna unguiculata* (L.) Walp. Colloids and Surfaces B: Biointerfaces 2007;57(1):69-74.

Manolov I, Antonov D, Stoilov G, Tsareva I, Baev M. Jordanian zeolitic tuff as a raw material for the preparation of substrates used for plant growth. Journal of Central European Agriculture 2005; 6(4):485-94.

Merah O. Potential importance of water status traits for durum wheat improvement under Mediterranean conditions. Journal of Agricultural Science 2001; 137:139-45.

Mirzaei M, Akbar A, Mohsen S. Aggregation stability and organic carbon fraction in a soil amended with some plant residues, nanozeolite, and natural zeolite. International Journal of Recycling of Organic Waste in Agriculture 2015;4:11-22.

Mumpton FA. La roca magica: Uses of natural zeolites in agriculture and industry. Proceedings of the National Academy of Sciences of the United States of America 1999;96:3463-70.

Najafi-Ghiri M. Effects of zeolite and vermicompost applications on potassium release from calcareous soils. Soil and Water Research 2014;9:31-7.

Ni X, Song W, Zhang H, Yang X, Wang L. Effects of mulching on soil properties and growth of tea olive (*Osmanthus fragrans*). PLoS ONE 2016;11(8): ID e0158228.

Owais SJ, Abdel-Ghani AA, Ghrair AM, Al-Dalain SA, Almajali N. Effect of natural Jordanian volcanic tuff on growth, irrigation water saving and leaves mineral content of *Salvia officinalis*. Jordan Journal of Agricultural Sciences 2013;9(4):439-56.

Ozbahce Aynur A, Tari F, Gönülal E, Simsekli N, Padem H. The effect of zeolite applications on yield components and nutrient uptake of common bean under water stress. Archives of Agronomy and Soil Science 2015;61(5):615-26.

Paquin R, Mehuys GR. Influence of soil moisture on cold tolerance of alfalfa. Canadian Journal of Plant Science 1980;60:1351-66.

Perez-Caballero R, Gil J, Benitez C, Gonzalez JL. The effect of adding zeolite to soils in order to improve the N-K nutrition

of olive trees. American Journal of Botany 2008;2(1):321-4.

Pirzad A, Mohammadzade S. The effects of drought stress and zeolites on the protein and mineral nutrients of *Lathyrus sativus*. International Journal of Biosciences 2014;4(7):241-8.

Qin W, Hu C, Oenema O. Soil mulching significantly enhances yields and water and nitrogen use efficiencies of maize and wheat: a meta-analysis. Scientific Reports 2015;5:1-13.

Ramesh K, Reddy DD. Zeolites and their potential uses in agriculture. Advances in Agron 2011;113:219-35.

SAS Institute Inc. SAS User's Guide: Statistics Version 9 for Windows. Cary, NC, USA: SAS Institute; 2004.

Shalhevet J. Plants under salt and water stress. In: Fowden L, Mansfield T, Stoddart J, editors. Plant Adaptation to Environmental Stress. London, UK: Chapman and Hall; 1993. p. 133-54.

Silberbush M, Adar E, De Malach Y. Use of a hydrophilic polymer to improve water storage and availability to crops grown in sand dunes. I. corn irrigated by trickling. Agricultural Water Management 1993;23(4): 303-13.

Singh BR, Singh DP. Agronomic and physiological responses of sorghum, maize and pearl millet to irrigation. Field Crops Research 1995;42:57-67.

Sinkevičienė A, Jodaugienė D, Pupalienė R, Urbonienė M. The influence of organic mulches on soil properties and crop yield. Agronomy Research 2009;7:485-91.

Van Reeuwijk LP. Procedures for Soil Analysis. 6th ed. Netherland: International Soil Reference and Research Center; 2002.

Wright PR, Morgan JM, Jessop RS, Cass A. Comparative adaptation of canola (*Brassica napus*) and Indian mustard (*B. juncea*) to soil water deficit: Yield and yield components. Field Crops Research 1995;42(1):1-13.

Yamanaka T, Inoue M, Kaihotsu I. Effects of gravel mulch on water vapor transfer above and below the soil surface. Agricultural Water Management 2014; 67:145-55.

Zhang P, Avudzega DM, Bowman RS. Removal of perchlorate from contaminated waters using surfactant-modified zeolite. Journal of Environmental Quality 2007;36(4):1069-75.

Pine Needle Energy Potential in Conifer Forest of Western Himalayan

Vishal Sharma* and Rajeev Kamal Sharma

Chitkara University Institute of Engineering and Technology, Chitkara University, Punjab, India

ARTICLE INFO

Received: 2 Apr 2019
Received in revised: 6 Aug 2019
Accepted: 13 Aug 2019
Published online: 23 Sep 2019
DOI: 10.32526/ennrj.18.1.2020.06

Keywords:
Pine needles/ Estimation/ Conifer forest/ Himalayan

*** Corresponding author:**
E-mail:
thevishsharma@gmail.com

ABSTRACT

The present study estimates the energy potential of pine needles in the western Himalayan territory. Both a single point estimation approach and tree-canopy density approach were carried out to determine the net annual pine needle litterfall for different types of conifer forest. The annual net and gross pine needles yield in the year 2018 have been estimated to be 67.99 million tonnes and 59.02 million tonnes respectively. It provides an annual primary energy (APE) potential in electric and thermal energy form. The calculated thermal energy varied from 1.16-1.34 pJ which can provide a backup of 0.09-0.1 billion kWh. Thus, the pine needle offers a source of renewable fuel with excellent combustion characteristics of 18.64 MJ/kg. Additionally, the massive pine needles would result in a net increment of economic energy to the Himalayan regions and also control the threats of forest fires and, most importantly, scale-down the environmental pollution.

1. INTRODUCTION

The most coniferous forests in the Himalayan territories cover 1.09 million km^2 and have a high potential of pine trees (*Pinus roxiburghii*) spreading across Nepal, Bhutan, China, Pakistan, and India (Bhagat et al., 2009). The western subalpine coniferous forests in the Himalayan territory cover 39,700 km^2 on the middle and lower elevations of Nepal, Pakistan, and India. These regions have a considerable potential of forest residues in term of pine needles (Gupta, 2013). The use of pine needles for energy source is progressively gaining the attention of researchers (Nunes et al., 2016; Polphan et al., 2009). Pine needles also act as an alternative to conventional sources, can improve the energy access options, and provides many environmental benefits (Bisht and Kumar, 2014). The pine needles fall off trees from the middle of March to the onset of rain in July and lounge for a more extended period. Shed pine needles have to make a thick layer of foliage on the pinewood floor, prevent natural growth of forest flora and also have relatively poor biodegradability due to high lignin content (Lal et al., 2013). Moreover, dried pine needles are the primary cause of forest fires in the summer days. Even a small ignition of such litter on the pinewood floor damages a large economy and slaughters mature pines and forest fauna. Besides this, the heat of the wildfire that consumes dried pine needles intercept seedling growth due to prematurely opening cones which spread seeds when exposed to the fire. The wildfire also creates drastic living conditions (Zhu et al., 2019; Joseph et al., 2009; Sairorkham, 2014). Adversely, dried pine needles current usage is limited for space heating, bedding for cattle, and other residential purposes (Malik and Mohapatra, 2013). The usage quantity is measured far less than the amount of pine needles that persist on the pinewood floor every year. Some necessary information is required to ensure that the pine needles would be suitable for use as an energy feedstock (Phrommarat, 2019; Sedpho and Sampattagul, 2015). The pine needles' calorific value as an energy source of 18.64 MJ/kg is comparable to some commonly available agricultural and forestry residues. For example, the calorific value is 16.91 MJ/kg for cotton stalk (Sharma and Mohapatra, 2016), 17.10 MJ/kg for wheat straw (Jain et al., 2014), 15.40 MJ/kg for rice husk (Malik and Mohapatra, 2013), 15.70 MJ/kg for wood chips (Parikh et al., 2005), and 17.32 MJ/kg for sugarcane baggage (Bilgen and Sarikaya, 2016). Moreover, its net calorific value is in good agreement with the other parts of the pine tree. For example, the calorific value is 18.55 MJ/kg for pine cone, 20.54 MJ/kg for pine pellet, 16.64 MJ/kg for pine chip,

Citation: Sharma V, Sharman RK. Pine needle energy potential in conifer forest of Western Himalayan. Environ. Nat. Resour. J. 2020;18(1):55-65. DOI: 10.32526/ennrj.18.1.2020.06

21.78 MJ/kg for pine bark, and 16.64 MJ/kg for pinewood (Nhuchhen and Salam, 2012). Additional main attractive features of pine needles are analyzed by proximate analysis and ultimate analysis ensure the high energy potential. Volatile matter confirms the way of thermochemical conversion of pine needles during the combustion process. Pine needle has a low bulk density, further enhancing the benefits for use in conversion.

Many researchers have worked on harnessing pine for various applications. The influence of climate on the structural growth of pine trees has been studied by Sharma and Lekha (2013) and Mahajan et al. (2016). Particular interest has also been paid to the knowledge of medicinal properties of pine trees for the treatment of various tropical disorders and its antioxidant characteristics (Parikh et al., 2005). Tiwari et al. (2013) studied the effect of altitude on the morphological, epidermal, and anatomical structure of pine needles. Sharma and Lekha (2013) studied pine resin, one of the essential non-wood products for the production of turpentine. Bisht et al. (2014), Dhaundiyal and Tewari (2015), and Dhaundiyal and Gupta (2014) made attempts to harness pine needles energy generation using gasification. Joshi et al. (2017) and Pandey and Dhakal (2013) worked on the pine needles briquettes for use as energy feedstock for gasification. The following are the potential applications of pine needles for energy feedstock:

1) It can provide extra fuel for electricity generation by various thermochemical conversion systems to meet the heat requirements of industries.

2) It creates a good source of employment by opening small or medium scale industries that provide the tasks of collection, transportation, and storage.

3) Suitable feedstock for water heating, space heating, and cooking necessities of residential and commercial installations.

Pine needles availability estimation is a challenging task as its density, shape-size, and quantity may vary along with climate, location, and species (Sharma and Lekha, 2013; Bisht et al., 2014). Utilization of unexploited source of pine needles has become the impetus for a future energy system due to their multiple environmental benefits. Additionally, recognition of pine needle distribution among the selected site and also undertake the calculation of the grid accessibility for power generation. The pine needle estimation study in a particular location should cover the present biomass status, its environment effect, availability, and approximate energy potential. The present work is primarily focused on the assessment of dried pine needles litterfall data as energy feedstock and predicting the annual primary, thermal, and electrical energy-producing capacity from it.

2. METHODOLOGY

2.1 Classification of conifer forest

Forest Survey of India uses remote sensing technology to generate satellite data of forests. The satellite LISS-III with a spatial resolution of 23.50 m provides statistical information of forest cover land. Table 1 shows the forest type and tree canopy relation (Gupta, 2013). According to Dasgupta et al. (2011), the state covers 15,100 km^2 of forest including particular forest, reserved forest, private forest, unclassified forest, demarcated protected forest, un-demarcated protected forest, and other forest managed by the forest department. Canopy density or crown cover is the part of the forest floor covered by vertical projections of trees as observed from top.

Table 1. Classification of pine forest basis of canopy density (Gupta, 2013).

Number	Forest type	Canopy density	Forest cover area (km^2)	
			Himachal Pradesh	Hamirpur
1	Very dense forest (VDF)	> 70%	3,224	39
2	Moderate dense forest (MDF)	40 - 70%	6,381	86
3	Open forest (OF)	10- 40%	5,074	188
4	Scrub	< 10%	300	2

2.2 Pine needles

Pine needles (*Pinus roxburghii*) were collected from conifer forest situated in the western Himalayan region were chosen for experimentation. Pine needles were collected from four different types of pinewoods, as mentioned in Table 1. These needles were dried in the box type solar cooker for 7-8 hours at 60-80 °C and were kept in an airtight poly bag

before experimentations. The solar drying removed 40% of the initial moisture content. Table 2 shows some measurements of the dimensions of freshly litter dried pine needles. The Pulverizer mill helps to convert dried pine needle samples into fine powder for ultimate analysis and proximate analysis, as shown in Table 2. The table also shows the energy characteristics of pine needles and indicates their suitability as feedstock for thermochemical conversion in a specially designed fluidized bed (Sharma and Sharma, 2018).

Table 2. Pine needle properties as an energy feedstock

Properties	Values
Bulk density (kg/m^3)	92.11-112.00
Net calorific value (MJ/kg)	18.64
Lignocellulosic analysis (%)	Alcohol benzene extractive = 6.23 Holo cellulose content = 53.46 Lignin = 37.50
Proximate analysis (%)	Volatile matter = 75.75 Fixed carbon = 16.67 Ash content = 3.45 Moisture = 3.83
Ultimate analysis (%)	Carbon (C) = 48.20 Hydrogen (H) = 6.10 Oxygen (O) = 38.30 Nitrogen (N) = Not detected (eligible) Sulphur (S) = 0.12

2.3 Study site description

The study site, located at the lower outer range of the Himalayas, extends between 31°25'-31°52' north latitudes and 70°18'-70°44' east longitudes. The study was conducted in the Hamirpur range forest of Himachal Pradesh, with a total geographical area of 1,118 km^2. The pine trees grow naturally in abundance in 9 out of 12 districts of the state, over the altitude varying from 350-2,500 m. Out of the total area, 19.58 % area is occupied by the conifer forest along with some broad-leaved trees (Gupta, 2013). The study area overall altitude varies from 400-1,100 m above mean sea level. The climate generally remains warm (average annual temperature 21.6 °C) with an average rainfall of 157.2 cm. The study area and sampling sites are shown in Figure 1 (Gupta, 2013).

The pine needle samples were collected from 20 different forest sites, located in the Hamirpur forest range. The structural standard variables such as above-ground pine needles, number of pine trees per km^2, pine tree height, and pine tree age were measured with non-destructive methods. From each selected site, pine needles samples were collected from a 1 × 1 m area in airtight polythene bags, after removing foreign particles, from March - June 2018. The selected sites of the conifer forest are according to the working plan reported by the work plan officer (WPO) of the forest division. The pine needles samples were weighed on an Electronic balance (CT-300, Contech Instruments Ltd., India) after drying in a domestic solar cooker for 7-8 hours to remove the interstitial moisture content. Allometric and statistical sampling technique is generally used to evaluate forest statics prior to available advance applications of remote sensing satellite technology.

2.4 Pine tree age and height estimation

A study was conducted to estimate the height-age of pine trees by measuring the diameter at breast height (DBH). The total of 209 observations of pine trees were taken, to figure out the approximate age and height of trees nearby each plot. The tree calliper (Long Jaw Vernier Caliper Series 534, Roorkee Survey House Sheikhpuri Roorkee, India) was used to measure DBH of pine trees. The collected data was statically analyzed through linear regression and correlations. The height and age of pine tree were estimated based on already developed equations (Sadiq et al., 2016; Gonzalez-Benecke et al., 2014):

$$\text{Age} = 1.1627 \times \text{DBH} - 2.7039 \quad (1)$$

$$\text{Height} = 0.1792 \times \text{DBH} + 8.8237 \quad (2)$$

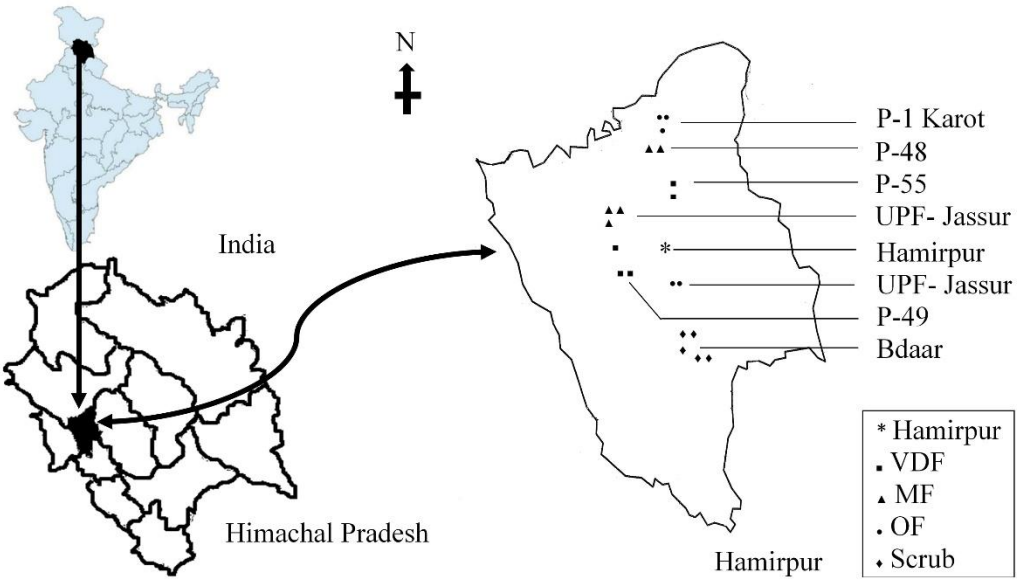

Figure 1. Pine needles collection sites surveyed in various forest range (Gupta, 2013)

2.5 Different approaches in the estimation of above ground pine needles data

2.5.1 Pine needle yield estimation per unit forest area

The pine needle litterfall generally occurs from March to the onset of the rain in July. This approach estimates the pine needle yield per square meter for different types of forest and is tabulated in Table 3. The approach is applied to the four different types of the forest canopy for potential estimation of annual pine needle yield. The collected pine needle samples varied from 2.00-2.93 kg/m^2/year for VDF, 1.12-2.20 kg/m^2/year for MDF, 0.94-1.60 kg/m^2/year for OF, and 0.18-1.10 kg/m^2/year for scrub.

Table 3. Litterfall data of pine needles in March, April, May, and June of the year 2018.

Plot number	Collection of pine needles from the forest (kg/m^2/year)			
	VDF	MDF	OF	Scrub
1	2.71	2.10	1.60	0.19
2	2.24	1.81	0.94	1.10
3	2.93	1.12	1.38	0.80
4	2.00	2.20	0.89	0.18
5	2.18	1.81	1.10	0.90
Average	2.41	1.81	1.22	0.62

The potential annual accessibility of pine needle yield along with VDF, MDF, OF, and scrub area was estimated with the average value of collected pine needles yield. Annual pine needle yield ($APNY_1$) can be estimated as (Kala and Subbarao, 2018),

$$APNY_1 = A_{VDF} \times PNY_{tree} + A_{MDF} \times PNY_{tree} + A_{OF} \times PNY_{tree} + A_{scrub} \times PNY_{tree} \quad (3)$$

Where, A_{VDF}, A_{MDF}, A_{OF}, and A_{scrub} indicate the area in km^2 under the VDF, MF, OF, and scrub, respectively, PNY_{tree} represents pine needle yield per tree.

2.5.2 Pine needle yield estimation as per canopy density based on the total number of pine tree per km^2

Canopy density characterized the percentage and helped to estimate the total number of pine tree per km^2. The forest is classified based on canopy density, as canopy density is greater for VDF as compared to MDF, OF, and Scrub. Estimating its yield per tree can predict the annual pine needle yield per km^2. Table 4 shows the pine needle yield collected from the conifer forest. The method used assumptions for calculating canopy density and the total number of trees in the known or selected area. All tree canopy

densities were measured carefully for estimation. Tree canopy density of the conifer can be a help to calculate the tree density of the forest. The tree canopy density can be described as follows (Kala and Subbarao, 2018; Gill et al., 2000; Wu, 2012):

$$D_i = 2 \times (b_o + b_1 \times DBH) \quad (4)$$

$$\text{Canopy cover} = \left(\frac{\pi}{4} \times D_i^2\right) \quad (5)$$

Tree canopy density is the measurement of tree cover per unit area of the forest land and can be described as:

$$\text{Tree canopy density} = \sum_{i=0}^{n} \left(\frac{\pi}{4} \times \frac{D_i^2}{\text{Forest area}}\right) \quad (6)$$

Where, D_i is the diameter of the tree crown, b_o=1.1817±0.2627 and b_1=0.0265±0.0040 are the regression coefficient, and DBH is the diameter at the breast height.

Table 4. Estimation of pine needle yield per tree

Forest Canopy	Pine needle yield (kg/2,500 m^2/year)	Number of Pine tree per 2,500 m^2	Pine needle per tree (kg/year)
VDF	6,023	307	19.62
MDF	4,519	268	16.86
OF	2,949	202	14.6
Scrub	1,548	195	7.94

Further trees packing in the forest are acknowledged by the green covering. For VDF the trees are packed more closely as compared to MDF, OF, and scrub. Gill et al. (2000) mentioned the average minimum crown radius for conifer trees is 2.21 m. It might be taken note that the effective diameter is smaller than the actual diameter of the canopy of the tree crown. By using this method, the total number of pine trees per 50 m × 50 m is achieved as 307 trees for VDF, 268 for MDF, 202 for OF, and 195 for the scrub area (by neglecting damaged trees and other species).

With this approach the annual pine needle yield is calculated in the following manner (Kala and Subbarao, 2018):

$$APNY_2 = A_{VDF} \times PNY_{tree} \times N_{tree,VDF} + A_{MDF} \times PNY_{tree} \times N_{tree,MDF} + A_{OF} \times PNY_{tree} \times N_{tree,OF} + A_{scrub} \times PNY_{tree} \times N_{tree,scrub} \quad (7)$$

These two simple methodologies have been considered to predict pine needle potential for all types of conifer forest canopy (VDF, MDF, OF, and scrub). Equation 3 and Equation 7 help to find the expected annual pine needle yield value in the year 2018. The first approach provides the single point estimates and the second approach gives the data based on tree canopy density of all types of conifer forest.

2.6 The annual energy potential of pine needle yield

The calorific value and the net annual pine needle yield are taken into account for available annual primary energy (APE). Electric and thermal energy from pine needles is estimated. These are the primary form of energy. The energy estimation has been carried out by using the following equation (Nhuchhen and Salam, 2012):

$$HHV_{PA} = 19.2880 - 0.2135 \times \frac{\%VM}{\%FC} - 1.958 \times \frac{\%Ash}{\%VM} + 0.0234 \times \frac{\%FC}{\%Ash} \quad (8)$$

$$HHV_{UA} = 32.7934 + 0.0053 \times (\%C)^2 - 0.5321 \times \%C - 2.87 \times \%H + 0.0608 \times \%C \times \%H - 0.2401 \times N \quad (9)$$

$$LHV_{moist\ basis} = HHV_{PA/UA} - 24.44 \times (9 \times \%H + \%M) \quad (10)$$

$$LHV_{dry\ basis} = \frac{LHV_{moist\ basis} \times 100}{100 - \%H} \quad (11)$$

Where, NCV = Net calorific value (MJ/kg) wet basis, GCV = Gross calorific value (MJ/kg) dry basis, w = Water content of the fuel as % of weight, and h = Hydrogen concentration as % of weight.

The thermal energy potential of pine needles (Given et al., 1986):

$$Q = 328.4 \times \%C + 1422 \times \%H + 92.7 \times \%S - 138 \times \%O + 636 \quad (12)$$

Where, Q = heat combustion per unit weight kJ/kg.

3. RESULTS AND DISCUSSION

3.1 Pine tree age and height

The growth rate among individual trees in the four study areas varied with diameter. The estimated DBH of pine trees range from 56.97-117.65 cm. The present work found that there was a strong relationship between diameter and age of the tree; the diameter has a direct proportion to the age of the pine tree.

From Equation 1, the age of the VDF, MDF, OF, and scrub has been calculated as 134.09 (±10.33) years, 97.7 (±6.50) years, 81.52 (±6.67) years, and 63.53 (±7.99) years respectively. The average age of pine trees lies between 30 years to 47 years for VDF, 30 years to 45 years for MF, 25 years to 35 years for OF, and 20 years to 33 years for a scrub as shown in Figure 2. A similar study revealed that growth rates changing among individual trees at study sites (Shackleton, 2002). In the comparison of the present study, it was found that the tree diameter and tree age relation have significant correlation.

The study also reported that the height of the pine trees varied from 7.9-10.6 m. The results found that the maximum height was 12.6 m with a 133.5 cm diameter and the minimum height was 7.6 m with a 56 cm diameter. The average height of all conifer forest trees was 9.6 (±1.59) m, 8.9 (±1.00) m, 8.9 (±1.02) m, and 8.9 (±1.23) m for VDF, MF, OF, and scrub, respectively as shown in Figure 2. In all types of forest canopy, the height and age increased with an increase in diameter. There is a strong direct relationship between diameter, age, and height. The pine tree environmental conditions have a significant role in regulating forest growth. A similar study by Ferguson and Carlson (2010) reported that the estimation of height and age relation was adopted to predict ages for the future. It has been concluded from the present study that forest growing stock parameters have a significant role in balancing forest growth. Thus, diameter increment has a substantial relationship with the height and age of the conifer forest and it directly affected the estimates of production in a forest area when statistically analysed (Khan et al., 2016).

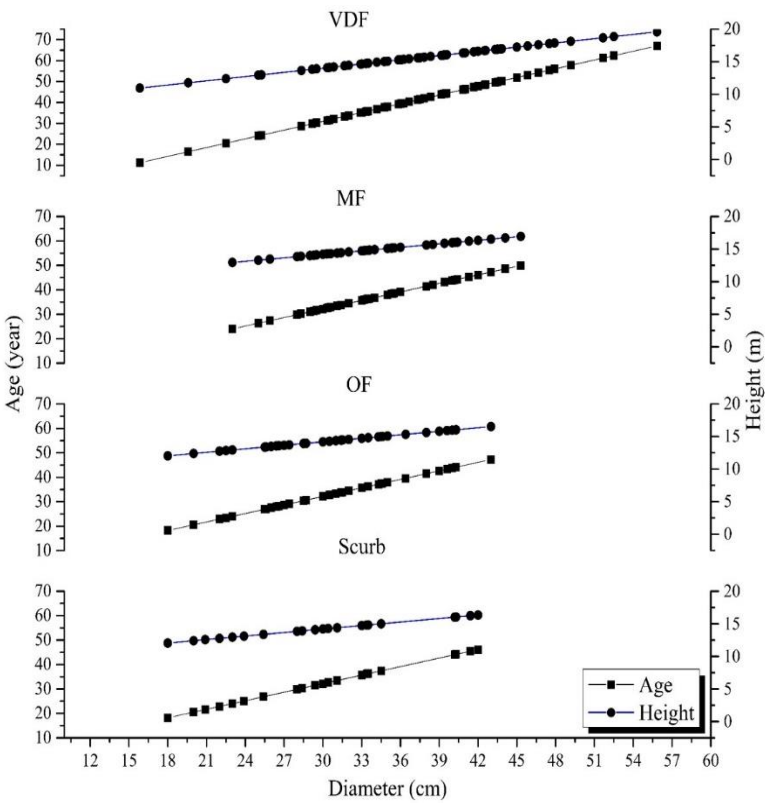

Figure 2. Relationship between the diameter, tree age, and height.

3.2 Pine needle litterfall data

The samples were collected four times at the end of each month from March - June 2018 from 20 randomly selected plots of 1 × 1 m for VDF, MF, OF, and scrub. The litterfall was lower for plot 4 in March to June as compared to all other forest canopy densities. From Figure 3, it reveals that all the forest canopies followed the same trend in terms of litterfall of pine needles in all fall-out months. The variation in the litterfall data of pine needles was due to some environmental factors like temperature, light intensity, location etc. (Lal et al., 2013). The litterfall of pine needles has shown enormous potential in VDF as compared to MF, OF, and scrub. From Figure 4, the litterfall in March showed lower potential, which tends to increase in April and May then decrease in June although this value for MF in May showed significantly different results. The maximum and minimum litterfall recorded was 1.45 kg in May of VDF (plot 3) and 0.02 kg in March of scrub (plot 4). The total observation period of litterfall was four months which is applicable for the year. The mean annual standard-litterfall rate of VDF, MF, OF, and scrub was estimated to be 3.41, 2.40, 1.22, and 0.14 (dry weight kg/m^2/year) respectively. The mainly seasonal trend for litterfall was followed in which needle fall was more significant during May. Some other environmental conditions also affect litterfall rates (Rawat et al., 2011). The proportion of each set of pine needle litterfall data is shown in Figure 4. The pine needles have the massive potential in VDF plots as compared with the MF, OF, and scrub plots in all fall-out months. The litterfall data has shown a significant variation ranging from 0.02 kg from the scrub in March (plot 4) to 1.45 kg from VDF in May (plot 3).

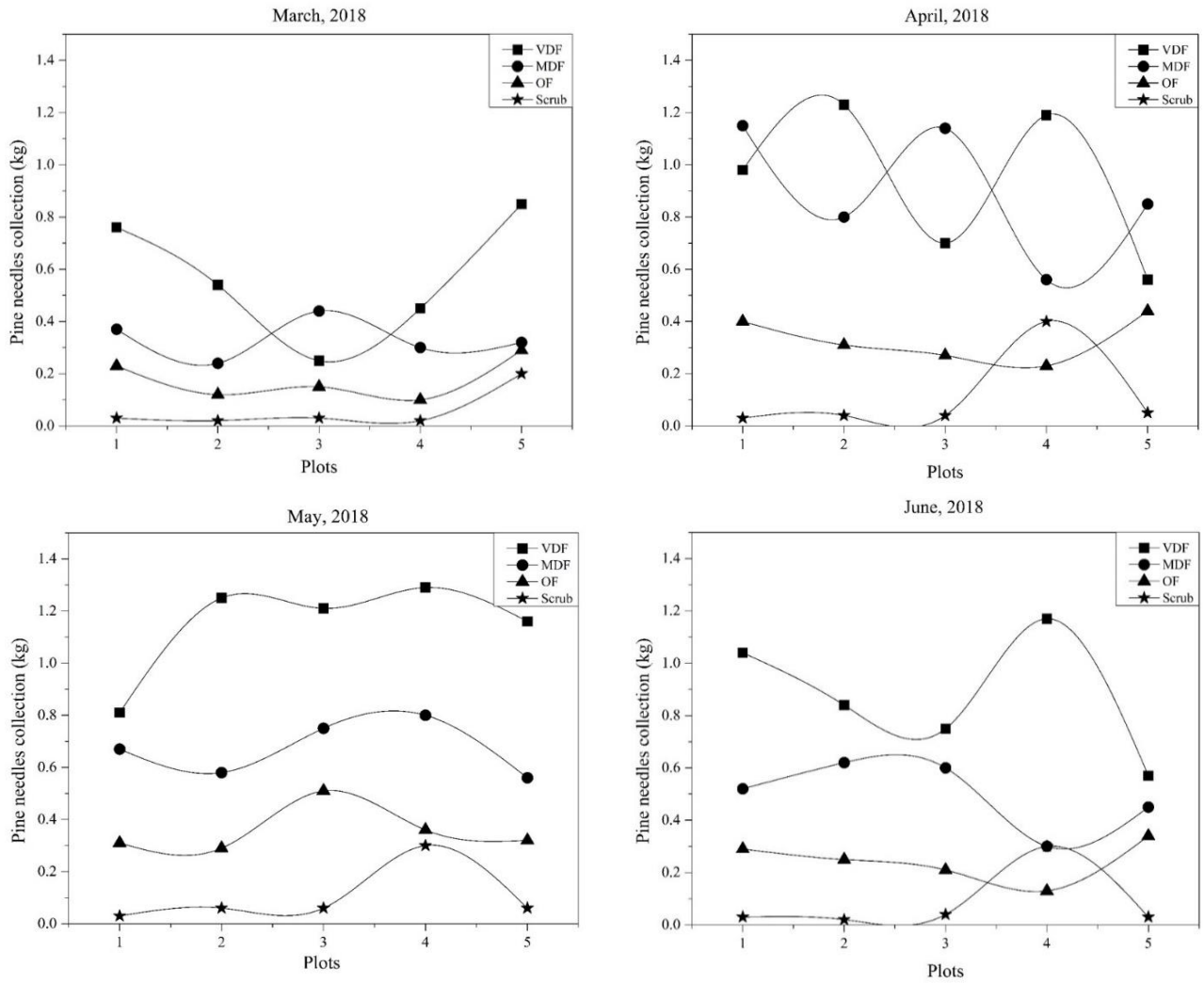

Figure 3. Litterfall data of pine needles in the month of March, April, May, and June 2018

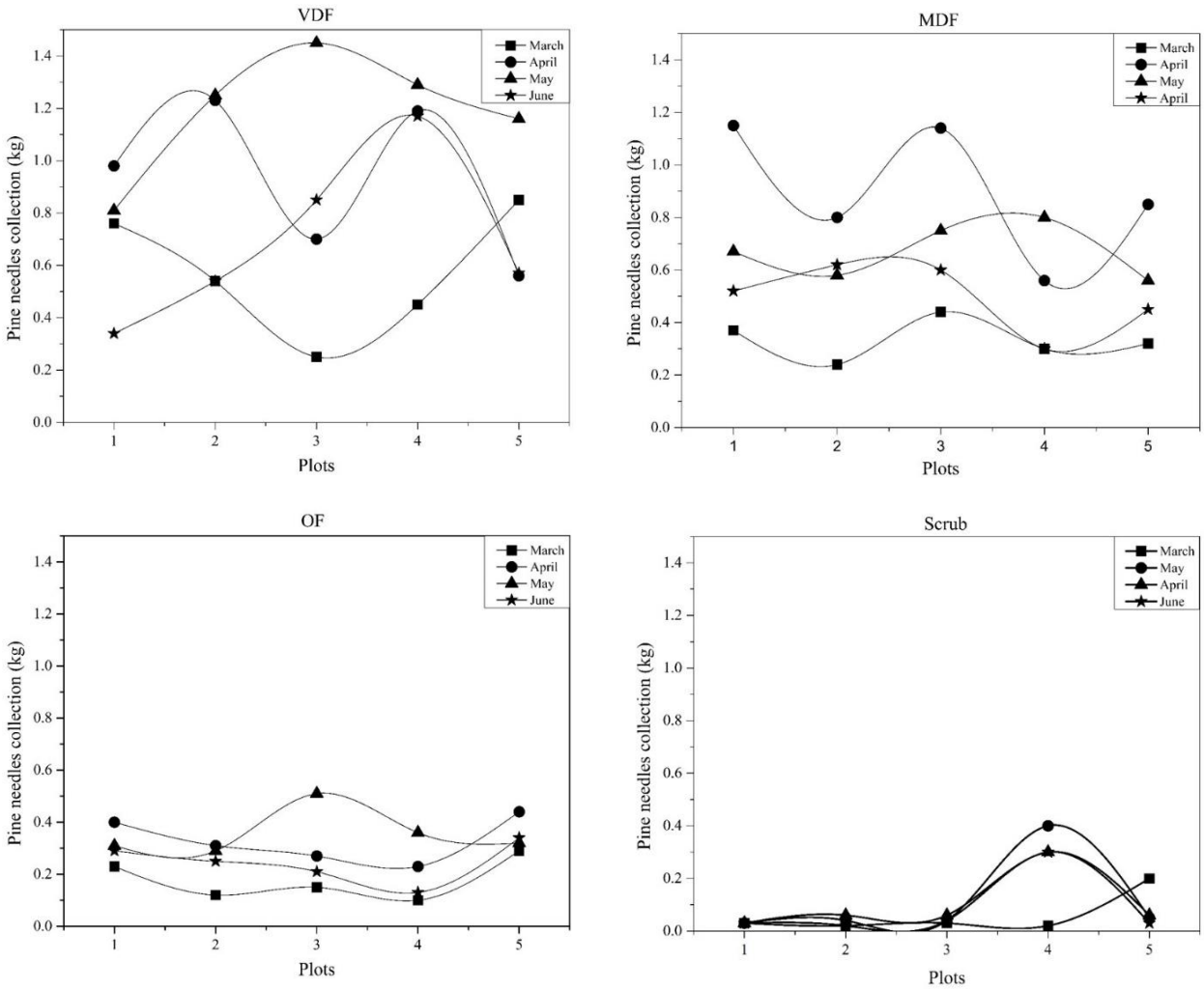

Figure 4. Litterfall data of pine needles according to forest canopy (VDF, MF, OF, and scrub).

3.3 Above ground pine needle estimation

3.3.1. Determine above ground pine needle

The estimation of gross pine needles yield has been carried out with two approaches based on the pine needle samples collection. The total annual above ground litterfall of pine needles collection can also be affected by almost 30 % due to poor accessibility, some domestic usage, rains, forest fires, various other losses, etc. (Kala and Subbarao, 2018; Gupta, 2013; Runyan et al., 2015). Table 5 presents a summary of the pine needle yield within the state.

The two different approaches for estimation of gross annual pine needle availability in the state are given in Table 5 and Table 6. The estimated results of gross annual pine needle yield is 25.5 million tonnes and net pine needle yield is 17.85 million tonnes with a single-point estimation approach (Table 5). The annual gross and net pine needle is 22.3 million tonnes and 15.61 million tonnes respectively when calculated using the tree-canopy density approach (Table 6). The most probable values of gross annual pine needle yield, 25.5 million tonnes and 22.3 million tonnes using the Approach I and Approach II, respectively. Thus Approach I shows the high value of the pine needles potential in the state. Kala and Subbarao (2018) revealed similar results by using the Approach I for Uttrahhund. Equation 8-11 help to calculate the APE, thermal energy and annual electrical energy as shown in Table 7 (Kala and Subbarao, 2018; Klass, 2004; Mckendry, 2002). The annual primary energy from dried pine needle yield is 0.44-0.50 pJ, which would provide 37.22-42.77 million kWh annual energy back up in the state.

Table 5. Gross pine needle yield estimation

Number	Parameters	Value
1	Area $_{VDF}$ (km^2)	3,224
2	Area $_{MF}$ (km^2)	6,381
3	Area $_{OF}$ (km^2)	5,074
4	Area $_{scrub}$ (km^2)	300
5	Pine needle collected from VDF (kg/2,500 m^2)	6,023
6	Pine needle collected from MF (kg/2,500 m^2)	4,519
7	Pine needle collected from OF (kg/2,500 m^2)	2,949
8	Pine needle collected from scrub (kg/2,500 m^2)	1,548
9	Gross pine needle yield per year (million tonne)	25.50
10	Net pine needle yield per year (million tonne)	17.85

Table 6. Estimated annual pine needle evaluated through the number of the pine trees

Number	Parameters	Value
1	Number of pine trees, $N_{tree\ VDF}$ (Tree/2,500 m^2)	307
2	Number of pine trees, $N_{tree\ MF}$ (Tree/2,500 m^2)	268
3	Number of pine trees, $N_{tree\ OF}$ (Tree/2,500 m^2)	202
4	Number of pine trees, $N_{tree\ scrub}$ (Tree/2,500 m^2)	195
5	Pine needle yield per tree, PNY_{tree} (kg/tree)	14.75
6	Gross pine needle yield per year (million tonnes)	22.30
7	Net pine needle yield per year (million tonnes)	15.61

Table 7. Annual pine needle energy potential.

Number	Approach	Annual thermal energy (pJ)	Annual Primary Energy (APE)		Annual electrical energy	
			pJ	Ktoe	pJ	million kWh
1	Approach I	0.506	0.77	18.39	0.154	42.77
2	Approach II	0.443	0.67	16.12	0.134	37.22

By neglecting the scrub forest densities, Figure 5 shows the district-wise distribution of pine needles in Himachal Pradesh. In this distribution, Chamba and Kangra have huge pine needle potential in VDF and MF, respectively. Shimla and Kullu has an old forest with very old-age trees and therefore has a little difference between the pine needle potential of VDF and MF within the district. Bilaspur, Hamirpur, and Lahul-Spiti have little pine needle contribution among all regions.

Pine needles estimation by using two approaches are considered to better account for biofuels in the subtropical pine forest of western Himalayan territories. From the results, the gross annual pine needles yield (APNY) as an energy feedstock in western Himalayan was concluded. The minimum and maximum values of the estimated gross yearly pine needle yield are 59.02-67.99 million tonnes. The annual pine needle yield as an energy feedstock ranges between 41.31-47.59 million tonnes. This work has achieved ranges of values for both the gross and net annual pine needle yield availability in the western Himalayan regions. The APE has a minimum value of 1.76 pJ and a maximum value of 2.03 pJ obtained from the thermochemical conversion processes. It amounts to 42.05-48.48 ktoe in term of tonnes of oil. The annual thermal energy ranges from 1.16-1.34 pJ. The annual electrical energy available has a minimum value of 0.09 billion tonnes and the maximum value of 0.1 billion kWh. This is a considerable amount of electricity left after technical and commercial losses.

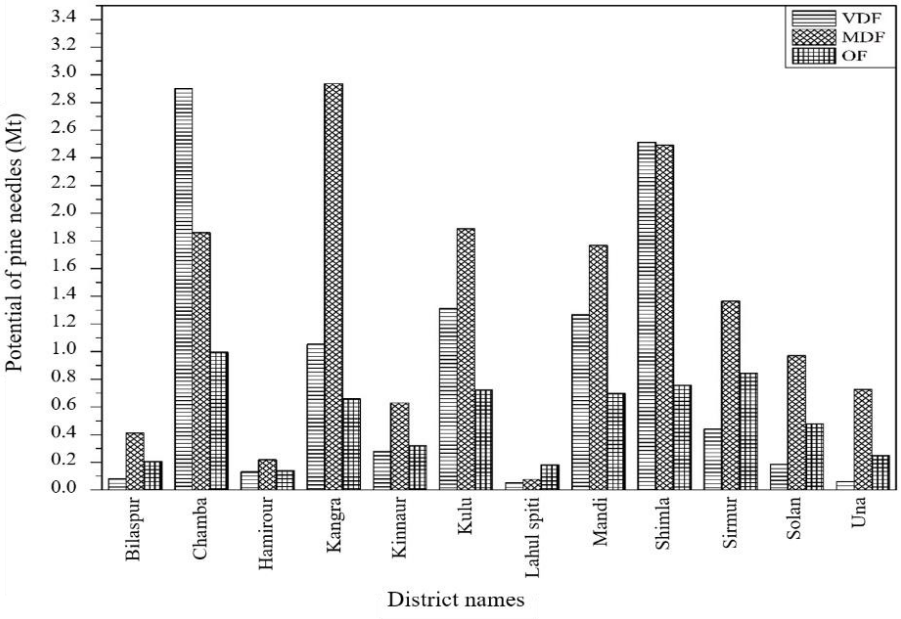

Figure 5. District-wise distribution of pine needles in the state.

4. CONCLUSION

Himalayan territories generate a tremendous amount of conifer forest waste, in terms of pine needles, that lounge on the forest floor every year for a more extended period. Some conclusions on the annual estimation of pine needle in the western Himalayan region have been discussed in the present study. The gross annual pine needle yield attained in this study using two different approaches has a minimum value of 59.02 million tonnes and a maximum value of 67.99 million tonnes. The annual pine needles yield use as an energy feedstock has also been estimated by reducing the yield by 30% due to various type of difficulties and issues in its availability. The estimations as energy feedstock of pine needles varies from 41.31 million tonnes to 47.59 million tonnes with the mean value of 44.45 million tonnes. The estimated annual primary energy 1.91 pJ as a most feasible value. Further, the estimation of annual thermal energy ranged from 1.76-2.03 pJ. It offers yearly electrical power back up of 0.09-0.10 billion kWh. This energy will be further supporting the regional commercial grid sector of Himalayan territories in the future.

ACKNOWLEDGEMENTS

We thank Mr Salig Ram Badala, retd. Assistant Conservator of forest (HPFS) for assistance with calculating pine needle potential through single-point estimation approach and tree canopy density-based approach. We are also appreciative to staff members of Himachal Pradesh Forest Department (HPFD) of Hamirpur and Solan for assisting in sampling.

REFERENCES

Bhagat RM, Rana RS, Singh S, Kalia V. Developing district-wise land use of Himachal Pradesh. Centre of Geo-information: Research and training CSK Himachal Pradesh agricultural University; 2009.

Bilgen S, Sarıkaya I. Utilization of forestry and agricultural wastes. Energy Sources, Part A: Recovery, Utilization and Environmental Effects 2016;38(23):3484-90.

Bisht AS, Kumar SR. Use of pine needle in energy generation. International Journal for Research in Applied Science and Engineering Technology 2014;2(11):59-63.

Bisht MS, Singh D, Kumar MR. Pine needles a source of energy for Himalayan region. International Journal of Scientific and Technology Research 2014;3(12):161-4.

Dasgupta S, Sharma SD, Nautiyal R, Chauhan AS, Singh S. Forestry statistics India 2011- New forest, Uttrakhand. Division of Statistics: Indian Council of forestry Research and Education; 2011.

Dhaundiyal A, Gupta VK. The analysis of pine needles as a substrate for gasification. Hydro Nepal: Journal of Water, Energy and Environment 2014;15:73-81.

Dhaundiyal A, Tewari PC. Comparative analysis of pine needles and coal for electricity generation using carbon taxation and emission reductions. Acta Technologica Agriculture 2015;18(2):29-35.

Eskin N, Hepbasli A. Development and applications of clean coal fluidized bed technology. Energy Sources, Part A: Recovery, Utilization and Environmental Effects 2006;28(12):1085-97.

Ferguson DE, Carlson CE. Height-age relationships for regeneration-size trees in the northern Rocky Mountains, USA. Fort Collins, US Department of Agriculture: Rocky Mountain Research Station; 2010.

Gill SJ, Biging GS, Murphy EC. Modeling conifer tree crown radius and estimating canopy cover. Forest Ecology and Management 2000;126(3):405-16.

Given PH, Weldon D, Zoeller JH. Calculation of calorific values of coals from ultimate analyses: Theoretical basis and geochemical implications. Fuel 1986;65(6):849-54.

Gonzalez-Benecke CA, Gezen SA, Samuelson LJ, Cropper WP, Leduc DJ, Martin TA. Estimating *Pinus palustris* tree diameter and stem volume from tree height, crown area and stand-level parameters. Journal of Forestry Research 2014;25(1):43-52.

Gupta RK. Himachal forest statistics 2013. Forest Department, Himachal Pradesh 2013:1-65.

Jain N, Bhatia A, Pathak H. Emission of air pollutants from crop residue burning in India. Aerosol and Air Quality Research 2014;14:422-30.

Joseph S, Anitha K, Murthy MSR. Forest fire in India: A review of the knowledge base. Journal of Forest Research 2009;14(3):127-34.

Joshi UC, Singh Y, Singh SA. Review on pine needle and its potential to develop energy. International Journal of Scientific and Engineering Research 2017;8(12):229-35.

Kala LD, Subbarao PMV. Estimation of pine needle availability in the Central Himalayan state of Uttarakhand, India for use as energy feedstock. Renewable Energy 2018;128:9-19.

Khan MS, Shah W, Hussain A, Masaud S. Height growth, diameter increment and age relationship response to sustainable volume of subtropical Chir pine (Pinus roxburghii) forest of Karaker Barikot forest. Pure and Applied Biology 2016;5(4):760-7.

Klass DL. Biomass for renewable energy and fuels. Encyclopedia of Energy 2004;1:193-212.

Lal PS, Sharma A, Bist V. Pine needle - An evaluation of pulp and paper making potential. Journal of Forest Products and Industries 2013;2(3):42-7.

Mahajan R, Nikitina A, Litti Y, Nozhevnikova A, Goel G. Autochthonous microbial community associated with pine needle forest litterfall influences its degradation under natural environmental conditions. Environmental Monitoring and Assessment 2016;188(7):1-10.

Malik A, Mohapatra SK. Biomass-based gasifiers for internal combustion (IC) engines: A review. Sadhana-Academy Proceedings in Engineering Sciences 2013;38(3):461-76.

McKendry P. Energy production from biomass (part 1): Overview of biomass. Bioresource Technology 2002;83(1):37-46.

Nhuchhen DR, Salam PA. Estimation of higher heating value of biomass from proximate analysis: A new approach. Fuel 2012;99:55-63.

Nunes LJR, Matias JC, Catalão JPS. Biomass combustion systems: A review on the physical and chemical properties of the ashes. Renewable and Sustainable Energy Reviews 2016;53:235-42.

Pandey S, Dhakal RP. Pine needle briquettes: A renewable source of energy. International Journal of Energy Science 2013;3(3):254-60.

Parikh J, Channiwala SA, Ghosal GK. A correlation for calculating HHV from proximate analysis of solid fuels. Fuel 2005;84:487-94.

Phrommarat B. Life cycle assessment of ground coffee and comparison of different brewing life cycle assessment of ground coffee and comparison of different brewing methods: A case study of organic Arabica coffee in northern Thailand. Environment and Natural Resources Journal 2019;17(2):96-108.

Polphan S, Phongkhieo NT, Chimchome V. Impacts from forest area utilization of local communities to habitat utilization of wildlife: A case study of Kaeng Krachan national park. Environment and Natural Resources Journal 2009;7(1):84-93.

Puri A, Srivastava AK, Singhal B, Mishra SK, Srivastava S, Lakshmi V. Antidyslipidemic and antioxidant activity of Pinus roxburghii needles. Medicinal Chemistry Research 2011;20(9):1589-93.

Rawat S, Upreti DK, Singh RP. Estimation of epiphytic lichen litter fall biomass in three temperate forests of Chamoli district, Uttarakhand, India. Tropical Ecology 2011;52(2):193-200.

Runyan CW, Odorico PD, Shobe W. The economic impacts of positive feedbacks resulting from deforestation. Ecological Economics 2015;120:93-9.

Sadiq M, Khan S, Shah W, Hussain A. Height growth, diameter increment and age relationship response to sustainable volume of subtropical Chir pine (Pinus roxburghii) forest of Karaker. Barikot forest. Pure and Applied Biology 2016;5(4):760-7.

Sairorkham B. Stagnation of community forest management: A case study of Nam Kian Sub-District, Phupiang district, Nan Province. Environment and Natural Resources Journal 2014;12(1):80-94.

Sedpho S, Sampattagul S. Exergetic evaluation of renewability for renewable electricity generation in Thailand. Environment and Natural Resources Journal 2015;13(1):39-46.

Shackleton CM. Growth patterns of Pterocarpus angolensisin savannas of the South African lowveld. Forest Ecology Management 2002;166:85-97.

Sharma KR, Lekha C. Tapping of *Pinus roxburghii* (Chir pine) for Oleoresin in Himachal Pradesh, India. Journal of Advances in Forestry Letters 2013;2(3):51-5.

Sharma V, Sharma RK. Fluidized bed combustion: Technology for efficient utilization of biomass residues. Proceeding of the Society of Materials and Mechanical Engineers: International Conference on Advancements and Futuristic Trends in Mechanical and Materials Engineering; 2018 Nov 15-17; Asian journal of engineering and applied technology, Hoshiarpur: India; 2018.

Sharma RK, Mohapatra SK. Thermo-economic analysis of a biomass-fired bubbling fluidised bed thermal power plant. International Journal of Exergy 2016;21(1):1-20.

Tiwari SP, Kumar P, Yadav D, Chauhan DK. Comparative morphological, epidermal, and anatomical studies of Pinus roxburghii needles at different altitudes in the North-West Indian Himalayas. Turkish Journal of Botany 2013;37(1):65-73.

Wu W. Derivation of tree canopy cover by multiscale remote sensing approach. International Archives of the Photogrammetry, Remote Sensing and Spatial Information Sciences 2012;38(4):142-9.

Zhu X, Liua W, Chenc H, Dengh Y, Chena C, Zenga H. Effects of forest transition on litterfall, standing litter and related nutrient returns: Implications for forest management in tropical China. Geoderma 2019;333(1):123-34.

Effect of Plant Spacing and Organic Fertilizer Doses on Methane Emission in Organic Rice Fields

Andin Muhammad Abduh, Eko Hanudin*, Benito Heru Purwanto and Sri Nuryani Hidayah Utami

Department of Soil Science, Universitas Gadjah Mada, Yogyakarta-55281, Indonesia

ARTICLE INFO

Received: 9 May 2019
Received in revised: 30 Jul 2019
Accepted: 14 Aug 2019
Published online: 18 Sep 2019
DOI: 10.32526/ennrj.18.1.2020.07

Keywords:
Cropping pattern/ Methane emission/ Organic fertilizer/ Rice field

*** Corresponding author:**
E-mail: ekohanudin@ugm.ac.id

ABSTRACT

Methane (CH_4) emission from paddy rice fields is a global concern; however, engineering plant spacing can decrease CH_4 emission. Due to this, field research was conducted to measure CH_4 emissions from rice fields planted using *jarwo 2:1* spacing, which has a 25 × 12.5 cm and 50 cm for the plant-free area (PFA), compared to *tegel*, which has a spacing of 25 × 25 cm. Each field was treated with organic fertilizer (mixture of cow manure and neem compost in a ratio of 1:1) with one of four doses: 0, 3, 6 and 9 tons/ha. The results showed that chemical properties such as soluble-Fe, soil organic matter (SOM), soil acidity (pH), and redox potential (Eh) were significantly correlated with CH_4 emissions (0.52***, 0.47**, 0.36*, and -0.27* respectively). *Jarwo 2:1* had lower CH_4 emissions than *tegel* on all doses of fertilizer. The most efficient dose of fertilizer was 3 tons/ha applied *jarwo 2:1* because it was able to produce rice up to 12 tons/ha with CH_4 emissions of only 34 kg/ha/season, while CH_4 emissions in *tegel* was 39 kg/ha/season. It is concluded that *jarwo 2:1* with 3 tons/ha organic fertilizers can be recommended to farmers because it produces lower CH_4 emissions and higher rice yield.

1. INTRODUCTION

Climate change is one of the issues intensively discussed in the 21st century. Rice fields are one of the sources of greenhouse gas (GHG) emissions such as CH_4 and contributed 16% of total anthropogenic greenhouse gas in 2010 in which the agriculture sector itself contributed more than half, reaching 51% of anthropogenic CH_4 emissions at the global level. Of those emissions, 20% was from rice fields (IPCC, 2014). CH_4 is a major component of greenhouse gases and their quantification is essential to address the issues of Climate Change (Mandal et al., 2013).

Rice cultivation needs a high production with low GHG emission to protect environmental sustainability. However, increasing rice growth can stimulate CH_4 emissions which aggravate global climate change, since rice cultivation as one of the primary sources of this potential greenhouse gas. However, Jiang et al. (2017) stated that a rice cultivar with high yield can decrease CH_4 emission from rice fields that have high organic-C content. A rice cultivar with high yield significantly increased the abundance of methanotroph microorganisms and root porosity, suggesting that the larger and more porous root systems of high-yielding cultivars facilitated CH_4 oxidation by promoting O_2 transport to soils. High organic carbon-rich soils indicate that the soil has a high C/N ratio that causes the soil to lack nitrogen for protein synthesis during microbial growth and induces a decrease of CH_4 production (Prayitno, 2016). A high soil C/N ratio causes slow SOM decomposition that inhibits methane production due to the lack of available carbon as a source energy for methanogens (Liu et al., 2016). The promotion of organic farming practices will help to improve sustainable, environmentally friendly agricultural production (Yuttitham, 2019).

Plant spacing can affect CH_4 emission, and when spacing is tighter emissions are lower (Watanabe et al., 2000). Tight plant spacing causes more plants per unit surface area, thus increasing the volume of the root zone. If the transport of methane

Citation: Abduh AM, Hanudin E, Purwanto BH, Utami SNH. Effect of plant spacing and organic fertilizer doses on methane emission in organic rice fields. Environ. Nat. Resour. J. 2020;18(1):66-74. DOI: 10.32526/ennrj.18.1.2020.07

to the atmosphere is slowed down, more methane is oxidized because it spends a longer time in the oxidation zone (Khalil et al., 1998). Therefore, it needs a plant spacing engineered with tight spacing and PFA that is suspected to decrease CH_4 emission. Indonesia has developed this plant spacing engineering called *jarwo 2:1*, a cropping pattern that manipulates the location of the plant so that more rice grows at the edge of the crop, where every two rows of rice plants are interspersed with a wide row spacing (Nurhayati et al., 2015) (Figure 1). Thus, it obtains an optimal growing space for the growth and development of plants, facilitates the conduct of the treatment plants, creates a sub-optimal environment for plant-disturbing organisms and increases the population resulting in high yield (Susilastuti et al., 2018). Meanwhile, *tegel* is a conventional cropping pattern that is generally performed by farmers in Indonesia with a distance of 25 × 25 cm or wider which forms like tiles (Darmawan, 2016).

Even so, there are no reports of this plant spacing engineering on CH_4 emission. Due to that, this research was conducted to find out the effect of plant spacing engineering *jarwo 2:1* compared to *tegel* with different doses of fertilizer on CH_4 emission.

2. METHODOLOGY

This research was carried out in organic rice fields in Imogiri, Indonesia (07° 56' 014" N, 110° 22' 292" E). The soil was classified into Inceptisols according to USDA (2014), and its parent material originated from volcanic deposits of young Merapi Mount. It has clay loam class texture (33% sand, 37% silt, 30% clay), with soil pH 6.6, Eh 9 mV, organic-C 2.3%, total-N 1.1%, available-P 1.4 mg/kg, available-K 0.15 mg/kg, soluble-Fe 8 mg/kg, and cation exchange capacity 29 cmol(+)/kg. There were two treatment factors selected in this experiment: *tegel* and *jarwo 2:1* cropping pattern, and doses of organic fertilizer (mixture of cow manure and neem fertilizer with a ratio of 1:1) applied at 0, 3, 6 and 9 tons/ha. Treatment areas were arranged in a Randomized Complete Block Design with three replications.

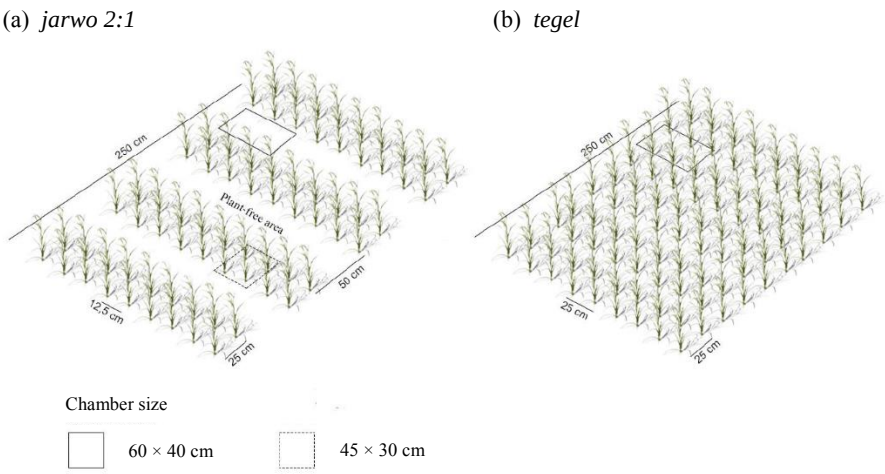

Figure 1. Chamber position when gas investigation conducted in (a) *jarwo 2:1* and (b) *tegel* cropping pattern.

The rice cultivar was cv. Mentik Wangi that was transplanted 20 days after germination into 2.5 × 4 m plot according to the cropping pattern applied (Figure 1). Organic fertilizer was applied a week before transplanting. Irrigation was carried out using the intermittent method, i.e., Flooded at 15, 45, 75 days and drained at 30, 60, 90 days after transplanting (DAT).

Soil observation was carried out on the variables of CH_4 flux (Abduh and Annisa, 2016), pH H_2O (Kabała et al., 2016), Eh (Toma et al., 2019), soluble-Fe (NH_4OAc extract at pH 4.8) (Shahandeh et al., 1994) and organic materials (Jha et al., 2014) with observational intervals of 15 DAT. CH_4 flux was measured by the closed chamber method. Gas extraction for *tegel* was carried out with one chamber, whereas for *jarwo 2:1* it was carried out with two chambers in plant area (PA) and PFA (Figure 1). Flux in each treatment was calculated using following equation (Abduh and Annisa, 2016):

$$E = \delta Csp/\delta t \times Wm/Vm \times Vch/Ach \times Tst/T+Tst \quad (1)$$

In order to balance the observation results with *tegel*, flux calculation in *jarwo 2:1* was transformed. The CH_4 flux of PA was multiplied by 5.2 m^2. Meanwhile, the flux of the PFA was multiplied by 4.8 m^2 then the two emissions from PA and PFA were added up. The two values above were obtained based on the PA and the PFA in the planting plots. The formula used for CH_4 flux on *jarwo 2:1* is as follows:

$$CH_4 \text{ flux } jarwo\ 2{:}1 = \frac{[\text{flux PA}\times 4.8]+[\text{flux PFA}\times 5.2]}{10} \quad (2)$$

Data were analyzed with Analysis of Variance using GenStat. Significant effect between treatments then were tested using Least Significant Difference. After that, Pearson Correlation test was conducted to find out a close relationship between the variables. Statistically significant differences are reported at level 5%.

3. RESULTS AND DISCUSSION

There was dynamic in CH_4 flux value during the plant growth due to intermittent drainage. The highest CH_4 flux was observed at 45 DAT at vegetative stage (Figure 2). It occurred because of the high availability of organic substrates from root exudates which release acetic acid higher than at the generative stage which can stimulate methanogenic bacteria to actively produce CH_4 (Kerdchoechuen, 2005). The low CH_4 flux at transplanting and generative stages is due to the lack of active methanogens caused by drainage, which make soils have aerobic conditions that inhibit CH_4 production and increase CH_4 oxidation (Conrad, 2007).

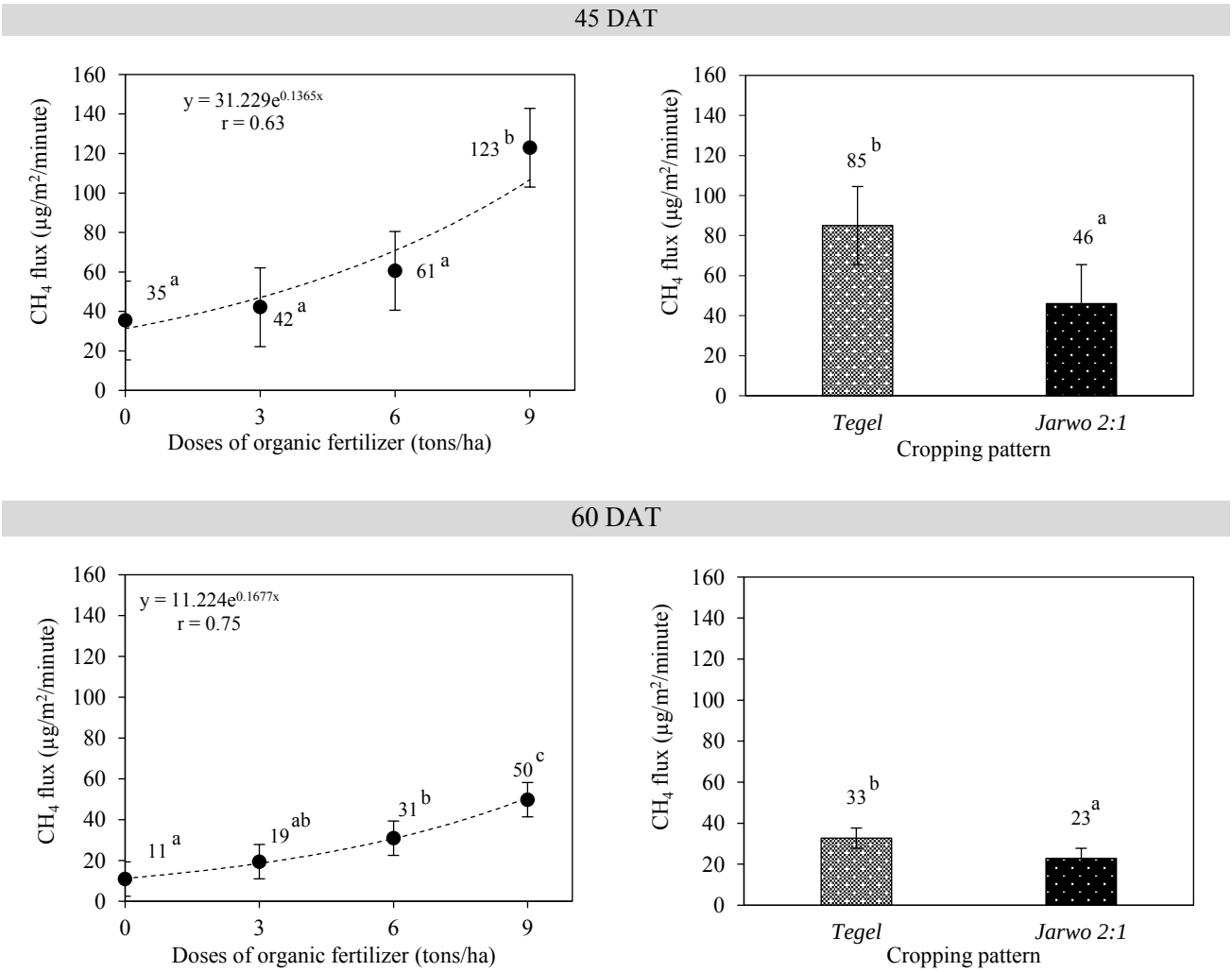

Figure 2. CH_4 flux in *jarwo 2:1* compared to *tegel* (right) and due to different organic fertilizer doses (left) at 45, 60, and 75 DAT. Data at left and right panels are showing the mean value of single factor of organic fertilizer doses and cropping pattern, respectively. Error bars represent standard error. A row of the continuous and dotted lines show the trend between doses of organic fertilizer with CH_4 flux. Mean values followed by the same letter are not significantly different based on the LSD test at a significance level of 5%.

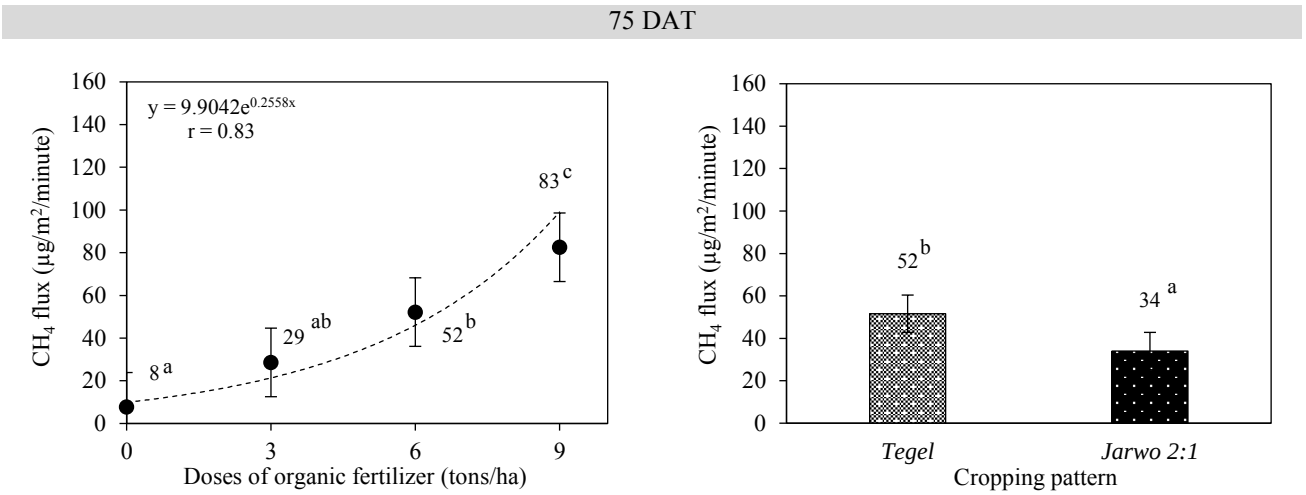

Figure 2. CH_4 flux in *jarwo 2:1* compared to *tegel* (right) and due to different organic fertilizer doses (left) at 45, 60, and 75 DAT. Data at left and right panels are showing the mean value of single factor of organic fertilizer doses and cropping pattern, respectively. Error bars represent standard error. A row of the continuous and dotted lines show the trend between doses of organic fertilizer with CH_4 flux. Mean values followed by the same letter are not significantly different based on the LSD test at a significance level of 5% (cont.).

Single treatment of cropping patterns and doses of organic fertilizer had significant effect on CH_4 flux. Doses of 3 and 6 tons/ha resulted in lower CH_4 flux compared to 9 tons/ha. Meanwhile, *jarwo 2:1* resulted in lower CH_4 flux compared to *tegel* (Figure 2). The combination of cropping patterns and doses of organic fertilizer has significant interaction effect on total CH_4 emissions. *Jarwo 2:1* could decrease CH_4 emissions by 17 kg/ha/season. Meanwhile, the best treatment is *jarwo 2:1* combined with 3 tons/ha organic fertilizers (Figure 3).

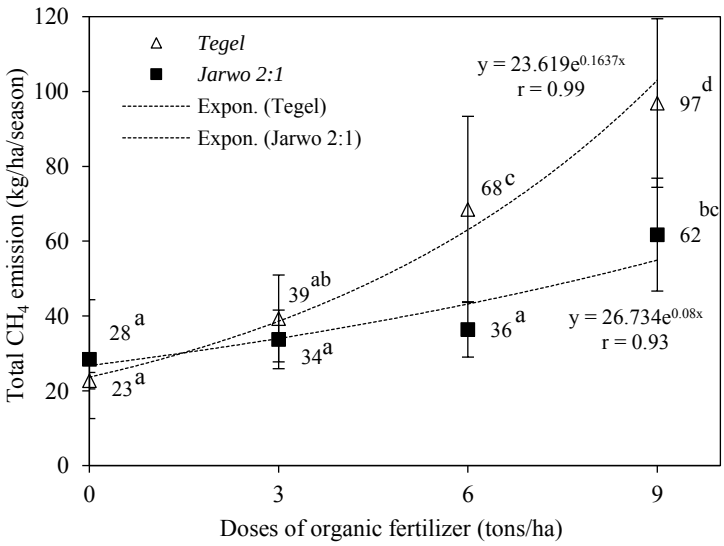

Figure 3. Total CH_4 emissions in *jarwo 2:1* compared to *tegel* with differents organic fertilizer doses. Error bars represent standard deviation. Arrow of the continuous and dotted lines show the trend between doses of organic fertilizer with CH_4 flux at *tegel* and *jarwo 2:1*. Mean followed by the same letter was not significantly different based on the LSD test at a significance level of 5%.

Figure 4, clearly shows the total CH_4 emission among *tegel*, *jarwo 2:1* PFA, and *jarwo 2:1* PA. The existence of PFA in *jarwo 2:1* can decrease CH_4 emissions because CH_4 flux tends to be very low due to the absence of a direct pathway of CH_4 from soil to the atmosphere, such as rice plants have through aerenchyma and this process contributes about 80-90% of the total CH_4 flux emitted to the atmosphere from the rice field (Cheng et al., 2006; Setyanto et al., 2004). PFA causes plants and soil to get more sunlight. Accumulated sunlight could have affected the efficiency of the photosynthesis process and

make methanotrophs become more active (Arunrat et al., 2014; Wassmann et al., 2018). The methane oxidation rate in the rhizosphere was higher during warmer months which indicated more sunlight (Lombardi et al., 1997).

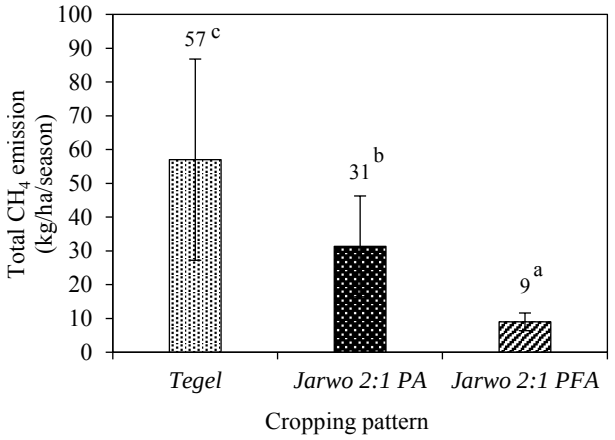

Figure 4. Total CH_4 emission in *tegel*, *jarwo 2:1* PA (plant area), and *jarwo 2:1* PFA (plant-free area). Error bars represent standard deviation. Mean values followed by the same letter were not significantly different based on the LSD test at a significance level of 5%.

Cropping patterns with tight plant spacing have a low CH_4 emission because tight spacing can lessen photosynthesis in old leaves of rice plants resulting in less substrate from root exudate for CH_4 production, so that it can delay soil reduction (Watanabe et al., 2000). Delay of soil reduction is caused by the ability of roots to oxidize by diffusing O_2 from the atmosphere to the rhizosphere through aerencyhma. So, that it is one of the important characteristics in rice cultivation which can control CH_4 production (Gutierrez et al., 2014). Therefore, the presence of PFA with tight plant spacing causes *jarwo 2:1* have lower total CH_4 emission than *tegel*.

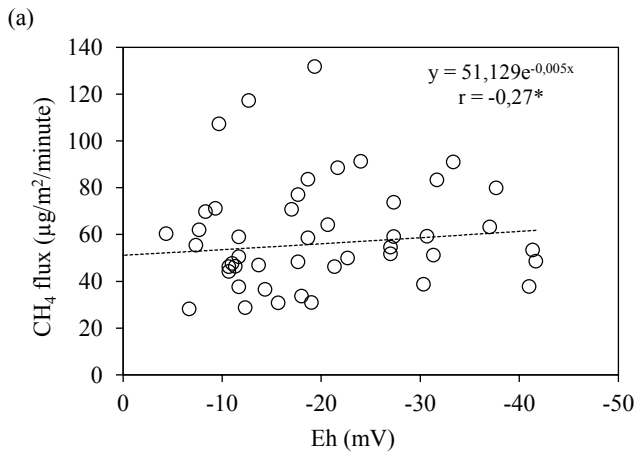

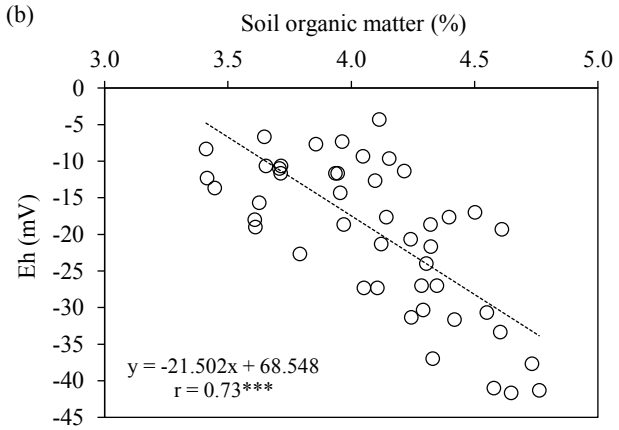

Figure 5. Relationship between Eh with CH_4 flux (a) and soil organic matter with Eh (b) in organic rice fields with different cropping patterns and organic fertilizer doses.

Redox conditions in the rhizosphere are influenced by the nitrogen content in the soil, if nitrogen in the soil is in a deficiency condition, the rhizosphere tends to be more reductive (Kyuma, 2004). Insufficient nitrogen supply will cause the roots to release more organic substances, thereby stimulating faster bacterial proliferation and increasing oxygen consumption in the rhizosphere (Trolldenier, 1977). This situation can be overcome by utilizing mature compost to diminish nitrogen loss that occurs due to NO_3^- leaching so it can minimize nitrogen deficiency (Opoku et al., 2014). The oxidative ability of roots and nitrogen availability for plants can maintain high soil redox potentials in soils. Soil Eh in this study only ranged from -42 to 2 mV which indicates that CH_4 formation does not run optimally. The results show soil Eh is negatively correlated with CH_4 flux (Figure 5(a)). This explains how the high value of Eh causes a decrease in the value of CH_4 flux.

Although CH_4 formation is not optimal in root areas due to high Eh, CH_4 formation can occur at the soil depth which is not reached by plant roots. In deeper soil the CH_4 production is greater in relation to the distribution of methanogenic bacteria in the soil (Dinel et al., 1988). CH_4 gas formed by methanogens will move by diffusion towards the root surface so that CH_4 will be partially oxidized, of which about 10-30% of CH_4 is consumed by methanotrophs associated with rice roots (Krüger et al., 2002).

The low CH_4 emissions in *jarwo 2:1* (40 kg/ha/season) compared to *tegel* (57 kg/ha/season) is an opportunity that can be developed to suppress CH_4

emissions. Based on this study the productivity of *jarwo 2:1* is not significantly different compared to *tegel*, but higher doses of organic fertilizer (9 tons/ha) provided higher productivity than those with lower rates (Figure 6(a)). However, based on quantitative values, *jarwo 2:1* showed productivity that tended to be higher. *Jarwo 2:1* according to Giamerti and Yursak (2013), has more optimal plant growth and higher productivity reaching 6.6 tons/ha compared *tegel* which only 5.1 tons/ha. A dose of 3 tons/ha is an efficient dose producing yields of 12 tons/ha. Thus, it is very good to recommend *jarwo 2:1* with a dose of 3 tons/ha to the farmers because it has low emissions but also results in higher productivity.

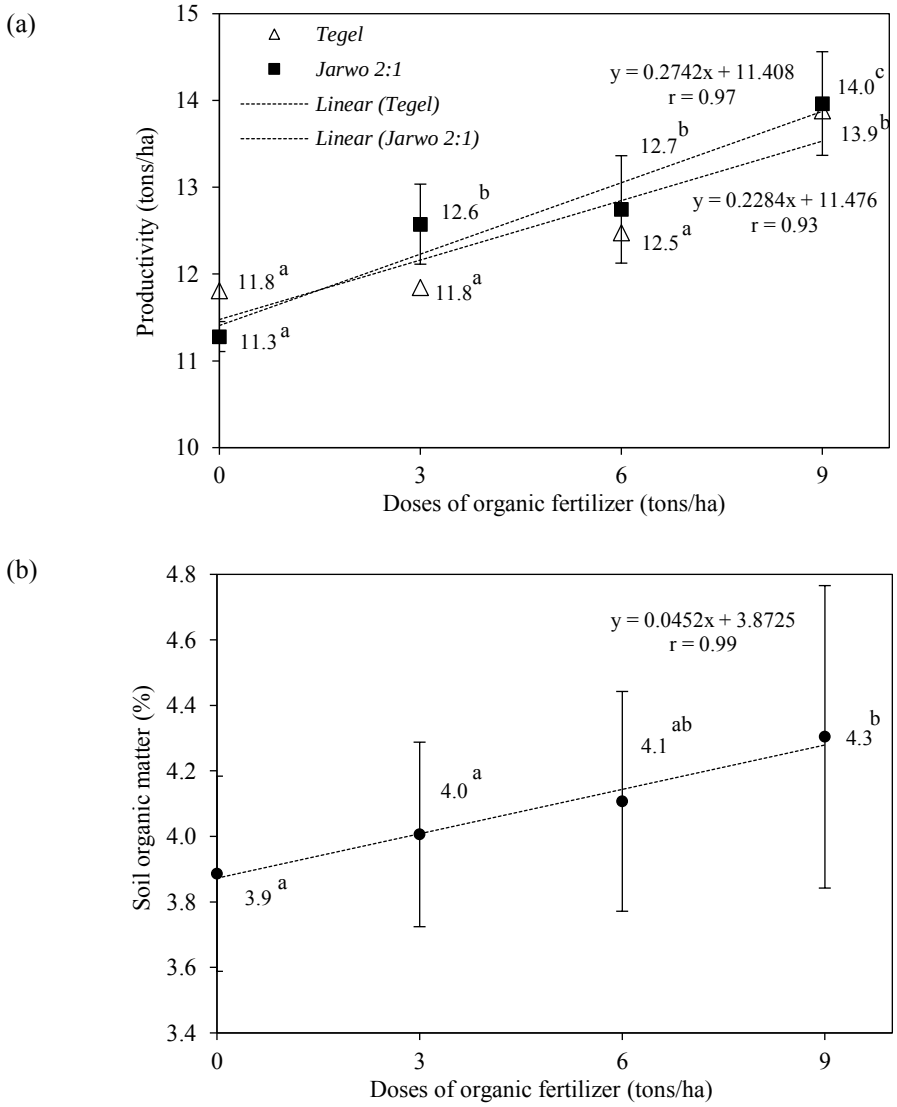

Figure 6. Productivity *jarwo 2:1* compared to *tegel* (a); SOM (soil organic matter) (b) with differents organic fertilizer doses. Error bars represent standard deviation. Arrow of the continuous and dotted lines show the trend among doses of organic fertilizer with productivity at *tegel*, *jarwo 2:1*, and SOM. Mean values followed by the same letter at same rows were not significantly different based on the LSD test at a significance level of 5%.

There is a relationship between the doses of organic fertilizer and CH_4 flux at 45, 60, and 75 DAT (Figure 2). The regression pattern is exponential in which the increase of organic fertilizer doses can increase CH_4 flux to a certain extent. CH_4 emissions are very strongly influenced by dosage of fertilizer application, where one unit of organic fertilizer dose increases emissions 2.7 to 4.1 compared to the absence of organic fertilizer (Wassmann et al., 1996). The application of organic fertilizer with different doses had significant effect on CH_4 flux in which the dose of 9 tons/ha gave the highest CH_4 flux. Meanwhile, the lowest CH_4 flux was found in the dose of 0 tons/ha even though it was not significantly different from the dose of 3 and 6 tons/ha (Figure 2). Furthermore, the increasing of dose of applied

organic fertilizer can elevate SOM content (Figure 6(b)) that leads to a surge of CH_4 fluxes (Figure 7(c)). It is very clear that this relationship occurs because (1) organic matter will be transformed into simple substrates such as formate, ethanol, and acetate then used by methanogens to produce CH_4 to get energy (Malyan et al., 2016), (2) organic matter application may change soil microbial communities and their activities which would increase production of CH_4 (Zheng et al., 2007). High amounts of organic matter provide an abundant source of energy for methanogens to produce CH_4. This study is similar to the study of Humphreys et al. (2019) that indicated CH_4 emissions increase as soil organic matter increases.

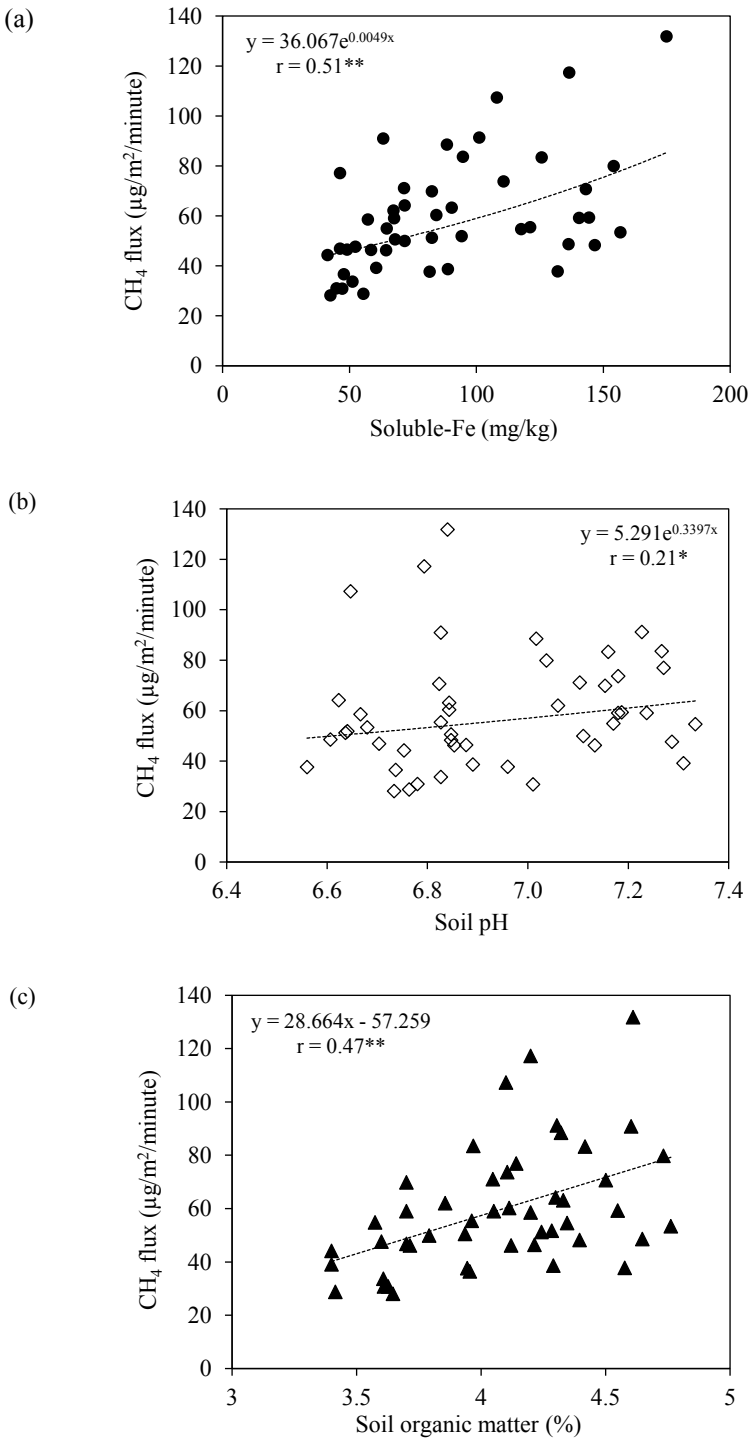

Figure 7. Relationship between soluble-Fe (a), soil pH (b), SOM (soil organic matter) (c), with CH_4 flux in organic rice fields with different cropping patterns and organic fertilizer doses.

The application of organic fertilizer with a mixture of neem compost functioning as a nitrification inhibitor can decrease CH_4 emissions by 8% compared to using only urea fertilization (Malla et al., 2005). The application of neem compost causes the nitrification process to be inhibited so that NH_4^+ is abundant in the soil causing competition with CH_4 oxidizing agents having the same site for O_2 as electron acceptors (Bédard and Knowles, 1989). This causes an increase in the population of nitrifier bacteria compared to methanotrophs, in which nitrifier bacteria can oxidize CH_4 but less effectively than methanotrophs (Malla et al., 2005).

There is a negative correlation between SOM and Eh (Figure 5(b)). Addition of SOM as electron donors can create a more reductive soil due to increases in the activity of heterotrophic bacteria (Sutton-Grier et al., 2011). Reductive soil conditions indicate that the soil is dominated by a reduction. One of them is the occurrence of iron reduction from Fe^{3+} to Fe^{2+}. This reduction affects the CH_4 emissions, in which higher amounts of Fe^{2+} in the soil causes an increase in CH_4 flux (Figure 7(a)). CH_4 flux is regulated by Fe reduction due to the electron flow in the soil concentrated to the reduction of Fe and CH_4 production, in which cumulative Fe^{3+} reduction acts as the dominant electron acceptor, which ranges from 79.5-99.7% of total electron consumption donors (Peng et al., 2015). Soil pH can affect CH_4 flux (Figure 7(b)). Methanogens are usually more active in soils with neutral pH ranging from 6.5-7.5 or slightly alkaline and are very sensitive to soil pH fluctuations (Weslien et al., 2009).

4. CONCLUSION

Soluble-Fe, OM, pH, and Eh influenced CH_4 emissions in which these factors showed Pearson correlation coefficients of 0.52***, 0.47**, 0.36*, and -0.27*, respectively. *Tegel* and *jarwo 2:1* produced CH_4 emissions of 57 kg/ha/season and 40 kg/ha/season, respectively. CH_4 emissions can be suppressed by 17 kg/ha/season using *jarwo 2:1*. Meanwhile, application of organic fertilizer at 3 tons/ha is the most efficient because it resulted in high rice productivity of 12 tons/ha and low CH_4 emissions. Total CH_4 emissions are affected by the interaction between cropping patterns and organic fertilizer doses, where the use of *jarwo 2:1* combined with 3 tons/ha organic fertilizers was able to suppress CH_4 emissions but could maintain high rice productivity.

ACKNOWLEDGMENTS

We would like to express our gratitude to Universitas Gadjah Mada for financial support in conducting this research.

REFERENCES

Abduh AM, Annisa W. Interaction of paddy varieties and compost with flux of methane in tidal swampland. Journal of Tropical Soils 2016;21(3):179-86.

Arunrat N, Pumijumnong N, Phinchongsakuldit A. Estimating soil organic carbon sequestration in rice paddies as influenced by climate change under scenario A2 and B2 of an i-EPIC model of Thailand. EnvironmentAsia 2014;7(1):65-80.

Bédard C, Knowles R. Physiology, biochemistry, and specific inhibitors of CH_4, NH_4^+, and CO oxidation by methanotrophs and nitrifiers. Microbiological Reviews 1989;53:68-84.

Cheng W, Yagi K, Sakai H, Kobayashi K. Effects of elevated atmospheric CO_2 concentrations on CH_4 and N_2O emission from rice soil: an experiment in controlled-environment chambers. Biogeochemistry 2006;77(3):351-73.

Conrad R. Microbial ecology of methanogens and methanotrophs. Advances in Agronomy 2007;96:1-63.

Darmawan M. Analysis of legowo row planting system and system of rice intensification (SRI) of paddy field (*Oryza Sativa* L.) toward growth and production. Agrotech Journal 2016; 1(1):14-8.

Dinel H, Mathur SP, Brown A, Levesque M. A field study of the effect of depth on methane production in peatland waters: equipment and preliminary results. Journal of Ecology 1988;76(4):1083-91.

Giamerti Y, Yursak Z. Yield component performance and productivity of rice Inpari-13 varieties in various planting system. Widyariset 2013;16(3):481-8.

Gutierrez J, Atulba SL, Kim G, Kim PJ. Importance of rice root oxidation potential as a regulator of CH_4 production under waterlogged conditions. Biology and Fertility of Soils 2014;50(5):861-8.

Humphreys J, Brye KR, Rector C, Gbur EE. Methane emissions from rice across a soil organic matter gradient in Alfisols of Arkansas, USA. Geoderma Regional 2019;15:e00200.

Intergovernmental Panel on Climate Change (IPCC). Climate Change: Impacts, Adaptation, and Vulnerability. Part A: Global and Sectoral Aspects. Contribution of Working Group II to the Fifth Assessment Report of the Intergovernmental Panel on Climate Change. United Kingdom and New York: Cambridge University Press; 2014. p. 1-32.

Jha P, Biswas AK, Lakaria BL, Saha R, Singh M, Rao AS. Predicting total organic carbon content of soils from walkley and black analysis. Communications in Soil Science and Plant Analysis 2014;45(6):713-25.

Jiang Y, Van-Groenigen KJ, Huang S, Hungate BA, Van-Kessel C, Hu S, Zhang J, Wu L, Yan X, Wang L, Chen J, Hang X, Zhang Y, Horwath WR, Ye R, Linquist BA, Song Z, Zheng C, Deng A, Zhang W. Higher yields and lower methane emissions with new rice cultivars. Global Change Biology 2017;23:1-11.

Kabała C, Muzstyfaga E, Galka B, Labunska D, Manczynska P. Conversion of soil pH 1:2.5 KCl and 1:2.5 H_2O to 1:5 H_2O: Conclusions for soil management, environmental monitoring, and international soil databases. Polish Journal of Environmental Studies 2016;25(2):647-53.

Kerdchoechuen O. Methane emission in four rice varieties as related to sugars and organic acids of roots and root exudates and biomass yield. Agriculture, Ecosystems and Environment 2005;108(2):155-63.

Khalil MAK, Rasmussen RA, Shearer MJ. Effects of production and oxidation processes on methane emissions from rice fields. Journal of Geophysical Research Atmospheres 1998;103(D19):25233-9.

Krüger M, Eller G, Conrad R, Frenzel P. Seasonal variation in pathways of CH_4 production and in CH_4 oxidation in rice fields determined by stable carbon isotopes and specific inhibitors. Global Change Biology 2002;8(3):265-80.

Kyuma K. Paddy Soil Science. Japan and Melbourne: Kyoto Unversity Press and Trans Pasific Press; 2004.

Liu M, Ussiri DAN, Lal R. Soil organic carbon and nitrogen fractions under different land uses and tillage practices. Communications in Soil Science and Plant Analysis 2016;47(12):1528-41.

Lombardi JE, Epp MA, Chanton JP. Investigation of the methyl fluoride technique for determining rhizospheric methane oxidation. Biogeochemistry 1997;36(2):153-72.

Malla G, Bhatia A, Pathak H, Prasad S, Jain N, Singh J. Mitigating nitrous oxide and methane emissions from soil in rice-wheat system of the Indo-Gangetic plain with nitrification and urease inhibitors. Chemosphere 2005;58(2):141-7.

Malyan SK, Bhatia A, Kumar A, Gupta DK, Singh R, Kumar SS, Tomer R, Kumar O, Jain N. Methane production, oxidation and mitigation: a mechanistic understanding and comprehensive evaluation of influencing factors. Science of the Total Environment 2016;572:874-96.

Mandal RA, Dutta IC, Jha PK, Karmacharya SB, Yadav BK, Kafle RR. CO_2 and CH_4 emission from domestic fuel and livestock in Tarai and Bhawar in Nepal: A household-level analysis. Environment and Natural Resources Journal 2013;11(1):1-11.

Nurhayati A, Lili W, Herawati T, Riyantini I. Derivatif analysis of economic and social aspect of added value minapadi (paddy-fish integrative farming) a case study in the village of Sagaracipta Ciparay Sub District, Bandung West Java Province, Indonesia. Proceedings of the Aquatic Procedia of 2nd International Symposium on Aquatic Products Processing and Health: 2015 Sep 13-15; Diponegoro University, Semarang: Indonesia; 2015.

Opoku A, Chaves B, DeNeve S. Neem seed oil: A potent nitrification inhibitor to control nitrate leaching after incorporation of crop residues. Biological Agriculture and Horticulture 2014;30(3):145-52.

Peng QA, Shaaban M, Hu R, Mo Y, Wu Y, Ullah B. Effects of soluble organic carbon addition on CH_4 and CO_2 emissions from paddy soils regulated by iron reduction processes. Soil Research 2015;53(3):316-24.

Prayitno HB. Methane formation in mangrove sediment. Oseana 2016;41(3):44-53.

Setyanto P, Rosenan AB, Boer R, Fauziah CI, Khanif MJ. The effect of rice cultivars on methane emission from irrigated rice field. Indonesian Journal of Agricultural Science 2004; 5(1):20-31.

Shahandeh H, Hossner LR, Turner FT. A comparison of extraction methods for evaluating Fe and P in flooded rice soils. Plant and Soil 1994;165:219-25.

Susilastuti D, Aditiameri A, Buchori U. The effect of jajar legowo planting system on Ciherang paddy varieties. Agritropica 2018;1(1):1-8.

Sutton-Grier AE, Keller JK, Koch R, Gilmour C, Megonigal JP. Electron donors and acceptors influence anaerobic soil organic matter mineralization in tidal marshes. Soil Biology and Biochemistry 2011;43(7):1576-83.

Toma Y, Sari NN, Akamatsu K, Oomori S, Nagata O, Nishimura S, Purwanto BH, Ueno H. Effects of green manure application and prolonging mid-season drainage on greenhouse gas emission from paddy fields in Ehime, Southwestern Japan. Agriculture 2019;9(2):29.

Trolldenier G. Mineral nutrition and reduction processes in the rhizosphere of rice. Plant and Soil 1977;47(1):193-202.

United States Department of Agriculture (USDA). Keys to Soil Taxonomy. 12th ed. Washington DC, Unites States of America: Natural Resources Conservation Service; 2014.

Wassmann R, Shangguan XJ, Cheng DX, Wang MX, Papen H, Rennenberg H, Seiler W. Spatial and seasonal distribution of organic amendments affecting methane emission from Chinese rice fields. Biology and Fertility of Soils 1996; 22(3):191-5.

Wassmann R, Alberto MC, Tirol-Padre A, Hoang NT, Romasanta R, Centeno CA, Sander BO. Increasing sensitivity of methane emission measurements in rice through deployment of "closed chambers" at nighttime. PLoS ONE 2018;13(2):e0191352.

Watanabe A, Kajiwara M, Yoshida S, Kimura M. Effect of planting density on methane emission from a rice paddy. Environmental Science 2000;13(2):223-7.

Weslien P, Klemedtsson ÅK, Börjesson G, Klemedtsson L. Strong pH influence on N_2O and CH_4 fluxes from forested organic soils. European Journal of Soil Science 2009;60(3):311-20.

Yuttitham M. Comparison of carbon footprint of organic and conventional farming of Chinese Kale. Environment and Natural Resources Journal 2019;17(1):78-92.

Zheng J, Zhang X, Li L, Zhang P, Pan G. Effect of long-term fertilization on C mineralization and production of CH_4 and CO_2 under anaerobic incubation from bulk samples and particle size fractions of a typical paddy soil. Agriculture, Ecosystems and Environment 2007;120(2-4):129-38.

Effects of *Agrobacterium* sp. I26, Manure and Inorganic Fertilizers to Pb Content of Rice Grains Planted in Pb Polluted Soil

Retno Rosariastuti[2*], Muhamad Sulthoni Fauzi[1], Purwanto[2], and Suntoro[2]

[1]*Bachelor Student of Soil Science Study Program Soil Science, Faculty of Agriculture, Universitas Sebelas Maret, Surakarta 57126, Central Java, Indonesia*
[2]*Soil Science Study Program, Faculty of Agriculture, Universitas Sebelas Maret, Surakarta 57126, Central Java, Indonesia*

ARTICLE INFO

Received: 21 June 2019
Received in revised: 17 Sep 2019
Accepted: 30 Sep 2019
Published online: 22 Oct 2019
DOI: 10.32526/ennrj.18.1.2020.08

Keywords:
Bioremediation/ Lead/ *Agrobacterium* sp. I26/ Manure/ Soil

***Corresponding author:**
E-mail: retnobs@staff.uns.ac.id

ABSTRACT

Chemical waste from textile industries discharged directly into rivers will affect paddy soil irrigation surrounding these factories. Thus, heavy metal pollution may occur in this paddy soil. Bioremediation can remediate polluted heavy metals by removing the pollutant. *Agrobacterium* sp. I26 and manure were studied as a bioremediation agent because both use biological processes in remediation. The effectivity of bioremediation agent (*Agrobacterium* sp. I26 or manure) and inorganic fertilizer in inhibiting the absorption of Lead (Pb) in rice, as well as the production of rice, was studied. This study used a factorial Randomized Completely Block Design (RCBD), which consisted of two factors: a) inorganic fertilizers (P): without inorganic fertilizers (P0) and with inorganic fertilizers (P1); b) bioremediation agents (K): without bioremediation agents (K0), with *Agrobacterium* sp. I26 (K1), with manures (K2). From these two factors, six treatment combinations with four repetitions, resulting in 24 experiment units were obtained. Results of this study showed that *Agrobacterium* sp. I26 and manures are able to inhibit Pb absorption in rice grains. The best treatment of this study was the combination of inorganic fertilizers with *Agrobacterium* sp. I26, which showed the highest weight of 1000 seeds (31.95 g), 14.96% higher compared to control, and was able to inhibit Pb absorption by rice grain up to a threshold (0.29 µg/g), 39.58% lower compared with control.

1. INTRODUCTION

This study was held in Waru, Kebakkramat Sub district, Karanganyar Regency, Central Java Province, Indonesia which has a lot of textile industries. The impact of the textile industry caused lead (Pb) pollution in paddy soil to be 16.18 mg/kg (Kharisma et al., 2018). Because of that, bioremediation research has been carried out in this area to absorb heavy metals in the soil using plants.

Industrial activities play an important role in developing countries, especially economically, socially and culturally (Syaifullah, 2009). Industries in Kebakkramat Sub-district are dominated by textile industries, using melamine as one of its raw materials. Melamine is used in dye coating processes so that textiles become water resistant, are not easily tangled and don't fade. Melamine is synthesized from urea at a temperature between 350-400 °C (Ullman, 2003), hence textile waste contains urea. Textile industries besides having a positive impact on a community also have a negative impact towards the environment from its chemical waste.

Wuana et al. (2010) stated that one of the heavy metals commonly found in industrial waste is lead (Pb). Another source of Pb, other than textile waste, can be found in inorganic fertilizers. Laboratory analysis of Pb in the inorganic fertilizers used in this research showed that urea fertilizer (source of Nitrogen) contained 0.32 µg/g of Pb, SP36 fertilizer (source of Phosphate) had the highest concentration of Pb with 1.63 µg/g and KCl fertilizer (source of Potassium) contained 0.52 µg/g of Pb. The manure used in this research contained 0.32 µg/g of Pb.

Based on Government Regulation of Indonesia number 101 (2014), soil Pb content is allowed at a level of 3 µg/g. Rice grains should not exceed the threshold

Citation: Rosariastuti R, Fauzi1 MS, Purwanto, Suntoro. Effects of Agrobacterium sp. I26, manure and inorganic fertilizers to Pb content of rice grains planted in Pb polluted soil. Environ. Nat. Resour. J. 2020;18(1):75-84. DOI: 10.32526/ennrj.18.1.2020.08

of 0.3 µg Pb/g of rice (Indonesia's Badan Standardisasi Nasional, 2009). Darmono (2001) explained that rice with heavy metal pollution, if consumed and accumulated in the human body will cause chronic toxicity and damage internal organ functions.

Bioremediation is the development in the field of environmental biotechnology that utilizes biological processes in controlling pollution with agents called bioremediation agents. Darmono (2001) found organic compounds can prevent heavy metal ion absorption in plant tissue. Another effort to minimize Pb absorption is application of bacterium *Agrobacterium* sp. I26. A previous study by Rosariastuti et al. (2013) found, addition of this bacterium will minimize Cr absorption to shoots. Pramono et al. (2013) also said that *Agrobacterium* sp. I26 can produce the reductase enzyme that can reduce chromium from toxic (available for plant) to non-toxic (non-available for plant) forms. Therefore, it is possible that the reductase enzyme can reduce Pb^{4+} (available for plants) to Pb^{2+}/Pb II (not available for plants). *Agrobacterium* sp. I26 and manure are included as bioremediation agents because both are using biological processes in remediation.

However, research on the effect of *Agrobacterium* sp. I26 and manures to heavy metals in soil is needed. *Agrobacterium* sp. I26 and manures play roles as bioremediation agents to minimize Pb absorption to shoots or rice grains, hence rice produced will be safe for consumption. This study compared the effectivity of bioremediation agents (*Agrobacterium* sp. I26 or manure) and inorganic fertilizers in inhibiting the absorption of Pb in rice and the production of rice.

2. METHODOLOGY

2.1 Study area

This study was held from April to September 2018 in Waru, Kebakkramat Sub-district, Karanganyar Regency, Central Java Province, Indonesia (7°30'36'26"S and 110°54'23'72'E) with an area of 651 m^2.

Figure 1. The study site

2.2 Materials

The materials used in this study were manure that comes from cow feces (produced by Jatikuwung Inovation Center), *Agrobacterium* sp. I26 isolated by Rosariastuti et al. (2013), inorganic fertilizer: Urea (source of Nitrogen), SP36 (source of Phosphate) and KCl (source of Potassium) (Figure 2), Luria Bertani medium (Tryptone 10%, NaCl 5%, Yeast extract 5%, Agar 15%), sulfuric acid, nitric acid, acid percolate, NaCl, $K_2Cr_2O_7$, Alcohol, Atomic Absorption Spectrophotometer (AAS), Autoclave, vortex, shaker, etc.

This study used 3 types of inorganic fertilizers: Urea, SP36, and KCl because the Nitrogen, Phosphate, and Potassium are essential macro nutrients which are more needed by plants than other nutrients.

Figure 2. Fertilizers used in this study: a) Manure; b) Urea; c) SP-36; d) KCl.

2.3 Experimental design

This study used a factorial and Randomized Completely Block Design (RCBD) consisting of two factors: a) inorganic fertilizers (P): without inorganic fertilizers (P0) and with inorganic fertilizers (P1); b) bioremediation agents (K): without bioremediation agents (K0), with *Agrobacterium* sp. I26 (K1), with manures (K2). From these two factors, six treatment combinations with four repetitions, resulting in 24 experiment units were performed.

Table 1. Treatments combination

Treatments	Information
P0K0	Without any treatment (Control)
P0K1	Without inorganic fertilizers + *Agrobacterium* sp. I26
P0K2	Without inorganic fertilizers + Manures
P1K0	Inorganic fertilizers + without bioremediation agents
P1K1	Inorganic fertilizers + *Agrobacterium* sp. I26
P1K2	Inorganic fertilizers + Manures

2.4 Procedure

2.4.1 Agrobacterium sp. I26 *inoculum preparation*

Bioremediation agents used in this study were *Agrobacterium* sp. I26 and manure. Phenotypic characterization such as cell morphology/cells type, gram stain reaction, motility, aerobicity, and ability to grow at 40 ºC was recorded. Propagation of *Agrobacterium* sp. I26 isolates was done using pure isolates of *Agrobacterium* sp. I26 grown in solid LB media on new slope media. After it was grown, it was transferred to 100 mL LB liquid media per one tube pure isolate of *Agrobacterium* sp. I26. Media was shaken until the density of its bacterial cells measured using a hemacytometer was 10^{10} CFU/mL. The dosage of bacteria was 10^6 CFU/g soil, therefore the quantity of bacteria needed were 1.25×10^{10} CFU/mL per sub plot obtained from the calculation results of the soil weight (Bulk density × Volume of soil).

2.4.2 Land preparation

The soil was hoed manually on the rhizosphere, the lower rhizosphere was moved to the upper part so that the nutrients in lower part of the rhizosphere were moved to the top where they could be used by plants. Twenty four plots (same as experimental units) at 1.25 × 1.25 m per-plot were prepared. The plots were made higher than the surrounding land to keep the land in a dry condition. The plant distance of this study was 25 × 25 cm (sub plots), so there were 25 sub plots per-plot. Three paddy seeds were planted per plot.

One application of manure and bacterial inoculum was performed seven days before planting. The application of bacterial inoculum was done by pouring the inoculum into the planting holes (per-sub plot). Inorganic fertilizers used in this study were urea (N), SP36 (P) and KCl (K), with dosages of: Urea 300 kg/ha, SP36 100 kg/ha and KCl 100 kg/ha (Minister of Agriculture Regulation Republic of Indonesia, 2007). The application of fertilizer was done by spreading out and was done three times; five days after planting (3/5 of dosage), 25 days after planting (1/5 of dosage) and 45 days after planting (1/5 of dosage). Manure was applied at 10,000 kg/ha (Rauf et al., 2000) and the application was spread out.

2.4.3 Harvesting

Harvesting was done three months after planting by taking all parts of the plant. Plant samples were separated into their roots, shoots, and grains. After that, everything was air dried, then dried in an

oven until constant weight. Next, each sample was ground prior to laboratory analysis.

Figure 3. Sample of plants.

2.5 Sample collection and analysis

Soil and plant samples were chosen randomly from the inner sub plots of each plot (Figure 4). Five soil and plant samples were taken from each plot. The samples were decomposed into one as a sample from the plot. It took two weeks to prepare the soil and plant samples, while laboratory analysis took 1 month.

The parameters measured and laboratory analysis methods, based on Indonesia's Balai Penelitian Tanah (2009), were pH (Electrometric method), Soil CEC (Ammonium Acetate Saturation Method), Soil Organic Matter that calculated from C-Organic (Walkey and Black Method), soil bacteria colonies (Plate Count Method), Soil Pb levels (Wet Destruction Method continued by reading the metal content using AAS), Removal Effectiveness (calculated from differences in initial heavy metal levels and final heavy metal content after treatment), Weight of 1000 Seeds (Direct Measurement Method using digital scales), and Pb content (roots, shoot, grain) in Plants (Wet Destruction Method continued by reading the metal content using AAS).

2.6 Data analysis

Data were analyzed by statistical analysis using ANOVA with a confidence level of 95%. If significant, then continued by the LSD or T-test with a level of 95%.

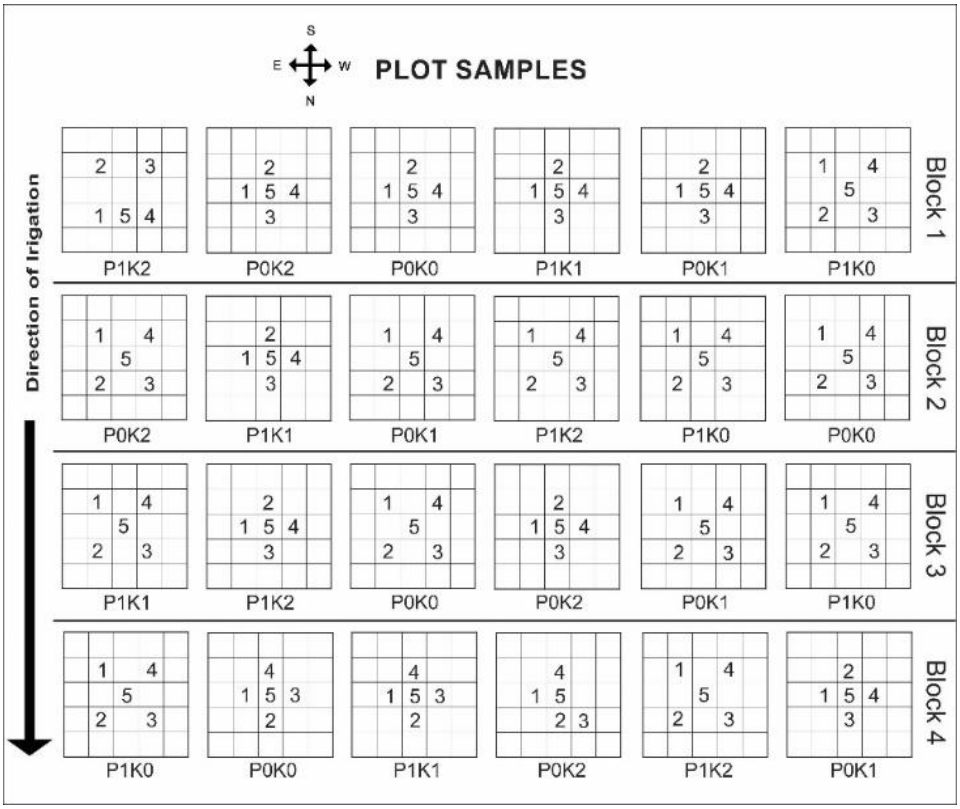

Figure 4. Samples of each sub plot

3. RESULTS AND DISCUSSION

3.1 Soil characteristics

3.1.1 Soil pH

Result of soil pH analysis can be seen in Figure 5 below.

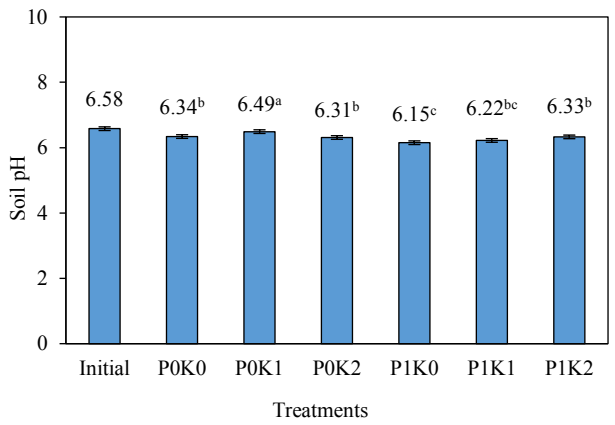

Figure 5. Soil pH

Figure 5 shows decreases of soil pH from its initial soil pH in all treatments. This is due to the nitrogen content in textile industry waste that flows in irrigation water. Foth (1995) stated that nitrogen in the form of ammonia or other can turn into nitrate because of the nitrification process that produces hydrogen ions. Based on the results of the laboratory analysis showed that Urea pH of 5.5; SP36 of 6 and KCl of 6. This causes the soil pH to drop from the initial soil.

ANOVA results showed that inorganic fertilizer treatment had a very significant effected on soil pH, whereas bioremediation agent treatments did not significantly affect the soil pH. The interaction between inorganic fertilizer and bioremediation agent treatments significantly affected the soil pH. Figure 5 shows the treatment P0K1 has the highest soil pH value and was significantly different with other treatments. The treatment has the lowest decrease of pH compared to initial soil pH by 1.37%. Meanwhile the control decreased by 3.64% from the initial soil pH. Soil pH in P0K1 treatment was higher than the control, this is in accordance with the study by Li and Zhang (2012) which found that microbial biology activity can increase Ca^{2+} cation availability, which can increase soil pH. Based on the soil bacterial colonies it can be seen the P1K1 treatment was the highest treatment followed by the P0K1 treatment, but in the P1K1 treatment there was an inorganic fertilizer that can reduce soil pH due to the substitution of H^+ in plant roots with cations in the soil, so the concentration of H^+ in the soil increases.

George et al. (2016) stated that biosorption process will be optimum around pH 5 for Pb ion. However, the soil pH in this study was greater than 6. Therefore, statistical analysis showed that soil pH had low correlation with soil Pb level.

3.1.2 Soil CEC (Cation Exchange Capacity)

Results of soil CEC analysis are shown in Figure 6 below.

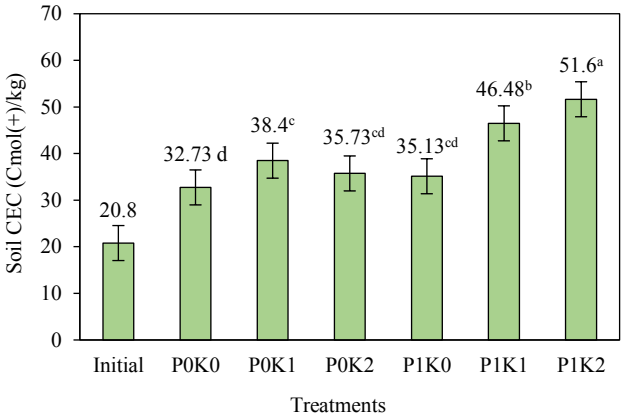

Figure 6. Soil CEC

Figure 6 shows soil CEC increase compared to its initial soil CEC in all treatments. This is caused by soil bacterial activities in soil organic matter decomposition thus it can increase soil CEC. Ferina et al. (2017) stated that soil bacterias can increase soil CEC with decomposition of soil organic matter. Hameed et al. (2015) stated soil microbes have an important role in immobilization of soil cations. The results of observations in this study showed that *Agrobacterium* sp. I26 has a dominant growth and its characteristics are stem, short, round, convex, flat, yellow colony and fine structure.

The ANOVA showed that inorganic fertilizer treatment, bioremediation agents and the interaction between these treatments had a significant affect on soil CEC. The P1K2 treatment had the highest soil CEC and was significantly different from all other treatments (51.65 Cmol(+)/kg), while the treatment with the lowest soil CEC was P0K0 (32, 73 Cmol(+)/kg) which was not significantly different with the P0K2 and P1K0. Walker et al. (2003) states that organic matter can increase CEC in soil. Treatment combinations of inorganic fertilizer and bioremediation agents made the increasing of soil CEC higher than treatment without inorganic fertilizer. Mujiyati and Supriyadi (2009) and Su et al. (2014) also stated that inorganic fertilizers can

increase the activity of plant roots in producing root exudates as a source of energy for bacteria to decompose organic matter, thereby increasing soil CEC.

The decomposition result of soil organic matter is organic acids which have a negatively charged functional group, thus it helps increase soil CEC (Kargar et al., 2015). Soil CEC have an important role in the exchange of cations in colloidal soil. Soils that have a lot of clay content can minimize the availability of Pb. In this study, *Agrobacterium* sp. I26 and fertilizer also act as bioremediation agents to immobilize Pb metal in the soil. Bacteria produce secondary metabolites consisting of many organic compounds such as enzymes, organic acids, hormones, etc., which can also increase soil CEC.

3.1.3 Soil organic matter

Result of soil organic matter analysis could be seen in Figure 7 below.

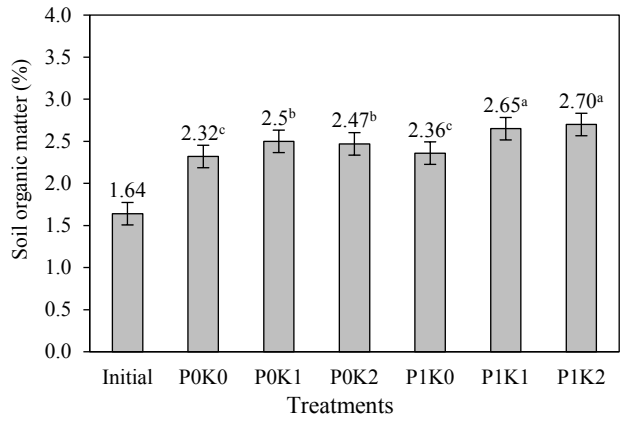

Figure 7. Soil organic matter

Figure 7 shows the content of organic matter increased from the initial soil in all treatments. This was due to soil bacterial activity in decomposing soil organic matter in the soil. The ANOVA showed that the treatment of inorganic fertilizers and bioremediation agents significantly affected the soil organic matter. The interaction between the treatment of inorganic fertilizers and bioremediation agents significantly affected the content of organic matter in the soil. Figure 7 shows that the treatment with the lowest soil organic matter was P0K0 (control) treatment at 2.32% which was not significantly different from P1K0 treatment.

The treatment with the highest organic matter content was P1K2 at 2.70% and not significantly different from P1K1 treatment. This suggests that bioremediation agents can increase the soil organic matter. The combination of inorganic fertilizer and bioremediation agents could increase the plant growth so plant would produce root exudate more than other treatments. Therefore the soil organic matter is also higher than other treatments. This is in accordance with the study of Johanto et al. (2019) and Rosariastuti et al. (2018) that revealed the combination of inorganic fertilizers with *Agrobacterium* bacteria can increase the highest value of organic matter compared to other treatment combinations.

Decomposition of organic matter will produce simple organic acids. According to Huang and Schnitzer (1997) and Ding et al. (2016), effective organic acids in soil mineral binding are the result of decomposition of organic matter with high molecular weight acid complexes, for example humic acid. Johanto et al. (2019) revealed that the process of decomposition of organic matter would release cation bonds in complex compounds of humic acid or fulvate and be replaced by Pb, so that Pb in the soil formed Pb II - Humic complexes.

3.1.4 Soil bacteria colonies

Result of soil bacteria colonies analysis could be seen in Figure 8 below.

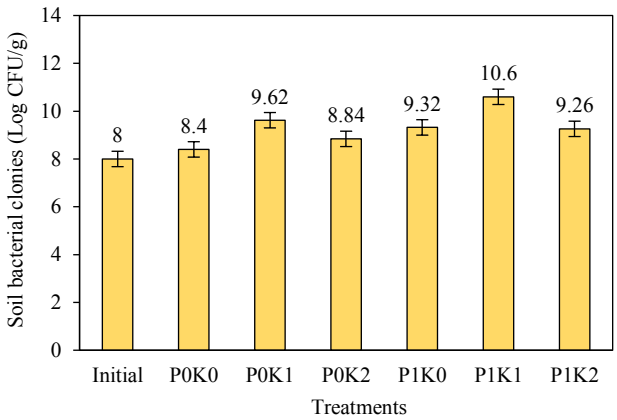

Figure 8. Soil bacteria colonies

Figure 8 shows that the average number of soil bacteria colonies increased compared with the initial soil bacteria colonies in all treatments including P0K0 (control). This was possible due to the bacterial activity from previous research. The bacteria colonies showed that *Agrobacterium* sp. I26 looked to be dominant with characterization such as cell rod morphology/cells type, negative gram stain reaction, and motility. The colonies morphology was spherical, convex, and the inner structure was smooth.

The ANOVA showed that the treatment of inorganic fertilizers, bioremediation agents and interactions between the two treatments had no significant affect on the soil bacteria colonies. Although the treatments had no significant affect, the treatment that used *Agrobacterium* sp. I26 had soil bacteria colonies higher than the other treatments.

According to Rosariastuti et al. (2013), the bacteria *Agrobacterium* sp. I26 is able to grow in aerobic conditions and temperatures around 40 °C. Paddy soil conditions in this research tended to be wet for several days due to rain, so that bacterial growth was less optimal and each treatment was not significantly different. The highest soil bacterial colonies was in P1K1 treatment of 10.6 Log CFU/g, while the treatment with the lowest soil bacterial colonies was P0K0 (control) treatment of 8.4 Log CFU/g.

Rosariastuti et al. (2018) stated that the combination of inorganic fertilizers and *Agrobacterium* sp. I3 can increase the highest total bacterial colonies compared to other treatments. Narayani and Shetty (2013) said that secondary metabolites produced by bacteria in soil can efficiently eliminate Pb through bioaccumulation. Bacteria can bind Pb ions in the soil by extracellular polymers or extracellular poly-saccharides produced by bacterial cells and have a reactive side of negatively charged cells.

3.1.5 Soil Pb level

Results of soil Pb level analysis are shown in Figure 9 below.

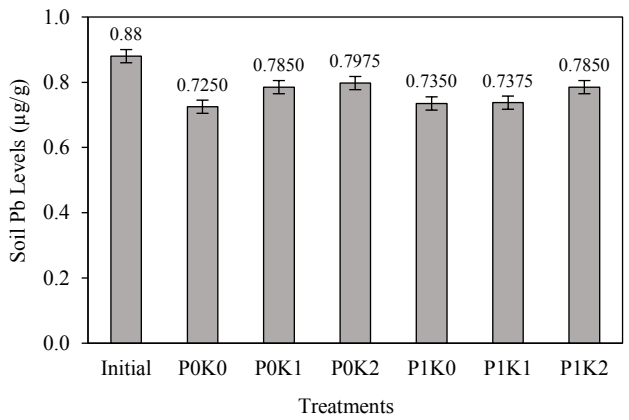

Figure 9. Soil Pb levels

Figure 9 shows that Pb soil levels decreased from the initial Pb soil level in all treatments. Factors that causes a decrease of Pb soil levels are Pb absorb by plant and Pb leaching caused by rainwater. The weather in the study area was rainy, so the rainfall intensity tends to be high. Johanto et al. (2019) stated decreasing Pb levels in soil was possible due to the presence of leaching factor. Based on Figure 9 it can be seen that the decrease in soil Pb level from the initial soil to the final soil was not high, this may be due to the influence of the soil type at the study site, namely vertisol (sand 6.294%, dust 25.756%, clay 67.950%). The texture that was dominant by clay will cause Pb to be bound by colloidal soil.

The result of ANOVA showed that inorganic fertilizer treatment had no significant affect on soil Pb levels, whereas the bioremediation agents treatment had a significant affect on soil Pb levels. The interaction between inorganic fertilizers and bioremediation agents treatments did not significantly affect soil Pb levels. Treatment with the highest soil Pb level was P0K2 treatment (0.7975 µg/g), while the treatment with the lowest soil Pb levels was P0K0 treatment (0.7250 µg/g).

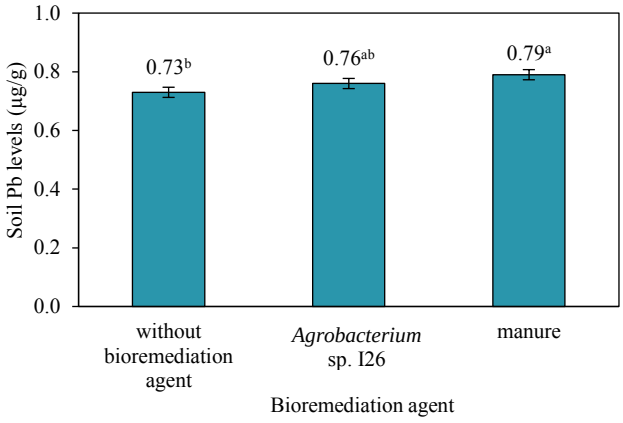

Figure 10. Effect of bioremediation agent on soil Pb level.

The treatments without bioremediation agents were significantly different from treatment using manure (sig 0.009). Treatment using *Agrobacterium* sp. I26 had no significant affect to other treatments. Although treatment with *Agrobacterium* sp. I26 was not significantly different from treatment without bioremediation agents, the soil Pb levels in treatment with *Agrobacterium* sp. I26 was higher than without bioremediation agents. This means the two bioremediation agents could inhibit the soil Pb absorbed by plants or immobilize the Pb in soil. Rosariastuti et al. (2013) stated that the addition of *Agrobacterium* sp. I26 can minimize Pb absorption so that it does not enter into the shoot of plants. Narayani and Shetty (2013) also said that bacteria can produce secondary metabolites which can efficiently eliminate Pb through bioaccumulation.

Decreasing Pb on land caused by phytoremediation activities can be used to calculate the effectiveness of phytoremediation. The effectiveness of bioremediation or often called Removal Effectiveness (RE) is the success of the phytoremediation process in soil which is calculated from differences in initial heavy metal levels and final heavy metal content after treatment

$$RE = \frac{\text{InitialPb level} - \text{final Pb level}}{\text{Initial Pb level}} \times 100\%$$

Removal effectivity values can see in the Table 1 below.

Table 2. Removal effectivity (RE)

Treatments	Removal effectivity (%)
P0K0	17.04
P0K1	10.39
P0K2	8.96
P1K0	16.10
P1K1	15.81
P1K2	10.39

Table 2 shows the decrease of soil Pb levels in all treatments. In this study, the treatment with the lowest effectiveness was the best treatment because this study aimed to minimize the absorption of soil Pb to the plant tissue, especially grain. Table 2 shows the best treatment with the lowest RE of 8.96% was P0K2 treatment. This phenomenon was in accordance with the soil organic matter that can bind the Pb in the soil with humic being Humic - Pb (II).

3.2 Plant characteristics

3.2.1 Weight of 1,000 seeds

Result of weight of 1,000 seeds analysis could be seen in Figure 11 below.

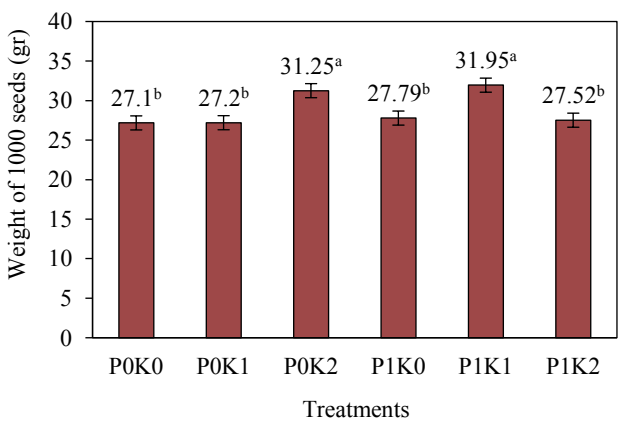

Figure 11. Weight of 1,000 seeds

Figure 11 shows the P0K2 and P1K1 treatments can increase the weight of 1,000 seeds compared with control. The lowest weight of 1,000 seeds was P0K0 treatment of 27.17 g, while the highest weight of 1000 seeds was P1K1 treatment of 31.95 g, but it was not significantly different from the P0K2 treatment. This showed that *Agrobacterium* sp. I26 affects the weight of 1,000 seeds of rice.

The ANOVA showed that inorganic fertilizer treatment did not significantly affect the weight of 1,000 seeds of rice, but bioremediation agents and interaction between inorganic fertilizer and bioremediation agent fertilizer had a very significant affect on the weight of 1,000 seeds of rice.

Manure can increase the weight of 1,000 seeds, but when combined with inorganic fertilizer it had a lower weight of 1,000 seeds than without inorganic fertilizer. This is because the immature organic matter in manure which have high molecular weight can bind the nutrients in soil. Nutrients that are bound by immature organic matter will be immobilized in soil. *Agrobacterium* sp. I26 can increase the weight of 1,000 seeds, but when combined with inorganic fertilizer it can increase more optimally the weight of 1,000 seeds. This is because the inorganic fertilizer can promote plant growth, so that the plant produced many root exudates that can be energy for bacteria (Vigliotta et al., 2016). Bacteria could produce enzymes which will increase the process of metabolism, so it could increase the weight of 1,000 seeds.

According to research conducted by Mulsanti et al. (2014) about the weight of 1,000 seeds in various varieties of paddy showed that the weight of 1,000 seeds of Ciherang varieties showed the highest weight of 1,000 seeds was 26.19 g. In this study the weight of 1,000 seeds were better than Mulsanti's research, including in the control treatment.

3.2.2 Pb Content in plant

Table 3 shows the average Pb content in roots higher than in plant shoot and rice grain. It means that paddy plants accumulated Pb in their roots and did not translocate the Pb in plant shoot.

ANOVA showed that inorganic fertilizers significant affected Pb content in roots, but not significantly affect Pb content in plant shoots and rice grain. Bioremediation agent treatments significantly affected Pb content in roots and rice grain, but did not significantly affect Pb content in plant shoots. Interaction between inorganic fertilizers and

bioremediation agent had significantly effected to Pb content in roots, but not significantly effected to Pb content in plant shoot and rice grains.

Table 3. Pb content in plant

Treatments	Pb content in plant (µg/g)			
	Roots	Shoots	Grains	Totals
0K0	0.84[b]	0.0280	0.48	0.31[b]
P0K1	0.93[b]	0.0080	0.30	0.22[d]
P0K2	0.87[b]	0.0009	0.41	0.26[bc]
P1K0	1.10[a]	0.0255	0.43	0.31[a]
P1K1	0.26[c]	0.0155	0.29	0.17[e]
P1K2	0.31[c]	0.0009	0.42	0.23[cd]

P1K1 treatment had the lowest Pb content: 0.17 µg/g, while the treatment with the highest Pb content was P0K0: 0.31 µg/g. In general, bioremediation agents can inhibit the entry of Pb into plant shoots, especially in the rice grain, but *Agrobacterium* sp. I26 can inhibit the entry of Pb more than manure. This is in accordance with Rosariastuti et al. (2013), which found that the application of *Agrobacterium* sp. I26 was able to minimize Pb absorption to plant tissue and accumulate in roots. Narayani and Shetty (2013) also said that bacteria application induced secondary metabolites that efficiently eliminate Pb through bioaccumulation. *Agrobacterium* sp. I26 can bind Pb ions in soil by extracellular polymer or extracellular polysaccharide produced by bacteria and has reactive cell with negative charges. Pramono et al. (2013) also said that *Agrobacterium* sp. I26 can produce the reductase enzyme that can reduce the chromium from toxic (available for plant) to non-toxic (non-available for plant). Therefore, it is possible that the reductase enzyme can reduce the Pb^{4+} (available for plants) to Pb^{2+}/Pb II (not available for plants).

The initial soil showed that soil Pb level was 0.88 µg/g and the final soil has an average that was not much different from the initial soil, while the soil Pb level showed the Pb that enters the plant tissue was higher than the difference between the initial and final soil. This is due to the addition of inorganic fertilizers thereby increasing soil pH, while initial soil pH sampling came before the application of inorganic fertilizers.

Based on Indonesia's Badan Standardisasi Nasional (2009), the maximum allowable Pb content in rice grains is 0.3 µg/g. This study (Table 3) showed that the only treatment that inhibited Pb absorption to the threshold or below was treatment using bioremediation agent *Agrobacterium* sp. I26, and the best combination treatments was P1K1 treatment.

4. CONCLUSION

Based on the results of this study it can be concluded that the highest production weight of 1000 seeds was P1K1 (inorganic fertilizer + *Agrobacterium* sp. I26) treatment of 31.95 g (14.96% higher than the control) followed by P0K2 (without inorganic fertilizer + manure) treatment of 31.25 g (13.06% higher than control). The treatment that can inhibit the absorption of Pb in rice grains to below the threshold was P1K1 (inorganic fertilizer + *Agrobacterium* sp. I26) treatment of 0, 29 µg/g (39.58% lower than control) followed by P0K1 (without inorganic fertilizer + *Agrobacterium* sp. I26) treatment of 0.30 µg/g (37.5% lower than control).

ACKNOWLEDGEMENTS

This research was funded by national strategic research funds year 2018 of the Ministry of Research, Technology and Higher Education of Indonesia.

REFERENCES

Darmono. Environment and Pollution; Its Relationship with Toxicology of Metal Compounds. Jakarta, Indonesia: Universitas Indonesia Press; 2001.

Ding L, Shen SG, Liang SX. Effect of different organic acids for heavy metal extraction from Pb, Zn, and Cd contaminated soil. International Conference on Energy Development and Environment Protection; 2016 Jun 11-12; Beijing: China; 2016.

Ferina P, Rosariastuti R, Supriyadi. The effectiveness of mendong plant (*Fimbrystilis globulosa*) as a phytoremediator of soil contaminated with chromium of industrial waste. Journal of Degraded and Mining Lands Management 2017;4(4):899-905.

Foth HD. Fundamentals of Soil Science. Yogyakarta, Indonesia: Gadjah Mada University Press; 1995.

George SK, Revathi BK, Deepa N. A study on the potential of moringa leaf and bark extract in bioremediation of heavy metals from water collected from Various Lakes in Bangalore. Procedia Environmental Sciences 2016;35:869-80.

Government Regulation of Republik of Indonesia. Management of hazardous and toxic wastes, No. 101. Indonesia: Government Regulation of Indonesia; 2014.

Hameed AHAE, Ewada WE, Abou-Taleb KAA. Biosorption of uranium and heavy metals using some local fungi isolated from phosphatic fertilizer. Annals of Agricultural Science 2015;60(2):345-51.

Huang PM, Schnitzer M. Soil mineral interactions with natural organics and microbes. Proceedings of the Symposium on the Soil Science Society of America; 1997 Aug 15-16; Washington DC: United states; 1997.

Indonesia's Badan Standardisasi Nasional. Maximum Limit of Metal Contamination in Food. Jakarta, Indonesia: Indonesia's Badan Standardisasi Nasional; 2009.

Indonesia's Balai Penelitian Tanah. Technical Guide, Chemical Analysis of Soil, Plants, Water and Fertilizers. Jawa Barat, Indonesia: Balai Penelitian Tanah Bogor; 2009.

Johanto A, Rosariastuti R, Vita R. Effort to get safe rice for consumption through bioremediation technology in paddy field contaminated by lead. Tropical and Subtropical Agroecosystems 2019;22:179-88.

Kargar M, Clark OG, Hendershot WH, Jutras P, Prasher SO. Immobilization of trace metals in contaminated urban soil amended with compost and biochar. Water, Air and Soil Pollution 2015;226:191.

Kharisma AY, Sri B, Rosariastuti R. Application of *Agrobacterium* sp. I30 and vermicompost to suppress lead (Pb) uptake by rice in Pb polluted soil. Journal of Degraded and Mining Lands Management 2018;6(1):1545-52.

Li J, Zhang Y. Remediation technology for the uranium contaminated environment: A review. Procedia Environmental Sciences 2012;13:1609-15.

Minister of Agriculture Regulation Republic of Indonesia. Recommendations for fertilizing N, P, and K in specific location rice paddy soils, No. 40. Indonesia: Ministry of Agriculture; 2007.

Mujiyati, Supriyadi. Effect of manure and NPK to increase soil bacterial population of Azotobacter and Azosprillum in chili (*Capscium annum*) cultivation. Nusantara Bioscience 2009;1:59-64.

Mulsanti I, Wahyuni S, Sembiring H. Multiple results from four different variety of rice. Food Crop Agricultural 2014; 3(33):169-76.

Narayani M, Shetty V. Chromium resistant bacteria and their environmental condition for hexavalent chromium removal: A review. Critical Reviews in Environmental Science and Technology 2013;43:955-1009.

Pramono A, Rosariastuti R, Ngadiman, Irfan DP. Bacterial Cr (Vi) reduction and its impact in bioremediation. Journal Ilmu Lingkungan 2013;11(2):120-31.

Rauf AW, Syamsuddin, Sihombing SR. The Role of NPK Fertilizer on Rice Plant. Irian Jaya, Indonesia: Workshop on Assessment of Agricultural Technology; 2000.

Rosariastuti R, Umi Barokah, Purwanto, Supriyadi. Phytoremediation of Pb contaminated paddy field using combination of *Agrobacterium* sp. I3, compost and ramie (*Boehmeria nivea*). Journal of Degraded and Mining Lands Management 2018;4(5):1381-8.

Rosariastuti R, Irfan DP, Ngadiman, Gani SP, Angry RP. Isolation and identification of plant growth promoting and chromium uptake enhancing bacteria from soil contaminated by leather tanning industrial waste. Journal of Basic and Applied Science 2013;9:243-51.

Su J, Ding L, Xie K, Yao H, Quensen J, Bai S, Wei W, Wu J, Zhou J, Tiedje JM, Zhu Y. Longterm balanced fertilization increases the soil microbial functional diversity in a Phosphateuslimited paddy soil. Molecular Ecology 2014;24(1):136-50.

Syaifullah. Industrialization, industrial man and social change. Journal Geografi GEA 2009;9(1):39-50.

Ullman. Encyclopedia of Industrial Chemistry. Germany: VCH; 2003.

Vigliotta G, Matrella S, Angela C, Guarino F. Effects of heavy metals and chelants on Phytoremediation capacity and on Rhizobacterial communities of Maize. Journal of Environmental Management 2016;179:93-102.

Walker DJ, Clemente R, Roig A, Bernal MP. The effects of soil amendments on heavy metal bioavailability in two contaminated Mediterranean soils. Environmental Pollution 2003;122:303-12.

Wuana RA, Okieimen FE, Imborvungu JA. Removal of heavy metals from a contaminated soil using organic chelating acids. International Journal Environmental Science Technology 2010;7:485.

Structural Durability Assessment of Stilt Houses to Flash Flooding: Case Study of Flash Flood-Affected Sites in Thailand

Olarn Charoenchai[1,2,*] and Kampanad Bhaktikul[1]

[1]*Faculty of Environment and Resource Studies, Mahidol University, Nakhon Pathom 73170, Thailand*
[2]*Faculty of Architecture, Kasetsart University, Bangkok 10900, Thailand*

ARTICLE INFO

Received: 22 Jun 2019
Received in revised: 1 Oct 2019
Accepted: 9 Oct 2019
Published online: 30 Oct 2019
DOI: 10.32526/ennrj.18.1.2020.09

Keywords:
Stilt house/ Flash flood/ Durability assessment/ Structural durability/ Main structure/ Flood loads/ Reactive stress

*** Corresponding author:**
E-mail: archolarn@gmail.com; archolc@ku.ac.th

ABSTRACT

The 'stilt house' is found in many flood-prone areas and represents local wisdom regarding building construction to coexist with floodwaters. Most academic research projects have studied stilt houses based on two types of flood: inundation and coastal flooding. The study of pillar houses in flash floods is very limited. This research investigated whether the main structure of a stilt house could withstand strong water current to determine the suitability of the stilt house for flash flood sites. The study explored the physical appearance of stilt houses in five flash flood areas in Thailand. The styles of stilt houses in each area were simplified to generate models and to then test their tolerance toward moving water. The main findings were: 1) the main structure of the stilt house can resist flood loads at 1.00 m depth with a waterflow speed at 3.05 m/s; 2) the most vulnerable points on the main structure if struck by more rapid, deeper flows of water are the base of the column and the joint between the column and beams; and 3) the horizontal or diagonal bracing members perpendicular to the flow and not above the flood level become water blockades that increase the reactive force to the main structure.

1. INTRODUCTION

In recent years, the technology of flood control has been questioned due to devastating consequences since, despite the extensive implementation of flood control measures to prevent flooding, human settlements around the world remain vulnerable to flood hazards (Andersen and Shepherd, 2013). Flood control infrastructure cannot cope with extreme flows that exceed its design capacity and it can fail unexpectedly with smaller flows. The recognition that flooding cannot be completely prevented gave rise to integrated flood risk management that incorporates non-structural measures (Parker, 2000). The ideology that flooding should be prevented in the first place or the 'flood control paradigm' remains unchallenged (Liao, 2014). With increasing flood risks associated with climate change, relying solely on flood control would make many areas more vulnerable (Liao et al., 2016). For this reason, searching for new methods of flood management and 'living with floods' has been mentioned as a new alternative strategy. It is a flood adaptation paradigm which is concerned with preventing damage when flooding happens. This strategy is different from flood control; it does not try to change the flood regime but attempts to integrate with the actual or expected flood (Liao et al., 2016). Coexistence with floodwaters has always been a part of rural life in developing countries (Laituri, 2000), whereas people in urban areas continue to rely greatly on flood control mechanisms. Although the living-with-floods lifestyle is vastly dissimilar to modern urbanism, it has enlightened flood management discourses (Thaitakoo et al., 2013; Zevenbergen et al., 2011). The flood adaptation paradigm is most expressed in the built environment, particularly in buildings. Houses on stilts are commonly found in flood-prone locations and are likely to become a unique housing style in flood risk areas. During the flood season, these houses are above the flood water since the downstairs area such houses is almost empty, so the floodwaters can pass underneath through the gaps between the supporting columns. During the dry season, there is an additional shaded

Citation: Charoenchai O, Bhaktikul K. Structural durability assessment of stilt houses to flash flooding: Case study of flash flood-affected sites in Thailand. Environ. Nat. Resour. J. 2020;18(1):85-100. DOI: 10.32526/ennrj.18.1.2020.09

and dry space under the house for various activities (Kusar and Ut, 2014).

Many research projects have studied houses on stilts with various objectives. Mongkonkerd et al. (2013) studied the monetary damage of the big flood in 2011 to a pillar house in the Chao Phraya River Basin, Thailand. Ramasoot and Nimsamur (2014) estimated damages to a stilt house and the cost to repair or replace components due to flood inundation in a riparian community in the Chao Phraya River Basin. Liao et al. (2016) studied the physical appearance of stilt houses and how this influenced their coping capacity to seasonal flooding and utilization of ground level in dry season and explored ways to reinforce such stilt houses. They selected two hamlets in the Vietnamese Mekong Delta as study sites. Tikul and Thongdee (2015) estimated the coping capacity of pillar houses in three low-income communities of upper Northern Thailand to flood inundation. Kusar and Ut (2014) studied the structure and building materials of a modern house on columns built to coexist with flood inundation in the marshland of Ljubljana, Slovenia. Sastrawati (2009) examined the characteristics of stilt houses in a coastal area of Makassar, Indonesia, especially in terms of safety and security aspects, with the study focusing on the resistance of building construction to coastal flooding. Hryczyszyn and Neil (2014) studied stilt houses over inundating floodwaters in the Mekong Delta region of Southern Vietnam. They determined spatial characteristics and the importance of stilt houses and analyzed their distribution pattern in the area. From the above, it can be seen that these research studies were all concerned with stilt houses in events of inundation and coastal flooding. In fact, another type of flooding is flash flooding, which has generated severe damage to buildings and losses to people in various regions of the world. The above literature study revealed scarce attention has been paid to stilt houses in flash flood-prone areas. The current study aimed to fulfill such a conspicuous gap by exploring the physical characteristics of stilt houses in flash flooding locations and examined their structural durability to moving water. It was also expected that the research results would identify the vulnerable points of the pillar structure when struck by a flash flood and lead to the improvement and reinforcement of the house to better cope with this type of flood in the future. The completeness of the methodology, processes, and results of the structural durability assessment of a stilt house in this paper was accomplished by referring to some parts of a previous study (Charoenchai, 2018).

2. METHODOLOGY

2.1 Study areas

Five communities were selected as study areas because they had been struck by flash flooding almost every year or had experienced severe flash flooding in the past. The study areas were: Mae Phun community in Uttaradit Province, Nam Kor community in Phetchabun Province (these two communities are located in the lower Northern Thailand), Krung Ching community in Nakhon Si Thammarat Province, Tamot community in Phatthalung Province and Prig community in Songkhla Province (these three communities are located in the Southern (east coast) Thailand) as shown in Figure 1. To live with serious damage from flash flooding various adaptation strategies are required, including house modifications. The stilt house is one important solution and this type of house is commonly found in the five communities above.

Mae Phun community is located in Mae Phun Sub-district, Lap Lae District, Uttaradit Province. It is in the Nan Sector IV Basin (a branch of the Nan Basin) (Hydro and Agro Informatics Institute, 2012a). It covers 116 km^2 and consists of 11 villages, 3,685 households, and a population of 9,338. Mae Phun is settled in a valley surrounded by forests and mountains. The overall topography is plains between mountains. Many important waterways that flow through this community include: Mae Prong canal; Mae Phun creek; Kum Bi (Ban Di) Creek; Mae Bok creek; and Tai creek (Department of Mineral Resources, 2013). Mae Phun has experienced seasonal flash flooding almost every year, which frequently takes place from June to August. The average depth of floodwaters is 1.50 m and remains in the community from 4 h to 2 days. In 2006 and 2009 devastating flooding caused widespread damage. The flooding in 2006 was the most extreme, with a large number of houses and farming areas entirely destroyed and many fatalities (Nation Multimedia Group, 2006; Editorial Department of Komchadluek Newspaper, 2008).

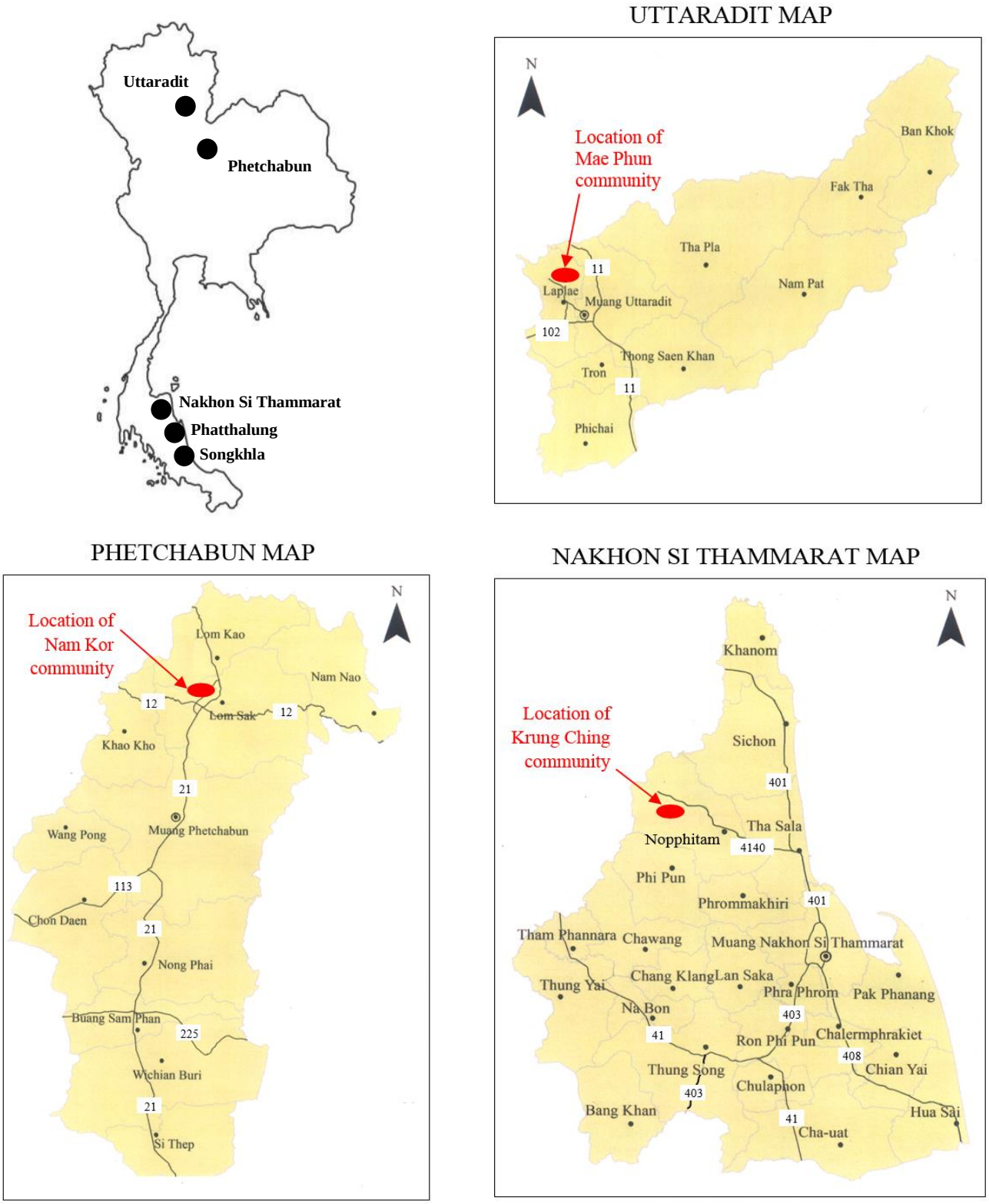

Legend:

Location of the community

Figure 1. Location of five study sites

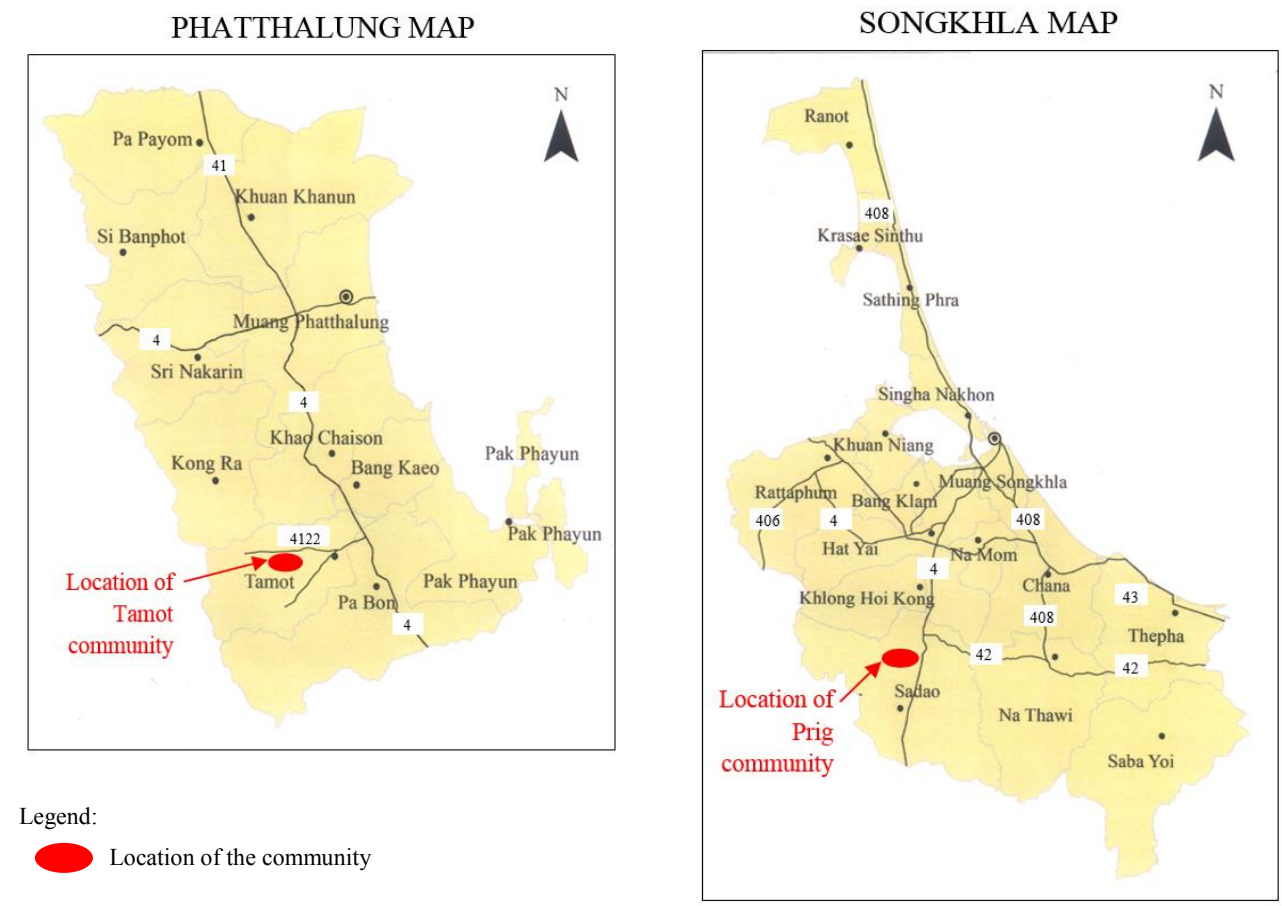

Figure 1. Location of five study sites (cont.)

Nam Kor community is located in Nam Kor Sub-district, Lom Sak District, Phetchabun Province. It is in the Huay Nam Phung Watershed (a branch of the Pasak Watershed) (Hydro and Agro Informatics Institute, 2012b). It covers 183 km^2, 13 villages, 2,365 households, and has a population of 6,720. The overall topography is high steep mountains and plains. The community is settled on the plains. Nam Kor creek is the only main water channel. In the rainy season every year (from June to September), Nam Kor always has flash flooding. The floodwaters have deluged the community from 2 h to 3 days with water depths of 0.20-2.00 m. In 2001, an enormous and unprecedented flash flood hit Nam Kor. This flood demolished a great number of houses, destroyed many livestock, farms, and rice paddies, and caused many injuries and deaths (Nam Kor subdistrict Administrative Organization, 2015).

Krung Ching community is in the Krung Ching Sub-district, Nopphitam District, Nakhon Si Thammarat Province. It is located in Klong Klai Basin (a branch of the Eastside South Watershed) (Hydro and Agro Informatics Institute, 2012c). It covers 364 km^2, 11 villages, 3,537 households, and has a population of 9,740. Krung Ching is settled in a valley surrounded by mountains. The overall topography is plateaus and mountains. There are many waterways flowing through the community: Lek, Wat, Nopphitam creeks, Klai, Phitam, Pien, Pong, and Phot canal (Krung Ching subdistrict Administrative Organization, 2015). Flash flooding has taken place almost every year in Krung Ching during the peak rainfall season (November to December). Floodwaters have immersed the community from 1 h to 2 days with water depths of 1.0-2.0 m. In 2010, 2011, and 2013, this community was hit by serious flash floods that the residents there had never experienced before. Roads, bridges, para-rubber and fruit plantations, and houses were destroyed (Editorial Department of Naew Na Newspaper, 2011; Sunanta, 2011; Focus News Agency, 2011).

Tamot community is in Tamot Sub-district, Tamot District, Phatthalung Province. It is located on the western side of the Songkhla Lake Basin. The overall topography is hillocks and plains. Most of the

community is settled on the plains. There are four important canals that run through the community: Tamot; Kong; Hua Chang; and Lo Chang Kra. This community covers 176.65 km^2, 12 villages, 1,879 households and has a population of 7,000 (HelpAge International, 2013). Tamot has faced flash flooding almost every year, particularly during the rainy season in November and December. The depth of floodwaters has been in the range 0.50-1.00 m with deluges lasting from 1 h to 1 day. Large flash floods were recorded in Tamot in 1970, 1998, 1999, 2010, and 2011.

Prig community is in Prig Sub-district, Sadao District, Songkhla Province. It is situated in the Songkhla Lake Watershed (Hydro and Agro Informatics Institute, 2012d). It covers 164.2 km^2, 11 villages, 5,349 households, and has a population of 16,364. Around 70% of the topography is plains and the remainder is foothill slopes. There are five important canals: U-Tapao; Prig; La Pang; Lay; and Sadao (Nopphaket, 2011; Prig Sub-district Health Plan Working Group, 2008). The basin-shaped catchment receives water from many canals, in the monsoon season during November and December, so that the canals overflow and flood the community with fast flowing water. Floodwaters have submerged Prig for around 1-3 days with a depth of 1.0-2.0 m. This community has been hit by flash flooding almost every year with notable severe flooding in 1959, 1966, 1972, 1978, 1988, 1998, 2010, and 2011 (Society and Health Institute, 2014).

2.2 Survey method

A guided field walk technique was used to explore and record the appearance of stilt houses at the five study sites. Recording involved roughly measuring some elements of each stilt house, such as size and dimension of columns, distance between columns, height from ground to stilt floor, elevation from stilt floor to roof beam, roof shape and its slope. In addition, notes and photos were used to record building materials of the house principal structure (columns and beams), roof structure, upper wall, stilt floor, and ground floor. The guided field walks were accompanied by well-known community figures to ensure households would co-operate and allow measurements to be taken. Guided field walks of the Tamot, Prig, and Krung Ching communities took place in March 2016 and surveys of the Nam Kor and Mae Phun communities occurred in July 2016.

2.3 Analysis

The assessment of structural sturdiness of stilt houses to flash flooding was conducted using software named Robot Structural Analysis Professional (Educational Version) (Autodesk, 2015). This software is an integrated program used for modeling, analyzing, and designing various types of structures. Data from the field surveys could be used to categorize the stilt houses into seven types. The physical appearance of each type was simplified and used as raw data to generate basic graphical models for testing structural durability. Flood loads were calculated and then applied to the models (Figure 2).

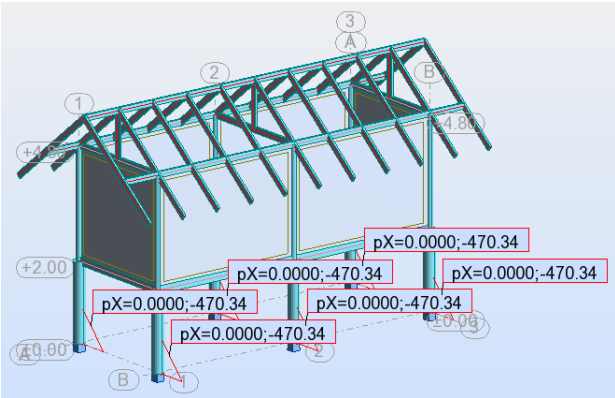

Figure 2. Example of basic graphical model of stilt house with applied flood loads on its downstairs columns.

The software processed and analyzed data and then showed the responsive stresses at any point on the main structure of the model. Such reactive stresses were compared with the ultimate strength of the material being used in the main structure. If the reactive stress is less than the ultimate strength, then the main structure of that house can resist flood loads. Conversely, if the reactive stress is higher than the ultimate strength, then the main structure is likely to be damaged by flood loads.

3. RESULTS AND DISCUSSION

3.1 Types of stilt house

From the field surveys at the five study sites, stilt houses could be categorized into seven types based on their physical characteristics, as shown in Table 1.

Table 1. Types of stilt house.

	Physical characteristics
Type I	Wooden roof structure, square wood columns 15 × 15 cm, wood walls, and wood floors (upstairs), round wood columns diameter 30 cm and earth ground (downstairs).
Type II	Wooden roof structure, round wood columns diameter 15 cm, wood walls, and wood floors (upstairs), round wood columns diameter 15 cm and earth ground (downstairs).
Type III	Wooden roof structure, square wood columns section 15 × 15 cm, wood walls, and wood floors (upstairs), square wood columns section 15 × 15 cm and earth ground (downstairs).
Type IV	Wooden roof structure, square wood columns section 15 × 15 cm, wood walls, and wood floors (upstairs), square wood columns section 15 × 15 cm, bracing wooden bars, and earth ground (downstairs).
Type V	Wooden roof structure, square wood columns section 15 × 15 cm, wood walls, and wood floors (upstairs), square concrete columns section 20 × 20 cm and concrete floor slabs on ground (downstairs).

Table 1. Types of stilt house (cont.)

	Physical characteristics
Type VI	Wooden roof structure, square concrete columns section 20 × 20 cm, bricked walls, and concrete floor slabs on beams (upstairs), square concrete columns section 20 × 20 cm and concrete floor slabs on ground (downstairs).
Type VII	Wooden roof structure, square concrete columns section 20 × 20 cm, bricked walls, and concrete floor slabs on beams (upstairs), square concrete columns section 20 × 20 cm and concrete floor slabs on beams (downstairs).

However, there were some common characteristics that were found in every type of stilt house. The distance between each column in the cross-sectional direction of the house was approximately 3.00 m while in the longitudinal direction it was approximately 4.00 m. The average height from the ground to the stilt floor was 2.00 m and from the stilt floor to the roof beam was 2.80 m. These common attributes were used as basic distances to create models of each type for subsequent durability testing.

3.2 Durability assessment of stilt house

Almost all houses in Thailand, including stilt houses, have been constructed using the post and lintel system where the main structure consists of columns and beams assembled as a frame to support other components including the roof, walls, floors, and staircases. The ability of the house to maintain its shape depends greatly on the stability of the main structure. If the main structure is damaged, other components of the house connected to the main structure will be damaged as well. For this reason, durability assessment of the stilt house to flash flooding in this research focused on evaluation of the stability of its main structure, including ground floor columns, ground floor or grade beams, stilt floor beams, stilt floor columns, and roof beams.

3.2.1 Calculation of flood loads

Flood loads are the loads on the building surface or structure induced by floodwaters. There are two basic types: hydrostatic and hydrodynamic. Hydrostatic loads are caused by water either above or below the ground surface, which results from either inundation or movement at a speed lower than 1.52 m/s. These loads are the product of the water pressure multiplied by the surface area on which the pressure acts. Hydrostatic pressure at any point is equal in all directions and acts perpendicular to the surface on which it is applied (American Society of Civil Engineers, 2014) and it can be calculated using the following equation (White, 1999):

$$p = q\,g\,h \tag{1}$$

Where: p = pressure (Pa or pascal)
q = density of water (1,000 kg/m^3)
g = acceleration of gravity (9.81 m/s^2)
h = depth in the water at which the pressure is measured (m)

Hydrodynamic loads are the loads that are induced by the flow of water moving at moderate-to-high speed above the ground. They are usually horizontal loads caused by the impact of a moving mass of water and the drag forces as the water flows around the obstruction. This type of load can be calculated using the following equation:

$$d_h = aV^2/2g \tag{2}$$

Where: d_h = surcharge depth (m)
V = average water velocity (m/s)
g = acceleration due to gravity (9.81 m/s^2)

a = coefficient of drag or shape factor (not less than 1.25)

Selection of the correct value of the drag coefficient "a" in Equation (2) depends on the shape and roughness of the object exposed to the flood flow. Generally, the smoother and more streamlined the object, the lower the drag coefficient. Drag coefficients of elements common in buildings and structures (round or square columns and rectangular shapes) will range from 1.0 to 2.0. However, the American Society of Civil Engineers (2014) recommends a minimum value of 1.25 be used. Equation (2) requires that the water velocity does not exceed 3.05 m/s. The dynamic effects of moving water should be permitted to be converted into hydrostatic pressure by increasing an equivalent surcharge depth (d_h) on the upstream side of the structure and above the ground only. Once the surcharge depth (d_h) is determined from Equation (2), it is added to the flood depth (h) in Equation (1) to calculate the resultant hydrostatic pressure. If different flow directions are considered, then each direction is an independent load case.

The calculation of both hydrostatic and hydrodynamic pressure is inevitably related to flood depth. Information on the flood depth at each study site resulted in defining the average flood depth as 1.00 m above the ground. Therefore, calculation of water pressure in this research was based on a 1.00 m depth for floodwaters. Flash flooding is an event where the mass of water moves above the ground and strikes obstructions at a certain speed, so it is absolutely related to hydrodynamic loads. In calculating the hydrodynamic pressure, the flow velocity is the key variable. In practice, it is very difficult to estimate the flow velocity precisely (American Society of Civil Engineers, 2014). From field investigations, it was found that there was no recording of flood velocity and a check with the state agencies working in water management revealed it has never been measured or recorded in small creeks or canals, only in large waterways. Each study site was located in a sub-basin having only canals as the main waterways; thus there were no data on the flood velocity for each site. Consequently, the current research used information on the average speed of flash floodwaters from other reliable sources. The American Society of Civil Engineers/Structural Engineering Institute Standard 7-05 (American Society of Civil Engineers, 2014) was used as a reference in this study. Such a standard classifies the flow of floodwaters into low velocity flow (the floodwater speed does not exceed 3.05 m/s) and high velocity flow (the water speed is greater than 3.05 m/s). Thus, 3.05 m/s is the velocity used to divide the kinds of flow and it was considered reasonable to apply this figure as the average velocity of flash floodwaters in this research.

3.2.2 Flood loads applying to each type of stilt house

Since the average height from the ground to the stilt floor of every type of stilt house in this study was 2.00 m (Table 1), for a flood depth of approximately 1.00 m, the members of the main structure directly impacted by the floodwaters are the columns at ground level. In addition to the flow velocity and the depth of floodwaters, the physical characteristics of downstairs column are another key factor influencing flood loads. The shape of the column determines the drag coefficient in Equation (2). Furthermore, it influences the value of the surcharge depth that is added to the flood depth in Equation (1) and finally, it affects the value of the hydrostatic pressure calculated using Equation (1). The size of the column determines the degree of surface area to impede floodwaters and then influences the extent of flood loads that impact each column because the flood loads are the product of the water pressure multiplied by the surface area on which the water pressure acts. Flood loads that are applied on downstairs columns of each type of stilt house were obtained using Equations (1) and (2).

A stilt house with round columns on the ground level has a surcharge depth (d_h) of 0.57 m and a water pressure at 1.57 m depth (h (1.00 m) + d_h (0.57 m)) of 1,567.80 kg/m^2. Flood loads which act on the surface area of each round column of stilt house Type I were 470.34 kg while for Type II they were 235.17 kg because the diameter of columns for stilt house Type II is smaller than for Type I (15 cm for Type II, 30 cm for Type I), so the surface area against the water is smaller, too (0.15 m^2 for Type II, 0.3 m^2 for Type I). A pillar house with square columns on the ground has an additional depth (d_h) of 0.95 m and so the water pressure at 1.95 m depth (h (1.00 m) + d_h (0.95 m)) is 1,947.50 kg/m^2. The value of 292.13 kg is the flood load acting on the surface area of each column of stilt house Types III and IV that have square columns of section 15 × 15 cm (surface area of each column against the floodwaters is 0.15 m^2). The flood load on each square column section 20 × 20 cm of stilt house

Types V-VII is 389.50 kg (surface area of each column against floodwaters is 0.20 m^2).

3.2.3 Results of structural durability assessment

When floodwaters at 1.00 m depth strike the downstairs columns of each type of stilt house, the main structure of the house reacts by generating responsive stresses at all points of its components as shown in Figure 3. The marks "-" and "+" do not represent the numerical meaning, they just indicate the type of stress that is compressive if a negative sign and tensile if there is a positive sign.

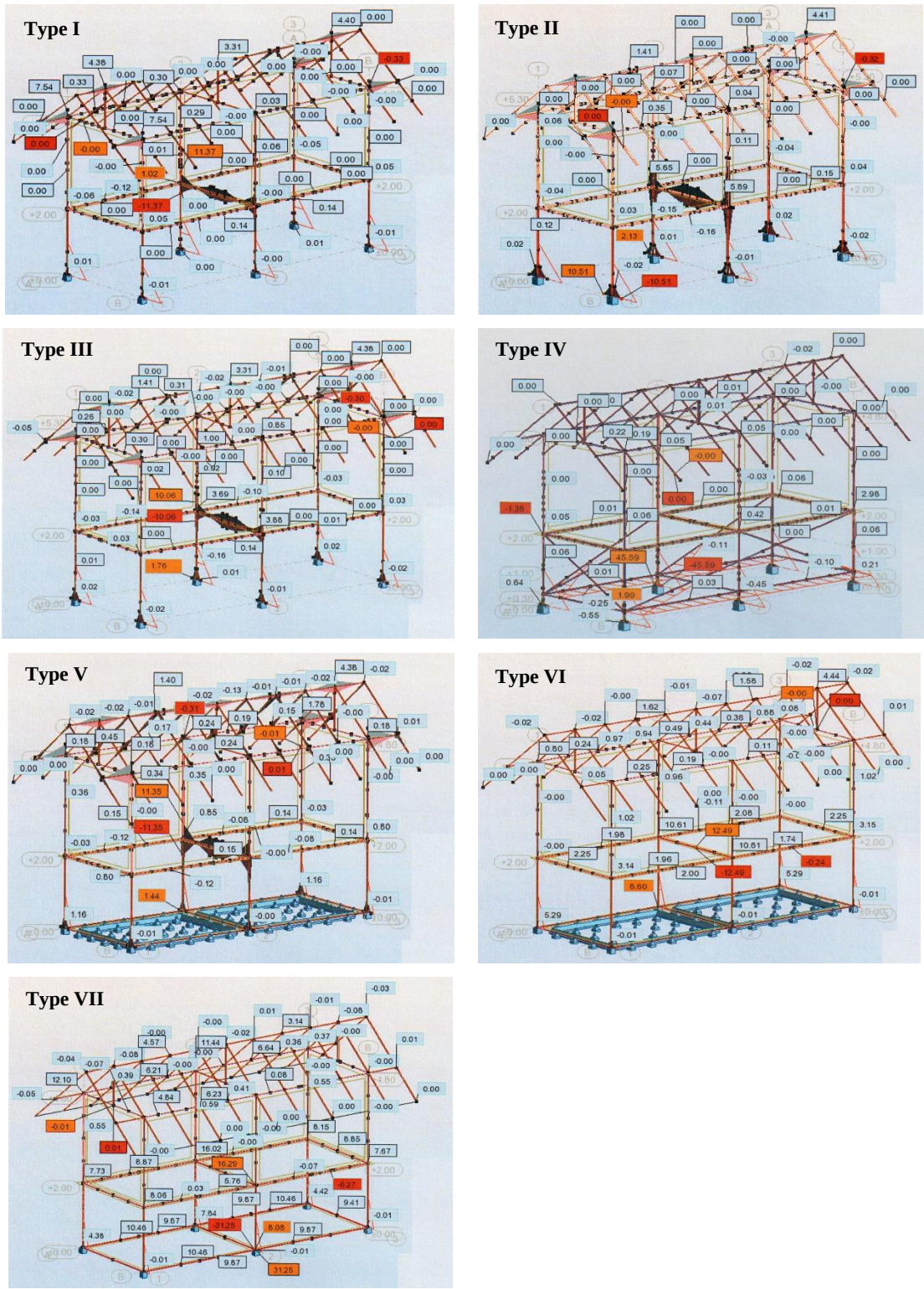

Figure 3. Reactive compressive and tensile stresses at any points of main structure of each type of stilt house, when struck by moving water at downstairs columns

Information on the mechanical properties of Thailand's timber species provided by the Royal Forest Department as cited by Chorwichien (2014) indicated the ultimate compressive and tensile strength of each kind of hardwood in the country and these strengths are divided into strength in the direction that is parallel and strength that is perpendicular to the wood grain. The current study only considered compressive and tensile strength normal to the grain because all timber columns and beams (the main structural elements) were produced with the grain parallel to the length of the component. Thus in the main frame of the house, their lateral surfaces along their length are impacted by the floodwater resulting in the flood loads acting in the direction that is perpendicular to the grain. The lowest value of ultimate compressive strength of hardwood (perpendicular to grain) is 99 kg/cm^2. The ultimate tensile strength normal to grain is approximately 10% of the tensile strength parallel to the grain (Chorwichien, 2014). The data on the mechanical properties of Thailand's timber species provided by the Royal Forest Department as referred to by Chorwichien (2014) specified the lowest ultimate tensile strength of hardwood (parallel to grain) as 806 kg/cm^2, so the lowest ultimate tensile strength that is perpendicular to grain is 80.6 kg/cm^2. For pillar house Types I-IV, for which the ground floor pillars were hardwood, their maximum compressive stresses (-11.37, -10.51, -10.06, -45.59 kg/cm^2, respectively) were not greater than 99 kg/cm^2. Similar to tension, their highest tensile stresses (+11.37, +10.51, +10.06, +45.59 kg/cm^2, respectively) were not over 80.6 kg/cm^2. The results indicated that flood loads at 1.00 m depth would not induce compressive and tensile stresses in the main structure that exceeded its ultimate strength; therefore these 4 types of stilt house could withstand the water current from a flash flood without any damage being caused to their main structures.

There are many factors affecting the ultimate compressive strength of concrete including: the type, quality and amount of cement, the quality, cleanness and grading of the aggregate, the quality and amount of water, the presence or lack of admixtures, the methods followed in handling and placing the concrete, the age of the concrete when placed in the forms, the temperature and curing conditions, and the age of the concrete when tested (Neville, 2015). The ultimate compressive strength of concrete is determined by casting some concrete specimens and curing them (by soaking) for 28 days, then subjecting those specimens to a specific force with a specific machine in the laboratory to determine the precise value of ultimate compressive strength of each sample. This method is extensively acknowledged as the general index to measure the ultimate compressive strength of concrete (CPAC Concrete Academy, 2000). In practice, on construction sites for general houses, no concrete specimens are used to test the ultimate compressive strength. Construction workers always mix concrete themselves and use it immediately, so there is no way to know accurately the ultimate compressive strength of that concrete. For this reason, this research had to refer to other trustworthy sources instead to obtain information on the ultimate compressive strength of concrete.

The review of the relevant literature indicated there were some sources mentioning the ultimate compressive strength of concrete. First, the ACI 318-14 standard (Section 19.2.1.1) indicated that a minimum specified ultimate compressive strength for structural concrete should be approximately 180 kg/cm^2 (American Concrete Institute, 2014). Second, Neville (2015) based on the 2015 IBC® and ACI 318-14: Concrete Quality and Field Practices specified that the ultimate compressive strength of concrete to make columns, walls, slabs, and beams should be in the range of 210-492 kg/cm^2. This research adopted the value of 180 kg/cm^2 as the ultimate compressive strength for the concrete used to build the main structures of the stilt houses at the five study sites since there was no general quality control associated with the common practice of mixing concrete on site without any strict quality control; thus, its ultimate compressive strength was not likely to be high. The figure of 180 kg/cm^2 was derived from the lowest value of the ultimate compressive strength of concrete indicated in the reference sources above.

Regarding the ultimate tensile strength of concrete, Neville (2015) mentioned that "Concrete in the structure is rarely loaded in pure tension, the tensile stresses being in connection with flexure, torsion or a combination of loadings. Research indicates that direct tension averages about 10 percent of the compressive". In addition, Al-Sahawneh (2015) stated that there is a variety of values of the ultimate tensile strength of concrete obtained from tests and measures, however, it could be concluded that the ultimate strength of concrete in tension is in the range of 7 to 11 percent of its ultimate compressive strength. Particularly, if the ultimate compressive strength of concrete was between 140 and 210 kg/cm^2, its ultimate tensile strength was approximately 10 percent of the compression. Thus,

the current study used 10 percent to calculate the ultimate tensile strength of concrete based on the ultimate compressive strength. Thus, for an ultimate compressive strength of 180 kg/cm^2, the capacity to bear maximum tensile stress would be 18 kg/cm^2.

The downstairs columns of stilt house Types V and VI were made of concrete and the testing results of structural durability revealed that the highest compressive and tensile stress in their main structure when hit by flood loads were not beyond the ultimate compressive and tensile strengths of the concrete. Stilt house Type V responded to flood loads by establishing reactive compressive and tensile stresses of -11.35 and + 11.35 kg/cm^2, respectively, at one joint of the column and stilt floor beam, whereas pillar house Type VI generated reactive compressive and tensile stresses of -12.49 and +12.49 kg/cm^2, respectively at one stilt floor beam made of concrete. Such values were not over the respective maxima of 18 kg/cm^2 and 180 kg/cm^2 indicating that the main structures in these two types of stilt house could tolerate flood loads. Similar to Types V and VI, the downstairs piles of stilt house Type VII were concrete and the highest compressive and tensile stresses (each being 31.25 kg/cm^2) occurred at the bottom of one column. Regarding compression, 31.25 kg/cm^2 is much less than the ultimate compressive strength of concrete (180 kg/cm^2), so these columns could resist compressive loads induced from floodwaters. Regarding tension, 31.25 kg/cm^2 is greater than the critical tensile bearing capacity of concrete (18 kg/cm^2), indicating that this concrete column in stilt house Type VII would likely be damaged due to the stress of tension. The field surveys revealed that in fact every column of this type of stilt house still existed without any damage. In practice, the core structure of the house was not made of pure concrete, but rather was reinforced concrete containing steel bars or rods within the concrete to increase the tensile strength of the concrete core structure. Engineers know well that concrete has a very limited capacity to bear tension, so they put reinforcing steel bars inside the concrete to absorb tensile stress instead, because of the very high ultimate tensile strength of steel.

The TIS 20-2543 standard indicated that the ultimate tensile strength of a round steel bar is 3,900 kg/cm^2 and of a deformed steel bar is 4,900 kg/cm^2 (Thai Industrial Standard Institute, 2001). The current research adopted 3,900 kg/cm^2 because most house owners in rural areas of Thailand (including the five study sites in the current research) prefer to use round steel bar to reinforce the concrete columns and beams of their houses. For stilt house Type VII, reinforced steel bars in concrete columns could bear a tensile stress of 31.25 kg/cm^2 instead of the lower value for concrete and this is the reason why every pile in this type of house was not affected by the water flow. The consequences of the structural durability assessment of the seven types of stilt house regarding flash flooding are provided in Table 2.

Table 2. Maximum reactive stress and durability assessment of main structure of each type of stilt house to flash flooding.

Type of stilt house	Maximum reactive stress	Ultimate compressive strength of main structure	Ultimate tensile strength of main structure	Percentage of maximum compressive stress to ultimate compressive strength	Percentage of maximum tensile stress to ultimate tensile strength	Durability to flash flooding
Type I (hardwood round column diameter 30 cm)	+11.37 kg/cm^2, -11.37 kg/cm^2 (at one joint between column and stilt floor beam)	99 kg/cm^2 (hardwood)	80.6 kg/cm^2 (hardwood)	11.48%	14.11%	Durable
Type II (hardwood round column diameter 15 cm)	+10.51 kg/cm^2, -10.51 kg/cm^2 (at one base of column)	99 kg/cm^2 (hardwood)	80.6 kg/cm^2 (hardwood)	10.62%	13.04%	Durable
Type III (hardwood square column 15×15 cm)	+10.06 kg/cm^2, -10.06 kg/cm^2 (at one joint between column and stilt floor beam)	99 kg/cm^2 (hardwood)	80.6 kg/cm^2 (hardwood)	10.16%	12.48%	Durable

Table 2. Maximum reactive stress and durability assessment of main structure of each type of stilt house to flash flooding (cont.).

Type of stilt house	Maximum reactive stress	Ultimate compressive strength of main structure	Ultimate tensile strength of main structure	Percentage of maximum compressive stress to ultimate compressive strength	Percentage of maximum tensile stress to ultimate tensile strength	Durability to flash flooding
Type IV (hardwood square column 15×15 cm with bracing bars)	+45.59 kg/cm^2, -45.59 kg/cm^2 (at one base of column)	99 kg/cm^2 (hardwood)	80.6 kg/cm^2 (hardwood)	46.05%	56.56%	Durable
Type V (concrete square column 20×20 cm with slabs on ground)	+11.35 kg/cm^2, -11.35 kg/cm^2 (at one joint between column and stilt floor beam)	180 kg/cm^2 (concrete)	18 kg/cm^2 (concrete) 3,900 kg/cm^2 (steel bar)	6.31% (concrete)	63.06% (concrete) 0.29% (steel bar)	Durable
Type VI (concrete square column 20×20 cm with slabs on ground)	+12.49 kg/cm^2, -12.49 kg/cm^2 (at the middle of one stilt floor beam)	180 kg/cm^2 (concrete)	18 kg/cm^2 (concrete) 3,900 kg/cm^2 (steel bar)	6.94% (concrete)	69.39% (concrete) 0.32% (steel bar)	Durable
Type VII (concrete square column 20×20 cm with slabs on beams)	+31.25 kg/cm^2, -31.25 kg/cm^2 (at one base of column)	180 kg/cm^2 (concrete)	18 kg/cm^2 (concrete) 3,900 kg/cm^2 (steel bar)	17.36% (concrete)	173.61% (concrete) 0.80% (steel bar)	Durable

Remarks: + (stress value) = tensile stress
- (stress value) = compressive stress

3.2.4 Notable observations

The structural durability assessment of a stilt house to flash flooding of 1 meter-depth with a water speed of 3.05 m/s produced some noticeable findings. First, all types of stilt house considered could withstand flood loads of moving water. The highest reactive stress which occurred in the principal structure of each type of stilt house was not beyond the ultimate strength of the materials used. Thus, this type of house is safe and suitable to build in locations prone to flash flooding. This finding was consistent with several studies of stilt houses in flood risk areas. Idham (2018) reported that the elevated floor in a stilt house is the most suggested house structural system for confronting flood disaster, since such an elevated floor provides a safe place for dwellers while allowing the water to run through the structure as a first precaution against disaster vulnerability based on the environmental threat. Saharom et al. (2018) suggested that according to the condition and affordability for the house owner, the ideal house construction system was an elevated stilt house system that used lightweight material to reduce the load on unstable ground. The elevated ground floor provides protection for the house residents from flood danger compared to a non-elevated house system which is more prone to flooding. Tikul and Thongdee (2015) reported that a suitable housing style helped to reduce livelihood problems during flooding, with a one-story house with a high basement being the most suitable housing style because it lets the water flow through the basement. Ourn and Suntornvongsagul (2015) studied one community experiencing repeated flooding in Cambodia and found that the houses in the community were built on high stilts to let the floodwaters pass through, clearly reflecting a mechanism adapted to flooding.

Second, although a stilt house can resist lateral loads of moving floodwaters at 1 meter-depth with a water speed of 3.05 m/s, if the level of floodwaters is deeper than 1 meter and flow with the velocity faster than 3.05 m/s there will be increased flood loads hitting the house. Under such conditions, the most vulnerable points at high risk of damage before other parts of the house are the base of columns and the joint between columns and stilt floor beams. The maximum reactive stress at those two vulnerable points might exceed the ultimate strength of their materials resulting in serious damage to the primary structure. Considering in detail the structural durability assessment of stilt houses, where the house consists of columns which extend from ground up to the roof without any joints in them,

the most vulnerable point was the base of the column as this is the connection point between the superstructure (structural members above the ground) and substructure (structural members under the ground, namely foundations) of the house. For a house with columns having joints on them (such as where the columns meet the stilt floor beams and are clearly a change in the column size or in the column material between under and above the joint), the most vulnerable point is the joint between the column and the stilt floor beam. Such a joint is the connection point between a vertical structural member (a column) and a horizontal structural member (a beam) in the house.

The connection points between the superstructure and substructure and between vertical and horizontal structural members are always the weakest points of the post and lintel structural system of a stilt house because they are the first point that will sway and move and then get damaged when struck by a lateral force. This is consistent with Allen et al. (2010) who studied lateral load resistance capacity in a bay of framing. They remarked that a bay of framing (a post and beam system) is mainly designed to resist axis or gravity loads. If a lateral load is applied to a bay of framing with ordinary joints, the bay will deform and collapse with a twisting motion and the top of a column that connects to a beams and the foot of the column will slide from its position. Such lateral load tends to push over beams and columns and then separate them (Figure 4).

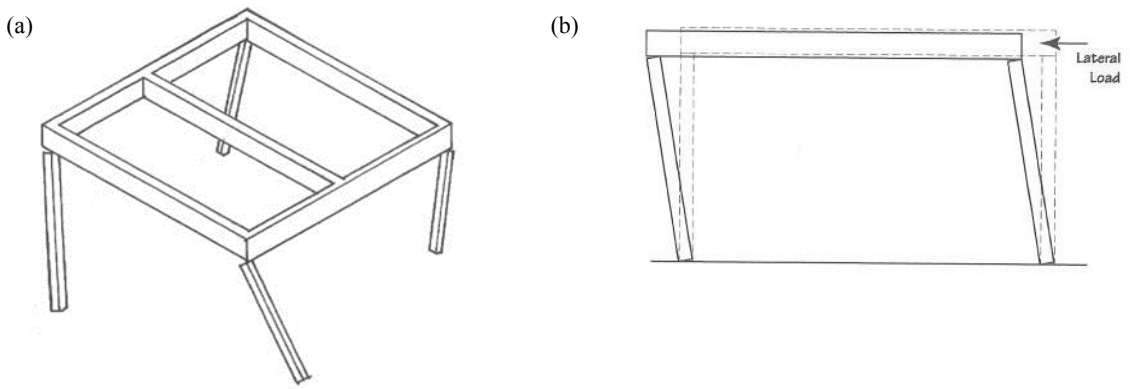

Figure 4. (a) Unbraced bay of framing will often collapse with a twisting motion; (b) lateral load tends to push over a beam and column (Allen et al, 2010)

Therefore, strengthening should be done to the base of the column and the joint between the column and the stilt floor beam in order to make the main structure of the house more resistant to any moving water force. Several studies have implied that the bottom of the post and the junction between the post and beam are the weakest points when struck by flood loads as well as remarking on how to make those weakest points more resistant to water force. Stephenson et al. (2018) indicated that the effect of lateral pressure from floodwaters is considered in relation to the resistance of the structure to being washed away. Concerning wash out, the connection of the structure to the foundation is a significant factor, since the friction action of the embedment of the post to the foundation is considered to resist flood loads and provide vulnerability reduction. Dilhani and Jayaweera (2016) found that reinforcing the superstructure of the house is one effective method to reduce flood damage. The building structure should be fixed to strong and deep foundations. The base of columns should not be free standing, but rather vertical reinforcement in columns should link foundations to the top of the superstructure walls and the roof. Zain (2016) found that the ways of making traditional houses in West Kalimantan, Indonesia to resist flood loads efficiently used posts which extended from the foundation up to the roof structure and the main columns are strengthened by roof and floor beams which go through the columns.

In addition, there have been some research projects studying the structural durability of stilt houses to lateral forces that are not flood loads. They definitely confirmed that the bottom of the column and the joint between the column and beam are the points that should be strengthened to better resist lateral loads. Madeali et al. (2018) reported that in the primary structure of Bugis traditional houses in Indonesia formed using a column and beam system, the joint between the column and the beam (both roof and floor beams) should be fixed or have a rigid joint such as a mortise and tenon. With this type of joint, Bugis houses can withstand wind loads at higher levels. Wasilah (2019) stated that the success of

Ammotoan stilt houses in South Sulawesi regarding their resistance to earthquakes was the system of columns and joints. The columns used a deep pile system where the main piles of the structure are embedded about 1.00 m into the ground. Rigid joints are used to connect the pillars and beams to the floor.

Third, diagonal and horizontal bracing members, fixed among stilt columns and perpendicular to the flow direction of floodwaters, were nearly useless if they were not above the flood level. Instead of permitting floodwaters to flow through rapidly, such bracings became water obstructions which increased reactive stresses and resulted in a high risk of severe damage to the core structure of the house. This does not mean that bracings are not permitted but rather that diagonal and horizontal bracing elements should be aligned in parallel with the water flow direction and installed above flood height so they do not hinder the flow of floodwaters and can increase the strength of the main structure to resist lateral forces (flood loads) efficiently. This finding corresponded to Liao et al. (2016) who studied stilt houses in the Vietnamese Mekong Delta, especially in areas subjected to floodwaters that coincided with a storm to produce waves that could collapse the house. They found that to mitigate the flood hazard, many households in those areas reinforced their stilt houses by tying bamboo poles between the stilts. Dilhani and Jayaweera (2016) mentioned attributes of flood risk mitigation strategies in dwellings, with one being to strengthen the main structure of the house by using bracing members. They suggested bracing of the adjacent posts diagonally in order to keep the house from leaning. Parekh (2018) reported that where a building is constructed so that the lowest floor is elevated above the regulatory flood height, the stilts should be compact and free from unnecessary appendages which would tend to trap or restrict free passage of debris during a flood. Bracing, where used to provide lateral stability, should be of a type that causes the least obstruction to the flow and the least potential to trap floating debris. Chaves (2015) stated that the horizontal structural members of the building not above the flood height are considered to be obstructions that can transmit the force of water impacts to the rest of the structure.

The above observations and discussion strongly reinforce that stilt houses can be constructed in flash flood-affected areas with some specific reinforcement methods to some particular parts of the house. In the five study locations (referring to the numerical data from the field survey), the income/year/household of most local residents was approximately USD 9,000 whereas the expenses/year/household were approximately USD 7,100. Each household had savings of USD 1,900 per year, or 21% of the income which is considered high. In Thailand, the current cost of a concrete stilt house is between USD 20,000 and 23,000 and the cost of wooden stilt housing is approximately USD 25,000 to 26,000 (Thai Appraisal and Estate Agents Foundation, 2018). A comparison between the construction costs of a stilt house and the savings proportion of the household indicated that the households could take out a loan to build their stilt house and their high proportion of savings would likely enable them to meet the repayment. With this financial status, owning a stilt house should be affordable to local residents.

The stilt house is an obvious example of flood damage mitigation. This type of house is representative of a flood adaptation paradigm that does not try to control or change the flood regime but rather it attempts to coexist with flooding as well as minimizing damage. The field survey showed it was a fact that some flood risk areas that have engineering structures to control or prevent flooding still face flood events. Moreover, some locations do not have such structures. This might emphasize that flooding cannot be completely prevented. Therefore, it might be better if people in flood risk areas were self-reliant by adopting flood adaptation measures instead of depending solely on flood controls. In addition, one important thing that local residents need to learn after the flood event is that they must adapt to be able to cope with flooding properly and safely. This means not only adapting their livelihoods during flood, but that adaptation should cover adjustment of their housing style. They should observe and learn which types of house are the best for coexisting with water current and suffer the least damage and they should also look for opportunities to build such a house.

Nevertheless, the structural durability assessment of stilt houses to flash flooding in this study was undertaken based on conditions of a flood depth of 1.00 m and a water flow velocity of 3.05 m/s. Consequently, these results cannot be generalized to the structural durability of stilt houses in all locations of flash flooding. The flood depth used in this research was the average value derived from only five study sites and as such, it cannot represent water depths at all locations of flash flooding. The flood velocity used in this research was based on some reliable sources instead of actual data from the study sites because of the lack of

recording instruments. Consequently, the velocity does not necessarily represent the real speed of flow water in a real place. In fact, flood depth and speed vary depending on the topography of each area. Further research should be undertaken on sites having different flood heights from those in the current study (deeper and shallower than 1.00 m) and on sites that have accurate measurement or recordings of the speed of floodwaters. Knowing the flood depth and velocity accurately will result in more precise calculations of flood loads and more closely reflect reality, this making the assessment more valid.

4. CONCLUSION

The results from this study revealed that the main structure of both wood and concrete stilt houses can resist flood loads of moving water at 1.00 m depth with a flow speed of 3.05 m/s. However, if the house is subjected to water deeper than 1.00 m and faster than 3.05 m/s, the house might be damaged. The points having a high risk of damage are the base of the column and the joint between the column and beam; these points require some strengthening. Where a house has horizontal or diagonal bracing members fixing the main structure and these are perpendicular to the flow and not above flood level, instead of making the house structure more stable, they become water obstructions that increase the reactive force to the main structure.

It can be concluded that for a stilt house to effectively withstand flash flooding, the main structure needs to be reinforced. First, the column base should be embedded into the ground and fixed to deep and strong foundations. The friction of the embedment of the column into the foundation helps to resist flood loads. Second, the connections between the column and beam (both roof and floor beams) should be rigid or fixed joints to reduce the opportunity for twist motion at these joints when they are hit by moving water. Third, the bracing members (both diagonal and horizontal) that are fixed to the main structure should be aligned in parallel with the water flow direction and be above the flood height to avoid becoming flow obstructions that can transmit the stress of water impacts to the main structure.

ACKNOWLEDGEMENTS

We thank everyone in the five study communities for greatly assisting with interaction with their communities to explore and record the physical characteristics of stilt houses. We also thank the stilt house owners who allowed us to survey and measure their houses.

REFERENCES

Allen E, Zalewski W, Foxe DM, Anderson J, Hriczo K, Ramage MH, Ochsendorf JA, Block P, Iano J. Form and Forces: Designing Efficient, Expressive Structures. New Jersey: John Wiley and Sons, Inc; 2010.

Al-Sahawneh EI. A new approach for the determination of tensile and shear strengths of normal weight concrete. Journal of Engineering 2015;5(8):38-48.

American Concrete Institute (ACI). ACI 318-14. Building Code Requirements for Structural Concrete. Michigan: ACI; 2014.

American Society of Civil Engineers (ASCE). ASCE/SEI 7-05. Minimum Design Loads for Buildings and Other Structures. Virginia: ASCE; 2014.

Andersen TK, Shepherd JM. Floods in a changing climate. Geography Compass 2013;7(2):95-115.

Autodesk. Robot Structural Analysis Professional. (Educational Version) [Software] Autodesk, Inc. 2015.

Charoenchai O. Flood Resilience Practical Adaptation in Flash and Inundation Flood-affected Areas in Thailand [dissertation]. Nakhon Pathom: Mahidol University; 2018.

Chaves DMM. Flood Resilient Housing Recovery Models: A Theoretical Case Study in Maldives [dissertation]. Lisbon: Universidade Nova De Lisboa; 2015.

Chorwichien W. Structural Timber Design. Bangkok: New-Thai-Mitr Press; 2014.

CPAC Concrete Academy. Standard Methods for Testing Aggregate and Concrete. Bangkok: The Concrete Products and Aggregate Co., Ltd; 2000.

Department of Mineral Resources. Map of Landslide Risk Community: Mae Phun subdistrict, Lap Lae district, Uttaradit province. Bangkok, Thailand: Department of Mineral Resources; 2013.

Dilhani KAC, Jayaweera N. A study of flood risk mitigation strategies in vernacular dwellings of Rathnapura, Sri Lanka. Built-Environment: Sri Lanka 2016;12(1):1-9.

Editorial Department of Komchadluek Newspaper. Landslide warning in 16 districts, 6 provinces [Internet]. 2008 [cited 2018 Sep 1]. Available from: http://hilight.kapook.com/view/23932.

Editorial Department of Naew Na Newspaper. Lesson learned from flood disaster to community disaster management plan [Internet]. 2011 [cited 2018 Sep 1]. Available from: http://www.measwatch.org/news/3183.

Focus News Agency. Flood rescue in Krung Ching [Internet]. 2011 [cited 2018 Sep 1]. Available from: http://songkhlatoday.com /paper/87404.

HelpAge International. Risk, Vulnerability, and Potential Analysis of Tamot Sub-district, Tamot District, Phatthalung Province within the Context of Climate Change. Bangkok, Thailand: Oxfam and alliance; 2013.

Hryczyszyn K, Neil D. Overwater stilt housing in Can Tho, Vietnam: distribution patterns and implications for development policy and master planning. International Development Planning Review 2014;36(4):475-501.

Hydro and Agro Informatics Institute. Nan Watershed. Bangkok, Thailand: Hydro and Agro Informatics Institute; 2012a.

Hydro and Agro Informatics Institute. Pasak Watershed. Bangkok, Thailand: Hydro and Agro Informatics Institute; 2012b.

Hydro and Agro Informatics Institute. Eastside South Watershed. Bangkok, Thailand: Hydro and Agro Informatics Institute; 2012c.

Hydro and Agro Informatics Institute. Songkhla Lake Watershed. Bangkok, Thailand: Hydro and Agro Informatics Institute; 2012d.

Idham NC. Riverbank settlement and humanitarian architecture, the case of Mangunwijaya's dwellings and 25 years after, Code River, Yogyakarta, Indonesia. Journal of Architecture and Urbanism 2018;42(2):177-87.

Krung Ching subdistrict Administrative Organization. Data Summary of Krung Ching subdistrict. Nakhon Si Thammarat, Thailand: Krung Ching subdistrict Administrative Organization; 2015.

Kusar DE, Ut MV. Construction of residential buildings on columns as an alternative to construction in areas exposed to floods. YBL Journal of Built Environment 2014;2(2):50-64.

Laituri MJ. Cultural perspectives of flooding. In: Wohl EE, editor. Inland Flood Hazards: Human, Riparian, and Aquatic Communities. Cambridge: Cambridge University Press; 2000. p. 451-68.

Liao KH, Le TA, Nguyen KV. Urban design principles for flood resilience: learning from the ecological wisdom of living with floods in the Vietnamese Mekong Delta. Landscape and Urban Planning 2016;155:69-78.

Liao KH. From flood control to flood adaptation: A case study on the lower Green River Valley and the city of Kent in King County, Washington. Natural Hazards 2014;76:723-50.

Madeali H, Suhendro B, Pradipto E, Kusumawanto A. Construction method and performance of Bugis traditional house in wind disasters. International Journal on Advanced Science Engineering Information Technology 2018;8(6): 2406-12.

Mongkonkerd S, Hirunsaree S, Kanegae H, Denpaiboon C. Comparison of direct monetary flood damages in 2011 to pillar house and non-pillar house in Ayutthaya, Thailand. Procedia: Environmental Sciences 2013;17:327-36.

Nam Kor subdistrict Administrative Organization. Flood and Landslide Prevention Plan. Phetchabun, Thailand: Nam Kor subdistrict Administrative Organization; 2015.

Nation Multimedia Group. Flooding in Uttaradit-Sukhothai-Chiang Mai [Internet]. 2006 [cited 2018 Sep 1]. Available from: http://www.thaiwater.net/current/floodphrae_Jun52.html.

Neville GB. Concrete Manual: Based on the 2015 IBC® and ACI 318-14: Concrete Quality and Field Practices. Illinois: ICC Publications; 2015.

Nopphaket N. Development for a Process of Community-active Planning: A Case of Prig Municipality's Landscape Master Plan. Thai Universities for Healthy Public Policies and Thai Health Promotion Foundation; Report number: TUHPP2553-0-012B, 2011.

Ourn V, Suntornvongsakul K. Copying mechanisms in repeated floods areas: A case study in Ba Baong commune in Prey Veng province, Cambodia. Environment and Natural Resources Journal 2015;13(2):33-43.

Parekh DN. Tsunami resistant design. International Journal of Technical Innovation in Modern Engineering and Science 2018;4(9):284-90.

Parker DJ. Floods. London, United Kingdom: Routledge; 2000.

Prig Sub-district Health Plan Working Group. Prig Sub-district Health Plan. Songkhla, Thailand: Thai Health Promotion Foundation and Health System Research Institute; 2008.

Ramasoot T, Nimsamur P. Vernacular Houses and Coping Capacity to Impact of Climate Change: A Case Study of Riparian Community in Sena District, Phra Nakhon Si Ayutthaya Province. Thailand Research Fund; Report number: RDG5530010, 2014.

Saharom NS, Diana SC, Kusyala D. Alternative housing system and materials criteria for land subsidence area (case study: Bandarharjo, Semarang). Proceedings of International Conference of Earth and Environmental Science; 11 Nov 2017; Bandung: Indonesia; 2018.

Sastrawati I. The characteristics of the self-support stilt-houses towards the disaster potentiality at the Cambaya coastal area, Makassar. Dimensi 2009;37(1):33-40.

Society and Health Institute. Learning to Live with Disasters: Cultural Ecology, Medias, Public Sector, and Community Dynamic. Bangkok, Thailand: Society and Health Institute; 2014.

Stephenson V, Finlayson A, Morel LM. A risk-based approach to shelter resilience following flood and typhoon damage in rural Philippines. Geosciences 2018;8(76):1-24.

Sunanta. Lesson from 'Nopphitam' to community disaster management plan [Internet]. 2011 [cited 2018 Sep 1]. Available from: www2.thaihealth.or.th/Content/18684-lessonfrom 'Nopphitam' to community disaster management plan.html.

Thai Appraisal and Estate Agents Foundation. The 2018 cost of construction [Internet]. 2018 [cited 2019 Aug 21]. Available from: http://www.thaiappraisal.org/english/the2001/default.php.

Thai Industrial Standards Institute. TIS 20-2543. Steel Bars for Reinforced Concrete: Round Bars. Bangkok: TISI; 2001.

Thaitakoo D, McGrath B, Srithanyarat S, Palopakon Y. Bangkok: The ecology and design of an aqua-city. In: Pickett STA, Cadenasso ML, McGrath B, editors. Resilience in Ecology and Urban Design - Linking Theory and Practice for Sustainable Cities. New York: Springer: 2013. p. 427-42.

Tikul N, Thongdee S. Development of Low Income Communities and Housing in Chiang Mai to Cope with the Risks of Climate Change: A Case Study on Flood Risks. Thailand Research Fund; Report number: RDG5630017, 2015.

Wasilah W. The structural effectivity of bent piles in Ammatoan vernacular houses. Buildings 2019;9(42):1-11.

White FM. Fluid Mechanics. Philadelphia, USA: McGraw-Hill; 1999.

Zain Z. The ecological responsive buildings: traditional houses in the Kapuas riverside of West Kalimantan. Komunitas 2016;8(2):295-308.

Zevenbergen C, Cashman A, Evelpidou N, Pasche E, Garvin S, Ashley R. Urban Flood Management. London: CRC Press; 2011.

Association of Community-level Traits with Soil Properties in a Tropical Coastal Sand Dune

Dokrak Marod[1,2], Sarawood Sungkaew[1], Hiromi Mizunaga[3], and Jakkaphong Thongsawi[1*]

[1]*Department of Forest Biology, Faculty of Forestry, Kasetsart University, Bangkok 10900, Thailand*
[2]*Center for Advanced Studies in Tropical Natural Resources, National Research University-Kasetssart University, Kasetsart University, Bangkok 10900, Thailand*
[3]*Department of Bioresource Sciences, Faculty of Agriculture, Shizuoka University, Shizuoka 422-8017, Japan*

ARTICLE INFO

Received: 25 Jul 2019
Received in revised: 1 Oct 2019
Accepted: 17 Oct 2019
Published online: 7 Nov 2019
DOI: 10.32526/ennrj.18.1.2020.10

Keywords:
Community-weighted mean/ Functional traits/ Non-metric multidimensional scaling/ Redundancy analysis/ Soil properties

*** Corresponding author:**
E-mail:
ma_muang6975@hotmail.com

ABSTRACT

There is limited information regarding plant functional traits for plant communities in tropical coastal sand dunes. This study investigated differences in species trait compositions and the relationship between community-weighted mean (CWM) traits and soil properties on the windward and leeward sides of the Bang Boet coastal sand dunes in southern Thailand. Ten sampling plots were randomly selected from each side of the dune. All woody plant species were collected and their functional traits were assessed. Soil samples were also collected. A redundancy analysis (RDA) was used to examine the relationship between CWM traits and soil properties. The results showed that species trait compositions and the CWMs of specific leaf area, leaf thickness, and leaf toughness were significantly different between windward and leeward sides. The RDA showed significant correlation between CWM traits and soil properties, particularly for specific leaf area, a functional trait that plays an important role in nutrient turnover on the leeward side. These results indicate that soil properties are predictable based on CWM traits and that leeward sand dune sides can support greater soil formation than windward sides. Hence, functional traits, as well as species, should be considered in coastal sand dune restoration and conservation programs.

1. INTRODUCTION

Recent natural disasters have focused global attention on societal responses to environmental hazards and the potential of natural systems to moderate disturbance effects, especially for coastal areas (Stanturf et al., 2007). Plant communities in coastal areas play an important role in protecting the coastline during major disturbance events, including tsunamis (Cochard et al., 2008). During the 2004 Indian Ocean tsunami event, ocean waters inundated beaches and flowed over adjacent aeolian sand dunes in Thailand (Choowong et al., 2007). After such events, plant recovery processes in coastal sand dunes are dependent on individual beach structure and the degree of anthropogenic disturbance, including trampling pressure and beach development. Plant functional traits are effective tools for assessing coastal sand dune status after disasters (Hayasaka et al., 2012). Although information concerning plant recovery after disasters in coastal ecosystems is relatively abundant, less research has focused upon plant functional traits in natural coastal sand dunes.

Plant functional traits are morphological, physiological, and phenological features that represent ecological strategies, determine how plants respond to crucial environmental factors and affect other trophic levels, and influence ecosystem properties (Kattge et al., 2011; Pérez-Harguindeguy et al., 2013). Functional traits allow for classifying species into functional types, providing insight into fundamental patterns and the effect of changing species composition on ecosystem functions. Assessing the community-weighted mean (CWM) of trait values is an approach used in plant ecology to

Citation: Marod D, Sungkaew S, Mizunaga H, Thongsawi J. Association of community-level traits with soil properties in a tropical coastal sand dune. Environ. Nat. Resour. J. 2020;18(1):101-109. DOI: 10.32526/ennrj.18.1.2020.10

describe ecosystem properties (Lavorel et al., 2008), especially during succession (Eichenberg et al., 2015; Pinho et al., 2017). According to Maun (2009), the landward zonation of coastal sand dunes is a special case of primary succession due to the greater influence of several abiotic factors including soil properties, wind velocities, and salt spray. In particular, soil properties developed by dune vegetation establishment are a major factor. Soil properties control plant growth and species composition in coastal sand dune systems (Kachi and Hirose, 1983), which are recovered via native species in sand dunes (Zhang et al., 2013). Additionally, topography, specifically windward and leeward sides of dunes, is instrumental in determining vegetation establishment (Moreno-Casasola, 1986; Maun, 2009). Soil variability in sites probably results from redistribution of litter by gravity and would be rather side-dependent (Wardenaar and Sevink, 1992). As sand dunes are a special case of primary succession, it is assumed that the initial soil properties are totally the same between the windward and the leeward sides (Walker and Moral, 2003; Maun, 2009). Therefore, evaluating species and plant communities via functional traits may be effective in assessing differences in soil properties on the windward and leeward sides of coastal sand dunes.

Coastal sand dunes are very common in temperate zones, but found less frequently in subtropical and tropical zones (Hesp, 2004; Cochard et al., 2008; Maun, 2009). In the tropical zone, Bang Boet is one of the largest dunes, located on the inner gulf of Thailand. Bang Boet has varied topography and habitats, including coastal grassland and coastal scrub, which is composed of woody plants (Laongpol et al., 2009). However, woody plant species covering in the natural areas are considered to be the final-stage in the successional process (Walker and Moral, 2003). Therefore, this study investigated the difference in woody plant community functional traits and the soil properties underlying these differences on the windward and leeward sides of coastal sand dunes in the Bang Boet. Two research objectives were addressed in this study, first, determining how species trait compositions, CWM traits and soil properties vary between leeward and windward sides, and second, identifying the relationship between CWM traits and soil properties. Although this study reflects sand dunes in the tropical zone, it is possible to generalise these results over broad geographic areas and diverse conditions for natural resource management after natural and anthropogenic disturbances (e.g., tsunami, flooding and mining).

2. METHODOLOGY

2.1 Study site

The study was conducted on the Bang Boet coastal sand dune (10°55′22″-10°56′6″N, 99°29′25″-99°29′49″E), Pak Klong sub-district, Pathio district, Chumphon Province, Southern Thailand (Figure 1), 425 km south of Bangkok. The highest elevation in the dune is approximately 20 m above mean sea level (Choowong, 2011). Bang Boet coastal sand dune experiences a tropical monsoon climate with three main seasons: rainy, winter, and dry seasons. The rainy season occurs from May to October and is influenced by the southwest monsoon. The winter season occurs from November to January, followed by a dry season from February to April. The mean annual rainfall between 1990 and 2017 was 1,730.52 mm, with a minimum of 1,148.10 mm in 1994 and a maximum of 2,656.50 mm in 1996. The mean monthly temperature over this period was 24.83 °C, with a minimum of 19.12 °C in April and a maximum of 30.54 °C in December, recorded by Saithong Silvicultural Research Station. The soil is sandy (99.55%) and rather acidic (pH 4.20-6.30), and has a low water-holding capacity and a low nutrient content.

2.2 Data collection

In early August 2016, ten sampling plots (10 m ×10 m) were randomly selected from three permanent transect plots (10 m × 100 m) established in 2012, on the windward and leeward sides of a dune, for a total of 20 sampling plots. Within each sampling plot, all woody plants with a diameter at breast height (DBH)≥1 cm were measured and identified to the species level. Species nomenclature was based on Smitinand (2014). Woody plants consisted of a total of 36 species representing 11 species in the windward and 32 species in leeward sides, with seven species present on both sides. In addition, ecological structures are explained in Table 1.

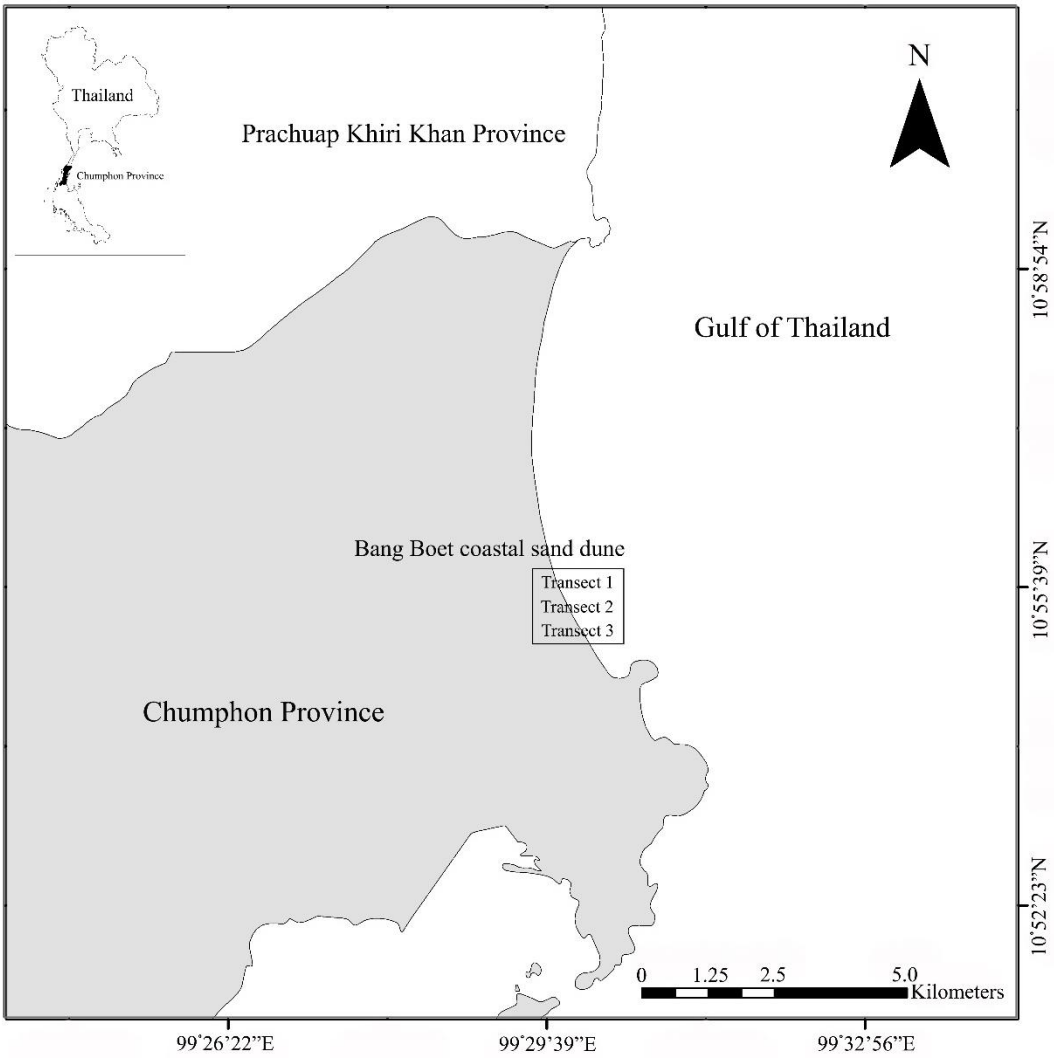

Figure 1. Study site in Bang Boet coastal sand dune on the inner gulf of Thailand.

Table 1. Ecological structure (mean±standard error) of all woody plants on the windward and leeward sides in the Bang Boet coastal sand dune.

Sides	Density (stem/0.01 ha)	Diameter (cm)	Height (m)
Windward	16±7	6.21±0.86	2.30±0.12
Leeward	111±13	3.75±0.31	3.45±0.25

Six plant functional traits were assessed, including leaf area (LA), leaf thickness (Lth), leaf toughness (LT), specific leaf area (SLA), leaf dry matter content (LDMC), and wood density (WD), using material collected from each species in accordance with Pérez-Harguindeguy et al. (2013). Each trait was quantified by measuring nine replicate samples from three different individuals randomly selected in each species from both the windward and the leeward sides. Mature sun-leaf samples from mature trees were collected to determine representative mean leaf trait values for each species. Fresh leaf weights were obtained before leaves were scanned. LA (mm^2) was estimated as the area of the fresh leaf, analysed using image analysis software (LIA for Win32, https://www.agr.nagoya-u.ac.jp/~shinkan/LIA32/index-e.html); Lth (mm) was estimated as the mean of a fresh leaf's thickness, measured in the middle of the leaf with a digital thickness gauge (model 547-401, MITUTOYO); LT (N/mm) was estimated as the mean of three punch tests per unit fracture length, performed with a digital penetrometer (2.0 mm diameter, model D2S, IMADA). SLA (mm^2/mg) was calculated using fresh leaf area divided by leaf dry weight (oven dried at 70 °C for 72 h), and LDMC (mg/g) was calculated using

leaf dry mass divided by leaf fresh weight. WD (mg/mm^3) was calculated using wood dry weight (oven dried at 105 °C for 72 h) divided by its fresh volume, which was collected at breast height from individual trees (DBH≥5 cm) using 5.15-mm increment borers.

In addition, soil samples were collected from each sampling plot. Each soil sample was collected using a soil core sampler, from the topsoil layer, at a depth between 0 and 15 cm. For chemical property analysis, five soil samples of 100 cm^3 each were collected from the four corner and centre points of each plot, then combined into one sample. For physical property analysis, one soil sample was collected using a soil core sampler at the centre of the plot. Chemical and physical properties were determined based on standard methods (National Soil Survey Center, 1996). Seven chemical properties (organic matter, pH, salinity, available phosphorus, exchangeable potassium, exchangeable calcium, and exchangeable magnesium) and two physical properties (bulk density and saturated hydraulic conductivity) were analysed at the Laboratory of Soil Science, Faculty of Agriculture, Kasetsart University (Bangkok, Thailand).

2.3 Data analysis

Non-metric multidimensional scaling (NMDS) ordination was performed to visualise patterns among species for all six measured functional traits using the *metaMDS* function in the Vegan package (Oksanen et al., 2015). Next, species trait compositions and soil properties between the windward and the leeward sides were examined using the *adonis* function to perform permutational multivariate analysis of variance (PERMANOVA), performed with 9999 random permutations. The CWM traits in each plot were calculated using the *functcomp* function in the FD package (Laliberté et al., 2014). One-way analysis of variance was used to quantify the difference in CWM traits and soil properties between dune sides. Finally, a redundancy analysis (RDA) was used to examine the relationship between CWM traits and soil properties using the *rda* function in the Vegan package. All analyses were performed using the data analysis software R (R Core Team, 2016).

3. RESULTS AND DISCUSSION

3.1 Species trait compositions

The results of the NMDS analysis of species trait compositions indicated a low stress value (0.08), suggesting reasonable performance. Two groups were created based on species trait compositions (Figure 2). The first group, representing a species trait community of LA, LT, and Lth, influenced the establishment of windward species, for example, *Casuarina equisetifolia* (6), *Hibiscus tiliaceus* (13), *Pandanus odorifer* (21), *Scaevola taccada* (28), *Syzygium grande* (33), and *Terminalia catappa* (35). The second group, representing a species trait community of WD, LDMC, and SLA, influenced the establishment of leeward species, including *Aporosa planchoniana* (1), *Chaetocarpus castanocarpus* (8), *Mischocarpus sundaicus* (19), *Ochna integerrima* (20), and *Planchonella obovata* (23). These results could be explained by heterogeneity in species trait compositions and differences in the availability of various environmental factors between the windward and leeward sites, suggesting that species occupying different dune sides do not share the same adaptive strategy. Maun (2009) and Santoro et al. (2012) previously demonstrated patterns of segregated coastal sand dune vegetation under stressful conditions. Soil property analysis showed that this sandy substrate is acidic, fine-grained, with a low water-holding capacity and low nutrient content; these properties represent stressful conditions for vegetation. Further, results from a PERMANOVA indicated that species trait compositions were strongly dissimilar and differed significantly between dune sides ($F_{1,41}$=3.44, R^2=0.08, P<0.05). Five of the six functional traits (LA, LT, Lth, LDMC, and WD) showed a significant correlation with the first two NMDS axes (P<0.01), excluding SLA (P=0.79) (Figure 2). WD and SLA are considered to be key functional traits explaining plant growth rates globally (Kunstler et al., 2016). A high WD, associated with a slow potential growth rate, indicates high tolerance to competition and a strong competitive effect, while a low SLA is generally associated with slow-growing plant species (Kunstler et al., 2016) and may be low as a consequence of low nutrient availability (Ordoñez et al., 2009), indicating that woody plant species in this coastal sand dune are slow growing. Furthermore, some species demonstrated adaptation strategy, and species trait compositions on the windward side showed high values of Lth, LT, and LA. Generally, a higher Lth values are considered an indicator of a plant's adaptations to highly sunlit, dry, less-fertile habitat (Onoda et al., 2011), influencing photosynthetic pigments and chlorophyll which are vital components to the uptake of CO_2, indicating that a thicker leaf

would contain more photosynthetic apparatus per unit area (Onoda et al., 2008). Higher LT relates to leaf life span, prolonging the longevity (Kitajima and Poorter, 2010). LA is related to drought stress, nutrient stress and high-radiation stress, all of which tend to select for relatively small leaves (Pérez-Harguindeguy et al., 2013), while in contrast, this area showed high LA. The results showed that woody plant species on the windward side showed high values of Lth, LT, and LA, those species adapted under environmental or nutrient stresses (Pérez-Harguindeguy et al., 2013). Interestingly, those species had a high LT and LA which has been attributed to longer palisade cells or an extra number of cell layers that can increase the capacity for area-based photosynthesis, and have high relative growth rates (Lambers et al., 1998). Collectively, these traits suggest adaptation strategy; therefore, it was concluded that those traits would represent the adaptation to stressful conditions in this tropical coastal sand dune that has a high mean annual rainfall, but low water-holding capacity and low nutrient content.

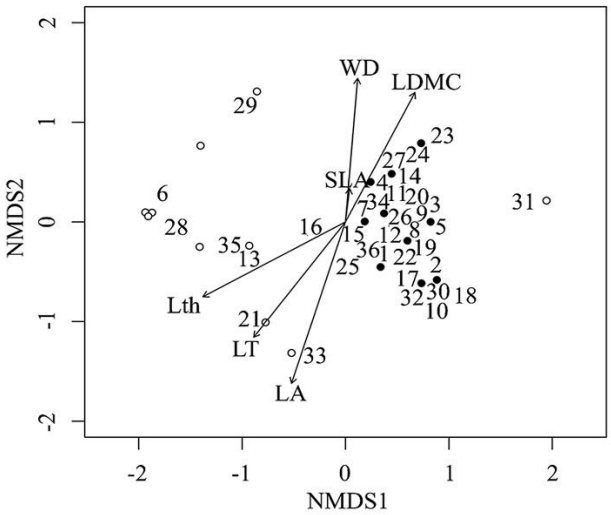

Figure 2. Non-metric multidimensional scaling (NMDS) plots showing trait dissimilarity occurring in 36 woody plant species. Open and solid circles represent plots from windward and leeward side of the sampled dune, respectively. LA, leaf area; SLA, specific leaf area; Lth, leaf thickness; LDMC, leaf dry matter content; LT, leaf toughness; WD, woody density. The numbers indicate species: 1=*Aporosa planchoniana*; 2=*Atalantia monophylla*; 3=*Breynia glauca*; 4=*Calophyllum calaba*; 5=*Carallia brachiata*; 6=*Casuarina equisetifolia*; 7=*Catunaregam tomentosa*; 8=*Chaetocarpus castanocarpus*; 9=*Champereia manillana*; 10=*Clausena excavata*; 11=*Diospyros vera*; 12=*Eurycoma longifolia*; 13=*Hibiscus tiliaceus*; 14=*Ixora cibdela*; 15=*Ixora javanica*; 16=*Lannea coromandelica*; 17=*Lepisanthes rubiginosa*; 18=*Microcos tomentosa*; 19=*Mischocarpus sundaicus*; 20=*Ochna integerrima*; 21=*Pandanus odorifer*; 22=*Pavetta indica*; 23=*Planchonella obovata*; 24=*Pleurostylia opposita*; 25=*Prismatomeris tetrandra*; 26=*Rhodamnia cinerea*; 27=*Rhodomyrtus tomentosa*; 28=*Scaevola taccada*; 29=*Sindora siamensis*; 30=*Suregada multiflora*; 31=*Syzygium antisepticum*; 32=*Syzygium claviflorum*; 33=*Syzygium grande*; 34=*Syzygium lineatum*; 35=*Terminalia catappa*; 36=*Vitex pinnata*.

3.2 Community-weighted mean (CWM) traits

The CWM traits differed between the windward and leeward sides (Figure 3). Of the five leaf morphology traits, the CWMs were significantly different between dune sides for all except LA and LDMC (Figure 3(a)-(e)). The CWM for SLA was significantly lower on the windward side, contrasting with Lth and LT, which were lower on the leeward side. The CWM for WD was slightly higher for the windward side, but this difference was not significant (Figure 3(f)). Overall, CWM traits suggested that the functional structure of communities may be determined by differential environmental conditions (Garnier et al., 2004; Lavorel et al., 2008). The windward side showed a higher CWM of Lth and LT values than the leeward side, suggesting that Lth patterns are dominated by pioneer species in younger successional plant communities (Pinho et al., 2017), while LT patterns are often affected by disturbance intensity (Avila et al., 2018). Interestingly, woody plant communities on the leeward side (9.65 mm^2/mg) showed a higher CWM of SLA than those on the windward side (7.54 mm^2/mg) but lower standardised effect sizes (9.89 mm^2/mg) (Bruelheide et al., 2018), suggesting that these communities are dominated by slow-growing species (Garnier et al., 2004; Kunstler et al., 2016).

3.3 Soil properties

Several soil properties differed considerably between the windward and leeward sides (Table 2). PERMANOVA indicated that soil properties were significantly different between dune sides ($F_{1,18}$=18.94, R^2=0.51, P<0.001). Soil properties presented low values in the windward and relatively high in the leeward side, except pH and bulk density. In the topsoil layer, plants leave a legacy in partially decomposed plant material, decomposing plant litters have an important role for fertility of soil properties (Adl, 2003). Although communities composed of slow-growing species tend to have low rates of litter accumulation, it is not yet known how litter production and decomposition could be estimated from litter input per unit of ground. The results from CWMs show that it differed between the windward and leeward sides. However, the CWMs of leaf traits

can reflect nutrient cycling and availability over forest succession (Eichenberg et al., 2015). Therefore, soil properties are likely to be predictable based on CWM traits, particularly nutrients that are indicators of decomposition dynamics in the Bang Boet coastal sand dune.

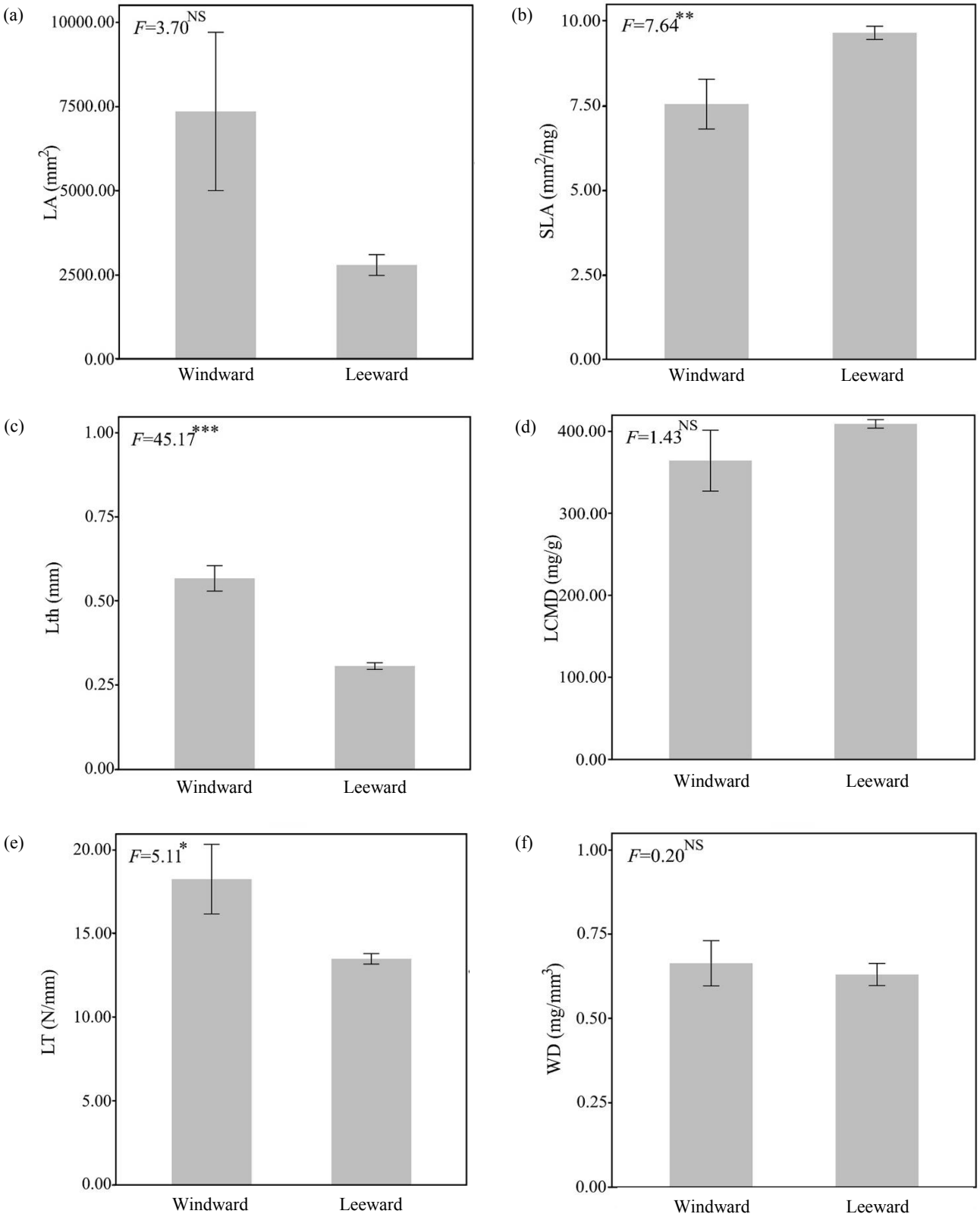

Figure 3. Community-weighted means (mean±standard error) for each functional trait measured from windward and leeward dune sides: (a) leaf area (LA), (b) specific leaf area (SLA), (c) leaf thickness (Lth), (d) leaf dry matter content (LDMC), (e) leaf toughness (LT), and (f) woody density (WD). NS indicates non-significant, and asterisks (*) represent significant differences at *P<0.05, **P<0.01, ***P<0.001.

Table 2. Soil properties (mean±standard error) in the Bang Boet coastal sand dune.

Soil properties	Windward	Leeward	$F_{(1,18)}$
Bulk density (g/cm^3)	1.42±0.03	1.04±0.07	25.46***
Organic matter (%)	0.48±0.15	2.18±0.28	28.65***
pH (in H_2O)	5.66±0.17	5.25±0.18	2.46^{NS}
Salinity (dS/m)	0.04±0.01	0.06±0.01	2.32^{NS}
Available phosphorus (mg/kg)	4.18±0.25	6.62±0.58	15.12**
Exchangeable potassium (mg/kg)	10.32±2.89	43.24±5.47	28.36***
Exchangeable calcium (mg/kg)	106.34±47.54	439.89±69.58	15.67***
Exchangeable magnesium (mg/kg)	31.28±16.58	89.99±10.89	8.71**
Saturated hydraulic conductivity (cm/s)	0.01±0.00	0.03±0.01	4.49*

NS indicates non-significant, and asterisks (*) represent significant differences at *P<0.05, **P<0.01, ***P<0.001.

3.4 Relationship between community-weighted mean (CWM) traits and soil properties

The RDA of soil properties explained 66% of total soil variation and included six CWM traits (Figure 4). The first and second axes of the model explained 53.64% and 10.87% of the variation, respectively. The first axis separated most of the assessed soil properties between windward and leeward sides, except for saturated hydraulic conductivity. The CWM for SLA (CWM.SLA), Lth (CWM.Lth), and LT (CWM.LT) contributed most to the first axis and explained 80.61% of the fitted variation. The second axis separated the saturated hydraulic conductivity from dune sides, explaining within-side differences. The CWM for LDMC (CWM.LDMC), WD (CWM.WD), and LA (CWM.LA) contributed most to the second axis and explained 16.34% of the fitted variation. However, this study focused on between-side differences (RDA axis 1). Therefore, only two CWM traits (CWM.SLA and CWM.Lth) explaining soil properties were significantly correlated with the axis (P<0.001 and P<0.01, respectively).

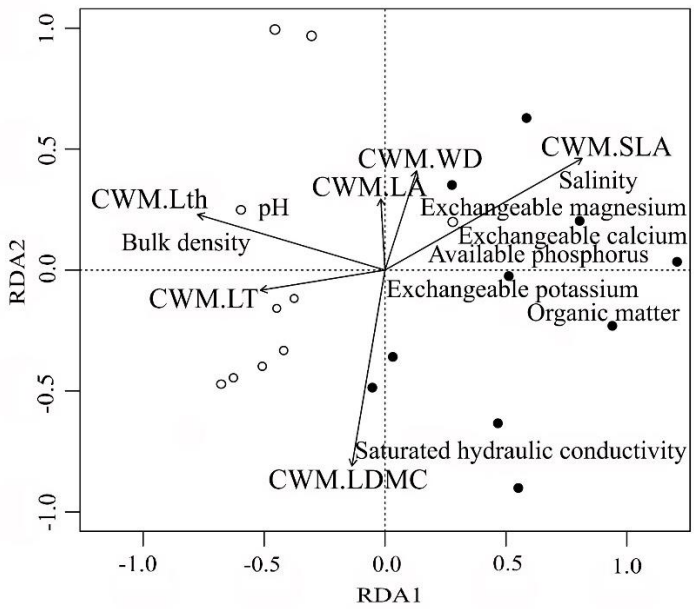

Figure 4. Redundancy analysis (RDA) of community-weighted mean (CWM) traits with soil properties. LA, leaf area; SLA, specific leaf area; Lth, leaf thickness; LDMC, leaf dry matter content; LT, leaf toughness; WD, woody density. Open and solid circles indicate plots from the windward and the leeward side, respectively.

The RDA results clearly indicate that the first axis separated most of the relationship between CWM traits and soil properties on both sand dune sides (Figure 4), which is a common approach in relating community-level trait responses to the environment (Kleyer et al., 2012). CWM trait values are important for explaining soil properties, particularly because CWMs of leaf traits reflect nutrient cycling through decomposing plant material available for soil resources (Eichenberg et al., 2015). Typically, CWMs for SLA are shown to relate

to nutrient cycling and dynamics (Garnier et al., 2004; Eichenberg et al., 2015). These results clearly show that in habitats with abundant soil resources (i.e. the leeward dune side) the CWM of SLA is higher, whereas the CWMs of Lth and LT (Figure 3(b), (c), and (e)) are lower. Rapid nutrient cycling on the windward dune side reflects the 'fast-slow' plant economics spectrum (Reich, 2014). In addition, LT is a physical defence trait relating to litter decomposition rates, where high LT relates to decreased litter decomposition (Eichenberg et al., 2015). These responses reflect a fundamental trade-off (leaf economics spectrum) between traits related to nutrient conservation and traits related to nutrient acquisition and turnover (Wright et al., 2004). Therefore, these results suggest that soil properties are predictable based on CWM traits, and that nutrient turnover and conservation are greater on the leeward side of coastal sand dunes.

4. CONCLUSION

Clear differences in functional trait composition between the windward and leeward sides indicate that the establishment of woody plant species on sand dunes reflects different successful adaptation strategies. The CWM of SLA was significantly greater on the leeward side, and SLA plays an important role in terms of soil turnover and nutrient conservation, particularly for these leeward sand dune sides. These results indicate that soil properties are predictable based on CWM traits and that leeward sand dune sides support nutrient turnover and conservation greater than windward sides. Therefore, to ensure success in restoration and conservation programs, management plans should focus on plant functional traits, specific conditions, and environmental factors.

ACKNOWLEDGEMENTS

This research was supported by the Center for Advanced Studies in Tropical Natural Resources, Kasetsart University, Bangkok, Thailand, and the Kasetsart University Research and Development Institute. We would like to thank the Royal Development Projects of His Majesty King Bhumibol Adulyadej for supplying essential facilities during the fieldwork. In addition, we thank the members of the Thai Forest Ecological Research Network, who supported field data collection and analysis.

REFERENCES

Adl SM. The Ecology of Soil Decomposition. Wallingford: CABI Publishing; 2003.

Avila AL, Sande MT, Dormann CF, Peña-Claroset M, Poorter L, Mazzei L, Ruschel A, Silva JNM, Carvalho JOP, Bauhus J. Disturbance intensity is a stronger driver of biomass recovery than remaining tree-community attributes in a managed Amazonian forest. Journal of Applied Ecology 2018;55(4): 1647-57.

Bruelheide H, Dengler J, Purschke O, Lenoir J, Jiménez-Alfaro B, Hennekens SM, et al. Global trait-environment relationships of plant communities. Nature Ecology and Evolution 2018;2(12):1906-17.

Choowong M, Murakoshi N, Hisada K, Charusiri P, Daorerk V, Charoentitirat T, Chutakositkanon V, Jankaew K, Kanjanapayont P. Erosion and deposition by the 2004 Indian Ocean Tsunami in Phuket and Phangnga Provinces, Thailand. Journal of Coastal Research 2007;23(5):1270-6.

Choowong M. Quaternary. In: Ridd F, Barber AJ, Crow MJ, editors. The Geology of Thailand. London: Geological Society of London; 2011. p. 335-50.

Cochard R, Ranamukhaarachchi SL, Shivakoti GP, Shipin OV, Edwards JP, Seeland KT. The 2004 tsunami in Aceh and Southern Thailand: a review of coastal ecosystems, wave hazards and vulnerability. Perspectives in Plant Ecology, Evolution and Systematics 2008;10(1):3-40.

Eichenberg D, Trogisch S, Huang Y, He JS, Bruelheide H. Shifts in community leaf functional traits are related to litter decomposition along a secondary forest succession series in subtropical China. Journal of Plant Ecology 2015;8(4):401-10.

Garnier E, Cortez J, Billès G, Navas M-L, Roumet C, Debussche M, Laurent G, Blanchard A, Aubry D, Bellmann A, Neill C, Toussaint J-P. Plant functional markers capture ecosystem properties during secondary succession. Ecology 2004; 85(9):2630-7.

Hayasaka D, Goka K, Thawatchai W, Fujiwara K. Ecological impacts of the 2004 Indian Ocean tsunami on coastal sand-dune species on Phuket Island, Thailand. Biodiversity Conservation 2012;21(8):1971-85.

Hesp PA. Coastal dunes in the tropics and temperate regions: Location, formation, morphology and vegetation processes. In: Martínez ML, Psuty NP, editors. Coastal Dunes: Ecology and Conservation. New York: Springer; 2004. p. 29-49.

Kachi N, Hirose T. Limiting nutrients for plant growth in coastal sand dune soils. Journal of Ecology 1983;71(3):937-44.

Kattge J, Diaz S, Lavorel S, Prentice C, Leadley P, Boenisch G, et al. TRY-A global database of plant traits. Global Change Biology 2011;17(9):2905-35.

Kitajima K, Poorter L. Tissue-level leaf toughness, but not lamina thickness, predicts sapling leaf lifespan and shade tolerance of tropical tree species. New Phytologist 2010;186(3):708-21.

Kleyer M, Dray S, Bell F, Lepš J, Pakeman RJ, Strauss B, Thuiller W, Lavoral S. Assessing species and community functional responses to environmental gradients: which multivariate methods? Journal of Vegetation Science 2012;23(5):805-21.

Kunstler G, Falster D, Coomes DA, Hui F, Kooyman RM, Laughlin DC, et al. Plant functional traits have globally consistent effects on competition. Nature 2016;529(7585): 204-7.

Laliberté E, Legendre P, Shipley B. Measuring functional diversity (FD) from multiple traits, and other tools for functional ecology [Internet]. 2014 [cited 2018 July 10]. Available from: https://cran.r-project.org/web/packages/FD/FD.pdf.

Lambers H, Chapin FS, Pons TL. Plant Physiological Ecology. New York: Springer; 1998.

Laongpol C, Suzuki K, Katzensteiner K, Sridith K. Plant community structure of the coastal vegetation of peninsular Thailand. Thai Forest Bulletin 2009;37(1):106-33.

Lavorel S, Grigulis K, McIntyre S, Williams NSG, Garden D, Dorrough J, Berman S, Quétier F, Thébault A, Bonis A. Assessing functional diversity in the field - methodology matters! Functional Ecology 2008;22(1):134-7.

Maun MA. The Biology of Coastal Sand Dunes. Oxford: Oxford University Press; 2009.

Moreno-Casasola P. Sand movement as a factor in the distribution of plant communities in a coastal dune system. Vegetation 1986;65(2):67-76.

National Soil Survey Center. Soil Survey Laboratory Methods Manual: Soil Survey Investigation Report No 42. Washington: Government Printing Office; 1996.

Oksanen J, Blanchet G, Kindt R, Legendre P, Minchin PR, O'Hara RB, Simpson GL, Solymos P, Stevens MHH, Wagner H. Community ecology package [Internet]. 2015 [cited 2017 Oct 1]. Available from: https://mran.microsoft.com/snapshot/2015-11-17/web/packages/vegan/vegan.pdf.

Onoda Y, Schieving F, Anten NPR. Effects of light and nutrient availability on leaf mechanical properties of Plant ago major: A conceptual approach. Annals of Botany 2008;101(5):727-36.

Onoda Y, Westoby M, Adler PB, Choong AM, Clissold FJ, Cornelissen JH, et al. Global patterns of leaf mechanical properties. Ecology Letters 2011;14(3):301-12.

Ordoñez JC, Bodegom PM, Witte J-PM, Wright IJ, Reich PB, Aerts R. A global study of relationships between leaf traits, climate and soil measures of nutrient fertility. Global Ecology and Biogeography 2009;18(2):137-49.

Pérez-Harguindeguy N, Díaz S, Garnier E, Lavorel S, Poorter H, Jaureguiberry P, et al. New handbook for standardised measurement of plant functional traits worldwide. Australian Journal of Botany 2013;61(3):167-234.

Pinho BX, Melo FPL, Arroyo-Rodríguez V, Piercee S, Lohbeck M, Tabarelli M. Soil-mediated filtering organizes tree assemblages in regenerating tropical forests. Journal of Ecology 2017;106(1):137-47.

R Core Team. R: A language and environment for statistical computing. R: foundation for statistical computing [Internet]. 2016 [cited 2017 Nov 5]. Available from: https://cran.r-project.org/bin/windows/base/old/3.2.5/.

Reich PB. The world-wide 'fast-slow' plant economics spectrum: A traits manifesto. Journal of Ecology 2014;102(2):275-301.

Santoro R, Jucker T, Carboni M, Acosta ATR. Patterns of plant community assembly in invaded and non-invaded communities along a natural environmental gradient. Journal of Vegetation Science 2012;23(3):483-94.

Smitinand T. Thai Plant Names. Bangkok: Department of National Parks, Wildlife and Plant Conservation; 2014.

Stanturf JA, Goodrick SL, Outcalt KW. Disturbance and coastal forests: A strategic approach to forest management in hurricane impact zones. Forest Ecology Management 2007;250(1-2):119-35.

Walker LR, Moral R. Primary Succession and Ecosystem Rehabilitation. Cambridge: Cambridge University Press; 2003.

Wardenaar ECP, Sevink J. A comparative study of soil formation in primary stands of Scots pine (planted) and poplar (natural) on calcareous dune sands in the Netherlands. Plant and Soil 1992;140(1):109-20.

Wright IJ, Reich PB, Westoby M, Ackerly DD, Baruch Z, Bongers F, et al. The worldwide leaf economics spectrum. Nature 2004;428(6985):821-7.

Zhang Y, Cao C, Han X, Jiang S. Soil nutrient and microbiological property recoveries via native shrub and semi-shrub plantations on moving sand dunes in Northeast China. Ecological Engineering 2013;53:1-5.

GUIDE FOR AUTHORS

Publication and Peer-reviewing processes of Environment and Natural Resources Journal

Environment and Natural Resources Journal is a peer reviewed and open access journal that is published twice a year (January-June and July-December). Manuscripts should be submitted online at https://www.tci-thaijo.org/index.php/ennrj/ by registering and logging into this website. Submitted manuscripts should not have been published previously, nor be under consideration for publication elsewhere (except conference proceedings papers). A guide for authors and relevant information for the submission of manuscripts are provided in this section and also online at: www.tci-thaijo.org/index.php/ennrj/navigationMenu/view/author. All manuscripts are refereed through a **double-blind peer-review** process.

Submitted manuscripts are reviewed by outside experts or editorial board members of **Environment and Natural Resources Journal**. This journal uses double-blind review, which means that both the reviewer and author identities are concealed from the reviewers, and vice versa, throughout the review process. Steps in the process are as follows:

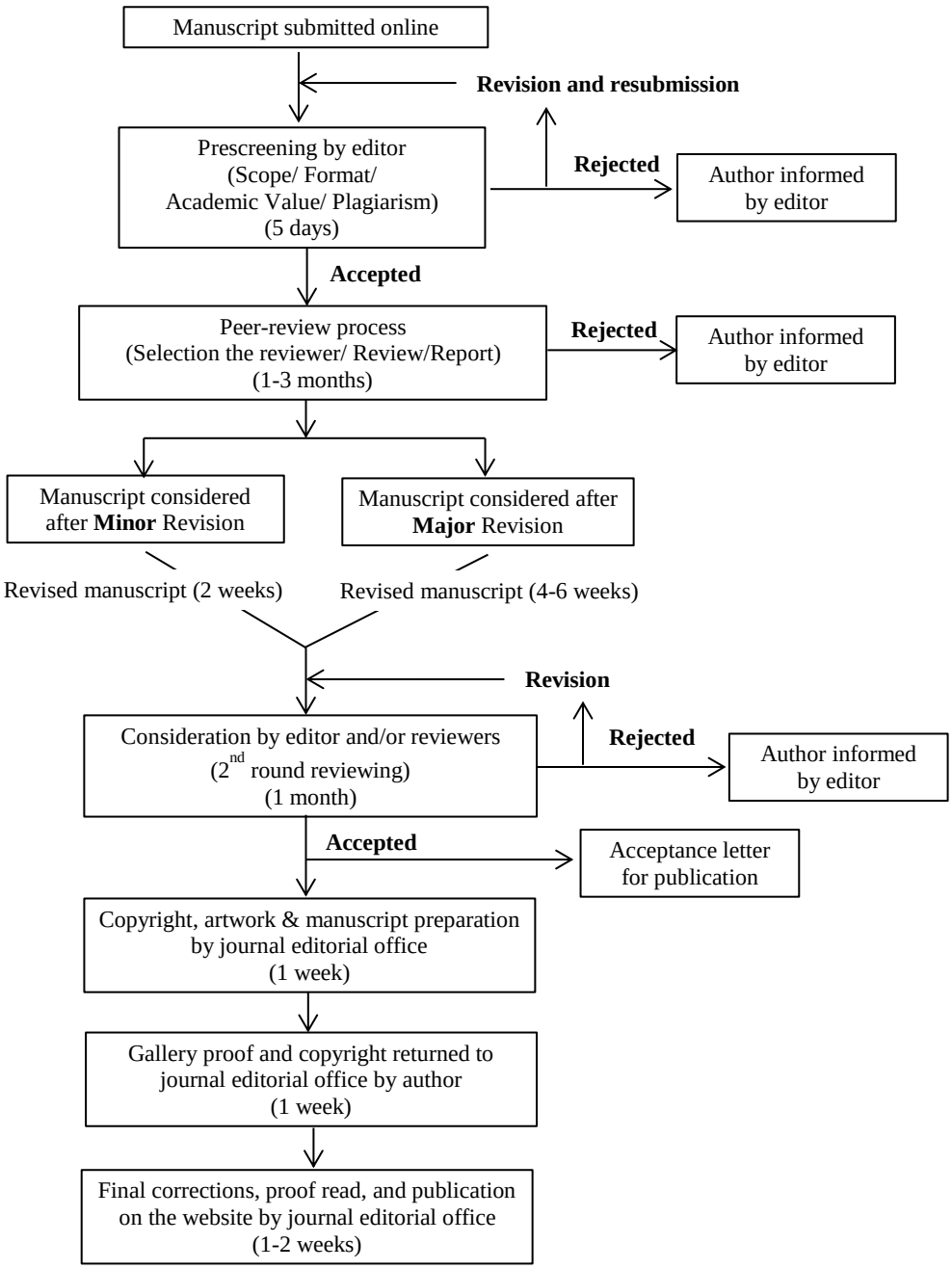

The Environment and Natural Resources Journal (EnNRJ) accepts 3 types of articles for consideration of publication as follows:

- *Original Research Articles:* Manuscripts should not exceed 3,500 words (excluding references).
- *Short Communications:* Manuscripts should not exceed 2,000 words (excluding references).
- *Review Articles:* This type of article focuses on the in-depth critical review of a special aspect in the environment and also provides a synthesis and critical evaluation of the state of the knowledge of the subject. Manuscripts should not exceed 6000 words (excluding references).

Preparation of Manuscripts

Manuscript should be prepared strictly as per guidelines given below. The manuscript (A4 size page) should be submitted in Microsoft Word (.doc or .docx) with Times New Roman 12 point font and a line spacing of 1.5. *The manuscript that is not in the correct format will be returned and the corresponding author may have to resubmit*. The submitted manuscript must have the following parts:

Title should be concise and no longer than necessary. Capitalize first letters of all important words, in Times New Roman 12 point bold.

Author(s) name and affiliation must be given, especially the first and last names of all authors, in Times New Roman 11 point bold.

Affiliation of all author(s) must be given in Times New Roman 11 point italic.

Abstract should indicate the significant findings with data. A good abstract should have only one paragraph and be limited to 200 words. Do not include a table, figure or reference.

Keywords should adequately index the subject matter and up to six keywords are allowed.

Text body normally includes the following sections: 1. Introduction 2. Methodology 3. Results and Discussion 4. Conclusions 5. Acknowledgements 6. References

Reference style must be given in Vancouver style. Please follow the format of the sample references and citations as shown in this Guide below.

Format and Style

Paper Margins must be 2.54 cm on the left and the right. The bottom and the top margin of each page must be 1.9 cm.

Introduction is critically important. It should include precisely the aims of the study. It should be as concise as possible with no sub headings. The significance of problem and the essential background should be given.

Methodology should be sufficiently detailed to enable the experiments to be reproduced. The techniques and methodology adopted should be supported with standard references.

Headings in Methodology section and Results and Discussion section, no more than three levels of headings should be used. Main headings should be typed (in bold letters) and secondary headings (in bold and italic letters). Third level headings should be typed in normal and no bold, for example;

2. Methodology

2.1 Sub-heading

2.1.1 Sub-sub-heading

Results and Discussion can be either combined or separated. This section is simply to present the key points of your findings in figures and tables, and explain additional findings in the text; no interpretation of findings is required. The results section is purely descriptive.

Tables Tables look best if all the cells are not bordered; place horizontal borders only under the legend, the column headings and the bottom.

Figures The journal does not normally use color for figures. Figures should be submitted in black and white; make sure that they are clear and understandable. Photographs converted from color to black and white format usually need to have their contrast adjusted. Regardless of the application used, when your electronic artwork is finalized, please 'save as' or convert the images to TIFF (or JPG) and separately send them to EnNRJ. Do not directly cut and paste them from MS Excel. The images require a resolution of at least 300 dpi (dots per inch). The lettering used in the artwork should be consistent in size and type.

Conclusions should include the summary of the key findings, and key take-home message. This should not be too long or repetitive, but is worth having so that your argument is not left unfinished. Importantly, don't start any new thoughts in your conclusion.

Acknowledgements should include the names of those who contributed substantially to the work described in the manuscript but do not fulfill the requirements for authorship. It should also include any sponsor or funding agency that supported the work.

References should be cited in the text by the surname of the author(s), and the year. This journal uses the author-date method of citation: the last name of the author and date of publication are inserted in the text in the appropriate place. If there are more than two authors, "et al." after the first author' name must be added. Examples: (Frits, 1976; Pandey and Shukla, 2003; Kungsuwas et al., 1996). If the author's name is part of the sentence, only the date is placed in parentheses: "Frits (1976) argued that . . ."

In the list of references at the end of the manuscript, full and complete references must be given in the following style and punctuation, arranged alphabetically by first author's surname. Examples of references as listed in the References section are given below.

Book

Tyree MT, Zimmermann MH. Xylem Structure and the Ascent of Sap. Heidelberg, Germany: Springer; 2002.

Chapter in a book

Kungsuwan A, Ittipong B, Chandrkrachang S. Preservative effect of chitosan on fish products. In: Steven WF, Rao MS, Chandrkachang S, editors. Chitin and Chitosan: Environmental and Friendly and Versatile Biomaterials. Bangkok: Asian Institute of Technology; 1996. p. 193-9.

Journal article

Muenmee S, Chiemchaisri W, Chiemchaisri C. Microbial consortium involving biological methane oxidation in relation to the biodegradation of waste plastics in a solid waste disposal open dump site. International Biodeterioration and Biodegradation 2015;102:172-81.

Published in conference proceedings

Wiwattanakantang P, To-im J. Tourist satisfaction on sustainable tourism development, amphawa floating marketSamut songkhram, Thailand. Proceedings of the 1st Environment and Natural Resources International Conference; 2014 Nov 6-7; The Sukosol hotel, Bangkok: Thailand; 2014.

Ph.D. thesis

Shrestha MK. Relative Ungulate Abundance in a Fragmented Landscape: Implications for Tiger Conservation [dissertation]. Saint Paul, University of Minnesota; 2004.

Website

Orzel C. Wind and temperature: why doesn't windy equal hot? [Internet]. 2010 [cited 2016 Jun 20]. Available from: http://scienceblogs.com/principles/2010/08/17/wind-and-temperature-why-doesn/.

Remark

** Please be note that manuscripts should usually contain at least 15 references and some of them must be up-to-date research articles.*

** Please strictly check all references cited in text, they should be added in the list of references. Our Journal does not publish papers with incomplete citations.*

Copyright transfer

The copyright to the published article is transferred to Environment and Natural Resources Journal (EnNRJ) which is organized by Faculty of Environment and Resource Studies, Mahidol University. The accepted article cannot be published until the Journal Editorial Officer has received the appropriate signed copyright transfer.

Online First Articles

The article will be published online after receipt of the corrected proofs. This is the official first publication citable with the Digital Object Identifier (DOI). After release of the printed version, the paper can also be cited by issue and page numbers. DOI may be used to cite and link to electronic documents. The DOI consists of a unique alpha-numeric character string which is assigned to a document by the publisher upon the initial electronic publication. The assigned DOI never changes.

Environment and Natural Resources Journal (EnNRJ) is licensed under a Attribution-NonCommercial 4.0 International (CC BY-NC 4.0)

Mahidol University

Wisdom of the Land

Research and Academic Service Section, Faculty of Environment and Resource Studies, Mahidol University
999 Phutthamonthon 4 Rd, Salaya, Nakhon Pathom 73170, Phone +662 441-5000 ext. 2108 Fax. +662 441 9509-10
E-mail: ennrjournal@gmail.com Website: https://www.tci-thaijo.org/index.php/ennrj

Crossref
Google Scholar